# Optimal Input Signal Design for Data-Centric Identification and Control with Applications to Behavioral Health and Medicine

by

Sunil Deshpande

A Dissertation Presented in Partial Fulfillment
of the Requirements for the Degree
Doctor of Philosophy

Approved April 2014 by the
Graduate Supervisory Committee:

Daniel E. Rivera, Chair
Matthew M. Peet
Jennie Si
Konstantinos S. Tsakalis

ARIZONA STATE UNIVERSITY

May 2014

ABSTRACT

Increasing interest in individualized treatment strategies for prevention and treatment of health disorders has created a new application domain for dynamic modeling and control. Standard population-level clinical trials, while useful, are not the most suitable vehicle for understanding the dynamics of dosage changes to patient response. A secondary analysis of intensive longitudinal data from a naltrexone intervention for fibromyalgia examined in this dissertation shows the promise of system identification and control. This includes data-centric identification methods such as Model-on-Demand, which are attractive techniques for estimating nonlinear dynamical systems from noisy data. These methods rely on generating a local function approximation using a database of regressors at the current operating point, with this process repeated at every new operating condition.

This dissertation examines generating input signals for data-centric system identification by developing a novel framework of geometric distribution of regressors and time-indexed output points, in the finite dimensional space, to generate sufficient support for the estimator. The input signals are generated while imposing "patient-friendly" constraints on the design as a means to operationalize single-subject clinical trials. These optimization-based problem formulations are examined for linear time-invariant systems and block-structured Hammerstein systems, and the results are contrasted with alternative designs based on Weyl's criterion. Numerical solution to the resulting nonconvex optimization problems is proposed through semidefinite programming approaches for polynomial optimization and nonlinear programming methods. It is shown that useful bounds on the objective function can be calculated through relaxation procedures, and that the data-centric formulations are amenable to sparse polynomial optimization. In addition, input design formulations are formulated for achieving a desired output and specified input spectrum. Numerical examples illustrate the benefits of the input signal design formulations including an example of a hypothetical clinical trial using the drug gabapentin.

In the final part of the dissertation, the mixed logical dynamical framework for hybrid model predictive control is extended to incorporate a switching time strategy, where decisions are made at some integer multiple of the sample time, and manipulation of only one

input at a given sample time among multiple inputs. These are considerations important for clinical use of the algorithm.

ACKNOWLEDGEMENTS

Although this document is single authored, the research presented in it would certainly not have been possible without the support of multiple individuals and help from various organizations. It is my intention to formally thank and show appreciation to those who have contributed to my professional, as well as personal, life.

First and foremost, I must thank my dissertation supervisor Professor Daniel E. Rivera. I have been very fortunate to have had him as my adviser during my graduate studies at Arizona State University. He hired me as a lowly masters student in his research group in the fall of 2009. I thank him for introducing me to system identification and model predictive control, and their applications in non-traditional settings. In all these years, Prof. Rivera has shown a great deal of confidence and patience in my work by giving me immense freedom to work independently and allowed me to pursue my interests. In the process, I hope to have learnt from him, among many things, how to conduct meaningful and impactful research by thinking clearly and working smartly. He is always supportive of students attending conferences and has convinced me that SYSIDs are among the most interesting conferences. He was also kind enough to present our work in conferences I could not attend. I would also like to acknowledge Prof. Rivera's help and extensive feedback in preparing papers for publication including this document. A big thank you for everything you have done for me.

I would like to thank my dissertation committee: Professors Jennie Si, Kostas Tsakalis and Matthew Peet. Their useful comments on my work has greatly improved the quality of this dissertation. I must also thank them for their graduate classes on systems and controls at ASU which have been very important stepping stones for me.

Given the multidisciplinary nature of this work, I would like to acknowledge the contribution and mentorship of my collaborators (many of whom are coauthors). First, I would like to thank Prof. Paulo Lopes dos Santos from the University of Porto for he has been very kind in including me in his research projects on linear parameter varying system identification. I am always amazed at his knowledge of theory of system identification and its applications. Prof. Eric Hekler from the School of Nutrition and Health Promotion at

Arizona State University involved me in his passion of designing better health interventions and I thank him for patiently answering my questions. Next, I want to thank Prof. Diego Regruto from Politecnico di Torino and his student Dr. Dario Piga for enlightening discussions on polynomial optimization and its application in system identification. Prof. Jarred Younger from Stanford University School of Medicine has been very kind in providing the experimental data used in this dissertation, and I thank him for his unique clinical perspective and for inviting me to visit his research group. Finally, I would like to thank Prof. Linda M. Collins and other researchers from the Methodology Center, Penn State University for engaging discussions during our conference calls.

I have been fortunate to have had great student colleagues and friends through the years and I have enjoyed working with them. First, I would like to thank current members of the Control Systems Engineering Lab (CSEL): Yuwen Dong, Kevin Timms and César Martín. ERC 522, later ERC 416, has been a wonderful office because of them and I have enjoyed our conversations and sometime useful distractions from research. I wish them all the best. Among previous members, I would like to thank Dr. Naresh Nandola for his guidance and for allowing me to use his code, and many thanks to Nikhil K. P., Yunze Yang and Dr. Jesús Emeterio Navarro-Barrientos for being great office mates. My days spent in Tempe were made more pleasant due to the company I have had here. In particular, I would like to thank my housemate Ranjit Magendraraj for his friendship and for listening to my thoughts and rants. I also thank my previous housemates and other friends - Mayur, Harie, Rohit, Akshay, Divakar, Jaidev, Rajendra, Tushar, Subhasish for their company, and thanks to Srikanth Sridharan and Hui Zhang for all the additional interesting technical discussions. Many thanks to Shilpa and Aravindhan for their friendship and all the delicious food. Finally, I also would like to thank my friends from undergraduate days for all the wonderful memories.

I would like to acknowledge generous conference travel funding from the Graduate and Professional Student Association (GPSA) at ASU, the American Automatic Control Council

and the University of Illinois at Urbana-Champaign. Some of the results in this dissertation were produced using computing resources provided by the ASU Advanced Computing Center and I thank their staff for the help. I also thank the staff members in SEMTE and ECEE at ASU for taking care of paperwork with many thanks to Darleen Mandt who has entertained various mundane requests from me.

No words are enough for the consistent encouragement and support I have received from my mother and father: Drs. Rekha and Avinash Deshpande. They have always believed in me and have patiently endured my shortcomings. I sincerely thank them for the values they have developed in me. I must also thank my younger brother Saurabh Deshpande for his support as he has grown older and wiser in all these years. Thanks are also due to my extended family for their support with many thanks to Suhasinee Madge for all the help. Finally, I must also thank my teachers in high school and undergraduate college in India for inculcating my interest in science and mathematics with special thanks to Mr. Kamlesh Rathod.

This work would not have been possible without organizations which support research and development. This work has been principally supported by the Office of Behavioral and Social Sciences Research (OBSSR) and the National Institute on Drug Abuse (NIDA) of the National Institutes of Health (NIH) through grants R21 DA024266 and K25 DA021173. Additional support for this work was received from the Piper Health Solutions Consortium at Arizona State University. As a disclaimer, this work has not been officially endorsed by these institutions, and hence the views presented in this dissertation do not reflect views of the NIH or the Piper trust, and are of the author only.

TABLE OF CONTENTS

CHAPTER Page

CHAPTER Page

CHAPTER Page

CHAPTER Page

LIST OF TABLES

LIST OF FIGURES

Figure Page

Figure Page

# Chapter 1

# INTRODUCTION

## 1.1 Motivation

In the behavioral health and medical disciplines, there has been a shift towards recognizing the need for development of an effective paradigm for prevention, treatment and management of chronic and relapsing health disorders [1, 2, 3, 4]. In particular, there is an increasing interest in treatment strategies which are individualized and time-sensitive for maximizing the treatment effect while minimizing risks and waste [5, 6, 7, 8]. This is a multi-faceted problem involving modeling and manipulation of a complex system (a human being and its environment) by incorporating scientific theories from natural and social sciences, state-of-the-art mathematical tools and an ever-increasing access to experimental data. As an open research problem, this is being addressed in different fields under topics such as data-driven personalized medicine [1, 2], clinical decision support systems [7, 9], adaptive interventions [5, 6, 10, 11] and just-in-time interventions [12] among others. Increasingly diverse examples of focused strategies have been proposed in various health settings such as, for example, in behavior change [13, 14], smoking cessation [15], gestational weight gain [16], alcoholism [17], neuroscience [18], chemotherapy [19, 20], and management of pain [21, 22], AIDS [23] and diabetes [24, 25] to cite a few examples.

A large number of phenomena that evolve over time can be modeled using a dynamical systems approach [26, 27, 28]. Traditionally, it has been used to describe the dynamics of inanimate systems, for example, in chemical processes [29], mechanical and aerospace systems [30], power systems [31] and computing systems [32]. This approach has also been recognized in the biological and behavioral sciences as a means for building a more predictive model to describe the evolution of the system [33, 34, 35, 36, 37]. In particular, dynamical systems are useful for translating theories in behavioral science and psychology into more

predictive, falsifiable and testable forms [37, 38, 14, 39], which are amenable to optimal decision making under dynamics and uncertainty using control theory [5, 28, 40, 41].

Recently, an important enabler for improved modeling and decision making has been access to large amount of data [42, 43, 44]. Although building models from experimental data has been a fundamental exercise in science and engineering, the ubiquitous nature of sensor and computing devices is giving access to information previously untapped. Among the various statistical methods lies the field of system identification which particularly deals with building dynamical models from experimental data [45, 46]. Given that the performance of a control system depends strongly on the quality of a model, mathematical modeling continues to remain an important and challenging task in control design [47, 48].

However, not all data are created equal. Collected data may not be useful due to lack of proper excitation and hence will lack critical information about the system. In particular, the data is not conducive to infer dynamics if it does not show sufficient variations over time. Thus, the process of choosing the nature and quality of collected data or *experiment design* [49] is critical for building meaningful models. Experiment design in system identification involves selecting, often a finite-dimensional, input signal $u = [u(1), \ldots, u(N)]^T \in \mathbb{R}^N$ such that engineering requirements of performance and safety are satisfied while minimizing certain cost criteria related to the estimation procedure [50, 51, 52, 53]. Indeed, generation of this input signal is dependent upon certain assumptions on the model structure, its size and complexity and the nature of the estimator [45]. This dissertation explores the design of optimal input signals with focus on data-centric system identification estimators [54, 55, 56] while addressing specific constraints of importance in clinical practice [57]. It is argued that the better quality of data would lead to improved modeling and subsequently better closed-loop performance. Towards this end, the dissertation proposes enhancements to hybrid model predictive control to address clinical requirements, including switching time constraints and choosing only one input among multi-inputs at a given time.

This chapter is organized as following: Section 1.2 describes the nature of the experimental data from clinical trials and introduces the concept of patient-friendly designs. Section 1.3 discusses the questions in experiment design or input signal design for system identification, and Section 1.4 describes the control systems approach for assigning dosages over time. The research goals addressed in this dissertation are presented in Section 1.5. The contribution of this dissertation are listed in Section 1.6. The chapter ends with information on the organization of the dissertation and a list of publications in Section 1.7.

## 1.2 Experimental Data from Biological Systems and Clinical Trials

Biological and social systems are characterized by complexity and thus, use of experimental data is critical towards unraveling the inner workings of these system. The experimental procedures may involve testing the effect of external perturbations and measuring outcomes end-points at select time intervals. The experimental data collected in a clinical trial has historically yielded increased understanding, for example, in systems biology [58, 59] and cancer biology [60]. This section describes the nature of clinical data using a previously-conducted clinical experiment and contains a brief description of how input signal design can play a role in the development of more effective clinical trials that ultimately lead to optimized treatments.

A clinical trial is a controlled scientific experiment conducted to determine the effects of certain treatment procedure such as a new drug or a behavioral therapy such as counseling. The design of a clinical trial involves both clinical and statistical aspects [61]. Knowledge of drug pharmacokinetic-pharmacodynamic effects is also necessary for clinical trials involving a pharmaceutical component [62]. Issues related to the clinical aspects include recruitment of participants, preparation and implementation of a safe clinical protocol for different phases of a clinical trial among other important considerations. More details on this aspect can be found in [61]. From a modeling perspective, clinical trials are designed as statistical experiments. In many population-level clinical trials, the participants are

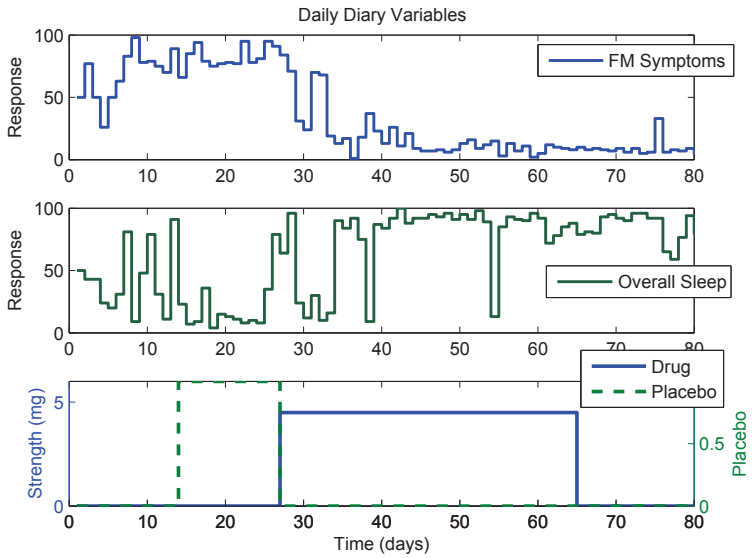


Figure 1.1: Plot of selected variables from naltrexone intervention of fibromyalgia as a function of time. This participant received placebo followed by drug in a single blinded trial. Decrease in FM Symptoms and increase in Overall Sleep over time indicate a dynamic response to the treatment.

randomly assigned to different treatment groups. The process of randomization guarantees independence between treatment procedure and desired outcome for causal inference [63, 64]. More commonly, crossover designs are employed where the participants receive different treatment in a sequential manner (e.g., drug followed by placebo). Furthermore, the experiments are also generally blinded: a single blind study is a clinical trial in which the participants do not know if they are taking the experimental treatment or a placebo. Similarly, a double blind study involves the scenario where both the participant and the experimenter are unaware of the actual treatment. Finally, many clinical trials measure the outcomes of interests over a period of time to deduce the efficacy of the intervention.

These concepts are illustrated with a clinical trial of naltrexone, an opiate antagonist, as a treatment for a pain disorder known as fibromyalgia [65, 66, 67, 68]. The study was designed as a single-blind, placebo-control while employing a crossover design [67]. Figure 1.1 shows data for a single participant of the pilot study to determine the efficacy

of this drug on fibromyalgia symptoms. In this blind controlled experiment, a unit dose is provided over a long period of time, and corresponding changes in symptom reports (on a scale of $0 - 100$) are noted over the period of the trial. As shown in Fig. 1.1, the participant in the trial reports lower overall fibromyalgia symptoms (primary endpoint), and improved sleep as a consequence of the drug. In addition, secondary endpoints were also measured during the course of the study [67]. The efficacy of the drug can be inferred through standard statistical tools [61, 67, 68]. The use of this data for dynamical modeling and subsequent closed-loop control is examined in Chapter 2. The secondary analysis of data revealed certain limitations in the design for producing an informative dataset for the purpose of system identification, and this has motivated this dissertation to address input design by incorporating requirements from clinical practice. More details on this secondary analysis can also be found in [21, 22, 69, 70].

As alluded to earlier, traditional population-level clinical data is generally not amenable for constructing dynamical models. This is not surprising given they are typically designed for 'static' systems and are geared towards hypothesis testing and finding treatment efficacy. For example, the following statements are true for the data collected in the naltrexone fibromyalgia trial:

- Continuous scales are used for variables measured in the study. Often data in clinical trials is represented in terms of categorical variables (e.g., binary or 'yes/no' variables) which are difficult to analyze using system identification.

- A rich dataset is available for many variables in this study. This is also know as intensive longitudinal data (ILD) in social science literature [71] which implies that many measurements were taken over time or that the signal was sampled fast enough to capture the underlying dynamics.

There are still a number of issues regarding using such clinical data that limit its usefulness for system identification such as:

1. Only *one dosage* level is present in the input signal:

    - *Modeling perspective*: The single step change in the dosage creates difficulties for assessing nonlinearity or distinguishing between the effect of disturbances versus the input, among other considerations.
    - *Pharmacological perspective*: The single step change (i.e. fixed dosage) may not cover the complete therapeutic window of the drug. This implies that it is possible to vary the drug dosages over time and to observe corresponding changes in reported pain condition. It is not uncommon to see *flexible* dosage trials [72] in literature, although they may be designed in an *ad-hoc* way.

2. Given the nature of the protocol, e.g., the drug signal followed by the placebo signal (Fig. 1.1), it is difficult to divide the dataset into estimation and validation subsets.

Considering some of these limitations, there has been increasing interest in using so-called 'n-of-1' or single-subject clinical trials [73, 74, 75]. These design are highly individualized and hence have specific advantages over population-level design by being more objective driven, capable of leveraging recent proliferation of mobile devices and hence are more compatible with the end goal of clinical practice [74, 75]. In the input signal approach, the drug dosages (input signals) can be manipulated to satisfy system identification objectives. Thus, the traditional shortcomings can be systematically addressed by approaching part of single-subject clinical trial design as an input signal design problem, and hence making the clinical data more useful for system identification [76].

However, embarking upon this task requires care, as many input design methods, even the state-of-the-art, may not incorporate human participant requirements that extend beyond commonplace issues relevant in industrial applications. This can be illustrated for pharmaceutical based proposed intervention for the drug *gabapentin* used to treat neuropathic pain. The drug has a broad therapeutic window [77] although the change in dosages should be slow. The following constraints are desired:

1. Typical dosage: $1200 - 3600$ mg,

2. Length of protocol : $90 - 240$ days,

3. Dosage change size : $100, 300, 600, 900$ mg,

4. Dosage assessment: 1 day (daily) to 7 days (weekly).

These constraints can be comprehensively addressed using input signal design procedures as shown in more detail in Section 1.5.1. Fig. 1.2 shows a dynamic simulation example to illustrate this point. The drug magnitude limit is translated as an amplitude constraint and the limitation on dosage change over time is enforced through a constraint on the signal rate of change. The simulation also shows two periods of the input signal, under daily assessment, along with a provision to gradually increase the drug dosage to 900 mg during baseline and similarly gradually decrease during the washout period. During the period of the experiment, the pain response is systematically manipulated under constraints. This simulation example has been discussed in more detail in Chapter 5.

To illustrate this point further, consider another example of an intervention aimed for improving physical activity among adults. The aim of the input design is to understand the dynamics of rewards on human behavior. The design provides a binary input (i.e. reward or no reward) such that the number of steps taken per day (by running or walking) match the goals for that day as close as possible through operant conditioning, and hence improve the physical activity of that individual [78]. The optimized experiment will take advantage of the dynamical model developed from behavioral theory [38] to determine optimal delivery of the intervention component over time. This optimization is performed under constraints that reflect clinical and practical guidelines. Fig. 1.3 shows the dynamic response to the optimal input for a simulation example. The optimized experiment is expected to result in superior information within allowable constraints in a single-subject fashion. This simulation example has been discussed in more detail in Chapter 6.

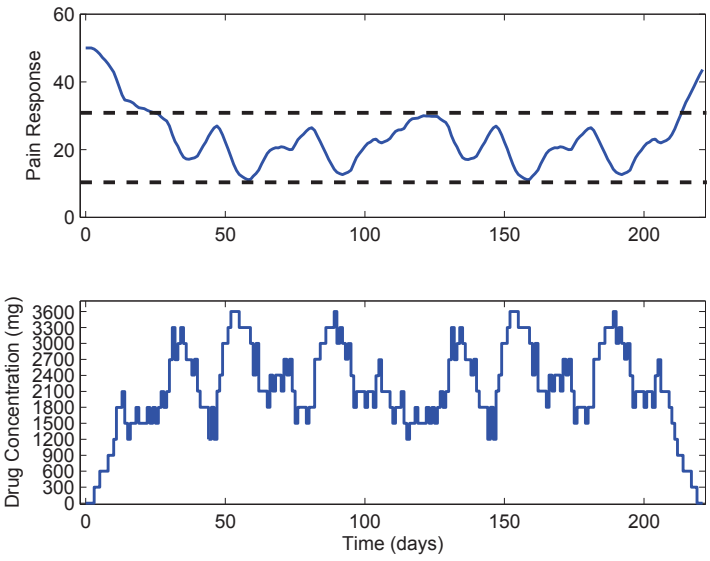


Figure 1.2: Dynamic simulation of pain response (from baseline 50) to a nine-level, two period input signal under daily assessment for the drug gabapentin. A first order system is used to simulate the pain response. The dashed lines denote the span of pain response which is a design variable in generating the input signal.

One of the aims of the dissertation is to address the issue of data-quality in a clinical setting such that the resulting data will carry more meaningful information about the response to different drug dosages. Based on this discussion, this section can be concluded with the following definition:

**Definition 1.** *The patient-friendly input signal design problem consists of the following:*

- *enhancements of single-subject clinical trial design by systematically addressing requirements of clinical practice,*
- *incorporation of system modeling requirements,*
- *end-use in adaptive interventions and personalized medicine.*

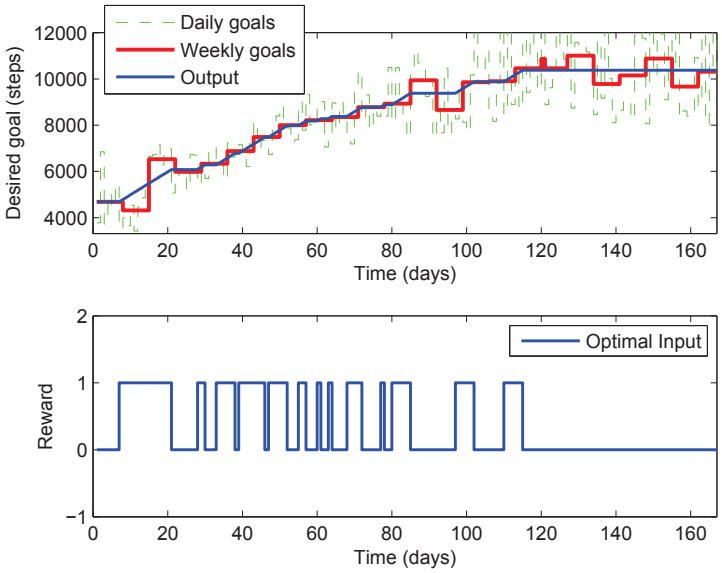


Figure 1.3: Dynamic simulation of steps per day (from baseline of 5000 steps) to a binary reward input for an intervention aimed at improving physical activity among adults. A dynamical model derived from social cognitive theory is for the simulation. The weekly goals are derived from averaging the daily goal setpoint.

## 1.3 Input Signal Design for System Identification

This section introduces input signal design for system identification with emphasis on data-centric methods.

### *1.3.1 Constraints and Objectives in Input Signal Design*

Input signal design is the key step for generating informative experimental data to be used in system identification. Broadly speaking, the goal of input signal design is to increase the information contained in the data by addressing the source of inaccuracy in the data generating process. For a given noise in the system, it is well known that the accuracy of the identified model is only a function of the design parameters chosen by the experimenter [49]. Conceptually, the input design problem in system identification can be posed

as an optimization problem

$$\begin{aligned} \min_{u} \quad & \text{Objective} \\ \text{subject to} \quad & \text{Time domain requirements} \\ & \text{Frequency domain requirements} \end{aligned} \tag{1.1}$$

where the input signal $u \in \mathbb{R}^N$ is the decision vector. The constraints in the optimization problem can be classified based on their native origin: time-domain and frequency domain. Prior work on input signal design at Arizona State has considered the concept of "plant friendliness" in input design to address practical time domain constraints that are part of industrial process operation; this includes limits on the signal length, amplitude and its rate of change.

One of the contributions of this dissertation is to explore how plant friendliness considerations can be extended for applications in health and medicine to the concept of "patient-friendly" input design. In addition to the traditional plant-friendly constraints, there may exist additional considerations that arise from clinical practice. These are typically limits on allowed drug dosages (e.g., number of treatment visits, medications, etc.) and their rate of change. Also among them is the presence of categorical constraints resulting from the fact that dosages cannot be continuously adjusted and can only assume certain discrete values within an interval. Likewise, dosage changes may only occur at certain prescribed time intervals (e.g., weekly) as a result of clinical requirements. The approach to "patient-friendliness" philosophically parallels, but is distinct from the "human-friendly" concept defined by [79] for patients with diabetes. Towards this goal, in previous work a simultaneous frequency and time domain formulation with plant-friendly constraints was shown in [50, 80, 81] using multisine signals. The input signals are designed using a predefined discrete power spectrum while the optimization procedure chooses the phases (and some amplitudes) to minimize a desired plant-friendly metric, such as the signal crest factor [45, 82].

The objective of the problem (1.1) relates to a certain metric of interest such as parameter variance of the identified model [45, 49, 83], input/output signal crest factor [81] or distribution of regressors [84, 85]. In addition, frequency domain requirements arise from aspects of persistence of excitation conditions on the input [45], robustness [86] and model quality [87]. The optimization problem 1.1 is generally found to be intractable. Many methods developed in literature take advantage of the fact that the inverse of the parameter covariance matrix is linear in the spectrum (which is the decision variable in those problems) [45] and hence such formulations can be posed as convex optimization problems [87]. However, they however have not been shown to explicitly consider all patient-friendly constraints required for a clinical trial. A major part of this dissertation is devoted towards developing tractable methods for solving a class of data-centric input design problems and the problem (1.1) is solved directly in the input signal $u$. A survey of experiment design in system identification is presented in Chapter 3.

### *1.3.2 Input Signal Design for Data-Centric System Identification Methods*

The traditional philosophy in system identification is to derive a parsimonious mathematical model as the best description (in some sense) of the input-output data generated from a dynamical system. The dataset is discarded following model validation and the estimated model serves as the exclusive basis for predicting system behavior. Linear time-invariant (LTI) system identification using prediction-error methods [45] and nonlinear identification methods such as neural networks, Nonlinear AutoRegressive with eXogenous input (NARX) and Hammerstein-Wiener models [45, 88] are few of the examples of this global approach. In general, the choice of a suitable structure is nontrivial, and often the associated optimization problem is nonconvex which may result in poor solutions. The data-centric approach, meanwhile, offers an effective modeling alternative, where computationally tractable methods are used to estimate an unknown function near a local neighborhood of the current operating point. In this approach, the data set is never discarded, but rather an estimate is generated "on demand" at each new operating condition. Examples of this approach in the

system identification literature include Model-on-Demand (MoD) estimation [55, 54, 89] and Direct Weight Optimization (DWO) [56, 90]. These approaches, and corresponding closed-loop design techniques, have been used in diverse applications, ranging from chemical process control to optimized behavioral interventions [55, 91].

With the advent of smart mobile devices, medical interventions can be conducted in real-time with new data continuously becoming available [8], and hence are enablers for data-centric methods. Data-centric system identification methods, such as MoD, build predictions from the collected dataset using estimator such as

$$\hat{f}(\varphi^*) = \sum_{k=1}^{N} w(k)y(k), \tag{1.2}$$

where $\varphi^*$ is the current *regressor* point, $y$ is the output and the weights $w$ are determined by an estimator specific algorithm. Thus, the success of data-centric methods hinges strongly on the availability of informative data. Consequently, input signal design is of critical importance for this class of methods. As argued earlier, recognizing constraints on the input and output is necessary to achieve practical requirements such as plant-friendly and patient-friendly operation [81, 57]. Input signal design requirements for data-centric methods are unique given that no fixed model is available, instead an estimate is formed at a current operating point, bounded by the dynamical constraints, on-line from a database of regressors. In fact, as data-centric methods are regressor centric, conventional inputs used in system identification, such as pseudo random binary sequence (PRBS) [45], may be suboptimal given they do not directly address spread or distribution in the regressor space. The input signal design framework proposed in this dissertation directly addresses distribution in the regressor space. The concept of developing coverage can also be extended to the case of highly interactive systems as discussed in Section 1.5.1. The arguments made in this section can be summarized in the following proposition:

**Proposition 1.** *Design an input signal to generate an informative database for data-centric system identification by achieving optimal coverage in the regressor and output space, and thus enabling effective local function estimation under noisy conditions.*

The overall aim of this dissertation is to combine the statements in Definition 1 and Proposition 1, and hence to develop algorithms that can generate informative data for data-centric methods while respecting clinical constraints.

## 1.4 Automated Dosage Assignment

The end-use of more accurate dynamical modeling of the system is to facilitate decision-making. The decisions are based on desired goals of the intervention, dynamics, uncertainty and constraints. As discussed in Section 1.2, many of the constraints under which clinical systems operate are hard and deterministic. In addition, the problems concerning automated dosage assignment may involve constraints which can be described only using propositional logic [92] and temporal logic [93]. For example, in cancer chemotherapy, it is common to provide a 'cocktail' of drugs to improve the efficacy of the treatment [60]. In some situations, it may be necessary to impose restrictions such as that one of the drug magnitude may not exceed a certain concentration unless the other drug has reached its peak saturation in the body. In addition, it may be required that multiple drug dosages are not changed at the same instant. These are examples of seemingly diverse constraints that can be addressed using tools of control engineering in a robust fashion [5]. In this dissertation, the following two requirements are considered:

- *Switching time requirement.* Due to clinical and resource considerations, it is often desirable to make decisions at frequencies other than the regular sampling interval. With more ubiquitous computing, samples can be collected as quickly as, for example, every second; however it is generally undesirable to make decisions at those

frequencies. The switching constraints gives the option to make decisions only at time intervals generally chosen in consultation with the domain expert.

- *Manipulating one input at a time requirement.* Clinical interventions generally feature multiple arms: some may be pharmaceutical in nature while some may be related with the behavioral aspects such as counseling sessions. In many situations, it is desired that only one of the components changes dosage at any given time. This condition meets a clinical requirement, and thus reduces the potential harmful effects of unknown interactions as much as possible.

These research questions are addressed, case-by-case, in the next section and, in detail, in the rest of chapters of this dissertation.

## 1.5 Research Goals

This section presents the three main research goals addressed in this dissertation. Section 1.5.1 contains the proposed algorithms for input signal design, Section 1.5.2 describes the computational algorithms to solve the input design problems and Section 1.5.3 contains the enhancement to the hybrid model predictive control algorithm. These topics are further explored in detail in the subsequent chapters of this dissertation.

### *1.5.1 Input Signal Design*

The research goals for patient-friendly input signal design are discussed under two categories: constraints and formulations.

#### 1.5.1.1 Constraints

Satisfying these input constraints is achieved by formulating the input design problem directly in the input variable $u$ which produces a *deterministic* finite length input signal. To illustrate the patient-friendly requirements, the previous example using the drug gabapentin is used to show how the clinical constraints can be translated as mathematical constraints for the input signal $u(k)\ \forall k$ of length $N$:

- Amplitude constraints: $u_{\min}(k) \leq u(k) \leq u_{\max}(\mathrm{k})$ - typical dosage of $1200 - 3600$ mg.
- Limit on $N$: length of protocol of $90 - 240$ days.
- Move size constraint: $|u(k+1) - u(k)| \leq b(k)$ - dosage change size of $100, 300, 600, 900$ mg.
- Switching constraint: $\sum_{j=1}^{T_{\mathrm{sw}}-1}(u(k) - u(k+j)) = 0 \quad \forall k = 1 + n_{\mathrm{sw}} \times T_{\mathrm{sw}},\ n_{\mathrm{sw}} = 0, 1, 2, \ldots$ - dosage assessment or switching time $T_{\mathrm{sw}}$ of 1 day to 7 days.

The patient-friendly constraints can be represented through an intersection of linear inequalities (amplitude and move size constraints) and equalities (switching constraint). Thus, the feasible set $\mathbb{U}$ in the variable $u$ is a convex set as described in Section 4.2 of Chapter 4.

#### 1.5.1.2 Formulations

In this dissertation, three distinct input signal designs are developed to extend Definition 1 and Proposition 1. The first problem formulation directly addresses the data-centric methods and the goal of formulating patient-friendly data-centric input signal design is achieved by developing a novel problem formulation using geometric distribution in the finite dimensional space. The proposed design is suited for data-centric system identification methods which do not produce a fixed parametric model. The other problem formulations address achieving a desired input spectrum and output. These are now briefly described.

1. Input signal for data-centric estimation methods:
    - *Using distribution of regressors*: The regressor is expressed as a function of the input and the algorithm then distributes the regressors (in some sense, as described later) to cover the regressor space under time domain constraints on the input. This is developed for linear time-invariant systems where the subsequent optimization problems correspond to nonconvex quadratic programs (which are NP-hard [94]) and for Hammerstein systems, where the subsequent optimization

problems are general nonconvex polynomial optimization problems. Two distinct problem statements are considered for distribution of regressors. The first problem statement can be described as *when given N regressor vectors of fixed finite dimension, distribute the regressor points as far apart from each other as possible in the regressor space under constraints on the input and output signals.* This can be represented as

$$\max_{u} \sum_{i=1}^{N-1} \sum_{j=i+1}^{N} d_{ij} \tag{1.3}$$
$$\text{s.t. } u \in \mathbb{U}$$

where $d_{ij}$ is the distance between regressor $\varphi(i)$ and $\varphi(j)$ or the regressor distance pair. The second problem statement can be described as *when given N regressor vectors of fixed finite dimension, distribute the regressor points such that* any two *regressors can be as far apart as possible in the regressor space under constraints on the input and output signals.* This can be represented as

$$\max_{u} \min d_{ij} \tag{1.4}$$
$$\text{s.t. } u \in \mathbb{U}$$

where $d_{ij}$ is the regressor distance pair. The two problem statements are compared and described in detail in Section 4.4.1. An initial formulation using semidefinite relaxation of one of these nonconvex quadratic problems is proposed in [84] with an extension proposed in [85]. The formulations developed are solved through semidefinite and nonlinear programming methods. Numerical examples and case studies are used to illustrate the proposed input design formulations and assess their benefits. An extension to other structured nonlinear systems such as Hammerstein-Wiener models and to multivariable scenarios is also proposed.

- *Using distribution of outputs*: For multivariable, highly interactive, ill-conditioned dynamical systems, it is difficult to obtain information in the low gain direction using convention open-loop input signal, and hence an input is required which can achieve a more uniform coverage to excite both low and high gain directions [95]. In this dissertation, it is proposed to spread the points in the output space such that the minimum distance between any two points is maximized:

$$\max_{u} \min dy_{ij} \qquad (1.5)$$
$$\text{s.t. } u \in \mathbb{U}$$

  where $dy_{ij}$ is the distance between any two time-indexed output points. This approach is described in Section 4.4.3.

- *Using Weyl's criterion*: Weyl's criterion:

$$\lim_{N\to\infty} \frac{1}{N} \sum_{k=1}^{N} e^{(2\pi\ell x(k))i} = 0 \quad \forall \ell \in \mathbb{Z} - \{0\} \qquad (1.6)$$

  gives the necessary and sufficient condition for a sequence $x$ to be uniformly distributed in $[0, 1)$. To achieve uniform coverage, Weyl's criterion on the output is minimized as

$$\min_{u\in\mathbb{U}\cap\mathbb{I}} \frac{1}{N} \sum_{k=1}^{N} e^{(2\pi\ell y(k))i} \qquad (1.7)$$

  where $\mathbb{U}$ is the set defined by input constraints and $\mathbb{I}$ is the additional categorical requirement on the input signal. Given the objective is a complex number, the real and imaginary parts are individually represented as shown in Section 5.2. The resulting optimization problem is nonlinear and nonconvex, and is solved (locally) using nonlinear programming. Examples are shown to prove the usefulness of this method. This approach is described in Section 4.4.4.

2. *Input signal for achieving a desired output under constraints.* Under the condition that the nature of output $y$ is known *a priori* as $y_{\text{des}}$, the input signal design problem

for LTI systems can be posed as convex optimization problem:

$$\min_{u} \quad \|y - y_{\text{des}}\| \tag{1.8}$$

$$\text{s.t.} \quad u \in \mathbb{U}. \tag{1.9}$$

This approach is described in Section 6.2. This is useful for applications where the changes in output has a trend over time.

3. *Input signal with a desired spectrum under time domain constraints.* The input signal design aim is to generate an input signal with a desired spectrum under time domain constraints. A "flat" spectrum ($\Phi_u(\omega)$) over a bandwidth is generally desirable

$$\Phi_u(\omega) \approx \gamma(\omega) = \begin{cases} \gamma_a & \omega_* \leq \omega \leq \omega^* \\ \gamma_b & \omega > \omega^* \end{cases} \tag{1.10}$$

where the frequency range is determined by

$$\omega_* = \frac{1}{\beta_s \tau_{\text{dom}}^H} \leq \omega \leq \frac{\alpha_s}{\tau_{\text{dom}}^L} = \omega^* \tag{1.11}$$

where typically $\alpha_s = 2$ and $\beta_s = 3$ [81] and estimate of $\tau_{\text{dom}}$ is obtained from drug pharmacokinetics metrics such as biological half-life. The problem is formulated as a nonlinear programming problem

$$\min_{u \in \mathbb{U}} \quad |\Phi_u(\omega) - |\gamma(\omega)|| \tag{1.12}$$

where $\mathbb{U}$ is the set defined by input constraints. This approach is described in Section 6.3.

In conclusion, the three formulations presented address the patient-friendly constraints. They fundamentally differ in the specific objective function: for example, the data-centric method's goal is to distribute the regressors while the spectral formulation aims at achieving desired input signal spectrum.

### 1.5.2 Computational Tools

A major focus of this work is to rely on optimization to solve the input signal design problems. As mentioned earlier, the problems are solved directly in the decision variable $u$. While the constraint set is convex, the specific objective functions considered are nonconvex. First, the problems can be locally solved using nonlinear programming. In many practical situations, this yields reasonable solutions. To improve the solution of the proposed problem formulations, semidefinite relaxation of polynomial optimization has been explored to approximate the original nonconvex problem. Using representation of nonnegative polynomial using sum-of-squares and theory of moments, a hierarchy of convex relaxation can be proposed as:

$$\begin{aligned} \mathbf{P}^{\xi}_{\mathbf{SOS}}: \quad & \max_{\lambda, s_0, s_j} \ \lambda \\ & \text{s.t. } g_0(u) - \lambda = s_0 + \sum_{j=1}^{m} s_j g_j, \ s_0, s_j \in \Sigma \\ & \deg(s_0), \deg(s_j g_j) \leq 2\xi, \end{aligned} \tag{1.13}$$

where $\mathbf{P}^{\xi}_{\mathbf{SOS}}$ can be written as a semidefinite program (SDP) to give a bound on the original nonconvex objective as a function of the relaxation parameter $\xi$. For the particular case of nonconvex quadratic programs, suboptimality bounds on the relaxation can also be found. These are explored in more detail in Chapter 5.

### 1.5.3 Model Predictive Control for Enhanced Clinical Use

Model predictive control (MPC) is a successful control technology particularly suited for use in clinical applications due to the flexibility it offers to address design objectives and constraints. To address categorical constraints, a *hybrid* model predictive control with three degree-of-freedom (3 DoF) tuning was developed in [96, 97]. The controller solves the following mixed-integer quadratic optimization problem

$$\min_{\{[u(k+i)]_{i=0}^{m-1},\, [\delta(k+i)]_{i=0}^{p-1},\, [z(k+i)]_{i=0}^{p-1}\}} \sum_{i=1}^{p} \|(y(k+i) - y_r)\|^2_{Q_y} + \sum_{i=0}^{m-1} \|(\Delta u(k+i))\|^2_{Q_{\Delta u}}$$

$$+\sum_{i=0}^{m-1}\|(u(k+i)-u_r)\|_{Q_u}^2+\sum_{i=0}^{p-1}\|(\delta(k+i)-\delta_r)\|_{Q_d}^2+\sum_{i=0}^{p-1}\|(z(k+i)-z_r)\|_{Q_z}^2 \tag{1.14}$$

$$\text{s.t.}\quad y_{\min}\leq y(k+i)\leq y_{\max},\ i\in\mathcal{T}_p \tag{1.15}$$

$$u_{\min}\leq u(k+i)\leq u_{\max},\ i\in\mathcal{T}_m \tag{1.16}$$

$$\Delta u_{\min}\leq \Delta u(k+i)\leq \Delta u_{\max},\ i\in\mathcal{T}_m \tag{1.17}$$

$$E_2\delta(k)+E_3z(k)\leq E_5+E_4y(k)+E_1u(k)-E_dd(k). \tag{1.18}$$

at each sampling instant under dynamical constraints, while only the first instance of the calculated optimal input is implemented as per the receding horizon framework. Specific details of the formulation can be found in Chapter 2, where it is used to assign dosages of naltrexone for treatment of fibromyalgia. This formulation allows inclusion of amplitude constraints on the manipulated variable and the controlled variable as well as limits on the rate of change of the manipulated signal, such as move size constraints. Logical constraints are enforced through a mixed-integer linear inequality shown in (1.18). However, there are certain clinical requirements which are not addressed in the current formulation. The proposed enhancements, developed in detail in Chapter 7, address the issues raised in the Section 1.4. They are as follows:

- *Switching time strategy*: In order to address the flexible assessment problem, it is proposed to include an additional constraint which will *block* the manipulated input for the fixed time, although the MPC algorithm is sampled at the original rate. Towards this, a linear equality can be added to the original formulation subject to additional constraints. This approach is described in Section 7.3.

- *Selection of single input at a multi-input scenario*: In order to address this requirement, additional binary variables $\phi$ and their associated logical specifications are introduced. They are converted into linear inequalities, and are implemented by appending them to (1.18) where the number of the additional binary variables will correspond

to the number of the manipulated inputs. The optimization problem solves and finds the solution such that only one input is manipulated. This approach is described in Section 7.4.

## 1.6 Contributions of the Dissertation

This dissertation has presented a framework for generating input signal for data-centric system identification under time-domain constraints which are inspired from the clinical applications, and enhancements to hybrid model predictive control. The contributions of this work in terms of input signal design can be summarized as follows:

- Enumeration of constraints on the input and output signal to address the requirements of practical importance originating in clinical applications. The problem formulations are written directly as a function of the input signal $u$ thus seamlessly addressing the patient-friendly requirements. This has allowed generation of finite length deterministic signals which can be applied in many applications.

- Development of a novel formulation for generating input signals using distribution in the finite-dimensional regressor space. The regressor points are distributed such that they generate sufficient support for the data-centric estimator.

- Development of a novel formulation for generating input signals for highly interactive systems using distribution of time-indexed output points.

- Development of an input signal design formulation to achieve distribution using Weyl's criterion. This formulation has been compared with the previous two formulations and has been shown for the case of gabapentin clinical trial.

- Development of an input signal design formulation for achieving desired output trajectory and desired input spectrum under input constraints. This desired output formulation has been shown for the case of physical activity intervention.

- The problem formulations have been mathematically written as optimization problems. For LTI systems, it has been shown that these correspond to nonconvex quadratic programs and for general block-structured nonlinear systems (which includes Hammerstein-Wiener systems), these correspond to polynomial optimization whose degree depends on the degree of the system nonlinearity.

- This dissertation has proposed numerical solution of these problems using semidefinite programming approaches for polynomial optimization and nonlinear programming. It has been shown that under certain conditions, useful bounds on the objective and a feasible input signal can be obtained.

- Enumeration of the condition under which the proposed input design problems are composed of few monomials and hence sparse. It has been shown that the input constraints are naturally sparse where as sparsity is induced by incorporating select regressor distance pairs. An alternative methods which utilizes the fact that the distances are already sum-of-squares has also been developed.

- The process of input signal design has been designed as a single-subject clinical trial with a proof-of-concept presented through simulation of a hypothetical clinical trial. It should be noted that the goal is to enhance, rather than replace the current clinical trial protocols. Post randomization and blinding, the participants can be given dosage plans which can be systematically designed using tools from system identification.

The contributions of this work in terms of updates to hybrid model predictive control can be summarized in following two points:

- Improvement of the hybrid model predictive control algorithm, as presented in [96, 97], to include constraints on the switching of the manipulated input. This updated implement in accordance with the receding horizon framework enables the manipulated input to change only at user supplied samples of importance to clinical practice.

- Extension of the mixed-logical dynamical (MLD) constraint of the hybrid model predictive control algorithm to address selection of only one manipulated variable in a multi-input scenario. Under this constraint, at any given sampling instants, only one of the inputs can change its magnitude.

Although the contributions of this dissertation have been highlighted using clinical applications, the formulations have been developed without any loss of generality and hence are capable of addressing requirements from other application areas. The ensuing section discusses organization of the dissertation.

## 1.7 Organization of the Dissertation

Including this Introduction, the dissertation has been organized into eight chapters. In brief, Chapter 2 describes modeling and control for fibromyalgia intervention. Chapter 3 provides a survey of data-centric methods in system identification. Chapter 4 describes the problem statements for data-centric input signal design under constraints and Chapter 5 formulates those statements as optimization problems. Chapter 6 discusses input signal design under desired objectives. Chapter 7 discusses enhancements to hybrid model predictive control. Finally, Chapter 8 summarizes the dissertation.

In detail, the document is organized as follows:

- Chapter 2 presents an optimized treatment plan for fibromyalgia using system identification and hybrid model predictive control (HMPC). The system identification models are developed from secondary analysis of actual clinical data and the application of HMPC is shown using simulation.

- Chapter 3 presents a brief survey of experiment design for system identification and mathematical optimization. The section on data-centric system identification methods serves as a reference for formulations developed in the ensuing chapters.

- Chapter 4 describes the constraints in input signal design, and develops the problem statements for data-centric input signal design using distribution of regressors, distribution of time-indexed output points and Weyl's criterion.

- Chapter 5 formulates optimization problems using problem statements from the previous chapter. Numerical illustrations are provided to further convey efficacy of the input design formulations. The problems are solved, separately for LTI and Hammerstein systems, using SDP relaxation of nonconvex quadratic programs, nonlinear programming and sparse polynomial optimization.

- Chapter 6 presents input signal design under desired objectives which are distinct from the previously developed data-centric designs. Numerical examples are shown for achieving a desired output and desired input spectrum.

- Chapter 7 describes updates to hybrid model predictive control by incorporating switching constraint and selection of one manipulated input in multi-input scenario. Simple numerical examples for switching time constraints are shown to highlight the proposed formulation.

- Finally, the document ends with summary and directions for future work in Chapter 8. The chapter summarizes the major contributions related to data-centric input signal design under constraints. The section on directions for future work presents some ideas about interesting extensions of the proposed input design and hybrid model predictive control problem formulations.

### *1.7.1 Publications*

The material presented in this dissertation has been taken from a series of published and submitted papers. In summary, the graduate work done at Arizona State has resulted in ten peer-reviewed conference papers, four of which are under review, and three journal publications of which one paper has been submitted for review, while one paper is being

revised after conditional acceptance as of submission of this dissertation. The details of the publications are as follows. The material for Chapter 2 has been taken from the following papers:

1. S. Deshpande, N. N. Nandola, D. E. Rivera, and J. W. Younger. Optimized treatment of fibromyalgia using system identification and hybrid model predictive control. Conditionally accepted to *IFAC Control Engineering Practice*, 2014.

2. S. Deshpande, N. N. Nandola, D. E. Rivera, and J. Younger. A control engineering approach for designing an optimized treatment plan for fibromyalgia. In *Proceedings of the 2011 American Control Conference*, pages 4798–4803, June 2011.

3. S. Deshpande, D. E. Rivera, J. Younger, and N. N. Nandola. A control systems engineering approach for designing optimized adaptive interventions: An illustration from the treatment of fibromyalgia. Submitted to *Translational Behavioral Medicine*, 2014.

The survey presented in Chapter 3 is previously unpublished. The material for Chapter 4 and Chapter 5 have been adapted from the following papers:

4. S. Deshpande, D. E. Rivera, and J. Younger. Towards patient-friendly input signal design for optimized pain treatment interventions. In *Proceedings of the 16th IFAC Symposium on System Identification*, pages 1311–1316, July 2012.

5. S. Deshpande and D. E. Rivera. Optimal input signal design for data-centric estimation methods. In *Proceedings of the 2013 American Control Conference*, pages 3930–3935, June 2013.

6. S. Deshpande and D. E. Rivera. Constrained optimal input signal design for data-centric estimation methods. *IEEE Transactions on Automatic Control* (to appear), 2014.

7. S. Deshpande and D. E. Rivera. A data-centric system identification approach to input signal design for Hammerstein systems. In *Proceedings of the 52nd IEEE Conference on Decision and Control (CDC)*, pages 5192–5197, Dec. 2013.

8. S. Deshpande and D. E. Rivera. Data-centric input signal design for highly interactive dynamical systems. Submitted to the *53rd IEEE Conference on Decision and Control*, 2014.

9. S. Deshpande and D. E. Rivera. Towards data-centric input signal design using sparse polynomial optimization. Submitted to the *53rd IEEE Conference on Decision and Control*, 2014.

The contents of Chapter 6 have been partially adapted into the following paper

10. C. A. Martin, S. Deshpande, E. B. Hekler, and D. E. Rivera. A system identification procedure for behavioral interventions based on social cognitive theory. Submitted to the *53rd IEEE Conference on Decision and Control*, 2014.

The contents of Chapter 7 have been partially taken from the following paper

11. Y. Dong, S. Deshpande, D. E. Rivera, D. S. Downs, and J. S. Savage. Hybrid model predictive control for sequential decision policies in adaptive behavioral interventions. In *Proceedings of the 2014 American Control Conference* (to appear), 2014.

Finally, the following two papers are part of ongoing collaboration on developing linear parameter varying (LPV) system identification for use in adaptive interventions; these two papers have not been included in this dissertation. The following paper

12. P. L. dos Santos, S. Deshpande, D. E. Rivera, T.-P. A. Perdicoulis, J. A. Ramos, and J. Younger. Identification of affine linear parameter varying models for adaptive interventions in fibromyalgia treatment. In *Proceedings of the 2013 American Control Conference*, pages 1976–1981, June 2013.

presents an alternate hypothesis that the secondary inputs only affect the perception of fibromyalgia symptoms and not directly drive it, and hence an affine linear parameter varying (A-LPV) system, where the secondary variables are the scheduling variables, can be used to model the fibromyalgia dynamics. Finally, the following paper proposes using a support vector machine approach to address basis selection problem in LPV identification.

13. P. L. dos Santos, T.-P. A. Perdicoulis, J. A. Ramos, S. Deshpande, D. E. Rivera, and J. L. M. de Carvalho. LPV system identification using a separable least squares support vector machines approach. Submitted to the *53rd IEEE Conference on Decision and Control*, 2014.

### *1.7.2 Mathematical Notation*

The mathematical notation used in this dissertation is fairly standard and as per the prevailing conventions in system identification, automatic control and mathematical optimization literature. The notation $\mathbb{R}^N$ is used denote real vector space of dimension $N$ where the elements of $\mathbb{R}^N$ are denoted by column vectors. In most cases, the definition of a variable is made clear in the context it has been used. In general, the scalar and vector variables are denoted in lower case and matrix variables in upper case. The notation $\mathbf{X} \succeq 0$ implies that the matrix $\mathbf{X}$ is positive semidefinite where as the notation $u \leq u_{\max}$ implies element-wise inequality or in other words, that each element of the vector $u$ is less that the corresponding entry of the vector $u_{\max}$. Finally, the optimization problems are written in terms of more informal semantics; for example as 'max' and 'min' assuming that the maxima and minima are achieved and a 'solution' signifies a local solution unless noted otherwise.

# Chapter 2

# OPTIMIZED TREATMENT OF FIBROMYALGIA USING SYSTEM IDENTIFICATION AND HYBRID MODEL PREDICTIVE CONTROL

## 2.1 Introduction

With rising health care costs, there is increasing interest in the medical community towards developing improved strategies for treating chronic diseases [106, 107]. Among these lie adaptive interventions, which consider adjusting treatment dosages over time based on participant response. Control engineering offers a broad-based solution framework for optimizing the effectiveness of such interventions and has been proposed as an enabler for more efficacious treatments that minimize waste, increase compliance, and enhance the intervention potency [5, 108, 8].

Conventional medical practice is based on treatment plans designed for a standard response that does not necessarily incorporate individual characteristics or optimization procedures. Many of these dosage strategies are inspired from the acute care model and in spite of effective drugs, are not necessarily efficient for relapsing, chronic disorders. The use of adaptive dosage strategies, where dosages are adjusted based on participant response over time, is the key motivation for use of control systems engineering principles. In particular, this chapter is intended to demonstrate how control engineering can impact the treatment of a pain condition known as fibromyalgia (FM) [65, 66, 67, 68, 22]. The method is based on secondary analysis of information collected from a previously conducted clinical trial using naltrexone for the treatment of FM. This problem is approached from a systems and controls point-of-view: first, system identification techniques are applied to develop models from daily diary reports completed by intervention participants. These diary reports include self-assessments of outcomes of interest (e.g., general pain symptoms, sleep quality) and additional external variables that affect these outcomes (e.g., stress, anxiety, and mood).

The dynamical systems model serves as the basis for applying model predictive control as a decision algorithm for dosage selection of naltrexone. The categorical/discrete-event nature of the dosage assignment creates a need for hybrid model predictive control schemes. Furthermore, instead of relying on conventional tuning using weight matrices, a multiple degree-of-freedom formulation is evaluated in this chapter that enables the user to adjust the speed of setpoint tracking, measured disturbance rejection and unmeasured disturbance rejection independently in the closed loop system. Simulation results are presented to illustrate the benefits of the proposed control scheme in addressing the hybrid dynamics, clinical constraints and plant-model mismatch typically present in such applications.

The chapter is organized in the following sections: Section 2.2 briefly describes the intervention and nature of the associated clinical data. Section 2.3 discusses the procedure of building parsimonious models using system identification. The MPC formulation used for dosage assignment is presented in Section 2.4. Section 2.5 demonstrates the application of hybrid control for delivering adaptive interventions under disturbances and model uncertainty. The chapter ends with a summary and conclusions in Section 2.6.

## 2.2 Naltrexone Intervention for Fibromyalgia

Fibromyalgia (FM) is a disorder characterized primarily by chronic widespread pain. The characteristic symptoms of FM are diffuse musculoskeletal pain and sensitivity to mechanical stimulation at soft tissue tender points [109, 110]. Other important symptoms of FM include fatigue, sleep irregularities, bowel abnormalities, anxiety, and mood dysfunction. While no specific laboratory test can confirm FM, most patients present with a history of widespread pain and fatigue conditions. Another important issue with FM is that its etiology is largely unknown and without any scientific consensus [111], although the condition is suspected to involve central sensitization of pain processing [112]. As the causes for FM are uncertain, unknown or disputed; and due to its chronic nature, it has been difficult to single out a specific type of treatment for this disease. Depending on dif-

ferent approaches for the mechanisms of the symptoms, there have been experiments with various drugs. There is a good evidence to suggest that naltrexone, an opioid antagonist, has a neuroprotective role and may be a potentially effective treatment for diseases like FM [67, 113]. The data for this chapter has been taken from clinical trials of a low dose naltrexone (LDN) intervention conducted by Dr. Jarred Younger and colleagues at the Stanford Systems Neuroscience and Pain Lab (SNAPL), Stanford University School of Medicine.

### *2.2.1 The Data*

The study was conducted in two phases: a single blind pilot study on 10 participants and a double blind full study on 30 participants (with longer protocol). A crossover design was employed where participants received both treatments and hence act as their own control (i.e. each participant takes both drug and placebo). A fixed naltrexone dose of concentration 4.5 mg was administered. In the pilot study, the participants received placebo followed by drug (P-D protocol) where as the full study participants were randomized to receive either drug first (D-P protocol) or placebo first (P-D protocol). The time line is split into baseline (during this phase participants do not receive any kind of medication), placebo/drug and finally washout phase (all kinds of medications are stopped) with the number of data points ranging from 98 to 154 sampled daily ($T = 1$). Participants entered their responses in a handheld computer to questions like 'Overall, how well did you sleep last night?' on a scale of $0 - 100$ as well as visited a clinic every two weeks to undergo a series of physical sensory tests. The daily diary data consists of one primary endpoint 'Overall, how severe have your FM symptoms been today?' [FM sym] and 13 secondary endpoints: fatigue, sadness, stress, mood, anxiety, satisfaction with life, overall sleep quality, trouble with sleep, ability to think, headaches, average daily pain, highest pain and gastric symptoms [67]. Fig. 2.1 shows data of selected variables for two representative participants. It can be observed that with introduction of drug, the participants report marked change in pain levels and sleep quality. The appropriate description of this dynamical phenomena will be the focus of modeling discussion further in the chapter. One of the important issues in data analysis

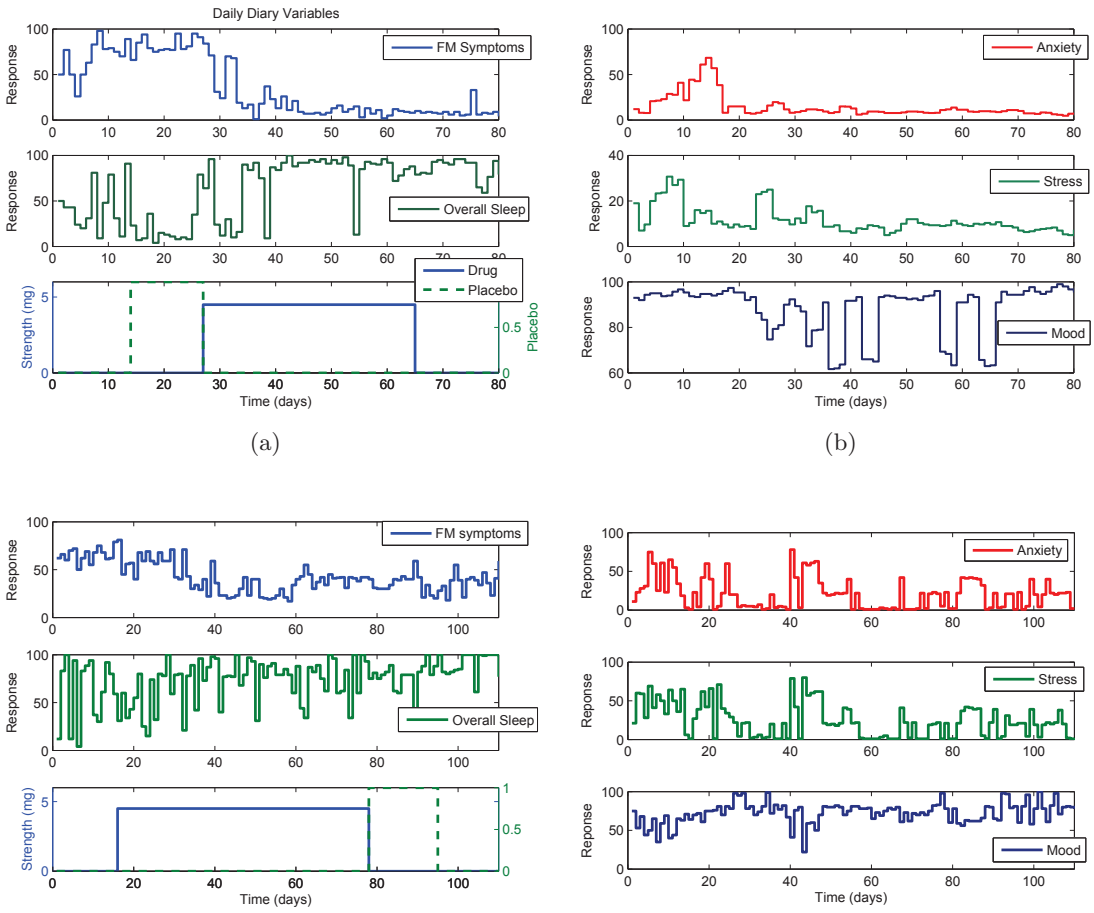


Figure 2.1: Primary self-report variables associated with naltrexone intervention of fibromyalgia as shown for two representative participants: participant from pilot study with placebo-drug (P-D) protocol ((a),(b)) and participant from full study with drug-placebo (D-P) protocol ((c),(d)). With introduction of drug, there is significant decrease in FM symptoms and increase in sleep quality over time.

from human subject research, and particularly from clinical trials, has been on the focus on a single subject (idiographic) vs multiple subject (nomothetic) analysis [114]. From a perspective of adaptive interventions, the focus in this chapter has been on performing single subject analysis where the participant is considered as a whole experiment in itself and their changes in symptoms (if any) are analyzed.

### *2.2.2 General Description of Variables*

From an input-output dynamical systems perspective, the variables from the naltrexone trial can be classified as following:

- Outputs: There is a clinical interest in understanding the magnitude and speed at which naltrexone affects various FM symptoms during the intervention. Hence typical symptoms like pain, fatigue, sleep disturbance, which correspond to dependent variables in the system, are classified as outputs.

- Inputs: Drug and placebo are classified as the primary inputs in this analysis, as they are introduced externally to the system and can be manipulated by the clinician. In addition to these primary inputs, there are other exogenous or disturbance variables affecting the outputs. Variables in the self-reports such as anxiety, stress, and mood are treated as measured disturbance inputs that when coupled with the primary inputs can help better explain the output variance, and ultimately improve the overall goodness-of-fit of the model.

As biological systems are characterized by complex interdependent components, it is difficult to define purely exogenous variables and dependent variables. This interconnection or feedback mechanism (both positive and negative) can result in cross correlation between endpoints and unmeasured noise collected from medical treatments and hence such experiments can be classified, in a classical system identification sense, as closed loop experiments. There may be a relationship between variables such that 'output' affects 'input' e.g., elevated pain condition may effect anxiety levels, although the existence of the feedback path

is not clear. In the absence of *a priori* information, this problem is tackled using direct methods by considering it as an open loop system [45]. In ensuing section, the modeling methodology does not attempt to model the internal mechanisms of FM but rather build an overall pharmacodynamic response model on how the drug and external factors affect a number of FM symptoms, so that the predictive information can be used by a controller to assign dosages based on measured participant responses.

## 2.3 Using System Identification to Model FM Intervention Dynamics

In light of the unknown dynamics of FM, an empirical modeling approach is proposed where input-output data of a single participant is used to build a model describing the effect of drug and external factors on FM symptoms.

### *2.3.1 System Identification Procedure*

The modeling process undertaken in this study can be summarized in three subparts as follows:

1. *Data preprocessing.* Initially the data is pre-processed for missing entries using a simple mean of immediate neighbors for single missing items, and interpolation for multiple consecutive missing items. To reduce the high frequency content in the time series, a three-day moving average filter $L(q)$ is applied:

$$L(q) = (1 + q^{-1} + q^{-2})/3, \tag{2.1}$$

   where $q$ is forward shift operator defined as $qy(k) = y(k+1)$.

2. *Discrete-time modeling using multi-input ARX models.* The filtered data is fitted to a parametric multi-input ARX-[$n_a$ $n_b$ $n_k$] model:

$$A(q)y(k) = \sum_{i=1}^{n_u} B_i(q)u_i(k - n_{k_i}) + e(k), \quad \forall k = 1, 2, \ldots \tag{2.2}$$

   where $n_u$ represents the number of inputs, $n_a$, $n_b$ and $n_k$ are model orders, $e(k)$ is the prediction error, and $A(q) = 1 + \sum_{j=1}^{n_a} a_j q^{-j}$ and $B_i(q) = \sum_{j=1}^{n_{b_i}} b_j q^{-j+1}$ are

polynomials in $q$. The philosophy is to start with a simpler parametrization (ARX) and add complexity as required. ARX models are computationally simple to estimate and can be consistently estimated provided the inputs are persistently exciting and the model structure is sufficiently high. In examination of multiple participants, ARX-[4 4 1] models were the highest order needed, and in many cases ARX-[2 2 1] models were suitable (as determined by the classical prediction-error validation criteria, per [45]).

The procedure for the choice of input signals is to begin with drug and placebo, which are expected to contribute significantly to FM symptoms for all participants. Additional input variables are then introduced sequentially to improve the goodness of fit. From a statistical perspective, it can be shown that adding extra inputs results in improved covariance of the parameter estimate (stronger for ARX/ARMAX structure) under the assumption that they are independent [115]. Consequently, while increasing the number of inputs improves the overall fit, an exceptionally high fit may not necessarily imply a highly predictive model. As the protocol applied in this study did not allow for a crossvalidation data set, proper judgement on the choice of input variables that adequately describes the data across all participants must be made.

3. *Simplification to a continuous time model.* The step responses from the ARX model are individually fit to a parsimonious continuous second-order model structure of the form:

$$G(s) = \frac{K_p(\tau_a s + 1)}{\tau^2 s^2 + 2\zeta\tau s + 1}. \tag{2.3}$$

From (2.3), useful dynamical system information such as gain, time constant, overshoot, rise and settling times for each input can be obtained which can be used to classify participants as responders or non-responders to the drug. The estimation procedure applied in this step follows according to the `Process Models` routine in Matlab's System Identification Toolbox.

The use of prediction-error models, and ARX models in particular, is justified because one can rely on well-established bias relations to obtain insight. For purposes of illustration, consider a system described by one manipulated input (e.g., drug), one measured disturbance input (e.g., anxiety) and noise, with plant and estimated models as follows:

$$y(k) = p(q)u(k) + p_d(q)d(k) + H(q)\nu(k) \tag{2.4}$$

$$= \tilde{p}(q)u(k) + \tilde{p}_d(q)d(k) + \tilde{p}_e(q)e(k). \tag{2.5}$$

The one-step-ahead prediction error can be written as:

$$e(k) = \tilde{p}_e(q)^{-1}(y(k) - (\tilde{p}(q)u(k) + \tilde{p}_d(q)d(k))). \tag{2.6}$$

Parseval's theorem can be used to relate the filtered prediction-error ($e_F(k) = L(q)e(k)$) with its power spectrum ($\Phi_{e_F}(\omega)$), which is defined as:

$$\Phi_{e_F}(\omega) = \frac{|L(q)|^2}{|\tilde{p}_e(q)|^2}\big(|p - \tilde{p}|^2\Phi_u(\omega) + |p_d - \tilde{p}_d|^2\Phi_d(\omega) + 2\mathrm{Re}((p - \tilde{p})(p_d - \tilde{p}_d)^*)\Phi_{ud}(\omega) + |H|^2\sigma_\nu^2\big), \tag{2.7}$$

where $\nu(k)$ is assumed to be uncorrelated with $u(k)$ and $d(k)$, $L(q)$ is the prefilter, Re denotes the real part of a complex number and $*$ is used to represent its complex conjugate. From (2.7), it is possible to obtain insights into how input power, model structure, cross-correlation between signals, and other factors can influence the goodness-of-fit in the identification process.

### *2.3.2 Case Studies*

#### 2.3.2.1 Participant from Pilot Study

In this subsection, the focus is on the application of the system identification modeling procedure to a participant from the pilot study with data as seen in Fig. 2.1. Equation (2.7) is used to systematically look at ways to minimize the role of model structures, inputs signal spectral information and input cross correlations.

- *Model structure.* An incorrect plant model structure corresponds to the $|p - \tilde{p}|$ term being non-zero and results in an asymptotic bias. Similarly incorrect structure $\tilde{p}_e$ for the noise model will result in a bias. In this work, ARX models of reasonable dimension were found to be sufficient and no improvement was observed with more complex parametrization.

- *Input signals.* Input signals must show sufficient power in the frequency range of interest. As in this secondary analysis, the excitation signals were not designed and hence, the inference of estimated models is limited to the bandwidth provided by the available signals. It was observed that input power spectrum bandwidth was approximately 0.6 radians/day (Fig. 2.2).

- *Input cross correlation.* Since various variables are measured in the experiment, the procedure is to choose inputs which have minimum cross spectra ($\Phi_{ud}(\omega)$). The sample cross correlation function [116] is used to better understand the relationship between different variables and with drug and placebo. For this participant, the headache and gastric variables (See Fig. 2.3b) have high degree of cross-correlation, and gastric is also correlated with the FM symptoms output (See Fig. 2.3c). Adding them as inputs did not yield good estimates. In comparison, anxiety and mood variable (See Fig. 2.3d) are essentially uncorrelated and offer good estimates when included as inputs. Details of this participant data with additional cases can be found in [22].

The multi-input ARX-[221] models (with respective input(s) and FM symptoms treated as the primary output) are as follows:

1. Model 1 (Drug)

2. Model 2 (Drug, Placebo)

3. Model 3 (Drug, Placebo, Anxiety)

4. Model 4 (Drug, Placebo, Anxiety, Stress)

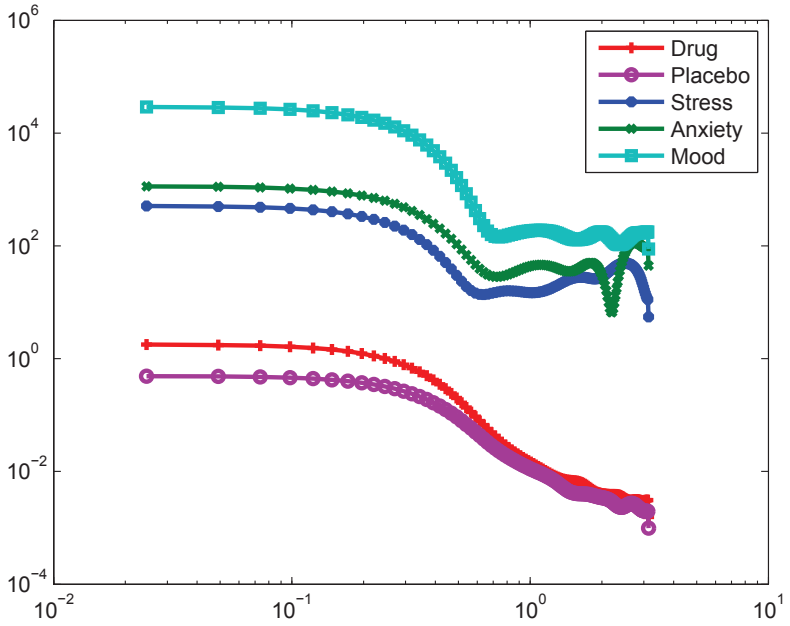


Figure 2.2: Signal power spectrum comparison, calculated using the Welch's method, for variables used as inputs for participant from the pilot study.

5. Model 5 (Drug, Placebo, Anxiety, Stress, Mood)

6. Model 6 (Drug, Placebo, Anxiety, Stress, Mood, Gastric)

7. Model 7 (Drug, Placebo, Anxiety, Stress, Mood, Gastric, Headache)

8. Model 8 (Drug, Placebo, Anxiety, Stress, Mood, Gastric, Headache, Life)

9. Model 9 (Drug, Placebo, Anxiety, Stress, Mood, Gastric, Headache, Life, Sadness)

Fig. 2.4 shows the corresponding fits for models 1 through 9, which explain 46.57% to 79.69% of the output variance. Beyond the five inputs noted in model 5, adding more variables did not improve the fit significantly and ultimately (for model 9) results in overparameterization. Hence, the inputs from model 5 are used as the base for multi-input ARX models for this participant. Fig. 2.5 shows the step responses resulting for the ARX models for the specific

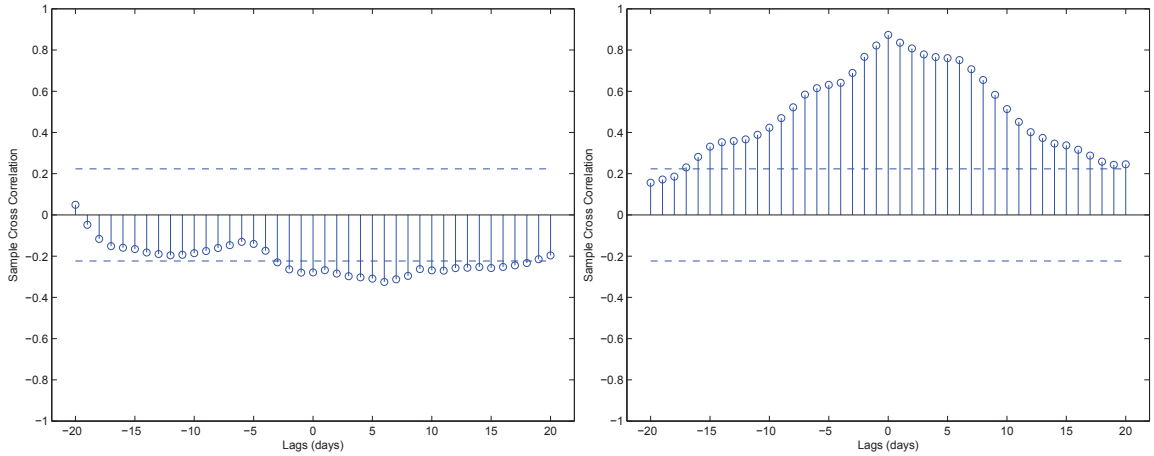


(a) Drug and Stress.




(b) Gastric and Headache.

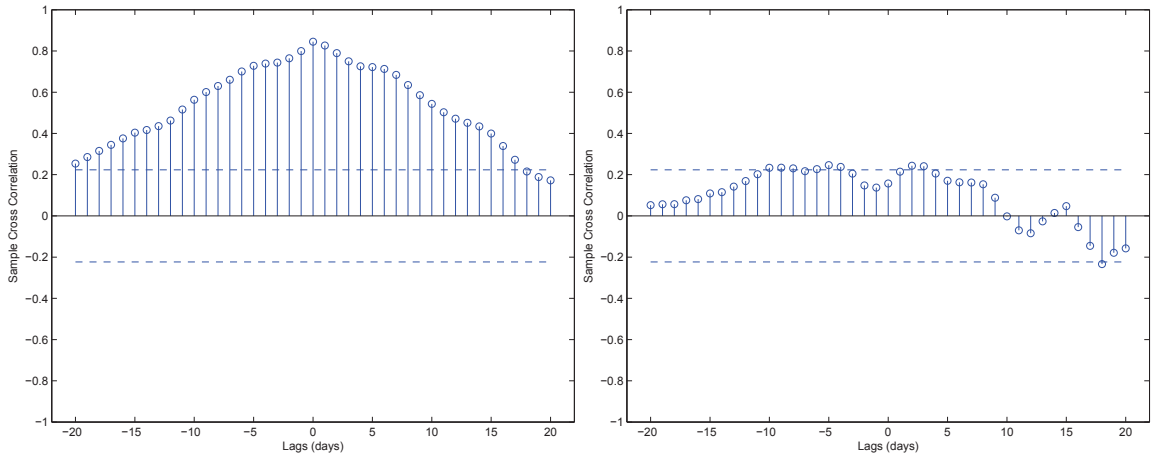


(c) FM sym and Gastric.




(d) Anxiety and Mood.

Figure 2.3: Sample cross correlation function plots between drug and other variables with two standard error bounds over ± 20 lags for participant from the pilot study.

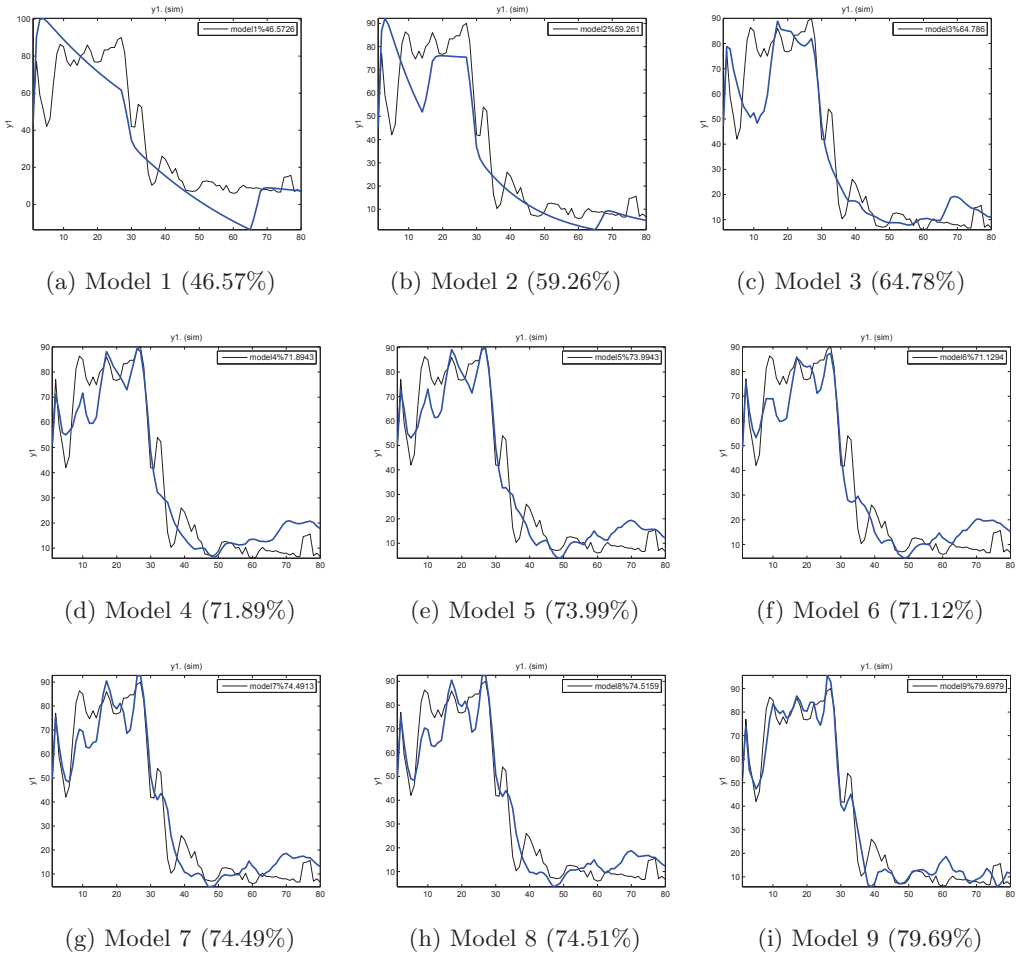


(a) Model 1 (46.57%) (b) Model 2 (59.26%) (c) Model 3 (64.78%)

(d) Model 4 (71.89%) (e) Model 5 (73.99%) (f) Model 6 (71.12%)

(g) Model 7 (74.49%) (h) Model 8 (74.51%) (i) Model 9 (79.69%)

Figure 2.4: Estimated models 1 through 9, output vs. actual (FM sym) output using ARX [2 2 1] structure for participant from the pilot study. The percent fits for each model are shown in parenthesis. It can be observed that any significant improvement in model fit is not obtained beyond model 5.

case of the naltrexone drug input. The final model has a gain of $-2.47$, indicating a nearly 2.5 point drop in the pain report per mg dose of naltrexone. The negative gain for drug classifies this participant as a responder to the treatment. A rise time ($T_r$) of slightly over 5 days, and a 98% settling time ($T_s$) of nearly 11.5 days characterizes the naltrexone response for this participant. Table 2.1 shows how including additional inputs improved the goodness-of-fit for this participant.

Table 2.2 summarizes the transfer functions for all inputs (manipulated and disturbance) for the Model 5 structure. For all these transfer functions the settling times and rise times (with the exception of Mood-FM) are essentially similar. The positive gain for the placebo input indicates that in the case of this participant, the administration of placebo has a detrimental effect. The large magnitude of the placebo gain is in part a consequence of how the input signal is coded (1 when present and 0 when not). Examining the gains for the measured disturbance models (anxiety, stress, and mood), these correspond to 0.86, 2.29, and $-0.091$, respectively. The positive values for the anxiety and stress gains and negative for mood agree with the clinical observations that increase in anxiety and stress and decrease in mood should worsen FM symptoms. The low magnitude of the mood gain, coupled with the relatively small contribution of this input to the percent variance described by the model (approximately 2%) indicates the low importance of this variable as a contributor to FM symptoms. Table 2.2 also includes the model resulting from the effect of drug to overall sleep. The positive gain in this transfer function demonstrates improved sleep quality with drug administration; however, the fact that $\tau_a < 0$ for this model denotes the presence of inverse response.

#### 2.3.2.2 Full Study Participants

Table 2.3 shows the summary of participant response from the fully study for placebo-drug protocol. In general for participants from the full study, additional inputs like sadness and headache as well as ARX models with higher orders (e.g., [4 4 1]) were required for improved fits. For example in case of most participants, the inputs corresponding to model 9 gave

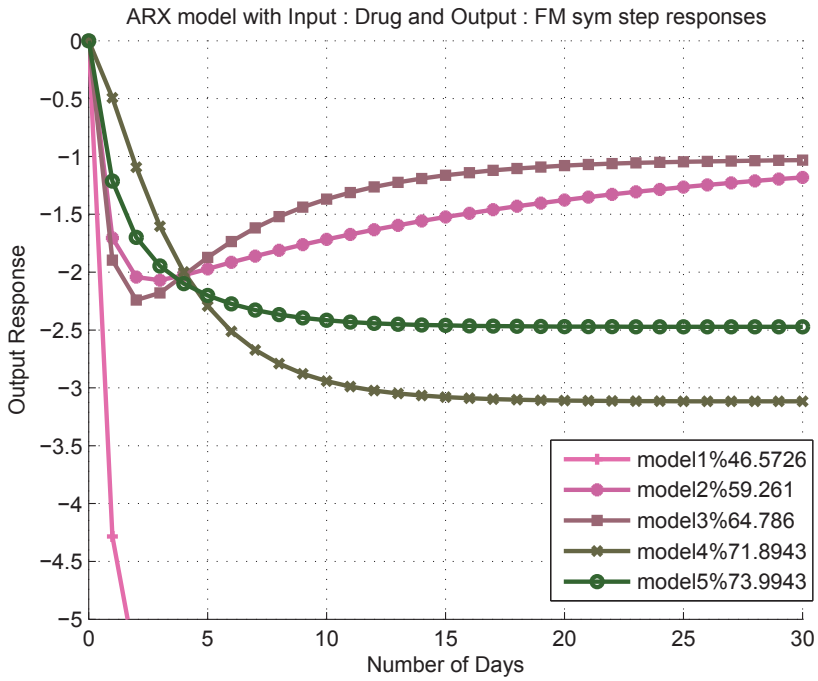


Figure 2.5: ARX model step responses for the drug-FM symptoms transfer function. As the model fit improves from model 1 to 5, the steady-state gain settles at approximately -2.5.

Table 2.1: Model estimate summary for the drug-FM model for pilot study participant. Percent (%) fit corresponds to the multi-input ARX-[2 2 1] model structure.

| Model | %fit | $K_p$, $\tau, \zeta, \tau_a$ | $T_r$(days) | $T_s$(days) |
|---|---|---|---|---|
| 1 | 46.5 | -12.03, 5.67, 4.14, 21.3 | 75.5 | 139.69 |
| 2 | 59.2 | -0.91, 3.5, 2.67, 44.4 | 0.43 | 75.06 |
| 3 | 64.7 | -1.02, 2.09, 1.5, 15.3 | 0.43 | 25.6 |
| 4 | 71.8 | -3.11, 1.62, 1.24, 0.22 | 7.53 | 14.38 |
| 5 | 73.9 | -2.47, 1.57, 1.26, 1.96 | 5.12 | 11.49 |

a better fit. For a total 15 participants in this protocol, 9 were classified as responders and 6 as non-responders based on the estimated model gain for drug as input and FM sym as output ($K_p$(DFM)). Settling time (in days) for each case are also noted. The gains for each participant are shown with one standard deviation on estimated gains (from

Table 2.2: Model parameter tabulation for various inputs-FM continuous models as well as the drug-overall sleep (Drug-Overall Sleep) model for pilot study participant. The participant shows reduction in pain and improvement in sleep with drug intake.

| Model | $K_p$, $\tau, \zeta, \tau_a$ | $T_r$(days) | $T_s$(days) |
|---|---|---|---|
| Drug-FM | -2.47, 1.57, 1.26, 1.96 | 5.12 | 11.49 |
| Placebo-FM | 45.81, 1.57, 1.26, 1.15 | 6.59 | 13.06 |
| Anxiety-FM | 0.86, 1.57, 1.26, 0.24 | 7.45 | 14.24 |
| Stress-FM | 2.29,1.57, 1.26, 0.49 | 7.31 | 13.94 |
| Mood-FM | -0.091, 1.57, 1.26, 4.67 | 0.8 | 11.93 |
| Drug-Overall Sleep | 4.98, 2.13, 1.04, -3.35 | 7.06 | 15.83 |

system identification) where as, in rows corresponding to average values, the deviation of mean of each participant's response is noted. It can be noted that the average model gain ($K_p$(DFM)) for responders was $-3.56$ where as for non-responders was 2.06. Overall, for all participants of this protocol the gain was $-1.31$. Similarly gain for drug as input and overall sleep as output ($K_p$(DS)) together with the settling time was also tabulated and it was noted that the response of sleep to drug was not strong in many cases with average gain for all participants being $-0.23$. In general, the drug response of full study participants was weaker compared to cases in the pilot study as can be noted by the gain magnitudes and large error bounds which make the classification of participants difficult.

### *2.3.3 Model Validation*

The following standard methods are used to validate the estimated models [45]:

- *Residual analysis.* A residual analysis is conducted on all estimated models using auto correlation of the residual and cross correlation between the inputs and residual. For most of the participants in this study, ARX [2 2 1] or [4 4 1] models met classical prediction error criteria.

- *Step responses from estimated ARX models.* After a model has passed residual analysis, the model step responses are analyzed. From second model onwards in Fig. 2.5,

Table 2.3: Tabulation of system responses to drug for Placebo-Drug (PD) protocol for selected participants from the full study. Corresponding model fits are also noted. Model 9 was used unless noted otherwise as $*$ implying input combination as {Drug, Placebo, Anxiety, Stress, Mood, Life, Sadness and Gastric} and # where inputs corresponding to model 7 are used. In case of bad data, no model was formed.

| | | | Responders | | | |
|---|---|---|---|---|---|---|
| # | % fit(DFM) | $K_p$(DFM) | $T_s$(DFM) | % fit(DS) | $K_p$(DS) | $T_s$(DS) |
| 1 | 64.92* | -4.70*±7.67 | 23.23* | 72.50 | -3.28±6.98 | 27.24 |
| 2 | 48.71 | -0.66±1.15 | 15.28 | 35.19 | 0.668±1.52 | 16.12 |
| 3 | 29.82 | -0.6±1.71 | 15.89 | 23.17 | -2.83±4 | 45.55 |
| 4 | 29.23# | -11.66#± 12.36 | 67.01# | 28.89 | 1.59±2.7 | 13.02 |
| 5 | 18.08 | -0.83±2.3 | 10.51 | 29.87 | -4.89±3.7 | 20.39 |
| 6 | 54.70 | -2.79±1.88 | 23.11 | 17.93 | 0.4±2.77 | 11.57 |
| 7 | 40.00 | -2.27±3.99 | 27.1 | 43.38 | -0.92±1.16 | 17.19 |
| 8 | 54.13 | -8.44±5.12 | 12.63 | 64.55 | -1.88±1.46 | 19.11 |
| 9 | 59.00 | -0.112±0.83 | 16.04 | 44.58 | 2.27±0.77 | 13.05 |
| | | | Average Values (std. deviation for nominal gain only) | | | |
| — | 44.28±15.8 | -3.56±4 | 23.42±17.2 | 40±18.4 | -0.98±2.4 | 20.36±10.5 |
| | | | Non Responders | | | |
| 10 | 44.68 | 3.96±3 | 33.05 | — | — | — |
| 11 | 2.19* | 4.09*±3.96 | 39.21* | 20.57 | -2.53±2.47 | 15.54 |
| 12 | 27.99 | 0.82±1.73 | 30.37 | 38.45 | 1±1.16 | 17.8 |
| 13 | 31.17 | 1.94±2.07 | 34.97 | 22.47 | 6.23±4.94 | 42.46 |
| 14 | 40.31 | 0.37±1.24 | 16.24 | 26.7 | 0.85±1.33 | 22.67 |
| 15 | 34.57 | 1.17±2.85 | 15.4 | 49.14 | 0±1.16 | 18.34 |
| | | | Average Values (std. deviation for nominal gain only) | | | |
| — | 30.15±14.9 | 2.06±1.6 | 28.2±10 | 31.46±12 | 1.11±3.17 | 23.62±10.9 |
| | | | Total Average Values (std. deviation for nominal gain only) | | | |
| — | 38.63±16.5 | -1.31±4.27 | 25.33±14.5 | 36.95±16.4 | -0.23±2.77 | 21.43±10.4 |

the responses tend to settle to a steady state with some dynamics with improved goodness-of-fit.

While it would have been desirable to have applied cross-validation to this analysis, when the data was partitioned into estimation and validation sets, it was found to lack the excitation required to support multi-input crossvalidation. This is a consequence of the limited number of data points in this study and the experimental procedure that was followed for the naltrexone and placebo dosages. Instead, how the percent fits improve with additional inputs added to the model are noted, simultaneously examining the step response results

to avoid the consequences of overparametrization (e.g., large changes in gain and settling time with parameters that do not agree with physical insight).

In summary, most of the pilot study participants were adequately modeled with model 5 using the ARX [2 2 1] structure, and in the full study with model 9 using the ARX [4 4 1] structure. It was noted that the response to drug was stronger in the pilot study as compared to the full study; likewise, a large number of full study participants showed placebo response. For those participants whom the modeling results would classify them as responders to treatment, the estimated models are used as the basis for adapting the intervention using control engineering. This is described in the next section.

## 2.4 Model Predictive Control of Naltrexone Intervention for Fibromyalgia

In this dissertation, model predictive control (MPC) is used as the algorithmic framework for making systematic dosage assignments. This control technology effectively combines the feedback-feedforward control action by on-line optimization of a cost function using a receding horizon as shown in Fig. 2.6 [117]. The MPC approach allows for flexibility to integrate critical clinical objectives and constraints, and hence is particularly suited for designing treatment regimens. It has seen medical applications from diabetes mellitus control to HIV/AIDS management [118, 119]. To achieve the required performance, a three degree-of-freedom (3 DoF) approach is used to tune the controller [120, 121]. This tuning methodology enables performance requirements associated with setpoint tracking, anticipated measured disturbance rejection and unmeasured disturbance rejection to be adjusted independently by varying parameters $\alpha_r$, $\alpha_d$ and $f_a$ respectively (as discussed later). These parameters can be adjusted between values 0 and 1; they in turn alter the response of a filter which supplies a filtered signal to the controller (for setpoint tracking ($\alpha_r$) and measured disturbance rejection ($\alpha_d$)) or adjust the observer gain ($K_f$) for unmeasured disturbance rejection ($f_a$). The hybrid extension of this 3 DoF approach [97] is considered here.

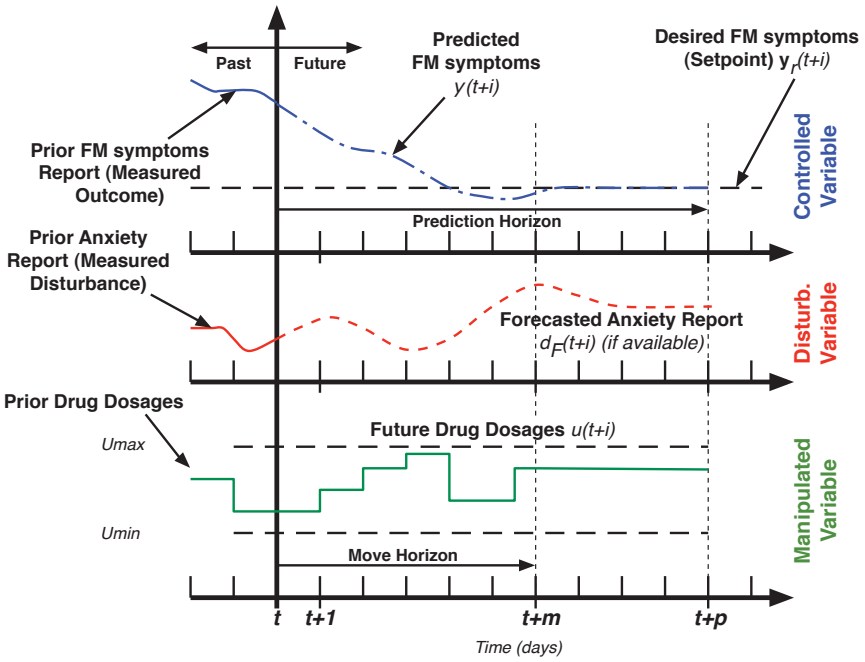


Figure 2.6: Receding horizon philosophy used in model predictive control. Only the first control input value calculated using the optimization procedure is implemented and this process is repeated at each sampling instant.

### *2.4.1 Clinical Goals*

Adaptive interventions employ decision rules and repeated assessments of participant response to improve outcomes. In this control engineering approach to adaptive interventions, the controller assigns dosages to each participant as dictated by model dynamics, problem constraints, and disturbances (both measured and unmeasured). The control system aims at functionally performing the following three tasks:

- *Setpoint tracking.* Drug dosages are assigned to take an outcome of interest (such as FM symptoms or overall sleep quality) to a desired goal. For example, clinician may decide on a goal or setpoint of 45% reduction in general pain symptoms within two weeks of drug administration.

- *Measured disturbance rejection.* The controller manipulates drug dosages to mitigate the effect from *reported* external influences using estimated disturbance models. For instance, if some external event (e.g., anxiety) which can lead to elevated FM symptoms is known *a priori*, then dosages can be adjusted in anticipation to compensate for that disturbance.

- *Unmeasured disturbance rejection.* The controller manipulates drug dosages to mitigate the effect of unknown and un-modeled external influences. For example, consider a sudden event which leads to worsening pain (FM symptoms). In such cases, the controller adjusts dosages to mitigate the unmeasured disturbance.

In addition to accomplishing the three functional modes of the control system, a number of practical clinical requirements have to be integrated into the controller design. These are:

- *Limit on possible dosages.* Drug efficacy is generally defined on some dosage levels, as well as dosage magnitudes has to be limited to certain bounds to ensure safe usage. In this work, the drug naltrexone is varied for simulation purposes as

$$0 \leq u(k) \leq 13.5 \text{ mg} \quad \forall k \in \{1, \ldots, N\}, \tag{2.8}$$

  where $N$ is the length of simulation.

- *Gradual change in dosages.* Dosage changes should not be very abrupt due to concerns with drug withdrawal and toxicity. This translates into limit on the move size of the signal as:

$$\Delta u_{\min} \leq |u(k+1) - u(k)| \leq \Delta u_{\max}, \tag{2.9}$$

- *Discrete dosages.* This is the most important clinical consideration which necessitates the use of hybrid models. In this work, the hybrid control results are shown using eight drug dosage levels defined in the range as

$$u(k) \in \mathbb{I} = \{0, 1.92, 3.85, 5.76, 7.68, 9.6, 11.58, 13.5\} \text{ mg}. \tag{2.10}$$

Subsequently in this chapter, the nomenclature *hybrid* MPC is used to define a controller which assigns dosages categorically where as a *continuous* MPC will assign dosages anywhere in the given range.

### *2.4.2 MPC Problem Formulation*

The details of the proposed MPC formulation are now presented. As was pointed out earlier, an important consideration in adaptive interventions is that intervention dosages can assume only discrete levels, and therefore it is necessary to consider hybrid algorithms [97]. A mixed logical dynamical (MLD) framework is used to represent linear hybrid systems which are systems with real and integer states, inputs and constraints [92], as shown:

$$x(k+1) = Ax(k) + B_1u(k) + B_2\delta(k) + B_3z(k) + B_dd(k) \tag{2.11}$$

$$y(k) = Cx(k) + d'(k) + \nu(k) \tag{2.12}$$

$$E_2\delta(k) + E_3z(k) \leq E_5 + E_4y(k) + E_1u(k) - E_dd(k), \tag{2.13}$$

where, in general, $x \in \mathbb{R}^{n_x}$ and $u \in \mathbb{R}^{n_u}$ represent states and inputs of the system. $y \in \mathbb{R}^{n_y}$ is the output and $d \in \mathbb{R}^{n_d}$, $d' \in \mathbb{R}^{n_d^{'}}$ and $\nu \in \mathbb{R}^{n_\nu}$ represent measured disturbances, unmeasured disturbances and measurement noise signals respectively. $\delta \in \{0,1\}^{n_d}$ and $z \in \mathbb{R}^{n_z}$ are discrete and continuous auxiliary variables respectively, which along with the input $u$, output $y$ and disturbance $d$ form the linear inequality constraint shown in Equation 2.13 in order to enforce logical/discrete decisions. The effect of all unmeasured disturbances is lumped as $d'$ in the measurement equation. Further, the MLD system is augmented with the disturbance model:

$$\begin{aligned} x_w(k+1) &= A_wx_w(k) + B_ww(k) \\ d'(k+1) &= C_wx_w(k+1), \end{aligned} \tag{2.14}$$

where $w$ is an *integrated* white noise and $x_w$ is the state of the noise model. This model is motivated from process control where disturbances may be non-stationary and hence this offers a general representation for a large class of scenarios. However in this chapter,

$B_w, C_w = I$ and $A_w = diag\{\bar{\alpha}_1, \ldots, \bar{\alpha}_{ny}\} = 0$, given asymptotically step inputs, $\bar{\alpha_j} = 0$ [121]. The augmented model is written in *difference form* as follows:

$$X(k+1) = \mathcal{A}X(k) + \mathcal{B}_1\Delta u(k) + \mathcal{B}_2\Delta\delta(k) + \mathcal{B}_3\Delta z(k) + \mathcal{B}_d\Delta d(k) + \mathcal{B}_w\Delta w(k) \tag{2.15}$$

$$y(k) = \mathcal{C}X(k) + \nu(k) \tag{2.16}$$

where,

$$X(k) = [\Delta x^T(k) \quad \Delta x_w^T(k) \quad y^T(k)]^T$$

$$\mathcal{A} = \begin{bmatrix} A & 0 & 0 \\ 0 & A_w & 0 \\ CA & A_w & I \end{bmatrix}; \quad \mathcal{B}_i = \begin{bmatrix} B_i \\ 0 \\ CB_i \end{bmatrix}, \; i = 1, 2, 3, d; \quad \mathcal{B}_w = \begin{bmatrix} 0 \\ I \\ I \end{bmatrix};$$

$$\mathcal{C} = [0 \quad 0 \quad I].$$

Equations 2.15-2.16 are used to generate system prediction which can then be used by an optimizer. A standard quadratic cost function ($|| \star ||^2_{Q_\star} = (\star)^T Q_\star(\star)$) is used to calculate the decision vector as:

$$\min_{\{[u(k+i)]_{i=0}^{m-1},\, [\delta(k+i)]_{i=0}^{p-1},\, [z(k+i)]_{i=0}^{p-1}\}} \sum_{i=1}^{p} \|(y(k+i) - y_r)\|^2_{Q_y} + \sum_{i=0}^{m-1} \|(\Delta u(k+i))\|^2_{Q_{\Delta u}}$$
$$+ \sum_{i=0}^{m-1} \|(u(k+i) - u_r)\|^2_{Q_u} + \sum_{i=0}^{p-1} \|(\delta(k+i) - \delta_r)\|^2_{Q_d} + \sum_{i=0}^{p-1} \|(z(k+i) - z_r)\|^2_{Q_z} \tag{2.17}$$

$$\text{s.t.} \quad y_{\min} \leq y(k+i) \leq y_{\max}, \; i \in \mathcal{T}_p \tag{2.18}$$

$$u_{\min} \leq u(k+i) \leq u_{\max}, \; i \in \mathcal{T}_m \tag{2.19}$$

$$\Delta u_{\min} \leq \Delta u(k+i) \leq \Delta u_{\max}, \; i \in \mathcal{T}_p, \tag{2.20}$$

and also subjected to state and output equations with mixed integer constraints as shown in (2.11)-(2.13), where $p$ is the prediction horizon, $m$ is the control horizon, $\mathcal{T}_p = \{1, \ldots, p\}$ and $\mathcal{T}_m = \{0, \ldots, m-1\}$. The vector 2-norm are weighted by matrix $Q_*$ as in

$$Q_y, \; Q_{\Delta u}, \; Q_u, \; Q_d, \text{ and } Q_z \tag{2.21}$$

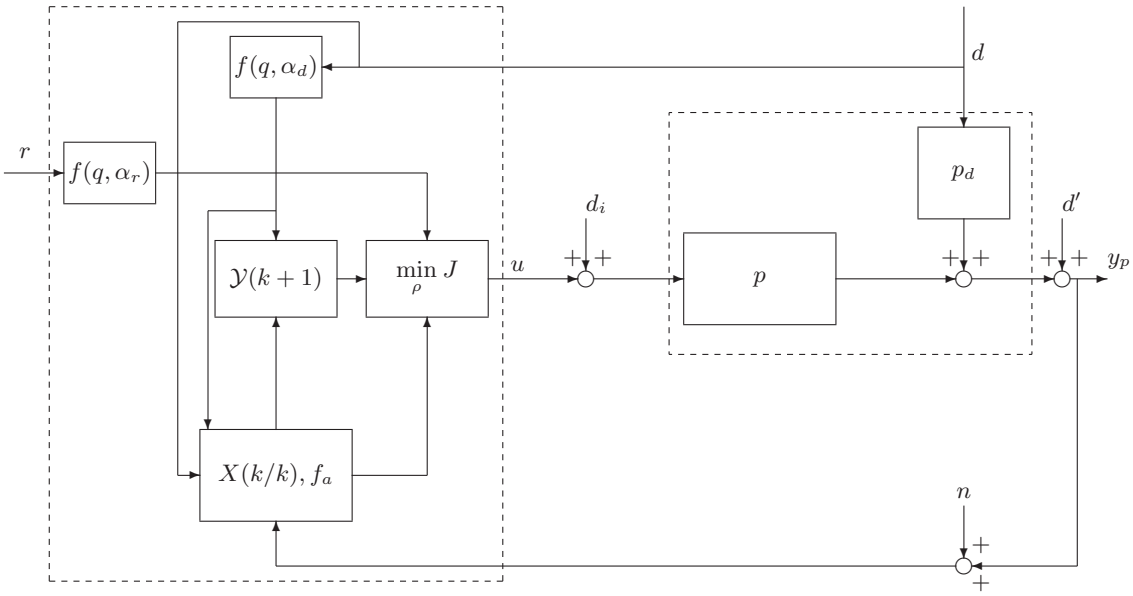


Figure 2.7: A block diagram depicting the three degree-of-freedom (3 DoF) controller formulation of model predictive control. $p$ and $p_d$ are the system plants models, $X(k/k), f_a$ is the observer block, $\mathcal{Y}(k+1)$ is the predictor block, min $J$ is the optimizer block, $\rho$ is the vector of the decision variables and $f(q, \alpha_{\{r,d\}})$ are the filters for reference and measured disturbance signals respectively.

are the penalty weights on the error, move size, control signal, auxiliary binary variables and auxiliary continuous variables, respectively. The problem is formulated as a tracking control system using references $y_r, u_r, \delta_r$ and $z_r$ for output, input, discrete and continuous auxiliary variables, respectively. Full details of the controller formulation, including applications to preventive behavioral interventions and supply chain management, can be found in [97].

### *2.4.3 Controller Tuning*

Fig. 2.7 shows the block diagram depicting 3 DoF controller formulation of model predictive control. This tuning approach for MPC can be discussed broadly in two sub topics as:

- *Setpoint tracking and measured disturbance rejection.* In 3 DoF approach, the feedback action (setpoint tracking) and feedforward action (measured disturbance rejection) can be directly manipulated using a filter, and hence the closed loop response can be

varied to achieve a desired performance. The choice of the filter depends on whether the set point or disturbances changes are asymptotically step or ramp, and on type of the system (integrating, for example). In this chapter, a Type I filter is used for both cases, described as:

$$f(q, {\alpha_{r,d}}^j) = \frac{(1 - {\alpha_{r,d}}^j)q}{q - {\alpha_{r,d}}^j},\ j \in \{1, \ldots, n_y\}, \tag{2.22}$$

where $\alpha_{r,d} \in [0, 1)$ and $n_y$ is the number of outputs.

As noted earlier, the tuning parameter to alter the setpoint response is denoted by $\alpha_r$ and the tuning parameter for measured disturbance filtering by $\alpha_d$. Hence the controller can be tuned for slower rejection of measured disturbances, for example, by more extensive filtering of the disturbance signals. Additional information on filters can be found in [122].

- *State estimation (unmeasured disturbance rejection).* Considering the uncertain nature of self reports and estimated models, the feedback loop is augmented with a state observer to influence the error in system prediction. In this system, unmeasured disturbances can be applied externally and/or can originate from the plant-model mismatch. A parametrized observer [120, 121, 97] is used, where the observer gain can be written as:

$$K_f = \begin{bmatrix} 0 & F_b^T & F_a^T \end{bmatrix}^T \tag{2.23}$$

$$F_a = \text{diag}\{(f_a)_1, \cdots, (f_a)_{n_y}\} \quad F_b = \text{diag}\{(f_b)_1, \cdots, (f_b)_{n_y}\} \tag{2.24}$$

$$(f_b)_j = \frac{{(f_a)_j}^2}{1 + \bar{\alpha_j} - \bar{\alpha_j}(f_a)_j},\ j \in \{1, \ldots, n_y\}, \tag{2.25}$$

where $(f_a)_j$ is a tuning parameter that lies between 0 and 1. As $(f_a)_j$ approaches zero, the state estimator increasingly ignores the prediction error. Where as $(f_a)_j$ approaches 1, the state estimator tries to compensate for all prediction error and hence may cause the controller to be extremely aggressive.

## 2.5 Closed-Loop Simulation Results

This section demonstrates a drug dosage assignment problem on the representative participant discussed in Section 2.3.2.1. The system under consideration is a five input-one output dynamical model with one manipulated variable (drug), four disturbance variables (placebo, anxiety, stress and mood) and one output (FM symptoms). The FM symptoms variable serves as the primary outcome in the analysis, while anxiety (assumed to be reported daily by the participant) serves as the measured disturbance signal. All other disturbances are set equal to zero. The drug dosages range from 0 to 13.5 mg with eight possible values. The eight discrete inputs form an arithmetic progression and can be represented logically in the MLD framework as:

$$\delta_i(k) = 1 \Leftrightarrow z_i(k) = 13.5 - (i-1) \times 1.9286, \quad i \in \{1, 2, ..., 8\} \tag{2.26}$$

$$u(k) = \sum_{i=1}^{8} z_i(k), \qquad \sum_{i=1}^{8} \delta_i(k) = 1. \tag{2.27}$$

These conditions and implications ($\Leftrightarrow$) are then converted into inequality constraints as represented in (2.13). Further, the simulation parameter values are as follows. The prediction horizon ($p$) is set to 25 days and the control horizon ($m$) to 15 days. As the 3 DoF approach is used to tune the controller, the weights will not be manipulated and hence are fixed as follows: $Q_y = 1,\ Q_{\Delta u} = \ Q_u = \ Q_d = \ Q_z = 0$. The three "knobs" in the controller are varied as: $\alpha_r \in [0, 1),\ \alpha_d \in [0, 1),$ and $f_a \in (0, 1]$. Finally for the single-output system ($n_y = 1$), it is assumed that there is no measurement noise in the system $n = 0$ and also no input disturbance or $d_i = 0$. These simulation parameters are now used to generate the closed-loop control results which are shown in two sections:

1. Evaluation of nominal performance for tracking and disturbance rejection (Section 2.5.1), and

2. Evaluation of robust performance under plant-model mismatch (Section 2.5.2).

In this hypothetical simulation of a control-oriented naltrexone intervention, the goal is to demonstrate how the 3 DoF formulation gives the flexibility to achieve a broad range of time-domain responses, and hence the controller can be tuned as per clinical requirements. An initial general proof-of-concept is followed by an analysis involving more rigorous performance metrics.

### *2.5.1 Nominal Performance*

This section evaluates the performance of the controller when a true model of the system is known. Three independent events take place in the simulation: the setpoint tracking starts at $k = 0$, a measured disturbance acts at $20 \leq k \leq 40$ with magnitude 16.52 and an unmeasured disturbance at $k = 55$ of magnitude 9.63. The output variable starts with a baseline value of 50 and a change of $-9.5$ is applied at $k = 0$ as shown by the reference in Fig. 2.8. The result is shown for tuning parameters set as: $(\alpha_r, \alpha_d, f_a) = (0.5, 0.5, 0.5)$. The length of the simulation is $N = 75$ days. MPC where $u(k)$ can take any continuous value on its range and with no filtering represents the best possible performance by the controller. Clinically, this can be the first benchmark which can be used to get a sense of treatment regimen from the control system. Next, depending on the clinical constraint of drug dosage levels, a new treatment regimen has to be generated which can be contrasted with the continuous case. However, the drug dosage changes may be perceived as too aggressive by the clinician and hence, in that scenario based upon the exact requirements (e.g., pain reduction by 30%), the hybrid controller can be de-tuned using 3 DoF tuning variables. For setpoint tracking, $\alpha_r$ can be adjusted to suit the expected response. Similarly, the response to disturbances can be varied by $\alpha_d$ and $f_a$ to suit the conditions at hand. In general, by increasing the filtering action, dosage assignments are more smoother and clinically acceptable. For measured disturbances, continuous MPC offers perfect compensation through the use of feedforward action where as in the case of hybrid MPC, the action is less effective due to constraints. At $k = 55$ an abrupt change

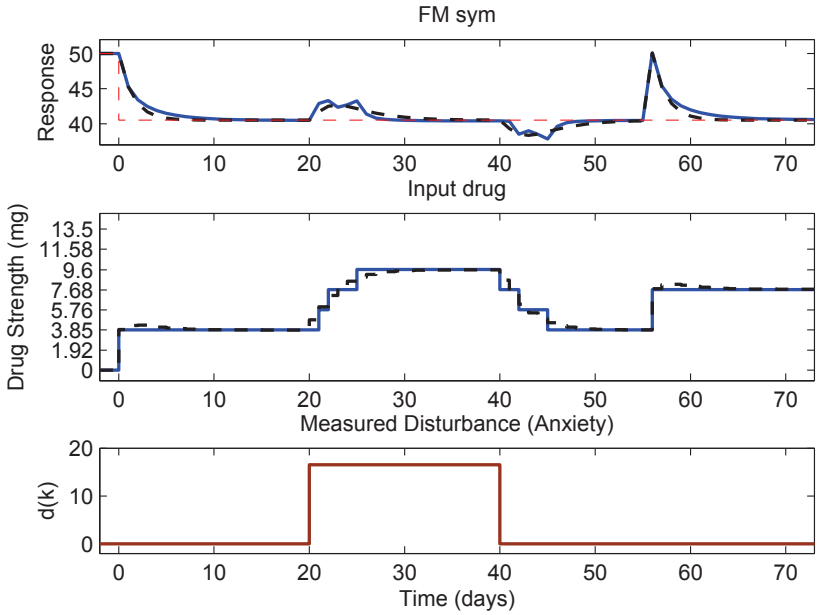


Figure 2.8: Performance of hybrid MPC (eight levels) with tuning parameter $(\alpha_r, \alpha_d, f_a) = (0.5, 0.5, 0.5)$. The performance of hybrid MPC is also compared to the continuous MPC.

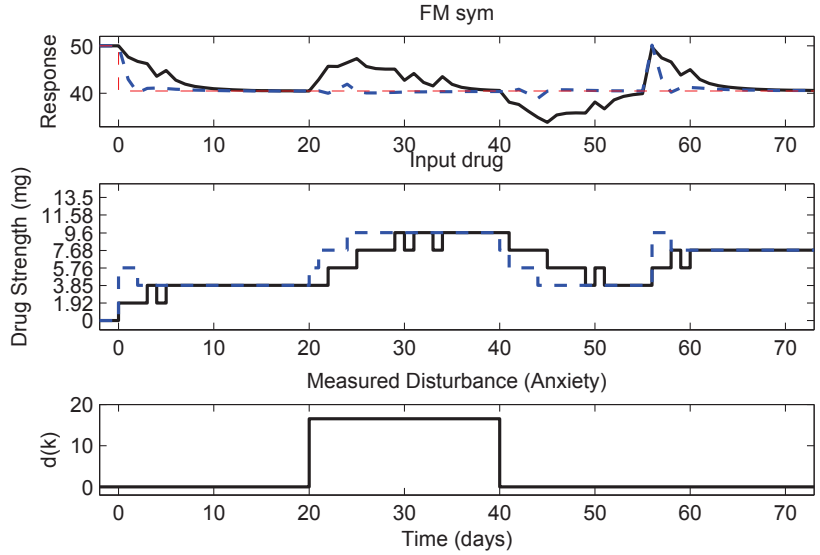


Figure 2.9: Performance of hybrid MPC (eight levels) with 3 DoF tuning parameters $(\alpha_r, \alpha_d, f_a) = (0.8, 0.8, 0.2)$ (slower) and $(\alpha_r, \alpha_d, f_a) = (0.2, 0.2, 0.8)$ (faster).

in the pain report occurs due to an unmeasured disturbance; this change is not part of the model prediction. The controller reacts by increasing the drug dosage to compensate.

Fig. 2.9 compares the performance of hybrid MPC for two set of tuning. The aim is to show that the 3 DoF formulation allows the user to tune the controller independently for setpoint tracking and disturbance rejection. The first case showcases a faster tuning ($(\alpha_r, \alpha_d, f_a) = (0.2, 0.2, 0.8)$) and it is then compared with a slower case ($(\alpha_r, \alpha_d, f_a) = (0.8, 0.8, 0.2)$). The manipulated variable changes smoothly for the slower tuning but results in more sluggish output response when compared to the case of faster tuning.

In practice, setpoint tracking has to be done in presence of disturbances and hence it is now shown that the treatment scheduling algorithm used here is robust to events occurring simultaneously. Both measured and unmeasured disturbance (of magnitude as before) act at $k = 0$ as shown in Fig. 2.10. The tracking is considered under both measured and unmeasured disturbances, where a smoother (but more aggressive controls) response is obtained for $\alpha_d = 0, f_a = 1$ where as the less aggressive controls for tuning $\alpha_d = 0.9, f_a = 0.2$. In both of the cases, the variation of $\alpha_r$ from 0 to 0.8 (as seen on the Y-axis) results in more sluggish setpoint tracking speed for fixed set of tuning parameters $\alpha_d, f_a$. It can also be observed that to compensate the effect of disturbance, more dosage magnitude is required. The length of the simulation is $N = 20$ days. In order to quantify the achieved performance under different sets of tuning, two metrics are defined: first, related to square of $2-$norm of error $e$ as:

$$J_e = \sum_{k=1}^{N} e(k)^T e(k), \tag{2.28}$$

where $e(k) = y(k) - y_r$ and second, square of $2-$norm of change in control ($\Delta u$) as:

$$J_{\Delta u} = \sum_{k=1}^{N-1} \Delta u^T \Delta u, \tag{2.29}$$

where $\Delta u(k) = u(k+1) - u(k)$. These are tabulated in Table 2.4, where it can be observed that de-tuning the controller (i.e. decreasing $f_a$ and increasing $\alpha_r, \alpha_d$ ) results in higher $J_e$ (more error) but lowering of $J_{\Delta u}$ (less aggressive controls).

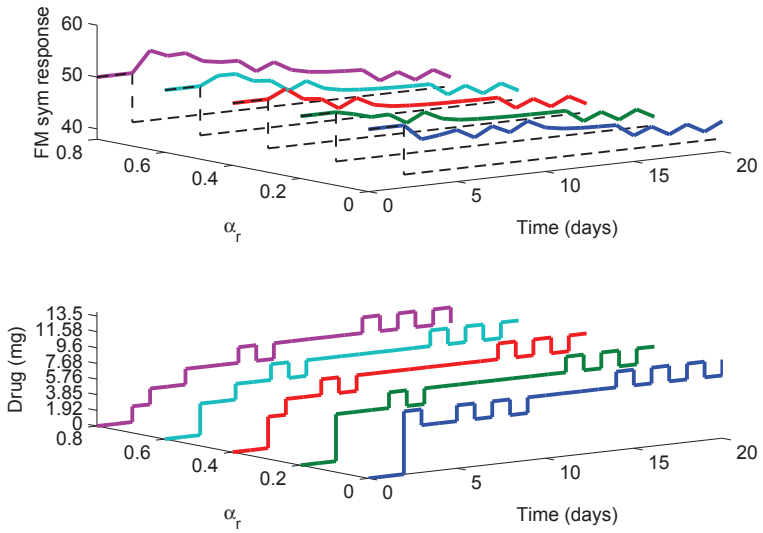


(a) $\alpha_d = 0.9,\ f_a = 0.2$

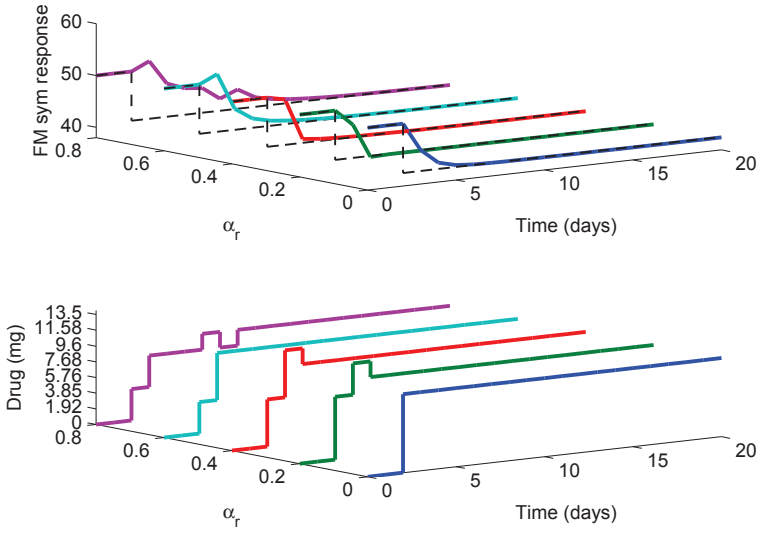


(b) $\alpha_d = 0,\ f_a = 1$

Figure 2.10: Setpoint tracking under both unmeasured and measured disturbance for various tuning ($\alpha_r$) values with two sets of settings for $\alpha_d, f_a$. The setpoint is denoted by dotted lines.

Table 2.4: Performance index of the signal under different tuning for setpoint tracking under disturbances. It can be observed that increases in $\alpha_r$ (implying more filtering action) leads to less aggressive control responses.

| $\alpha_d = 0.9, f_a = 0.2$ | | | $\alpha_d = 0, f_a = 1$ | | |
|---|---|---|---|---|---|
| $\alpha_r$ | $J_e$ | $J_{\Delta u}$ | $\alpha_r$ | $J_e$ | $J_{\Delta u}$ |
| 0 | 602.93 | 107.86 | 0 | 108.41 | 92.98 |
| 0.2 | 628.82 | 63.22 | 0.2 | 131.51 | 78.1 |
| 0.4 | 710.67 | 48.35 | 0.4 | 167.88 | 70.66 |
| 0.6 | 855.79 | 48.35 | 0.6 | 235.03 | 48.35 |
| 0.8 | 1181.53 | 44.63 | 0.8 | 327.85 | 40.91 |

Table 2.5: Performance index of the hybrid MPC under stochastic unmeasured disturbance. The observer gain can be varied to obtain a trade off between the metric of tracking error ($J_e$) and control moves ($J_{\Delta u}$).

| $f_a = 0.1$ | | $f_a = 1$ | |
|---|---|---|---|
| $J_e$ | $J_{\Delta u}$ | $J_e$ | $J_{\Delta u}$ |
| 9211.26 | 55.79 | 6203.99 | 1205.08 |

So far, only deterministic setpoint and disturbance signals have been considered. A scenario of practical interest is when the unmeasured disturbance is of stochastic nature; this is now introduced through an AutoRegressive Moving Average (ARMA) model to evaluate the controller performance. By changing the observer gain through $f_a$, it is possible to influence disturbance rejection. Consider an ARMA model as follows:

$$d(k) = \frac{(q-0.3)}{(q-0.7)^2} a(k) \quad \forall k, \quad a(k) \sim \mathcal{N}(0, 30), \tag{2.30}$$

where $d, a$ are discrete signals with $q$ as the forward shift operator. The time plot of this ARMA noise is shown in Fig. 2.11a where the unmeasured disturbance varies on a scale of 100. The length of the simulation is $N = 90$ days.

The two simulation cases are shown in Figure 2.11b. Two settings are considered to change the observer gain: $f_a = 1$ (which is more aggressive) and then $f_a = 0.1$ (which is more sluggish). Table 2.5 compares the performance indices related to the error and change in control from both simulations. It can be noted that under $f_a = 1$, a lower error performance ($J_e$) is observed but under a trade off with more aggressive control action

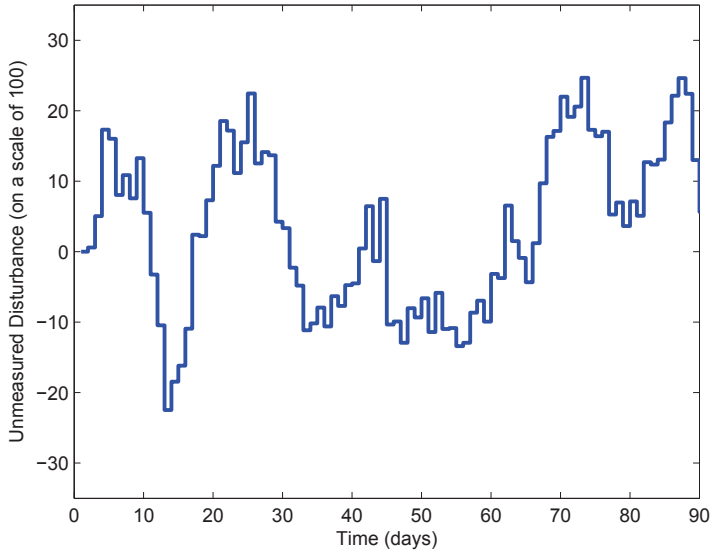


(a) Time series of ARMA noise.

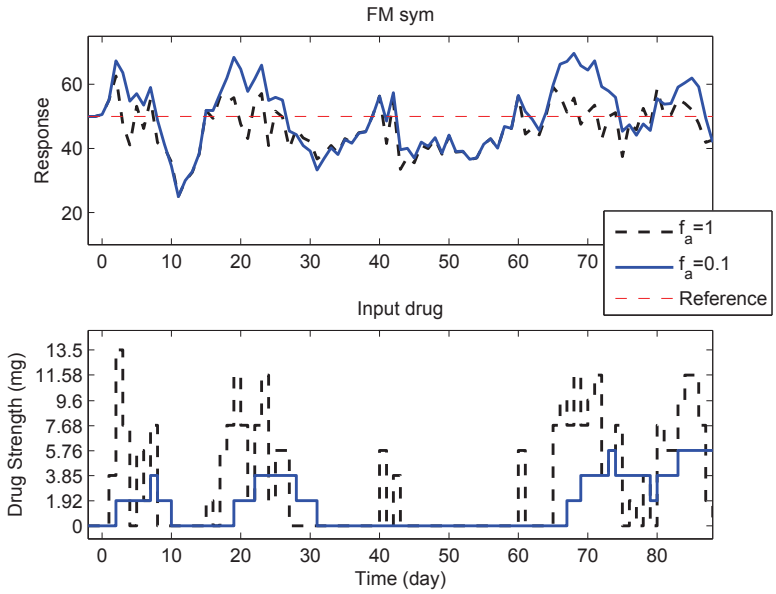


(b) Stochastic unmeasured disturbance rejection.

Figure 2.11: (a) Time series realization of unmeasured disturbance from the ARMA noise model. (b) Performance of hybrid MPC under different tuning ($f_a = 1, 0.1$) when the unmeasured disturbance is a realization of ARMA noise model.

where as using lower tuning value of $f_a = 0.1$ results in higher $J_e$ with the corresponding less change in control ($J_{\Delta u}$). To conclude, the novel tuning gives the user enough flexibility to choose the speed of response, for a given set of weight matrices, to satisfy certain clinical requirements.

### *2.5.2 Robust Performance*

It was previously indicated the importance of a suitable controller under model uncertainty and participant variability. That scenario is now addressed where the performance of the controller is evaluated when a perfect model is not available from the identification procedure. The approach used in this chapter is to showcase robustness via simulations. As before, one plant (drug-FM) and one disturbance (anxiety-FM) model are considered. To simulate model uncertainties, different parametric uncertainties on the estimated models (as shown by Equation 2.3) are used to generate scenarios for plant-model mismatch. The plant and disturbance model variations are chosen to illustrate participant variability expected in a cohort. For an individual treatment approach, these uncertainties may also correspond to unmodeled dynamics. These cases are noted in Table 2.6 for drug-FM model and anxiety-FM model. The modeling errors in plant will be compensated through the feedback action alone, although the modeling errors in disturbance model will be partially compensated by the feedforward action and the signal not compensated by the anticipation will enter the feedback loop as an unmeasured disturbance. It is assumed that none of the plant mismatch scenarios result in plant instability. Due to constraints on the input drug dosage levels, the uncertainties were not chosen to be arbitrarily very large.

The results for robust performance are shown in two sections: first, different uncertainties are evaluated for fixed tuning and the effect of different uncertainties ($\Delta*$) is observed as is shown in Section 2.5.2.1 and second, the uncertainty is fixed and the effect of tuning ($f_a$) on the response is observed as shown in Section 2.5.2.2.

Table 2.6: Tabulation of parametric perturbations on drug-FM model ($p$ or plant model) and on anxiety-FM model ($p_d$ or disturbance model).

| Case ($p$) | $\Delta K_p$ | $\Delta\zeta_p$ | $\Delta\tau_p$ | $\Delta(\tau_a)_p$ | Case ($p_d$) | $\Delta K_d$ | $\Delta\zeta_d$ | $\Delta\tau_d$ | $\Delta(\tau_a)_d$ |
|---|---|---|---|---|---|---|---|---|---|
| 1 | 0 | 0 | 0 | 0 | 1 | 0 | 0 | 0 | 0 |
| 2 | -29.1% | 0 | 0 | -23.46% | 2 | -15.1% | 0 | 0 | 66.66% |
| 3 | 29.1% | 0 | 0 | -23.46% | 3 | 15.1% | 0 | 0 | 66.66% |
| 4 | -29.1% | 16.6% | 259% | -23.46% | 4 | -15.1% | 16.6% | 259% | 66.66% |
| 5 | 29.1% | 79.3% | -29.1% | -23.46% | 5 | 15.1% | 79.3% | 191% | 66.66% |

#### 2.5.2.1 Robustness Evaluated under Fixed Tuning

The first case is now evaluated: effect of different uncertainties for a fixed instance of tuning of the control system. Since the plant-model mismatch will contribute to an unmeasured disturbance, it is not applied *externally* in the simulation. The observer gain is changed through $f_a$ for tuning and other parameters are kept constant ($\alpha_r = \alpha_d = 0$). The setpoint is kept constant at 50 and a measured disturbance is applied at $k = 2$ of magnitude 11.05. The length of the simulation is $N = 35$ days. Before describing the results, it is important to mention how the results are displayed for clinical inferences. The following two functional groupings are used:

1. *When a fixed nominal model is used.* A nominal model is used as a basis by the controller to assign dosages for different plants (typical robustness scenario). Clinically, this can be interpreted in two ways: first, that the (estimated) nominal model is an approximation of the true system (and hence the different scenarios represent different uncertain plants) for an individual participant and second, the nominal model represents an average or representative model for a population of participants (and hence the different scenarios represent different participants). This is shown in Fig. 2.12a-2.12b.

2. *When the true plant serves as the nominal model.* For each scenario considered in the previous case, the true plant is supplied as the nominal model to the controller. This case can be understood as when accurate modeling (through system identification or

otherwise) has been performed for each individual in a population. The key motivation for this is to get a clinical insight as the user can now compare how the controls will vary under plant-model mismatch and on the same page, it will help the user to assess the case when the correct model is available to the controller. Hence, the user can gauge the resultant change in dosing strategies due to modeling errors. This is shown in Fig. 2.12c.

In Fig. 2.12 each scenario (on 'Y' axis) represents five cases of uncertainty combinations of perturbations in both plant and disturbance model respectively. The following list shows the uncertainty cases $[P, P_d]$ used for simulation from Table 2.6: *a*) Scenario 1: [1,1] *b*) Scenario 2: [4,5] *c*) Scenario 3: [3,3] *d*) Scenario 4: [5,3] *e*) Scenario 5: [4,3] As can be noted, Scenario 1 in all plots is the case of nominal model (and hence no steady state error). When $f_a$ is changed from $f_a = 0.2$ (See Fig. 2.12a) to $f_a = 1$ (See Fig. 2.12b), more aggressive control are obtained, although this results in less output overshoot (max. pain) as noted in Table 2.7. In Fig. 2.12c, all the cases are compared with respective scenarios where a correct nominal model is available and it can be observed that the control is better as expected. It can be noted that only one plot is shown for correct nominal model case as both tuning values of $f_a$ result in the same response (no prediction error). Table 2.7 records the performance indices of this analysis; for $f_a = 0.2$, $J_e$ is higher when compared case-to-case with performance under tuning $f_a = 1$. However, using larger values of $f_a$ may result in aggressive control as in noted by some values of $J_{\Delta u}$. The metrics when a correct nominal model is available are also noted where, as expected, $J_e$ is lower with corresponding large values of $J_{\Delta u}$.

#### 2.5.2.2 Robustness Evaluated under Fixed Uncertainty

The second case is now evaluated: tuning of the control system is varied with a fixed uncertainty. If the user has some sense for the expected modeling uncertainties, different control inputs under different tunings are observed; a clinician can choose certain tuning

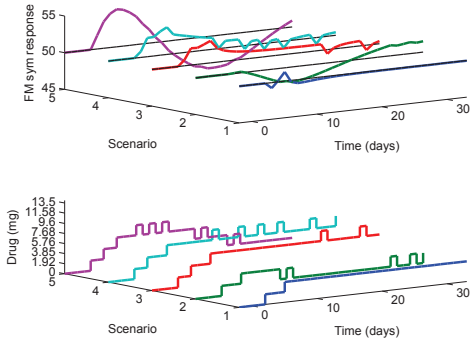


(a) Closed loop response with $f_a = 0.2$.

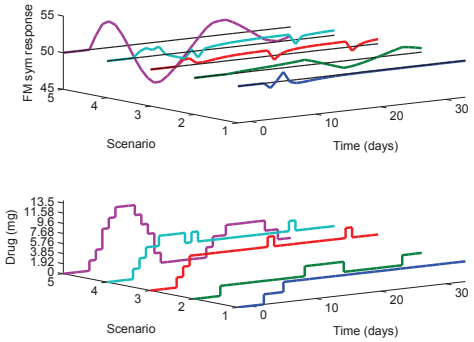


(b) Closed loop response with $f_a = 1$.

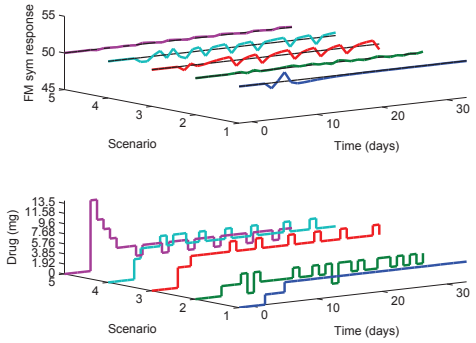


(c) Closed loop response where true plant serves as the nominal model (no plant model mismatch: $p = \tilde{p},\ p_d = \tilde{p}_d$).

Figure 2.12: Robustness evaluation when both plant model (drug-FM) and disturbance model (anxiety-FM) are perturbed under measured disturbance, with tuning $\alpha_r = \alpha_d = 0$ under different $f_a$. Plots (a) and (b) show the closed loop response with under model mismatch ($p \neq \tilde{p},\ p_d \neq \tilde{p}_d$ where scenario 1 represents the nominal model) under different tuning. Plot (c) shows the response under no plant-model mismatch hence independent of $f_a$.

Table 2.7: Performance index under two sets of tuning for robust performance with different scenarios of plant and disturbance model perturbations.

| | | $p \neq \tilde{p},\ p_d \neq \tilde{p}_d$ | | | $p = \tilde{p},\ p_d = \tilde{p}_d$ | | |
|---|---|---|---|---|---|---|---|
| Tuning | Uncertainty Case (plant ($p$), disturbance($p_d$)) | $J_e$ | $J_{\Delta u}$ | Max. pain | $J_e$ | $J_{\Delta u}$ | Max. pain |
| $\alpha_r = \alpha_d = 0, f_a = 0.2$ | 1,1 | 2.88 | 7.43 | 51.25 | 2.88 | 7.43 | 51.25 |
| | 4,5 | 44.47 | 37.19 | 51.55 | 0.39 | 126.46 | 50.23 |
| | 3,3 | 48.05 | 26.03 | 52.99 | 6.78 | 63.23 | 50.56 |
| | 5,3 | 75.48 | 52.07 | 53.7 | 8.55 | 70.66 | 50.72 |
| | 4,3 | 307.28 | 55.79 | 55.12 | 0.25 | 252.92 | 50.17 |
| $\alpha_r = \alpha_d = 0, f_a = 1$ | 1,1 | 2.88 | 7.43 | 51.25 | | | |
| | 4,5 | 9.05 | 14.87 | 50.97 | | | |
| | 3,3 | 12.04 | 26.03 | 50.91 | | | |
| | 5,3 | 14.44 | 33.47 | 51.17 | | | |
| | 4,3 | 216.33 | 78.1 | 53.57 | | | |

Table 2.8: Performance index under different tuning ($f_a$) for robust performance under fixed uncertainty of plant and disturbance model perturbations.

| Uncertainty Case (plant, disturbance) | $f_a$ | $J_e$ | $J_{\Delta u}$ | Max. pain |
|---|---|---|---|---|
| 4,3 | 0.2 | 345.87 | 81.827 | 55.12 |
| | 0.4 | 249.28 | 96.704 | 54.42 |
| | 0.6 | 248.51 | 63.23 | 53.9 |
| | 0.8 | 195.46 | 63.23 | 53.9 |
| | 1 | 226.92 | 89.265 | 53.57 |

parameters corresponding to the best possible treatment regimens. Fig. 2.13 shows how the tuning affects the performance more precisely than previous section as the uncertainty ($[p, p_d = 4, 3]$) is now fixed under different observer gains. It was further observed that used uncertainty combination is the most oscillatory of the cases and hence use of different $f_a$ can significantly vary the rate of change of dosing. Also, the simulation is run longer to allow the responses to settle ($N = 65$ days). The performance metrics are noted in Table 2.8 along with the maximum output overshoot, where it can be seen that best trade off between error and change in control is around $f_a = 0.8$. The proper trade off between modeling effort and controller performance will finally depend on clinical requirements.

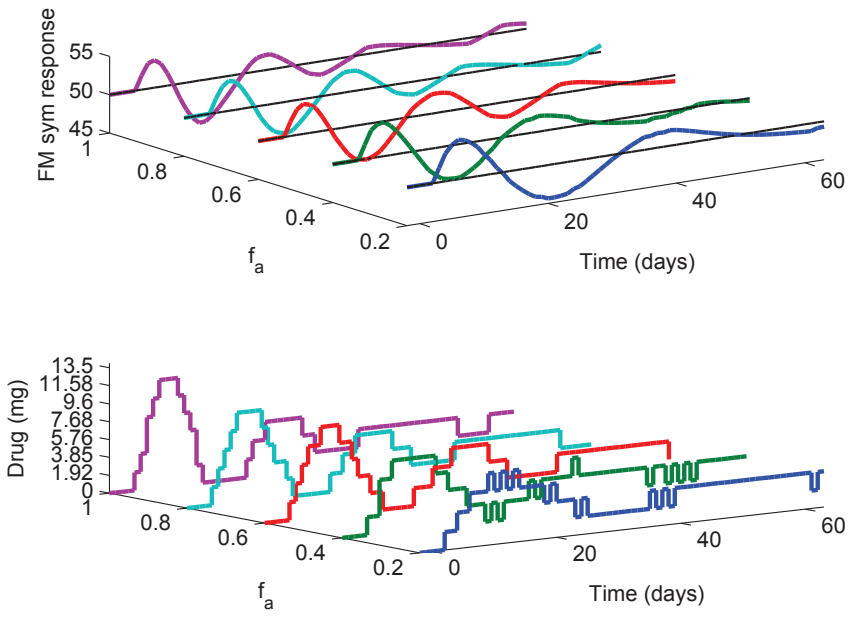


Figure 2.13: Robustness evaluation under different $f_a$ when both plant model (drug-FM) and disturbance model (anxiety-FM) are perturbed using plant uncertainty case number 4 as $\Delta K_p, \Delta\zeta_p, \Delta\tau_p, \Delta(\tau_a)_p = (-29.1\%, 16.6\%, 259\%, -23.46\%)$ and and using disturbance uncertainty case number 3 as $\Delta K_d, \Delta(\tau_a)_d = (15.1\%, 66.66\%)$.

## 2.6 Chapter Summary and Conclusions

This chapter demonstrated the design of an adaptive intervention for fibromyalgia that relies on system identification modeling and hybrid model predictive control to assign appropriate dosage levels of naltrexone as a treatment for fibromyalgia, a chronic pain condition. The approach described in this work generates models from clinical data and assigns categorical dosages by considering hybrid dynamics in a mixed logical dynamical (MLD) system framework.

Given the absence of first principles models, a secondary data analysis is performed to estimate parsimonious models from data available through clinical trials. Low-order multi-input ARX models are estimated and approximated to continuous-time second order

models. The effect of drug, placebo and other variables on outcomes of interest such as general FM symptoms are systematically included in the modeling procedure. The model yields the dynamical information that can be used to classify participants as responders or non responders to drug, and to make dosage changes over time.

Models from a representative participant from the clinical trial are used to show how model predictive control can be applied to assign dosages in the presence of disturbances and model uncertainties. The use of an improved 3 DoF tuning approach is demonstrated to give flexible independent tuning for a desired controller performance. The control results developed are broadly classified under nominal performance and robust performance. Under nominal performance, it is shown how by varying the three tuning parameters ($\alpha_r, \alpha_d, f_a$) related to filters and state observer dynamics, independent tuning for setpoint tracking, measured and unmeasured (deterministic and stochastic) disturbance rejection can be achieved, and their relationship to clinical goals in the intervention. In the robust performance evaluation, the model parameters are perturbed to create conditions of a plant-model mismatch which would be indicative of participant variability during the adaptive intervention. As part of this scenario, two cases are further considered: first, where controller tuning is fixed and the effect of different uncertainties are noted and second, when certain plant uncertainty is fixed and the effect of tuning is evaluated on the resulting response.

The results presented in this chapter can impact not only the treatment of fibromyalgia, but also the treatment of other chronic pain conditions and the development of adaptive behavioral interventions in general. It is envisioned that control engineering concepts will play a crucial role in novel individualized treatments, where a closed-loop system can adjust treatment dosages based on daily patient reports of pain and other symptoms of importance. In this way, an optimal dosage profile for that individual could be rapidly determined without requiring frequent office visits or substantial physician involvement. Thus, adaptive interventions relying on control systems engineering can be seen as a cost-effective and efficient method for accomplishing personalized pain interventions.

Finally, the secondary analysis conducted in this chapter has also pointed out the limitations of inferring dynamics from population-level clinical data. An experimental design where the drug dosages are adjusted to various signal levels will lead to significant observable changes in the outcomes. This change of drug magnitude can be brought about systematically such that the resulting signal has favorable theoretical properties from a system identification point-of-view under clinical constraints. Thus, the drug regimens changing magnitude over time can be used as a means to operationalize single-subject clinical trials and help create more informative intensive longitudinal dataset. The ensuing chapters discuss design of input signals to respect clinical constraints while achieving objectives derived from methods in system identification.

Chapter 3

# SURVEY OF METHODS IN SYSTEM IDENTFICATION, EXPERIMENT DESIGN AND OPTIMIZATION

## 3.1 Organization of the Chapter

This chapter presents a survey of methods in system identification, experiment design or input signal design and mathematical optimization. The presentation in this chapter is intended as a reference for development of problem formulations in subsequent chapters, and also to provide a brief overview of developments in system identification and input signal design. Given the mature nature of these fields, a comprehensive treatment will be forbiddingly long and is beyond the scope of this dissertation. The material presented in this survey is primarily based on texts on experiment design, system identification and optimization [49, 45, 123], and on research papers which have been cited in appropriate context. In particular, an overview of black-box modeling can be found in Sjöberg *et al.* [88]. A comprehensive survey of results for experiment design for system identification until the early 1970's can be found in Mehra [51] and recent reviews on optimal experiment design can be found in Pronzato [53] and Gevers *et al.* [52]. The material presented on optimization is based on the textbook by Nocedal and Wright [124], which covers the basics of numerical optimization and from the textbook by Boyd and Vandenberghe [123] which offers a more formulation or modeling oriented approach with focus on convex optimization.

The chapter begins with a brief overview of modeling in Section 3.2. Section 3.3 illustrates particular methods in system identification with description of key results which will serve as background for later chapters. The rest of the chapter focuses on survey of classical and recent results in experiment design for system identification, which is generally, and henceforth, referred to as *input signal design* in the context of dynamical systems. This is described in Section 3.4. Section 3.5 contains description of optimization methods and

related software. The chapter ends with a summary of described methods and conclusions in Section 3.6.

## 3.2 Philosophy of Modeling

Scientific methods consists of analysis of observed phenomena by testing or falsification of a proposed hypothesis using empirical, mathematical and logical techniques [125]. The scientific explanation takes shape, generally speaking, as a mathematical statement or a 'model'. In fact modeling forms the crux of the scientific enterprise, particularly in the natural sciences, where an accepted and validated model has both explanatory and predictive power, and which offers the best approximation of the perceived reality. Consequently, modeling is an important vehicle in building as well as complementing a scientific theory [126]. Without over stressing the explanatory role of mathematics in science, it should also be mentioned that not all models be necessarily described mathematically or quantitatively. This is sometimes observed in the social sciences where data and subsequently relationships between variables may be defined qualitatively. In this work, the term model is used in the sense of a mathematical model. Finally, the domain of model interpretation has to be carefully defined if the model is used as a way for predicting future behavior of the system. For example, there is debate in social sciences on the focus on an idiographic (single subject) vs nomothetic (multiple subject or towards generalization) analysis [13, 114].

Building of mathematical models using, and ultimately to explain, experimental data is universal in science and engineering. Experimentation is fundamental to the scientific method and hence model building is heavily dictated by data. Historical examples from astronomy such as discovery of Kepler's laws of planetary motion [127] and prediction of planetary orbits [128], to recent discoveries of a new particle (Higgs-like boson) from the Large Hadron Collider (LHC) experiment [129, 130] and evidence of cosmic inflation from BICEP2 experiment [131] highlight importance of using data to build, validate and falsify models. Learning from data is also a well observed behavior in living organisms,

particularly humans. In engineering, which involves application of scientific principles, models can also be constructed from known first principles. This is indeed true for the inanimate systems generally found in traditional engineering domains like electronic and electrical power systems, mechanical and aerospace systems, chemical processes and many more. With *a priori* knowledge and physical insight, observed data can be used to construct 'grey-box' or semiphysical models [45]. However, in many scenarios, only 'black-box' models from observed data can be constructed.

First and foremost, the collected data itself is the most basic model that can be constructed. In other words, in absence of any model structure, the best prediction that can be made is the data itself. Data visualization or 'eye balling' could give interesting insights in to the underlying dynamics such as possible nonlinear effects [132]. Generally, clinical data is collected as a function of time, e.g., the data shown in Fig. 2.1 indicated decrease in reported pain and improvement in sleep quality with drug intake. Hence, data visualization continues to be important in many scientific studies [133].

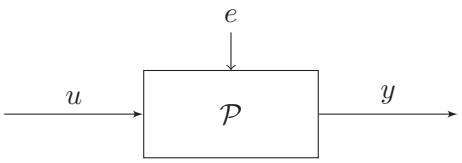


Figure 3.1: Input-output representation of a dynamical system.

Of particular interest in systems and control theory is the dynamical system framework, generally represented using state-space techniques [134], to describe the evolution of the system as a function of time. A dynamical system $\mathcal{P}$, shown in Fig. 3.1, is characterized by the fact that the value of a output variable $y$ depends not only on the current value of the input $u$ but also on its previous values [45]. Consider a dynamical system whose evolution in time as defined by a fixed rule:

$$\mathcal{P}: \quad y(k) = G(q,\theta)u(k) + H(q,\theta)e(k),\ k = 1,\ldots,N \tag{3.1}$$

where the transfer function $G, H$ are parametrized by $\theta$ and $e(k)$ is the uncertainty or the noise. In a stochastic framework, $e(k)$ is a random variable where as in a set-membership framework, the noise can be considered to be unknown but bounded.

Various types of dynamical models can be constructed: linear vs nonlinear, discrete-time vs continuous-time, time-invariant vs time-varying. In systems and control literature, the set of techniques for constructing dynamical models from data, usually with an exogenous input, are called system identification [48]. In conclusion to this section, it should be mentioned that like system identification, data-based modeling is pursued in many other areas like statistics [116], machine learning [135], artificial neural networks [136], econometrics [137], business and marketing [138], each with its own requirements, assumptions and conclusions. The method of system identification is discussed in the next section.

## 3.3 System Identification

System identification is the art and science of building *dynamical models* using observed input-output data from an experiment. The origins of system identification can be traced to early works in systems theory [26, 139]. Although a mature field now, significant interest continues to exist to tackle various theoretical and practical challenges [140].

Consider that an output $y$ is observed from a single-input single-output (SISO) dynamical system $\mathcal{P}$ subject to an input $u$. The data collected in practice is finite and noisy. It is often simpler to describe the modeling process as a mapping from the regressor space (which contains finite lagged data about the dynamical system) to the output space [88]. Hence, the modeling process would involve first construction of a regressor, and second a mapping to the output. The AutoRegressive with eXogenous input (ARX) regressor structure is commonly used [88, 54]:

$$\varphi(k) = [y(k-1),\ \dots, y(k-n_a),\ \ u(k-n_k),\ \dots, u(k-n_b-n_k+1)]^T, \tag{3.2}$$

where $y, u$ denote the output and input signals respectively, $n_a$, $n_b$ and $n_k$ denote the

number of previous instances of the output, input and the degree of delay in the model and the regressor vector $\varphi(k) \in \mathbb{R}^m$ where $m = n_a + n_b$. Along similar lines, the Finite Impulse Response (FIR) regressor structure can be written as

$$\varphi(k) = [u(k - n_k),\ \ldots\ , u(k - n_b - n_k + 1)]^T. \tag{3.3}$$

Given the regressor structure, consider a SISO process for which the dataset can be represented as $(\{y(k),\ \varphi(k)\}_{k=1}^{N})$ through the relation

$$y(k) = f(\varphi(k)) + e(k) \qquad k = 1, ..., N, \tag{3.4}$$

where $y(k) \in \mathbb{R}$, $f(\cdot)$ is an unknown smooth (possibly nonlinear) mapping, $\varphi(k) \in \mathbb{R}^m$ is the regressor vector and $e(k) \in \mathbb{R}$ is the noise [141]. Two broad approaches can be taken for system identification. The first approach uses a fully parametric method where a fixed model structure is estimated by minimizing a measure of model misfit for given model complexity. This also forms part of the 'global' methods which involve construction of fixed model to explain all of the data. The second approach involves use of nonparametric methods where a weighted average of neighboring points is used to estimate the unknown function for a given size of neighborhood. These 'local' methods involve construction of models in only local vicinity of the current operating point and hence the model is built on demand. These two approaches are now discussed in more detail.

### *3.3.1 'Global' Methods*

This section describes the prediction error methods which are among the most popular methods developed in system identification literature [45, 46]. This approach is based on minimization of certain cost function of observed data and parameter $\theta$ using classical statistical regression methods. The variable nomenclature adopted in this section has been taken from system identification literature (e.g., [45]). Consider that the true system can be represented as

$$y(k) = G(q, \theta_0)u(k) + H(q, \theta_0)e(k) \quad \forall k = 1, \ldots, N, \tag{3.5}$$

where $\theta_0 \in \mathbb{R}^{n_\theta}$ is the true parameter vector, $q$ is the forward-shift operator, $\{y(k), u(k)\}_{k=1}^{N} = Z^N$ are the input-output pair and $e(k)$ is zero mean white noise with variance $\sigma^2$. A model structure can be defined from a model set $\mathcal{M}$ as

$$y(k) = G(q,\theta)u(k) + H(q,\theta)\epsilon_e(k) \quad \forall k = 1,\ldots,N \tag{3.6}$$

where $\theta \in \mathbb{R}^{n_\theta}$. The one-step-ahead prediction can be defined as

$$\epsilon_e(k,\theta) = H^{-1}(q,\theta)(y(k) - G(q,\theta)u(k)). \tag{3.7}$$

Using the input-output data and quadratic criteria on the prediction error, the parameter estimate can be written as

$$\hat{\theta}_N = \arg\min_{\theta}\{V_N(\theta, Z^N)\} \tag{3.8}$$

$$= \frac{1}{N}\sum_{k=1}^{N}\epsilon_e^2(k,\theta). \tag{3.9}$$

If the true model is in the model set $\mathcal{M}$, then the following statements are true asymptotically [45, 46]

$$\sqrt{N}(\hat{\theta}_N - \theta_0) \to \mathcal{N}(0, P(\theta)) \tag{3.10}$$

$$P(\theta) = \sigma^2(\frac{1}{N}\sum_{k=1}^{N}[\psi(t,\theta)\psi(t,\theta)^T])^{-1}|_{\theta=\theta_0} \tag{3.11}$$

$$\psi(k,\theta) = \frac{\partial\hat{y}(k/k-1,\theta)}{\partial\theta} = -\frac{\partial\epsilon_e(k,\theta)}{\partial\theta} \tag{3.12}$$

where $\hat{y}$ is the one-step-ahead prediction. It can be shown that $\psi(k,\theta) \in \mathbb{R}^{n_\theta}$ is an affine function of the input $u(t)$ [45]. Equation (3.11) can be written in frequency domain using Parseval's theorem where it can be shown that inverse of the parameter covariance matrix is an affine function of the input power spectrum [45]. This fundamental result is used for the design of classical optimal inputs as discussed in Section 3.4.3. In other words, the quality of the estimated parameter directly depends upon $P(\theta) \in \mathbb{R}^{n_\theta \times n_\theta}$. These results can be used to construct an ellipsoidal confidence region which includes the true parameter $\theta_0$

$$(\theta - \hat{\theta}_N)^T(\frac{P(\theta)}{N})^{-1}(\theta - \hat{\theta}_N) \leq \chi^2_{\bar{\alpha}}(n_\theta) \tag{3.13}$$

with probability $\tilde{\alpha}$ as defined by $P(\theta)$ and the chi-squared distribution under sufficiently large $N$ i.e. $N \to \infty$ [45, 142].

The nature of optimization problem solved in (3.8) depends on the nature of parametrization. Commonly, the following parametric structures are used in system identification: ARX (Auto-Regressive with eXogeneous inputs), ARMAX (Auto-Regressive Moving-Average with eXogeneous inputs), FIR (Finite Impulse Response), BJ (Box-Jenkins) and OE (Output Error). The general structure describing these models can be written as

$$A(q)y(k) = \frac{B(q)}{F(q)}u(k - n_k) + \frac{C(q)}{D(q)}e(k) \tag{3.14}$$

where $A, B, C, D$ and $F$ are causal polynomials in $q$. The multi-input ARX equation was shown in (2.2). For these linear in the parameter models, relationship can be further represented using the regressor structure as

$$y(k) = \varphi^T(k, \theta) + e(k) \tag{3.15}$$

where for the FIR and ARX structure, the $\varphi^T(k, \theta)$ is independent of $\theta$ i.e. $y(k) = \varphi^T(k)\theta + e(k)$ and hence the quadratic criteria function reduces the optimization problem to linear least squares. For ARMAX, BJ and OE models, the optimization problem is nonlinear and nonconvex in nature, and the solution is calculated using iterative optimization schemes.

Of course, global methods are not limited to linear models. There is a rich literature of methods ranging from much flexible artificial neural networks, support vector machines and fuzzy logic based models to more structured approaches such as Nonlinear AutoRegressive with eXogenous input (NARX) and Hammerstein-Wiener models. The resulting optimization problems in these structures may be nonconvex. Although many results, such as shown in (3.11), generally hold true for any structure, the subsequent interpretations on model quality are not so straight forward as for the linear case. Recent efforts have been oriented to use the structural information in estimating nonlinear models [48].

### *3.3.2 'Local' Methods*

The local method philosophy deviates from the conventional modeling philosophy as fixed compact mathematical model as the best description is never derived; instead the input-output data generated from a dynamical system is used on demand to build local models. The methodology of building local linear models on-line is now briefly described. As before, consider a SISO process for a given data set $(\{y(k),\ \varphi(k)\}_{k=1}^{N})$ described by relationship as

$$y(k) = f(\varphi(k)) + e(k) \qquad k = 1, ..., N \tag{3.16}$$

where $\varphi(k)$ is composed of lagged output and input such as:

$$\varphi(k) = [y(k-1),\ ...\ y(k-n_a),\ \ u(k-1),\ ...\ u(k-n_b)]^T. \tag{3.17}$$

The local system identification methods such as Model-on-Demand (MoD) [55] attempt to estimate output predictions based on a local neighborhood of desired operating point $(\varphi^*)$ in the regressor space. The predictor function $\hat{f}$ is obtained by a linear combination of observed outputs

$$\hat{f}(\varphi^*) = \sum_{k=1}^{N} w(k)y(k) \tag{3.18}$$

where the weights are, in general, dependent on the distance of regressors from the current operating point $(\varphi^* - \varphi(k))$, noise variance and properties of $f$. The weights emphasize the size of the neighborhood from the desired operating point, and this is referred to as 'bandwidth' of the estimator. Thus, it governs the tradeoff between bias and variance errors of the estimate. To select these weights, the following two methods can be used:

- *Kernel-based approach*: The weights are assigned as per a kernel or window function $(W(\cdot))$ according to the distance of given regressors from $\varphi*$ to asymptotically minimize the mean square error of the estimate [55, 143, 45]

$$w(k) = W\left(\frac{\|\varphi^* - \varphi(k)\|_{M_1}}{h}\right) \tag{3.19}$$

where $M_1 \in \mathbb{R}^{m\times m}$ is scaling matrix for the Euclidean distance and $h$ is the bandwidth. The kernel function, which maps the regressors to weights, is generally of a symmetrical shape where certain kernel choice be shown to be optimal in the mean square error sense [143, 144]. In MoD [54, 89, 55], the bandwidth is selected using the classical methods such as Akaike Information Criteria (AIC) and crossvalidation [54].

- *Optimization-based approach*: Another approach of selecting these weights is through explicit use of optimization by minimizing the exact mean square error (MSE) or worst case MSE

$$w = \arg\min_{w} W(\varphi^* - \varphi(1), \ldots, \varphi^* - \varphi(N), f, w) \tag{3.20}$$

where $w = [w(1), ..., w(N)]^T$ and $W(\cdot)$ is some function of the MSE [56, 54]. Consequently, some of the resulting weights are zero and thus the 'bandwidth' of the estimator is automatically calculated. For example, these weights are obtained in the direct weight optimization (DWO) approach by solving following convex quadratic program (QP) at each time instant

$$\begin{aligned} \min_{w,s} \quad & \frac{1}{4}\left(\sum_{k=1}^{N} s_t \|\varphi^* - \varphi(k)\|^2_{M_2}\right)^2 + \sigma^2 \sum_{k=1}^{N} s(k)^2 \\ \text{s.t.} \quad & s(k) \geq w(k) \\ & s(k) \geq -w(k) \\ & \sum_{k=1}^{N} w(k) = 1 \\ & \sum_{k=1}^{N} w(k)\|\varphi^* - \varphi(k)\| = 0 \end{aligned} \tag{3.21}$$

where $M_2 \succeq 0$ is a function of the Lipschitz constant and $s$ is a vector of slack variables. For affine estimates, a new variable $w(0)$ can be defined. Since the choice of weights using statistical measures is only as per asymptotic arguments, the optimization-based approach is useful in practice when the number of data points is finite. Detailed formulation and proof can be found in [145, 56].

For both methods, predictions at other operating points in the regressor space can be obtained by recalculating using the kernel or by solving a new optimization problem, which will result in a new set of weights. The methods outlined so far have focused on obtaining the function approximation $\hat{f}(\varphi^*)$. In the next step, a local linear model can be obtained by solving

$$\hat{\beta} = \arg\min_{\hat{\beta}} \sum_{k=1}^{N} \ell(y(k) - \hat{m}(\varphi^* - \varphi(k),\ \hat{\beta})) \times W(\varphi(k) - \varphi^*) \tag{3.22}$$

where $\ell(\cdot)$ is a quadratic norm function, $W(\cdot)$ assigns weight as per the estimator bandwidth and the local model structure can be:

$$\hat{m}(\varphi^* - \varphi(k), \hat{\beta}) = \hat{\beta}_0 + \hat{\beta}_1(\varphi^* - \varphi(k)) \tag{3.23}$$

which is linear in the unknown parameters, and hence an estimate can be computed using least squares.

In conclusion, an important aspect for data based methods is availability of informative data and hence experiment design for system identification is a fundamental exercise in system identification. In the ensuing section, an overview of experiment design for system identification is presented.

## 3.4 Experiment Design for System Identification

Based on the discussion in the previous sections and Chapter 2, the procedure for system identification can functionally classified as:

1. *Experiment design.* This includes the task of selecting the input signal among other considerations such as choosing the sampling rate.

2. *Model structure.* This step involves selection of a parametric (e.g., ARX, Hammerstein-Wiener) or non parametric (e.g., frequency response) structure to capture the inherent relationship in the data. Technically, the Model-On-Demand approach is a hybrid of traditional parametric and nonparametric methods.

3. *Model estimation.* This step involves solving a specific optimization problem using the model structure previously selected. With assumptions on the stochastic nature of noise, certain statistical properties can be assigned to the calculated estimate.

4. *Model validation.* The final step involves various procedures to validate the model including quantifying the model fit.

The first stage of experiment design significantly determines the success of the later steps and hence is the most important design variable associated with system identification. Experiment design for system identification specifically involves the design of input signals to achieve various design objectives such as minimum variance parameters, distribution of regressors (as developed in this dissertation) or achieving desired input signal spectrum. A brief timeline of development of input signal design is shown in Fig. 3.2. Specifically for a dynamical system, the input design should address

1. Higher order moments of the input signal. For a linear system, the second order moment or the input spectrum uniquely defines the asymptotic properties of the estimated models [45]. This is discussed in Section 3.4.1, and

2. Shape of the input signal, i.e. the exact time domain realization of the input signal. This requirement can be grouped in the 'plant-friendly' category where the input signal should have limited amplitude and move sizes, among other considerations. This is discussed in Section 3.4.2 and in detail, in Section 4.2.

The topic of input design is discussed in the ensuing sections with focus on persistence of excitation in the signal, achieving plant-friendliness, and finally classical optimal input design.

### *3.4.1 Input Signals for Persistent Excitation*

In system identification, informative data sets are directly related to presence of the persistence of excitation (PE) in the input signal. This implies that the data allows to discriminate

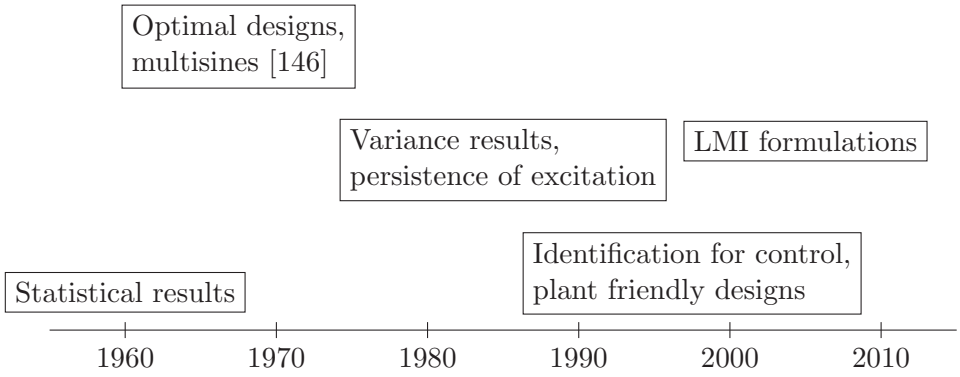


Figure 3.2: A brief timeline of development of input signal design. Early development in the 1970's utilized classical results from statistics for optimal designs. The later decades saw incorporation of variance of transfer function and plant friendly designs. The last ten years has seen resurgence of input design due to convex formulations.

between two rival models in a given model set and hence PE is a necessary condition to facilitate estimation in an unambiguous manner. The signal $u(k)$ is said to be persistently exciting if the following covariance matrix is positive definite:

**Definition 2.** *A quasi-stationary [45] input $u(k)$ is persistently exciting of order $n_{PE}$ if the matrix*

$$\hat{R} = \begin{bmatrix} r_u(0) & \cdots & r_u(n_{\mathrm{PE}}-1) \\ r_u(n_{\mathrm{PE}}-1) & \cdots & r_u(0) \end{bmatrix} \tag{3.24}$$

*is positive definite ($\hat{R} \succeq 0$),*

where $r_u(n)$ is defined as

$$r_u(n) = \sum_{k=-\infty}^{\infty} u(k)u(k+n). \tag{3.25}$$

In the frequency domain, this concept can be related to a condition on the input spectrum $\Phi(\omega)$ as follows:

**Definition 3.** *The input signal spectrum $\Phi(\omega)$ for a PE signal of order $n_{\mathrm{PE}}$ is non zero for at least $n_{\mathrm{PE}}$ distinct frequencies in $0 < \omega < \pi$:*

$$\Phi(\omega) > 0 \quad \forall \omega \in (0, \pi). \tag{3.26}$$

In addition to the PE condition, based on results derived in Section 3.3.1, it can be concluded that the parameter covariance matrix (or its inverse the information matrix) is a function only the spectrum and not of the signal waveform and hence, an input spectrum completely determines the quality of the LTI model. Historically, PE conditions have also played an important role in adaptive control [147]. Classical input signals that can be designed to satisfy this informative condition include [132]:

- *Pseudo Random Binary Sequence (PRBS)*: These are deterministic, periodic signals which can be uniquely defined by the number of shift registers $n_r$ and switching time $T_{\text{sw}}$ to excite the system bandwidth:

$$\omega_* = \frac{1}{\beta_s \tau^H_{\text{dom}}} \leq \omega \leq \frac{\alpha_s}{\tau^L_{\text{dom}}} = \omega^*, \tag{3.27}$$

  where $(\tau^H_{\text{dom}}, \tau^L_{\text{dom}})$ are the dominant time constant estimates of the system based on the high ($\alpha_s = 2$) and low ($\beta_s = 3$) frequency information [80], and $[\omega_*, \omega^*]$ is bandwidth for a flat spectrum $\Phi_u(\omega)$ defined as

$$\Phi_u(\omega) = \begin{cases} \gamma_a & \omega_* \leq \omega \leq \omega^* \\ \gamma_b & \omega > \omega^*, \end{cases} \tag{3.28}$$

  where $\gamma_a$ and $\gamma_b$ are real numbers defining the magnitude. Correspondingly, the switching time and the length of signal $N = N_{\text{cyc}} * T_{\text{sw}}$ can be calculated as:

$$T_{\text{sw}} \leq \frac{2.8\tau^L_{\text{dom}}}{\alpha_s}, \quad N_{\text{cyc}} = 2^{n_r} - 1 \geq \frac{2\pi\beta_s\tau^H_{\text{dom}}}{T_{\text{sw}}}. \tag{3.29}$$

- *Multisine signals*: These are deterministic, periodic signals designed to contain specific frequency information

$$u(k) = \sum_{i=1}^{n_s} a_i cos(\omega_i kT + \phi_i), \tag{3.30}$$

  where $n_s$ is the number of harmonics, $T$ is the sampling time, $a_i \in \mathbb{R}$ are constant for all $n_s$ and frequencies $\omega_i$ uniformly spread over the bandwidth. The phases $\phi_i$ can be determined, for example, by the Schroeder method [146]. In other cases, these

multisines can be designed to reach a desired plant friendly metric such as the crest factor under time domain constraints by selecting phases through an optimization procedure [81]. Finally, it can be shown the optimal input for a given information matrix (see Section 3.4.3) has a discrete spectrum. This implies that any optimal spectrum can be expressed using the multisine signal [52].

- *Multi Level Pseudo Random Sequence (MLPRS)*: These are deterministic, periodic signals designed to contain specific frequency information using the Galois field theory [82]. For a signal with $m_l$ levels, the number of elements $q$ in Galois field can be defined where $q \geq m_l$ to generate the pseudo-random numbers. Based on the given bandwidth, the variable switching time can be calculated as

$$T_{\text{sw}} \leq \frac{2.78}{\omega^*}, \quad \omega_* \geq \frac{2\pi}{T_{\text{sw}}(q^{n_r} - 1)}, \tag{3.31}$$

for $n_r$ shift registers and $\omega_*, \omega^*$ are as defined before. It should be noted that the length of the signal can increase exponentially given by the expression

$$N = (q^{n_r} - 1) * T_{\text{sw}}. \tag{3.32}$$

MLPRS has a distinct advantage over PRBS signal for identification of nonlinear systems due to limitation of PRBS to binary levels [45, 89].

- *Uniform random input signal*: These are random input signals directly sampled from a uniform probability distribution

$$u(k) \sim \mathcal{U}(u_{\min}, u_{\max}) \tag{3.33}$$

defined using the scalar amplitude bounds on the input signal. Indeed, an advantage of uniform random design is the capacity to address hard bounds on the inputs. Input signal derived from Gaussian distributions are also frequently in academic examples.

### *3.4.2 Plant-Friendly Input Signals*

Input signals used for system identification in practice need to take into consideration the limitations imposed by the plant, such as the minimum and maximum signal levels and the signal rate of change. In addition, they should contain a high enough signal-to-noise ratio to offset noise components in the system. Input signals that take into account these and other practical limitations are referred to as plant-friendly [50]. It can be noted that the plant-friendly requirements can be in direct conflict with traditional goals of input design, such as maximum power or high frequency excitation.

The design of plant-friendly signals has been a particular focus of the Control Systems Engineering Laboratory (CSEL) at Arizona State University. Initial work in the lab focused on design of input signals with low crest factor with connection to model uncertainty and robust control [148]. By considering constraints on the amplitude and move size constraints on both the input and output, multisine signals were used with a prescribed spectrum and the phases were chosen to minimize the signal crest factor through an nonlinear optimization procedure [89, 149, 81]. In an alternative algorithmic approach, plant-friendly multisine signals were designed using the simultaneous perturbation stochastic approximation (SPSA) methodology in [150, 151].

Later work on plant-friendly input design incorporated the issues associated with data-centric methods. The methods based purely on crest factor do not address the distribution required for data-centric methods. Towards this, a geometric discrepancy approach based on Weyl's criterion was used to address uniform distribution in the output space [152, 95]. Special attention was given to ill-conditioned plants to showcase the utility of the proposed input design [80, 153]. The next section deals with design of optimal input for minimum parameter variance.

### *3.4.3 Optimal Input Signal Design*

Optimal input signal design originated when the classical results from statistical experiment design, which are designed for *static* systems were re-interpreted from a *dynamical* system perspective. Thus, optimal experiment design for system identification deals with designing an input signal for optimal parameter estimation of the dynamical system. Like traditional statistical approaches, the central focus of optimal input signal design lies on the information matrix or the inverse of the parameter covariance matrix [45, 142].

Much of recent interest in optimal input signal design has been due amenable representation of these problems using linear matrix inequalities (LMI) as convex optimization problems. It comes from the fact that the parameter covariance matrix is affine in the input spectrum which itself is a linear function of the autocorrelation coefficients as shown in (3.34). These problems can be written as semidefinite programming (SDP) problems and can be efficiently solved. Recently, the MOOSE toolbox (Model Based Optimal Input Design Toolbox for MATLAB) [154] has been developed to implement these problems. MOOSE adds an extra layer over CVX [155] and SeDuMi [156] for these convex problems and offers much more simpler syntax for classical optimal input signal design.

Many formulations can be proposed to satisfy different design objectives for optimal design [53, 52]. The classical objective is to maximize some measure of the information matrix such as using determinant (D-optimal), eigenvalue (E-optimal) and trace (A-optimal) based designs [49]. In this survey, two particular formulation are discussed. The first formulation finds the specified input spectrum, whereas the second formulation minimizes the total power subject to model quality as a constraint [87].

The first formulation generates an input signal representation to follow bounds on desired input spectrum. The following equation

$$\Phi_u(\omega) = |U(\omega)|^2 = \sum_{k=-\infty}^{\infty} r(k)e^{-j\omega k} \geq 0, \tag{3.34}$$

is used to determine if there exists any autocorrelation coefficients which will result in a desired spectrum, with more details in Section 4.2. First, recall the following definition

**Definition 4.** *Positive Real (PR) Lemma [157]: Given a discrete time system, the transfer function $H(z)$ satisfies*

$$H(e^{j\omega}) + H^*(e^{j\omega}) \geq 0 \quad \forall \omega \in [0, 2\pi] \tag{3.35}$$

*iff for $S = S^T$, the following linear matrix inequality is true:*

$$\begin{bmatrix} S - A^T S A & C^T - A^T S B \\ C - B^T S A & D + D^T - B^T S B \end{bmatrix} \succeq 0 \tag{3.36}$$

*where $(A, B, C, D)$ are state-space matrices for the dynamical system.*

The first formulation is posed as a SDP feasibility problem. A critical notion here is to use the PR lemma to derive a LMI describing the non-negative condition on the spectrum. The power spectrum can be written as

$$\Phi_u(\omega) = H(e^{j\omega}) + H^*(e^{j\omega}) \tag{3.37}$$

with the important requirement for $\Phi_u(\omega)$ to qualify as a spectrum

$$\Phi_u(\omega) = \sum_{k=-\infty}^{\infty} r(k) e^{-j\omega k} \geq 0. \tag{3.38}$$

Since the above relationship is linear, the spectrum parametrization can be used to find $A, B, C, D$ as a function of $r(\tau)$ and hence, using PR lemma, express the problem as SDP [158]. This can be formally written as

$$\begin{aligned} \text{find} \quad & r \\ \text{s.t.} \quad & |\gamma^L(\omega)| \leq \Phi_u(\omega) \leq |\gamma^H(\omega)| \\ & \omega \in [0, \pi] \\ & \begin{bmatrix} S - A^T S A & C^T - A^T S B \\ C - B^T S A & D + D^T - B^T S B \end{bmatrix} \succeq 0 \end{aligned} \tag{3.39}$$

where $\gamma^L(\omega)$ and $\gamma^H(\omega)$ are the high and low bounds on desired spectrum. The optimization problem (3.39) is semi-infinite due to the presence of the variable $\omega$ which can take any values in the interval $[0, \pi]$. This can be addressed by frequency gridding [158]. This formulation is extended to account for time-domain constraints on the input in Section 6.3.

The second formulation aims to find a spectrum which is optimal with respect to model uncertainty set expressed in terms of the parameter covariance matrix shown in (3.11) and the objective is to minimize the input power [142]. It can be noted that since direct time domain input bounds cannot be specified (and this is revisited later in Section 6.3.1), the only way the signal can be restricted to not go too large is to minimize the total input power which, by Parseval's theorem, can be written as the area under the curve of the input spectrum. The resulting optimization problem can be written as a SDP:

$$\min_{r} \quad \mathcal{A} \tag{3.40}$$

$$\text{s.t.} \quad (\theta - \theta_0)^T (\frac{P(\theta)}{N})^{-1} (\theta - \theta_0) \leq \chi^2_{\tilde{\alpha}}(n_\theta)$$

$$\frac{1}{2\pi} \int_{-\pi}^{\pi} \Phi_u(\omega)\, \mathrm{d}\omega \leq \mathcal{A} \tag{3.41}$$

$$\begin{bmatrix} S - A^T S A & C^T - A^T S B \\ C - B^T S A & D + D^T - B^T S B \end{bmatrix} \succeq 0.$$

For both formulations, the final input signal is realized using spectral factorization as an output of a linear system driven by white noise [158] with more details in [142, 154].

A key point has to be mentioned, which unfortunately may be easily overlooked, that the optimal design requires knowledge of the (unknown) true parameter $\theta_0$ of the system as shown in (3.11). In other words, design of optimal inputs requires knowledge of the very parameters which the experiment is designed to estimate. Although this may seem as a contradiction at first, some inspection should convince the reader that this is indeed not surprising. To take an example from automatic control, 'optimal' control is optimal only for the given model. Similarly, an 'optimal' input can only be designed when the true parameters are known. Thus, the approach of optimal input is beneficial if a good initial

estimate is available [45]. The long-accepted approach in this situation is to use the best possible initial information and continue to refine it in an iterative fashion, as elucidated in the following excerpt from the book *System Identification: Theory for the User* [45, p. 443]

*"The optimal experiment design depends on the (unknown) true system and noise characteristics. This is the normal situation for optimality results, and in practice it has to be handled by using the best prior information available about the system".*

Recently, identification test monitoring [50], robust experiment design [86] and adaptive experiment design [159] have been proposed in literature as iterative schemes to address this issue. Finally in the context of optimal design, the following work address some plant friendly requirements: design of optimal input signals under amplitude constraints using dynamic programming is shown in [160], design of optimal input signals under input and output amplitude constraints using convex relaxation is shown in [161] and work in [162] specifically addresses input signal variance in an optimal input framework using Tchebysheff systems.

## 3.5 Mathematical Optimization

Most problems in decision and control can be formally posed as mathematical optimization problems. Historically, the interest in optimization has existed since antiquity. First formal development took place in the $17^{\text{th}}$ century, primarily by works of Euler and Lagrange, on the subject of calculus of variations [163]. Over the years, many ideas from Newton (particularly iterative algorithms) to Gauss and Legendre (least-squares [128]) were further incorporated. The real birth of modern optimization took place during and immediately after the Second World War as linear programming (LP) through the pioneering works of Kantrovich, Dantzig, Von Neumann and many others [164]. LP was primarily driven by economic and military needs for resource allocation. The word 'programming'

is now a vestigial term in the modern context where it was originally meant for general algorithm design. Over the next decades, many theories related to necessary and sufficient conditions related to optimality were quantified such as the Karush-Kuhn-Tucker (KKT) conditions along with algorithms for large scale nonlinear constrained optimization, integer constrained optimization and multiobjective optimization [124]. In addition, work was done on the framework of computational complexity and a general consensus had emerged that the fundamental structure of the optimization problem described in terms of the convexity or nonconvexity of the involved functions and sets determines the tractability of that problem [165, 166]. Significantly, in the last two decades rapid development has taken place in solving optimization problems, particularly convex problems, using interior point methods with much success in many applications [123, 124]. For the interested reader, the book 'Optimization Stories' contains many interesting historical notes [167].

### *3.5.1 Constrained Optimization*

Consider the following constrained optimization problem:

$$\begin{aligned} p^* = \min_x \quad & f_0(x) \\ \text{s.t.} \quad & f_i(x) \leq 0, \quad i = 1, \ldots, m, \\ & h_i(x) = 0, \quad i = 1, \ldots, p, \end{aligned} \tag{3.42}$$

where $x$ is the decision vector of finite dimension, $f_0$ is the objective function and the feasible set for this problem is defined by the intersection of domains of the inequality constraint functions $f_i$ and equality constraint functions $h_i$. The optimal objective is denoted by $p^*$ corresponding to an optimal feasible decision vector $x^*$ where $f_0(x^*) = p^*$. For problem (3.42), assuming that the functions are continuously differentiable, first-order optimality conditions known as Karush-Kuhn-Tucker (KKT) conditions can be written as [123]:

$$f_i(x^*) \leq 0, \quad i = 1, \ldots, m \tag{3.43}$$

$$h_i(x^*) = 0, \quad i = 1, \ldots, p, \tag{3.44}$$

$$\lambda_i{}^* \geq 0 \tag{3.45}$$

$$\lambda_i{}^* f_i(x^*) = 0 \quad i = 1, \ldots, m \tag{3.46}$$

$$\nabla f_0(x^*) + \sum_{i=1}^{m} \lambda_i{}^* \nabla f_i(x^*) + \sum_{i=1}^{p} \nu_i{}^* \nabla h_i(x^*) = 0 \tag{3.47}$$

where $x^*$ is the primal optimal point and $(\lambda^*, \nu^*)$ are the dual optimal points. When the objective function $f_0$ is convex, the inequalities $f_i$ are convex and equalities $h_i$ are affine, the problem is called convex optimization. In all other cases, the problem becomes nonlinear and nonconvex. The defining characteristic of convex optimization problems is that any local minimizer $x^*$ is also the unique global minimizer of (3.42). This implies that the KKT conditions are both necessary and sufficient for optimality and there are efficient polynomial time algorithms to solve the convex problem [166].

In brief, particular structure of optimization problems are now listed in increasing order of generality. The simplest form of convex optimization is linear programming (LP) where the constraints and the objective function are affine:

$$\begin{aligned} \min_x \quad & c^T x + d \\ \text{s.t.} \quad & Ax \leq b, \\ & Cx = d. \end{aligned} \tag{3.48}$$

When the objective function is convex quadratic, the optimization problem is quadratic programming (QP):

$$\begin{aligned} \min_x \quad & x^T Q x + c^T x + d \\ \text{s.t.} \quad & Ax \leq b, \\ & Cx = d. \end{aligned} \tag{3.49}$$

If $Q$ is not positive semidefinite, the problem becomes nonconvex [94]. Further generalization can be made by including quadratic inequality constraints (only and not quadratic equality constraints as they are nonconvex irrespective of properties of $Q$) resulting in

quadratically constraint quadratic programs (QCQP). Least-squares problem, which has historical origins in regression analysis, can also be written as unconstrained QP. The next order of generalized problem structure are the second-order cone programming (SOCP) problems, where the constraints can be written in 2-norm as:

$$\begin{aligned} \min_{x} \quad & c^T x + d \\ \text{s.t.} \quad & \|Ax\|_2 \leq p^T x + q, \quad i = 1, \ldots, m, \\ & Cx = d, \end{aligned} \tag{3.50}$$

and semidefinite programming (SDP) can be defined by minimizing a linear function subject to linear matrix inequalities (LMI):

$$\begin{aligned} \min_{x} \quad & c^T x \\ \text{s.t.} \quad & x_1 F_1 + ... + x_n F_n + G_0 \preceq 0 \\ & Ax = b \end{aligned} \tag{3.51}$$

where matrices $F_1 ... F_n$ and $G_0$ are symmetric. If the matrices are all diagonal, then the SDP reduces to a LP. Finally, the structures mentioned above can be connected with a more general, though abstract, notion of generalized inequalities [123].

Contrary to the common intuition, majority of optimization problems are difficult to solve. As mentioned earlier, the ease of solvability of an optimization problem is determined by its fundamental structure: convex vs nonconvex. With the development of field of computational complexity, many optimization problem structures can be classified as NP-hard and hence, in the worst case, are essentially intractable and *not* solvable in polynomial time (unless P=NP). Hence, nonconvex optimization problems are generally hard to solve and methods based on KKT conditions may give poor local solutions with arbitrary initial conditions. A powerful approach to approximately solve some of these problems is through *convex relaxation* where the main source of nonconvexity is replaced with a 'relaxed' version that is convex and hence more tractable [165, 168, 169, 166, 170]. Convex

relaxation gives a bound on the original objective function but generally no feasible solution unless the relaxation is tight. Clearly, there has be to a meaningful relationship between the original nonconvex problem and the relaxed convex problem. Semidefinite programming (SDP) relaxation for the case of nonconvex quadratic problems has been particularly successful in this regard. Since many of these structures can be represented as smooth polynomial functions, stronger bounds through convex relaxation can be derived using theory of moments and sum-of-squares representation of positive polynomials [171]. Through convex relaxation, the original nonconvex problem is approximated by a SDP which can be globally solved. Although limited by size of resulting SDP, the relaxation approach can be useful for certain special optimization structures. This has been discussed in more detail in Section 5.3.2.

### *3.5.2 Computational Tools*

It is often more productive to have a higher-level language to 'model' the optimization problem while leaving the low-level communications with the solver to an interface. This lets the user focus on the problem formulation and worry less about syntax and other formalities often associated with particular solvers. One of the earliest modeling languages were AMPL [172] and GAMS [173]. Recent years has seen development of specialized interfaces, with focus on convex optimization, such as CVX [155], YALMIP [174] and TOMLAB [175]. With impressive advances in single and parallel computing, there has been significant increase in efficiency of solvers as seen with introduction of web-based NEOS Server for Optimization [176]. It should be mentioned that a large number of these interfaces are for the MATLAB environment with recent increase in use of other open source software.

These specific interfaces interact with solvers which carry the algorithm to solve the particular optimization. The most popular solvers for certain convex optimization are Gurobi [177] and CPLEX [178] which can solve linear programming (LP), quadratic and quadratically constrained programming (QP and QCP), and mixed-integer programming

(MILP, MIQP, and MIQCP). For nonlinear programming, many options are available including KNITRO [179] which is traditionally used with AMPL/GAMS interface. Some other solvers are build as general purpose to solve complex nonlinear mixed integer programming such as Couenne [180] and Bonmin [181]. For conic programs, and particularly for SDP, SeDuMi [156], SDPT3 [182] and MOSEK [183] are the most popular solvers. In the MATLAB environment, the MATLAB optimization toolbox [184] offers various algorithms for convex and nonconvex programs include the useful general nonlinear programing function `fmincon`.

The polynomial optimization algorithm is coded in following software in MATLAB: GloptiPoly [185], YALMIP [174] and SparsePOP [186] among others. For polynomial optimization problems, at the algorithmic layer, although these many of optimization problems may be convex, the size of the resulting optimization problem is large for higher dimensional problem and it is potentially difficult to solve these problems with present interior-point based methods. The limitations are not only memory intensive but also relating to the numerical stability of the solver. Towards this, recent efforts have focused on development of so-called first-order methods for solving the convex problem approximately [187].

## 3.6 Chapter Summary

This chapter contained a brief treatment of developments in system identification, input signal design and optimization. In system identification, the methods were broadly grouped as global vs. local modeling and these two approach were described. The survey section for input signal design focused on persistence of excitation in the input signal, quality of plant-friendliness and finally on the topic of classical optimal input design. The chapter ended with a brief overview of numerical optimization and a summary of computational tools that will be relevant to the remainder chapters of the prospectus. The ensuing chapter discusses the process of design of constrained input signals with particular focus on data-centric system identification.

Chapter 4

# CONSTRAINED INPUT SIGNAL DESIGN FOR DATA-CENTRIC SYSTEM IDENTIFICATION: PROBLEM STATEMENTS

## 4.1 Overview

A distinguishing feature of many engineering problems is operation under *constraints*. Constraints or limitations naturally arise from the physics of a system such as, for example, defined by conservation laws. In most cases, constraints are enforced to satisfy certain performance and safety considerations. Typical examples of such restrictions are limits on drug dosages in medical treatment, limits on the rate of change of the angle-of-attack in an aircraft, actuator saturation in a chemical process plant, restrictions from environmental regulations in various industries, inventory limits in a supply chain and limited factors of production in economics.

This chapter develops problem statements to design input signals for data-centric system identification methods under these constraints. The data-centric approach systematically generates a local function approximation from a database of regressors at the current operating point. Broadly speaking, two approaches are presented to address unique requirements of data-centric system identification given that, in these methods, a fixed parametric model is not estimated. The first approach is a novel framework for input signal design based on the geometric spread or distribution in the regressor and output space. The second approach uses a classical result from discrepancy theory, the Weyl's criterion, to uniformly distribute the points in the feasible space. While the two approaches differ conceptually, they both are developed to directly address the constraints of interest.

The first approach addresses the distribution of regressors in the finite dimensional regressor space to generate *sufficient support* for the estimator [84, 85]. Two distinct problem statements are developed to distribute the regressors under time domain constraints on the

input, and this is shown by quantifying regressor distance pairs for the case of linear time-invariant (LTI) systems and Hammerstein systems. In particular, this chapter addresses the application of distribution of regressors to general multivariable and nonlinear systems to establish the importance of these results for solving a broader class of problems for which data-centric methods offer distinct advantages. Furthermore, to design input signals for highly interactive systems, the distribution in the output space is proposed as a means to additionally achieve *uniform coverage*. An alternative approach for achieving desired spread is using the concept of geometric discrepancy through Weyl's criterion, and this chapter explores this approach by extending previous work on highly interactive systems [80].

This chapter is the first of the two chapters which address data-centric input signal design. This chapter is arranged as follows: Section 4.2 describes the constraints considered in the process of input signal design. Section 4.3 discusses the requirements for experiment design in the context of data-centric methods. Section 4.4 develops the conceptual basis of the problem formulations for data-centric input signal design. The chapter ends with a summary and conclusions in Section 4.5. The ensuing Chapter 5 presents the mathematical formulations and numerical solutions for the problem statements developed in this chapter.

## 4.2 Constraints in Input Signal Design

This work considers a dynamical system $\mathcal{P}$ driven by a finite-time exogenous variable called the input $u = [u(1), \ldots, u(N)]^T \in \mathbb{R}^N$. The constraints are directly expressed as a function of time and are broadly grouped as: *1*) those originating from operating constraints which directly define the 'shape' or the time-domain realization of the signals, *2*) those defining frequency domain properties, and finally *3*) those originating from requirements on the spread or distribution of the signal in the given feasible signal space. It should be noted that some of these requirements may be in direct conflict with the requirements for achieving excitation. For example, restricting how fast a signal may change over time can limit the power of high frequency modes. Finally, since the constraints developed

here are relevant to clinical applications, the clinical interpretation will be pointed out using simple examples although the constraints considered in this work are universal in nature and broadly applicable.

### *4.2.1 Constraints Regarding the Shape of the Signal*

The three main constraints, which define the shape of the input signal, considered in this work are as follows:

1. *Amplitude constraints.* These are limits on the signal bounds that correspond to allowed maximum and minimum magnitude:

$$u_{\min} \leq u \leq u_{\max}. \tag{4.1}$$

   This constraint appears frequently in many practical applications mostly from point-of-view of safety. In a clinical application, such limitations are particularly required for medications with a smaller therapeutic window (e.g., anesthetic drugs such as ketamine) or in cases where physicians want to limit dosage changes (e.g., with opioid analgesics).

2. *Move size constraints.* These are limits on the rate of change of signal that correspond to allowed maximum change:

$$|u(k+1) - u(k)| \leq b(k). \tag{4.2}$$

   This can be written as a linear inequality in $u$:

$$Au \leq b \tag{4.3}$$

where $b \in \mathbb{R}^{2N-2}$ and $A \in \mathbb{R}^{2N-2\times N}$ is represented using two blocks of Toeplitz matrix as:

$$\left[\begin{array}{ccccc} 1 & -1 & 0 & \cdots & 0 \\ 0 & 1 & -1 & \cdots & 0 \\ \vdots & \vdots & \ddots & \vdots & \vdots \\ 0 & \cdots & 0 & 1 & -1 \\ \hline -1 & 1 & 0 & \cdots & 0 \\ 0 & -1 & 1 & \cdots & 0 \\ \vdots & \vdots & \ddots & \vdots & \vdots \\ 0 & \cdots & 0 & -1 & 1 \end{array}\right] \begin{bmatrix} u(1) \\ u(2) \\ \vdots \\ u(N) \end{bmatrix} \leq \begin{bmatrix} b \\ b \\ \vdots \\ b \end{bmatrix}. \tag{4.4}$$

Frequently in clinical applications, for patient safety and comfort, the drug dosage cannot be suddenly changed and hence has to be altered in a less abrupt manner. For example, drug gabapentin has been proposed to treat neuropathic pain and there the drug dosage profile over time cannot be abruptly modified [188]. This specific example is discussed in context of input signal design in Section 5.2.

3. *Switching time constraints.* These consider fixing the signal magnitude over a period of time ($T_{\text{sw}}$):

$$\sum_{j=1}^{T_{\text{sw}}-1} (u(k) - u(k+j)) = 0 \quad \forall k = 1 + n_{\text{sw}} \times T_{\text{sw}},\ n_{\text{sw}} = 0, 1, 2, \ldots. \tag{4.5}$$

This can be written as a linear equality in $u$:

$$A_{T_{\text{sw}}} u = 0 \tag{4.6}$$

where $A_{T_{\text{sw}}} \in \mathbb{R}^{(T_{sw}-1)\frac{N}{T_{sw}}\times N}$ is block diagonal matrix. This requirement is also commonly observed in clinical practice. For example, patients may have to visit a clinic to pick up their medication say every Monday. However, the dosages are assigned for daily consumption. As a result, dosage change is possible only at weekly frequencies $T_{\text{sw}} = 7$ rather than daily ($T_{\text{sw}} = 1$). For the case of weekly switching,

the system is sampled on a daily basis and the weekly input change is produced using switching time constraint. More broadly, this constraint satisfies the requirement that the dosages are not changing very frequently. For algorithmic details on generation of this constraint, see Section 7.3 where it has been developed in context of hybrid model predictive control.

**Definition 5.** *The constraints (4.1), (4.3) and (4.6) determine the shape of the input signal and form the set* $\mathbb{U}$ *as:*

$$\mathbb{U} = \{u \in \mathbb{R}^N : u_{\min} \leq u \leq u_{\max}, Au \leq b, A_{T_{\text{sw}}} u \leq 0, A_{T_{\text{sw}}} u \geq 0\}, \tag{4.7}$$

*which is convex and semialgebraic*[1]*.*

In addition to this convexity, the equations defining the set $\mathbb{U}$ are sparse in the variable $u$, i.e., it is not composed of all the elements $u(1)$ to $u(N)$. This fact has important implications for use in techniques from polynomial optimization. Without loss of generality, it can be assumed that the origin lies in this set (e.g., by assuming that the amplitude constraints are symmetric). Since the set $\mathbb{U}$ is defined by intersection of finite number of linear inequalities and equalities, it is a *polytope* [123]. The importance of these facts are discussed in more detail in Section 4.4 and Section 5.3.4. In addition to these three constraints, the following requirements may be desired:

4. *Length of signal* $(N)$ *constraint.* This considers a finite duration of the experiment as the costs incurred during testing may depend directly on the length of the experimentation [50]. Hence practical application of the condition under which asymptotic results of system identification hold true, i.e. $N \to \infty$, is not possible. For example, in a clinical trial, there are limitations on the overall duration i.e. the test cannot go on indefinitely. Typically the minimum length of the input signal design has to be such

[1]Loosely speaking, a semialgebraic set is defined by intersection of finite number of real polynomial inequalities [189]. Clearly, such a set may not be convex. Also note that the linear equality constraint has been written in terms of two inequality constraints.

that the dynamical effects can be captured. Furthermore, for the ease of validation, it is desirable that multiple periods of the signal can be implemented. Towards this, experiment can be designed such that it yields smallest possible signal length or least cost [190].

5. *Integer constraints.* These consider that input values can attain discrete or categorical values from a finite set $\mathbb{I} \subset \mathbb{Z}$ or in general:

$$u(k) \in \mathbb{I} = \{u_{-n}, u_{-(n-1)}, \ldots, u_0, \ldots, u_{n-1}, u_n\}. \tag{4.8}$$

In general, this constraint supersedes the amplitude constraints when both are enforced together. For example, the dosages of medication may be compounded into pills of a standard concentration, and hence any subsequent increase in dosage can be prescribed as an integer multiple of that basic dose. In other words, an arbitrary dosage magnitude can not be generally assigned.

From an optimization perspective, this implies that the problems require integer programming. To enable the use of tools from polynomial optimization, a reformulation can be proposed: $u(k) \in \mathbb{I}$ can be replaced by a polynomial which has roots at the desired integer points $u(k) \in \mathbb{I}$ iff

$$(u(k) - u_{-n})(u(k) - u_{1-n})...(u(k) - u_{n-1})(u(k) - u_n) = 0 \quad \forall k, \tag{4.9}$$

and can be further relaxed as

$$u(k) \in \mathbb{I} \quad \approx \quad |\prod_{i \in \mathbb{I}} (u(k) - i)| \leq \epsilon \quad \forall k \tag{4.10}$$

where $\epsilon$ is the parameter used for accuracy. The equality constraint version of (4.10) with $\epsilon = 0$ is an exact reproduction of the integer constraints.

6. *Norm constraints.* These are limits on the 2-norm and 1-norm of the input signal. The amplitude constraints (4.1) can be interpreted as limits on the infinity norm of the

signal. Similarly, the input signal can be constrained to have finite power by limiting the 2-norm of the finite signal

$$\|u\|_2^2 = \sum_{k=1}^{N} u(k)^2 \leq l_2^{\max} \tag{4.11}$$

which can be written as a quadratic function in $u$ and is convex. Similarly, the sum of absolute values can be constrained

$$\|u\|_1 = \sum_{k=1}^{N} |u(k)| \leq l_1^{\max} \tag{4.12}$$

which can be written as a linear function of $u$.

7. *Miscellaneous safety constraints.* These include additional safety constraints such as toxicity constraints based on how much drug has accumulated in the body and has yet to be metabolized by the patient. These can be represented as capacity constraints in a production-inventory system. Considerations such as these are common in cancer/chemotherapy trials, but will not be further developed in this dissertation.

In many practical situations, in addition to limitations on the input, there is a need to limit aspects of the output from the system. Consider an output signal $y = [y(1), \ldots, y(N)]^T \in \mathbb{R}^N$ generated by a linear time-invariant, discrete-time, stable, single input-single output system represented as

$$y = Gu, \tag{4.13}$$

where $G \in \mathbb{R}^{N \times N}$ is the Toeplitz matrix of system impulse response $h$:

$$G = \begin{bmatrix} h(1) & 0 & 0 & \cdots & 0 \\ h(2) & h(1) & 0 & \cdots & 0 \\ \vdots & \vdots & \ddots & \vdots & \vdots \\ h(N) & h(N-1) & h(N-2) & \cdots & h(1) \end{bmatrix} \tag{4.14}$$

and $N$ is chosen large enough to capture all of the dynamics. In other words, the output $y(k)$ is generated using discrete convolution. As shown for the input case, the following

constraints can be implemented: *Amplitude constraints* limit the output signal bounds that correspond to allowed maximum and minimum magnitudes:

$$y_{\min} \leq y \leq y_{\max}. \tag{4.15}$$

For a clinical example, consider the pain treatment problem shown in Chapter 2. The requirement is that the pain magnitude (measured on a scale of $0 - 100$) should be varied within certain limits for patient comfort and safety where the output is generated as per the linear dynamical constraint shown in (4.13). Next constraint considers limiting the rate of change of output deviation:

$$|y(k+1) - y(k)| \leq b_y(k). \tag{4.16}$$

In the pain intervention example, this constraint would limit the rate of change of reported pain as a sharp, sudden increase in pain symptoms is undesirable. For LTI systems, rate of change constraints on the output can be written as a linear inequality in $u$:

$$A(Gu) \leq b_y \tag{4.17}$$

where $b_y \in \mathbb{R}^{2N-2}$ is a bound on output changes. Similarly, equality constraints can be derived for switching time restrictions on the output. Since the output constraints for LTI systems can be described using linear inequalities, these can be added to the definition of set $\mathbb{U}$. By extension, output constraints are important in nonlinear dynamical systems. For example, the output from a Hammerstein system with input static nonlinearity $\mathcal{I}$ can be written as:

$$y = G\mathcal{I}(u). \tag{4.18}$$

It should be noted that the underlying notion of convexity of the feasible set $\mathbb{U}$ may be lost when output constraints are considered while it still remains semialgebraic. For example, the requirement $g(u) \geq y_{\min}$ is nonconvex when the nonlinearity $g(\cdot)$ is convex quadratic.

In conclusion, the constraints considered in this work are defined as part of "plant-friendly" or "patient-friendly" framework based on the fact that they cause minimum disruption to the normal operation of the system under constraints [81, 57]. As alluded in the Introduction, plant or patient friendliness considers the generation of a *deterministic* signal $u$ to satisfy hard bounds defined by the practical requirements. The ensuing section enumerates constraints defined in the frequency domain.

### *4.2.2 Constraints on the Spectral Properties of the Signal*

As discussed in Section 3.4.1, an experiment is considered informative if it allows discrimination between two parametric models and towards this, a condition on the autocorrelation or input spectrum ($\Phi_u(\omega)$) can be derived such that the input is persistently exciting [45]. Further, it can also be shown that the optimal input for minimum parameter variance for LTI system can be expressed in terms of its spectrum [45]. Thus, the input signal spectrum is an important design parameter in input design for linear systems. This is further discussed in Section 6.3.

The infinite dimensional variable ($\Phi_u(\omega)$) has to be properly parameterized to be used by an optimization procedure. As before, consider a real signal $u \in \mathbb{R}^{\mathbb{N}}$. For the purpose of illustration, quasi stationarity of the deterministic input is assumed [45]. The discrete-time Fourier transform (DTFT) of the signal is given as

$$U(\omega) = \sum_{k=1}^{N} u(k) e^{-j\omega k}, \quad \omega \in [0, \pi]. \tag{4.19}$$

Since the signal is finite ($u(k) = 0 \ \forall k < 1, k > N$) and bounded, the Fourier transform always exists. Next, the spectrum of $u$ is defined as the square of the magnitude of the DTFT as

$$\Phi_u(\omega) = |U(\omega)|^2 = |\sum_{k=1}^{N} u(k) e^{-j\omega k}|^2. \tag{4.20}$$

It should be noted that a linear relation can be found using the Wiener-Khinchin theorem as

$$\Phi_u(\omega) = |U(\omega)|^2 = \sum_{k=-\infty}^{\infty} r(k)e^{-j\omega k} \geq 0, \tag{4.21}$$

where $r(k)$ are the autocorrelation coefficients from the finite signal. However, it is difficult to formulate the problem using (4.21) with time domain constraints. Hence, the relation shown in (4.20) is used as the parametrization directly in $u$. Clearly, the DTFT shown in (4.20) is a semi-infinite constraint. Computationally, this can be effectively handled by defining a finite frequency grid

$$\Omega = \Big\{\omega : \omega = k\frac{\pi}{M} \quad \forall k = 1, \ldots, M\Big\}. \tag{4.22}$$

Equation (4.20) can be further simplified using Euler's formula as:

$$|U(\omega)|^2 = (a^T u)^2 + (b^T u)^2 \tag{4.23}$$

where,

$$a = [\cos\omega \ \ldots \ \cos N\omega]^T, \tag{4.24}$$

$$b = [\sin\omega \ \ldots \ \sin N\omega]^T. \tag{4.25}$$

It can be seen that (4.23) is a second-order polynomial in $u$ which is greater than zero $\forall\omega \in \Omega$. Consequently, this sum-of-squares condition can be expressed as

$$|U(\omega)|^2 = u^T Q(\omega) u, \quad Q(\omega) \succeq 0 \ \forall\omega \in \Omega. \tag{4.26}$$

As the expression (4.26) is already in sum-of-squares form, the matrix $Q(\omega)$ can be obtained by solving a SDP [174]. The requirement that the spectrum of the input signal exactly satisfy a certain frequency function $\gamma(\omega)$ is represented using quadratic equality and hence nonconvex:

$$u^T Q(\omega) u = \gamma(\omega), \quad \omega \in \Omega. \tag{4.27}$$

Expanding the equality constraint as two contrasting inequality constraint, the condition $u^T Q(\omega)u \leq \gamma(\omega)$ is convex, where as the condition $u^T Q(\omega)u \geq \gamma(\omega)$ is nonconvex. In

addition to this nonconvexity, the objective is also not sparse in the variable $u$, i.e., the function is composed of all the elements $u(1)$ to $u(N)$. This observation leads to the conclusion that the spectrum function cannot be used by sparse polynomial optimization procedures which work efficiently only when the objective and constraints are a function of few of the elements from the decision vector. Finally, it should be also emphasized here that these results hold true for a linear system where the information matrix can be completely characterized by second order moments (or the spectrum) of the input signal. For a nonlinear system, the information matrix depends on higher order moments of the input signal and additional conditions have to be derived.

### *4.2.3 Constraints on the Distribution of the Signal*

Among the requirements of plant-friendliness is that the input (and output) signals are distributed (in some sense) in the feasible signal space [50, 151]. In general, signal with desired spectral property, for example with persistence of excitation, are not well distributed over the signal span. Several criterion have been proposed in the literature to achieve certain signal distribution [191, 192, 80].

Among the metrics that can be used to quantify this distribution is crest factor [146, 191, 82] which can be defined as

$$\mathrm{CF}(x) = \frac{x_{\mathrm{peak}}}{x_{\mathrm{rms}}} = \frac{\max\limits_{k}|x(k)|}{\sqrt{\frac{\sum_k x(k)^2}{N}}}, \tag{4.28}$$

where $x = u$ or $y$ is a signal of length $N$. The crest factor varies as $1 \leq \mathrm{CF}(x) < \infty$ such that a low crest factor implies a fully even distribution of the signal. Another metric is the Performance Index for Perturbation Signals (PIPS) [192], which is defined as

$$\mathrm{PIPS}(\%) = 200 \times \frac{\sqrt{x_{\mathrm{rms}}^2 - x_{\mathrm{mean}}^2}}{\max(x) - \min(x)}. \tag{4.29}$$

PIPS is expressed in percent form ($0\% \leq \mathrm{PIPS}(x) \leq 100\%$). In practice, a high PIPS value corresponds to a signal which has low crest factor. Since PIPS is expressed in percent form, it can be argued that it is a more intuitive measure than the crest factor where higher PIPS

value suggests even signal distribution. Both metrics (crest factor and PIPS) force the signal to spread near its extremities (i.e. the signal histogram has peaks at the end) which gives it a better signal-to-noise ratio. The lower bound on the crest factor (i.e., $\mathrm{CF}(x) = 1$) can be obtained, for example, when the signal is binary and symmetric.

The spread in the extremities, however, is not always sufficient. In the case of a multi-variable system, it is often necessary to have good directionality for all inputs. One of the metrics to achieve uniform directionality is using results from discrepancy theory [193] such as Weyl's criterion [194]:

$$\lim_{N\to\infty} \frac{1}{N} \sum_{k=1}^{N} e^{(2\pi \ell x(k))i} = 0 \quad \forall \ell \in \mathbb{Z} - \{0\}, \tag{4.30}$$

which gives the necessary and sufficient condition for a sequence $x$ to be uniformly distributed in $[0, 1)$. A uniform distribution in the output is also an useful requirement for data-centric system identification methods which rely on generating models based on the current operating conditions. In general for data-centric methods, a more complete approach is to cover the regressor space. This has been discussed in more detail in Section 4.4.

From a computational point-of-view, the requirements shown in (4.28)-(4.30) are non-convex and nonsparse in $u$, and hence present difficult optimization problems [81]. For example, Figure 4.1 shows the surface plot of the crest factor function when the input signal is two dimensional. The function is nonconvex with multiple minimas. The minimum value the function is one, which is obtained when signal is binary or constant ('D.C.'). On the other hand, for amplitude constrained signal, the PIPS metric can be written as a smooth function by making the denominator constant. Thus, metrics such as PIPS can be added as constraints in nonlinear optimization problems which are easier to solve than the one involving crest factor. This can be written as

$$200 \times \frac{\sqrt{x_{\mathrm{rms}}^2 - x_{\mathrm{mean}}^2}}{\max(x) - \min(x)} \geq \kappa_x \quad x = u \text{ or } y, \tag{4.31}$$

where $\kappa_x$ is a minimum desired PIPS metric. It is generally not possible to know *a priori* the minimum metric, hence one has to proceed in an iterative way such that a feasible

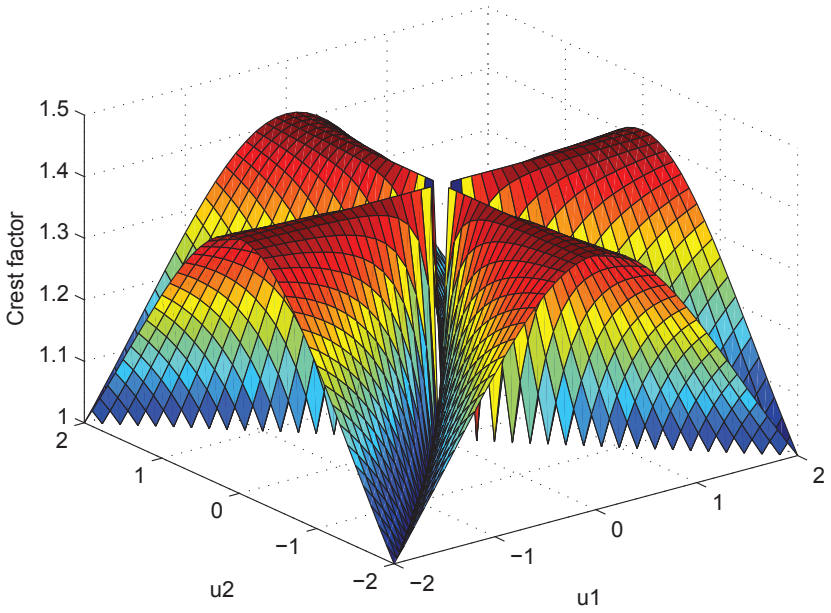


Figure 4.1: Surface plot of the crest factor function (4.28) where $u = [u(1), u(2)]^T$.

solution can be found. Finally, the expanded Weyl's criterion

$$\mathrm{Re}\left\{\frac{1}{N}\sum_{k=1}^{N} e^{(2\pi\ell x(k))i}\right\} \leq \delta \quad \forall \ell \in \mathbb{L} \subset \mathbb{Z} - \{0\} \tag{4.32}$$

$$\mathrm{Im}\left\{\frac{1}{N}\sum_{k=1}^{N} e^{(2\pi\ell x(k))i}\right\} \leq \delta \quad \forall \ell \in \mathbb{L} \subset \mathbb{Z} - \{0\}, \tag{4.33}$$

can be used where $\delta$ is a relaxation parameter used to approximately satisfy Weyl's criterion (given that only finite data points are available) using integers from a finite set $\mathbb{L} \subset \mathbb{Z} - \{0\}$. In the remainder of this dissertation, it is assumed that Weyl's criterion is satisfied only approximately. This assumption is not particular restrictive in practice, and good results have been reported by using this approximation as long as the signal length is not too short [153]. The ensuing section discusses data-centric estimation and associated experiment design issues to address design of input signals.

## 4.3 Data-Centric Estimation and Experiment Design

As before, consider a SISO process for a given data set $(\{y(k),\ \varphi(k)\}_{k=1}^{N})$ as:

$$y(k) = f(\varphi(k)) + e(k), \quad k = 1, \ldots, N, \tag{4.34}$$

where $y(k) \in \mathbb{R}$, $f(\cdot)$ is an unknown smooth nonlinear mapping, $\varphi(k)$ is the regressor vector and $e(k) \in \mathbb{R}$ is the noise. In a data-centric framework, a predictor function $\hat{f}$ can be obtained from a linear combination of observed outputs

$$\hat{f}(\varphi^*) = \sum_{k=1}^{N} w(k)y(k) = w^T y. \tag{4.35}$$

The weight $w$ is chosen by a procedure (based on a kernel or through optimization as discussed in Section 3.3.2) to minimize the mean square error (MSE) of the estimate

$$\mathbb{E}\{(\hat{f}(\varphi^*) - f(\varphi^*))^2\} \tag{4.36}$$

where $\mathbb{E}$ is the expectation operator. This error equation is a function of the distance of regressors from the current operating point $(\varphi^* - \varphi(k))$, the noise variance and properties of the mapping $f(\cdot)$ such as local smoothness [55, 90, 56]. In particular, the following factors determine the quality of the estimate for data-centric methods:

1. The structure of the regressor vector $\varphi(k)$ as a function of the input $u$. The regressor structure should correspond to what is suitable for a local linear model (e.g., from linearization of an *a priori* nonlinear model). Note that the distance between two regressors can become prohibitively large for higher dimensions of the regressor space. In practice, large number of systems can be well approximated with low dimension regressors.

2. The properties of the mapping $f(\cdot)$ such as local smoothness. For some data-centric estimators such as direct weight optimization (DWO), bounds on the Lipschitz constant and the Hessian matrix also influence the estimate quality.

3. The nature of the experimental data, for example, noise $e(k)$ and the number of data points ($N$). It is common to assume the stochastic nature of noise where $e(k),\ k = 1, \ldots, N$ can be defined using zero-mean, finite variance sequence of independent random variables.

4. The location of the current point $\varphi^*$ and the *distribution* of regressors in the regressor space.

For the case of global parametric methods, the classical optimal input signal design problem is conducted in the parameter space, for a fixed model, by minimizing some scalar measure of the parameter covariance matrix with specific requirements on higher order properties of the input, such as signal spectrum [45, 52, 53]. It should also be pointed out that the resulting design is optimized for that parametric structure and hence could be quite poor if these assumptions are not accurate [45]. In contrast, data-centric methods possess distinctive requirements, as the dataset is not expected to be captured by a single fixed parametric model. From the parametric school of thought, the biggest challenge with data-centric input signal design is that since no fixed parametric model is estimated, it is difficult to quantify the accuracy of the estimates globally. For example, consider the case of MoD estimator where a local linear model is estimated at each point [55]. Under certain conditions, it can be shown that this linear estimator optimally minimizes the mean squared error [144] as follows (for the 2-norm of the error):

$$\min \sum_{k=1}^{N} \{y(k) - (\beta_0 + \beta_1^T(\varphi(k) - \varphi^*))\}^2 \times W(\varphi(k) - \varphi^*) \tag{4.37}$$

where $W$ is a kernel function. The parameters, at point $\varphi^*$, are calculated by solving the linear least square problem

$$\hat{\beta} = (\mathcal{X}^T W \mathcal{X})^{-1} \mathcal{X}^T W Y \tag{4.38}$$

where $\mathcal{X}$ is formed using regressors $\varphi(k)$ and $\varphi^*$. An optimal input can be designed to maximize the information content for these parameters by minimizing some measure of the

error ellipsoid or the maximizing the information matrix, for example:

$$\max \det(\mathcal{X}^T W \mathcal{X}) \tag{4.39}$$

where $\det(\cdot)$ is the determinant function and the optimal design is a function of $\varphi^*$. However, the estimation problem will be repeated at a new point and a new set of parameters will have to be identified. In other words, the optimal design can be performed only for a fixed set of parameters but which keep on changing in data-centric system identification. Clearly, an input can be design for fixed or known operating point $\varphi^*$ but such an approach may not be directly practical for these class of methods. In a general function estimation setting, it is assumed that the regressors are distributed using random or fixed designs [56, 195, 196, 54]. In the nonparametric statistical literature, designs have considered some notion of parametric structure [197] or a Bayesian-based maxmin distance design for computer experiments and not in the context of dynamical systems [198, 53].

As noted earlier, the factors that can be influenced by experimental design include the distribution of regressors and the number of data points. For a dynamical system, the regressor distribution has to be shaped by an input signal where the regressors tend to be dependent. Frequently for data-centric estimation methods, a signal sampled from some probability distribution is used, but this is generally an arbitrary choice and may not result in an informative dataset. The other issue is limited length of data collected in experiments, specially those in biology and medicine, which may violate the strong assumptions made on the probability distribution of the uncertainty [58]. This chapter develops a novel method to address input design for data-centric system identification by developing *sufficient support* for the estimator by filling the regressors space. The formulation is inspired by its geometric interpretation, is not explicitly dependent on $\varphi^*$, and does not place conditions on the sources of uncertainty. Like other optimal designs, generating the optimal input requires *a priori* knowledge of the true system [45], although the requirements are not as stringent given the geometric nature of the formulation. This is achieved using two approaches:

by directly addressing the geometric distribution of regressors and by using the Weyl's criterion. This is now discussed in the ensuing section.

## 4.4 Data-Centric Input Signal Design: Problem Statements

This section introduces the problem statements and thus provides a mental picture associated with two approaches for data-centric input signal design: one based on distribution of regressors and output, and the other based on the Weyl's criterion.

### *4.4.1 Distribution of Regressors for Dynamical Systems*

As noted previously, it is often simpler to describe the modeling process in system identification as a mapping from the regressor space (which contains finite lagged data about the dynamical system) to the output space [88]. Following two regressor structures are commonly used [88, 54]:

1. Finite Impulse Response (FIR) structure

$$\varphi(k) = [u(k-n_k) \; ... \; u(k-n_b-n_k+1)]^T \tag{4.40}$$

2. AutoRegressive with eXogenous input (ARX) structure

$$\varphi(k) = [y(k-1) \; ... \; y(k-n_a) \;\; u(k-n_k) \; ... \; u(k-n_b-n_k+1)]^T, \tag{4.41}$$

where $y, u$ denote the output and input signals respectively, $n_a$, $n_b$ and $n_k$ denote the number of previous instances of the output, input and the degree of delay in the model and the regressor vector $\varphi(k) \in \mathbb{R}^m$ where $m = n_a + n_b$. Consequently, the regressor vector $\varphi(k)$, as shown in (4.41), can be written in terms of $u$ as:

$$\varphi(k) = \begin{bmatrix} P_k G \\ Q_k \end{bmatrix} u, \tag{4.42}$$

where $P_k \in \mathbb{R}^{n_a \times N}$, $Q_k \in \mathbb{R}^{n_b \times N}$ and the dynamical relation shown in (4.13). The case of the Finite Impulse Response (FIR) regressor structure can be derived as a special case

$$\varphi(k) = \begin{bmatrix} 0_{n_a \times N} \\ Q_k \end{bmatrix} u. \tag{4.43}$$

The matrices $P_k, Q_k$ are sparse with rank equal to $\max\{n_a, n_b\}$. For the FIR case, the dimension of the regressor $m$ has to be generally large to capture all of the dynamics. In contrast, a relatively low dimension is often suitable in the case of the ARX structure [88, 54]. Finally, keeping the same structural relationship, other regressors structures can be considered to incorporate separate noise models [54, 141].

The equation (4.42) establishes the relationship that the regressor is a function of the input signal for a dynamical system. Given that the input lies in the set $\mathbb{U}$, the regressor lies in the set $\mathbb{P}$ defined as

$$\mathbb{P} = \{\varphi(k) \in \mathbb{R}^m : \varphi(k) = f_k(u), u \in \mathbb{U}\}. \tag{4.44}$$

where $f_k$ is the unique mapping (depending on the system) for given $k$. Given the lagged nature of the discrete-time representation of the dynamical system, the initial regressors can be assumed to be at the origin. These observation leads to the following definition:

**Definition 6.** *The set of regressors $\mathbb{P}$ is a projection of the feasible set of input $\mathbb{U}$. For linear dynamical systems, the set $\mathbb{P}$ is a polytope containing the origin [199]. For general nonlinear dynamical systems, the projection is of nonlinear nature and hence, the convexity of the set may be lost.*

Since the aim of the formulation is to distribute the regressors points, the idea of regressor distance pair has to be defined. This is introduced initially for linear systems for which the set $\mathbb{P}$ is a polytope, and generalized later for block-structured nonlinear systems. The notion of distance in the space $\mathbb{R}^m$ can be defined using any $p$-norm distance. In this work, the Euclidean distance (2-norm distance) is used as the metric which is also used to calculate

the bandwidth of the estimator as discussed in Section 3.3.2. Based on the parametrization shown in (4.42), the square of the Euclidean distance between two regressor points can be defined as:

$$d_{ij}^2 = \|\varphi(i) - \varphi(j)\|_2^2 \tag{4.45}$$

$$d_{ij}^2 = (\varphi(i) - \varphi(j))^T(\varphi(i) - \varphi(j)), \tag{4.46}$$

which can be expanded as a polynomial

$$d_{ij}^2 = u^T \underbrace{\begin{bmatrix} (P_i - P_j)G \\ Q_i - Q_j \end{bmatrix}^T \begin{bmatrix} (P_i - P_j)G \\ Q_i - Q_j \end{bmatrix}}_{\mathbf{Q}_{ij} \in \mathbb{R}^{N \times N}} u, \tag{4.47}$$

where $d_{ij}$ is the distance between the $i$th and $j$th regressor as a function of the input. The unique regressor distances form a finite set $\mathcal{K}$:

$$\mathcal{K} = \{d_{ij} \in \mathbb{R} : i \in \{1, \ldots, N-1\}, j \in \{i+1, \ldots, N\}\}, \tag{4.48}$$

with the set cardinality given by $N(N-1)/2$ which is polynomial in $N$, e.g., the number of distance pairs $\simeq N^2/2 \; \forall N \gg 1$. In the case of a Hammerstein structure, the regressor vector can be written as

$$\varphi(k) = \begin{bmatrix} P_k G \\ Q_k \end{bmatrix} w_H. \tag{4.49}$$

Given that $w_H$ cannot be directly manipulated (as shown in Fig. 4.2), the regressor can be expressed ultimately as a nonlinear function of the system input $u$

$$\varphi(k) = \begin{bmatrix} P_k G \\ Q_k \end{bmatrix} \mathcal{I}(u). \tag{4.50}$$

Based on the nonlinear relationship between the regressor and the input signal, the distance between two regressor can be defined as:

$$d_{ij}^2 = \mathcal{I}(u)^T \underbrace{\begin{bmatrix} (P_i - P_j)G \\ Q_i - Q_j \end{bmatrix}^T \begin{bmatrix} (P_i - P_j)G \\ Q_i - Q_j \end{bmatrix}}_{\mathbf{Q}_{ij}} \mathcal{I}(u). \tag{4.51}$$

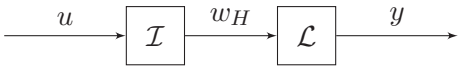


Figure 4.2: Noise-free input-output representation of a Hammerstein system where $\mathcal{I}$ is the static nonlinearity and $\mathcal{L}$ is the LTI system.

Similar expressions can be derived for the other block-structured systems such as Wiener and Hammerstein-Wiener systems.

The main argument made in this approach is now presented. Consider that, in general, a convex hull $\mathcal{D}$ can be constructed based on the available regressor points. Since the estimate is formed by *interpolation* of available outputs, as shown in (4.35), if the current operating point $\varphi^*$ lies beyond the convex hull $\mathcal{D} \subset \mathbb{R}^m$, the estimator would have to *extrapolate* rather than interpolate. Hence, the central idea is to generate sufficient support for the estimator where the extent of spread of regressors is fundamentally dictated by the constraints under which the system is operating and can be optimized by the choice of the input signal. On the other hand, the noise in the model is not a function of the input and hence cannot be optimized. For LTI systems, when the regressor points are vertices of the polytope $\mathbb{P}$, the set $\mathcal{D}$ and $\mathbb{P}$ are same; in other words a larger hull cannot be constructed [199]. The input signal design is achieved through two optimization-based formulations which consider spreading the regressor points in two different ways. The first formulation considers covering the complete regressor space under dynamical constraints. Thus, the input signal can be designed to cover the full span in the regressor space, under possible constraints, to generate enough support and thus to insure that the estimator is interpolating. This formulation is particularly useful when the system is operating close to saturation. These observations lead to the first problem statement:

**Problem Statement 1.** *Given $N$ regressor vectors of fixed finite dimension, distribute the regressor points as far apart from each other as possible in the regressor space under constraints on the input and output signals.*

Problem Statement 1 can be achieved by maximizing the sum of all the regressor distances:

$$J_1 = \max_u \sum_{i=1}^{N-1} \sum_{j=i+1}^{N} d_{ij} \tag{4.52}$$
$$\text{s.t.} \quad u \in \mathbb{U}$$

where $i$ and $j$ are selected to define unique distance pairs as per the finite set $\mathcal{K}$.

The second formulation considers a more uniform distribution of regressors given that the choice of weights is a function of the distance of $\varphi^*$ from the available regressor vectors $\varphi(k)$. This is more useful for kernel-based estimation methods, and leads to the second problem statement:

**Problem Statement 2.** *Given $N$ regressor vectors of fixed finite dimension, distribute the regressor points such that given any two regressors can be as far apart as possible in the regressor space under constraints on the input and output signals.*

Problem Statement 2 can be interpreted as maximizing the minimum regressor distance pair:

$$J_2 = \max_u \min d_{ij}, \ d_{ij} \in \mathcal{K} \tag{4.53}$$
$$\text{s.t.} \quad u \in \mathbb{U}.$$

In Section 5.3, these two formulations are developed and analyzed for LTI and block-structured nonlinear system under input constraints. In addition to the constraints on the input for these problem statements, if the operating point $\varphi^*$ is known *a priori* to lie in a convex polytope $\mathcal{D}_c \subset \mathcal{D}$, corresponding linear inequalities in $u$ can be derived using (4.42) [123]. Also, if the operating point $\varphi^*$ is fixed, the regressors can be centered around that point as

$$\frac{1}{N} \sum_{k=1}^{N} \varphi(k) = \varphi^*, \tag{4.54}$$

which can be expressed as a linear equality ($A_{\text{op}}u = b_{\text{op}}$) and added to the definition of set $\mathbb{U}$.

### *4.4.2 Extensions to Problem Statements Relating to the Distribution of Regressors*

The problem statements developed in the previous section addressed distribution of regressors under constraints. Various extensions can be proposed on these problem statements by incorporating multivariable dynamics, alternative distance metrics and noise models. These points are briefly described in the following paragraphs as themes for future research.

So far, the problem formulations have only considered single-input single-output (SISO) systems. It is of interest to extend these approaches to multivariable systems which consist of multiple manipulated inputs and disturbances interacting with multiple outputs, as these are commonly found in many practical applications ranging from high-purity distillation [80] to aerospace systems [41]. It is simple to show that the geometric concept of distribution of regressors can be logically extended to cases beyond SISO systems for data-centric estimation methods in a multivariable setting.

For purpose of illustration, consider a multi-input single-output (MISO) system described by $n_x$ inputs:

$$y(k) = P_1(q)u_1(k) + \cdots + P_{n_x}(q)u_{n_x}(k) \tag{4.55}$$

where $P_1(q), \ldots, P_{n_x}(q)$ represent open-loop stable transfer functions. In the worst case, each individual transfer function is parametrized uniquely by a regressor of different dimensions: $\varphi_i(k)$ which are defined as per (4.41). To be used by the data-centric methods, these individual regressors can be stacked together to form

$$\varphi(k) = [\varphi_1(k)^T, \varphi_2(k)^T, \varphi_3(k)^T, \ldots, \varphi_{n_x}(k)^T]^T \tag{4.56}$$

where the dimension of the new regressor space $m$ is equal to the sum of dimensions of the individual regressors

$$m = \sum_{i=1}^{n_x} (n_{ai} + n_{bi}), \tag{4.57}$$

where $n_a$ and $n_b$ are defined as per (4.41). To achieve optimal distribution in the regressor space, the stacked regressor replaces the SISO regressor in earlier derived formulations. Hence, all the problem statements derived in Section 4.4.1 for SISO systems naturally carry over to the MISO case. The multi-input multi-output (MIMO) case is handled on an output-by-output basis (i.e. multiple MISO systems, one output at a time) by the data-centric estimator. Since the input design based on distribution of regressors follows the structure of data-centric estimator, the subsequent design procedure can be described on a per output basis for MIMO systems. This implies that a regressor 'matrix' can be defined where each column, which would correspond to a particular output, contains the stacked regressors for the multiple inputs as shown in (4.56).

The other topic of interest is the parametrization of the regressor distance pairs. The 2-norm distance or the Euclidean distance is the most natural metric for calculating distances. In a finite dimensional vector space, the distance between two regressor can be measured in other norms. In particular, the infinity norm or the Chebyshev distance may be used which can offer distinct computational advantages as the distance $d_{ij}$ can be expressed as linear function of the input $u$. In that situation, selected distances pairs may be chosen so that the regressor space is completely covered. From a computational aspect, choosing selective Euclidean distance pairs in the context of inducing sparsity for polynomial optimization is discussed in Section 5.3.4.

Next, the patient-friendly constraints on the output signal developed in Section 4.2 consider only the plant part of the dynamical model. In case a detailed noise model is available, either through first principles or through system identification, the constraints on the measured output can be appropriately updated. Using the standard framework in parametric system identification [45], the dynamical model is updated as

$$y = Gu + He \tag{4.58}$$

where $G$ is defined in (4.14), $H \in \mathbb{R}^{N\times N}$ is the Toeplitz matrix of impulse response of the

noise model and $e \in \mathbb{R}^N$ is the noise. In the same parametric framework, $e$ is generally defined as vector of random variables with zero-mean and covariance matrix $\Lambda$. If the noise contribution belongs to a uniform distribution, the amplitude bounds, for example, can easily be shifted as the noise signal is known to be bounded. The Gaussian distribution, on the other hand, is unbounded and hence data up to three standard deviation can be included to approximately satisfy the amplitude constraints for Gaussian noise.

Progressing this further, the improved dynamical model implies that the distances $d_{ij}$ are now random variables. Consequently, the problem statements can be modified to account for this uncertainty by satisfying the objectives on an average. For example, Problem Statement 1 can be modified as

$$J_1 = \max_u \mathbb{E}\Big[\sum_{i=1}^{N-1}\sum_{j=i+1}^{N} d_{ij}\Big] \tag{4.59}$$
$$\text{s.t.} \quad u \in \mathbb{U}$$

where $\mathbb{E}$ is the expectation operator. Given the assumptions on the noise, it is simple to derive the effect of noise on the regressor distance pairs. For example, for LTI systems extending from (4.42), the regressor $\varphi(k)$ can be written as

$$\varphi(k) = \begin{bmatrix} P_k G \\ Q_k \end{bmatrix} u + \begin{bmatrix} P_k H \\ \mathbf{0} \end{bmatrix} e, \tag{4.60}$$

and the regressor distance pairs $d_{ij}^2 = (\varphi(i) - \varphi(j))^T(\varphi(i) - \varphi(j))$ can be derived as

$$\begin{aligned} d_{ij}^2 = e^T \underbrace{\begin{bmatrix} (P_i - P_j)H \\ \mathbf{0} \end{bmatrix}^T \begin{bmatrix} (P_i - P_j)H \\ \mathbf{0} \end{bmatrix}}_{\mathbf{Qee}_{ij}} e + e^T \underbrace{\begin{bmatrix} (P_i - P_j)H \\ \mathbf{0} \end{bmatrix}^T \begin{bmatrix} (P_i - P_j)G \\ Q_i - Q_j \end{bmatrix}}_{\mathbf{Qeu}_{ij}} u \\ + u^T \underbrace{\begin{bmatrix} (P_i - P_j)G \\ Q_i - Q_j \end{bmatrix}^T \begin{bmatrix} (P_i - P_j)H \\ \mathbf{0} \end{bmatrix}}_{\mathbf{Que}_{ij}} e + u^T \underbrace{\begin{bmatrix} (P_i - P_j)G \\ Q_i - Q_j \end{bmatrix}^T \begin{bmatrix} (P_i - P_j)G \\ Q_i - Q_j \end{bmatrix}}_{\mathbf{Q}_{ij}} u. \end{aligned} \tag{4.61}$$

The expected value of the regressor distance pair can be written as

$$\mathbb{E}[d_{ij}^2] = \mathrm{Tr}(\mathbf{Q}\mathbf{e}\mathbf{e}_{ij}\Lambda) + u^T \underbrace{\begin{bmatrix} (P_i - P_j)G \\ Q_i - Q_j \end{bmatrix}^T \begin{bmatrix} (P_i - P_j)G \\ Q_i - Q_j \end{bmatrix}}_{\mathbf{Q}_{ij}} u \tag{4.62}$$

using the fact that the input is a deterministic signal, properties of the noise vectors and expectation of a quadratic function [200]. Thus, the distribution of regressors under noisy conditions for LTI systems is fundamentally dictated by the deterministic part plus a constant term derived from noise. This brief analysis can be extended in more detail to work out other cases where the distribution of regressors is optimal under noise.

Finally, although the problem formulation has been derived for the data-centric system identification, the problem statements could be re-interpreted in the context of bounded-but-unknown error in the parametric model. Experiment design approaches for set membership identification methods try to minimize the volume of the set that contains the parameter [201], and a relationship could be derived in terms of distribution of regressors in the set $\mathbb{P}$.

### *4.4.3 Distribution of Time-Indexed Outputs for Highly Interactive Systems*

Highly interactive dynamical systems are multi-input multi-output (MIMO) systems where a given output of the system is affected by all or most of the inputs to the system. Quite naturally, these systems are found throughout the application domain of systems and controls, and in particular in chemical process control [202]. Invariably, there is a natural tendency of highly interactive systems to exhibit gain directionality; in other words, certain inputs have a stronger effect on the output compared to other inputs in the system. This behavior is captured by the steady-state gain matrix, and hence independent of the frequency, where the condition number of the gain matrix is high or the system is ill-conditioned [41]. Although the dynamic system is linear and time invariant, the presence of gain directionality due to ill-conditioning results in poor quality of input-output data, and hence these systems are quite challenging for identification and closed-loop control [95].

The MIMO distribution of regressors developed in the previous section, however, does not directly address requirements of certain MIMO systems which are highly interactive. The data-centric methods involve function estimation in only the local vicinity of the current operating point, and hence for highly interactive systems, coverage in the output space is important [80]. Fig. 4.3 shows a sample spread of output points, for a representative model shown in (4.67), which will be obtained by using standard input signals such as pseudo random binary sequence (PRBS). The natural system response is aligned along the high gain direction with very little information about the low gain direction. Hence, the resulting output data can be quite poor by using conventional inputs in system identification and subsequently, may result in poor closed-loop performance. Previous work in system identification literature has addressed design of input signal for highly interactive systems with emphasis on the input signal spectrum. Some of the proposed methods consider using correlated PRBS with high-amplitude colinear PRBS [203] and zippered multisines [95, 81] among others. A recent comparison of different input signals for ill-conditioned systems can be found in [204]. For data-centric methods, Weyl's criterion has been proposed to achieve uniform coverage in the output space [80, 153, 152].

Consider a $2 \times 2$ linear time-invariant (LTI), stable, noise-free, continuous-time system $G(s)$:

$$\begin{bmatrix} y_1(s) \\ y_2(s) \end{bmatrix} = \begin{bmatrix} G_{11}(s) & G_{12}(s) \\ G_{21}(s) & G_{22}(s) \end{bmatrix} \begin{bmatrix} u_1(s) \\ u_2(s) \end{bmatrix} \tag{4.63}$$

where $y_1(s), y_2(s)$ are the output variables and $u_1(s), u_2(s)$ are the input variables. The continuous-time models are discretized and by using the impulse response of each discrete-time transfer function, an input-output matrix representation can be derived as shown in (4.14). Subsequently, the MIMO system can be written as

$$y_1 = G_{11}u_1 + G_{12}u_2 \tag{4.64}$$

$$y_2 = G_{21}u_1 + G_{22}u_2 \tag{4.65}$$

where $G_{ij} \in \mathbb{R}^{N\times N}$ are the Toeplitz matrices of system impulse responses $h_{ij}$

$$G_{ij} = \begin{bmatrix} h_{ij}(1) & 0 & \cdots & 0 \\ h_{ij}(2) & h_{ij}(1) & \cdots & 0 \\ \vdots & \vdots & \ddots & \vdots \\ h_{ij}(N) & h_{ij}(N-1) & \cdots & h_{ij}(1) \end{bmatrix}, \tag{4.66}$$

and $u_i = [u_i(1), \ldots, u_i(N)]^T \in \mathbb{R}^N$ and $y_i = [y_i(1), \ldots, y_i(N)]^T \in \mathbb{R}^N$ are the inputs and outputs to the system respectively. In this dissertation, a simplified model inspired from a low-order linear representation of high-purity distillation column [205] is used for the purpose of illustration:

$$G(s) = \frac{1}{2s+1} \begin{bmatrix} 87.8 & -86.4 \\ 108.2 & -109.6 \end{bmatrix}. \tag{4.67}$$

Singular values from the singular value decomposition (SVD) of the steady-state gain matrix are given by

$$\begin{bmatrix} 197.2 & 0 \\ 0 & 1.39 \end{bmatrix} \tag{4.68}$$

where the condition number is $\gamma$ is equal to $\frac{197.2}{1.39} = 141.8$. This implies that the system is ill-conditioned and the output-space will be biased towards the high-gain direction as shown in Fig. 4.3.

For this system, any point in the two dimensional output space can be index by time $k$ and hence can be written as

$$\begin{gathered} \mathcal{Y}_1 : (y_1(1), y_2(1)) \\ \mathcal{Y}_2 : (y_1(2), y_2(2)) \\ \vdots \\ \mathcal{Y}_N : (y_1(N), y_2(N)). \end{gathered}$$

As shown in Fig. 4.3, the output points $\mathcal{Y}_1, \ldots, \mathcal{Y}_N$ are aligned along the high gain direction. In order to cover more of the constrained space, the distance between any two

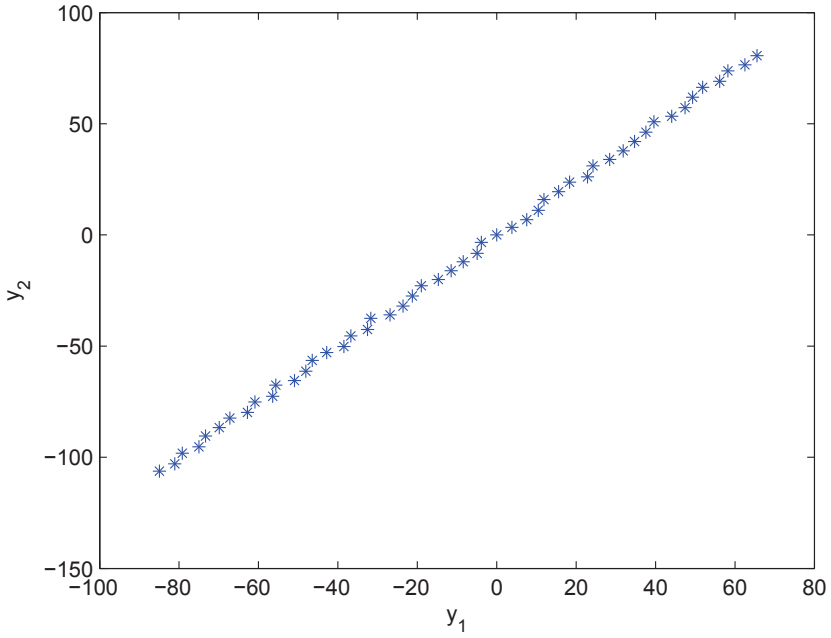


Figure 4.3: Distribution of noise-free output components $(y_1(k), y_2(k))$ showcasing alignment along the high-gain direction model for a representative system as shown in (4.67).

points has to be increased. Using the framework of distances in a finite dimensional space, the following input design problem statement is proposed:

**Problem Statement 3.** *Given finite $N$ data points $\mathcal{Y}_k$, distribute the points in the output space such that any two points are as far apart as possible under constraints on the input and output signals.*

Problem Statement 3 can be interpreted as maximizing the minimum distance between time-indexed output points:

$$J_3 = \max_u \min dy_{ij}, \ dy_{ij} \in \mathcal{K}_y \tag{4.69}$$
$$\text{s.t.} \quad u \in \mathbb{U},$$

where $dy_{ij}$ is the distance between $i$th and $j$th output point as a function of the input and the set $\mathcal{K}_y$ is defined as

$$\mathcal{K}_y = \{dy_{ij} \in \mathbb{R} : i \in \{1, \ldots, N-1\}, j \in \{i+1, \ldots, N\}\}. \tag{4.70}$$

Similar to the regressor distance pair $d_{ij}$ in Section 4.4.1, the notion of distance between two output points has to be quantified as a function of the input. The square of the Euclidean or 2-norm distance $dy_{ij}^2$ between $i$th and $j$th point in the output space can be written as:

$$dy_{ij}^2 = (y_1(i) - y_1(j))^2 + (y_2(i) - y_2(j))^2. \tag{4.71}$$

Based on the dynamical equations shown in (4.64)-(4.65), this can be algebraically simplified as:

$$\begin{aligned} dy_{ij}^2 &= \big((G_{11}(i,:)u_1 + G_{12}(i,:)u_2) - (G_{11}(j,:)u_1 + G_{12}(j,:)u_2)\big)^2 \\ &\quad + \big((G_{21}(i,:)u_1 + G_{22}(i,:)u_2) - (G_{21}(j,:)u_1 + G_{22}(j,:)u_2)\big)^2 \end{aligned} \tag{4.72}$$

$$\begin{aligned} dy_{ij}^2 &= \big((G_{11}(i,:) - G_{11}(j,:))u_1 + (G_{12}(i,:) - G_{12}(j,:))u_2\big)^2 \\ &\quad + \big((G_{21}(i,:) - G_{21}(j,:))u_1 + (G_{22}(i,:) - G_{22}(j,:))u_2\big)^2 \end{aligned} \tag{4.73}$$

where : denotes all the elements in the vector dimension, $u_1 \in \mathbb{R}^N$ and $u_2 \in \mathbb{R}^N$. The distance metric can be rearranged using matrix algebra

$$\begin{aligned} dy_{ij}^2 = \Big( \underbrace{\begin{bmatrix} (G_{11}(i,:) - G_{11}(j,:)) & (G_{12}(i,:) - G_{12}(j,:)) \\ (G_{21}(i,:) - G_{21}(j,:)) & (G_{22}(i,:) - G_{22}(j,:)) \end{bmatrix}}_{\Pi_{ij}} u \Big)^T \\ \Big( \underbrace{\begin{bmatrix} (G_{11}(i,:) - G_{11}(j,:)) & (G_{12}(i,:) - G_{12}(j,:)) \\ (G_{21}(i,:) - G_{21}(j,:)) & (G_{22}(i,:) - G_{22}(j,:)) \end{bmatrix}}_{\Pi_{ij}} u \Big) \end{aligned} \tag{4.74}$$

$$dy_{ij}^2 = u^T \Pi_{ij}^T \Pi_{ij} u = u^T \mathbf{Y}_{ij} u \tag{4.75}$$

where $u = [u1^T \; u2^T]^T$ and $\mathbf{Y}_{ij} \in \mathbb{R}^{2N \times 2N}$ is the matrix capturing the quadratic relationship. Section 5.4 presents the detailed mathematical formulation for design of inputs for highly interactive system by considering distribution in the multi-output space.

### *4.4.4 Uniform Distribution using Weyl's criterion*

An alternative to the distance-based objectives discussed earlier, is to utilize a metric which captures the 'non-uniformity' in space. One approach is to use concepts from discrepancy theory which deals with even distribution of points in space [193]. More formally, the theory tries to quantify discrepancy which tends to zero as the sequence of points are evenly distributed. A metric frequently used to capture discrepancy is the Weyl's Criterion, a classical result from number theory, which quantifies condition for equi-distributed modulo one sequences [194], and can be used to generate a low-discrepancy sequence.

To generate sufficient support for the data-centric estimator, the Weyl's criterion for uniform distribution can be applied either in the output space or in the regressor space. For data-centric methods which work by averaging the measured output, the uniform distribution in the SISO output space is more useful conceptually for this objective as well as it would be computationally more challenging to work in the regressor space. This leads to the following problem statement:

**Problem Statement 4.** *Given finite N data points, distribute the output signal uniformly in the output space by minimizing the Weyl's criterion under constraints on the input and output signals.*

This objective has been used earlier in context of input signal design for highly interactive multivariable systems [80, 95, 153, 152]. Section 5.2 presents input signal design problem formulations using the Weyl's criterion to produce an uniformly spread dataset for

data-centric estimation methods using a hypothetical example of a clinical trial, and Section 5.4 contrasts the Weyl's criterion with the earlier proposed distribution in the output space.

## 4.5 Chapter Summary and Conclusions

This chapter has presented problem statements for the design of constrained input signals for data-centric estimation methods. After defining the time domain and frequency domain requirements, a discussion is presented on experiment design issues for these class of estimators and a general inference is derived on the nature of the problem to build up on the ensuing problem statements. Problem statements for data-centric input design are developed using two approaches: based on distribution in the regressor and output space, and the other based on the Weyl's criterion.

For the distribution of regressors, two formulations are proposed towards achieving constrained input signal design for data-centric estimation methods. The objective is to distribute regressors, as measured by their Euclidean distances, in a given finite dimensional regressor space. The first formulation maximizes the total sum of all regressor pair distances under input constraints, while the second formulation maximizes the minimum distance pair under input constraints. These are developed subject to "plant-friendly" or "patient-friendly" constraints on the input such as amplitude constraints, move size restrictions and switching constraints. The chapter also briefly points out extensions of these problem statements as future topics. For highly interactive systems, it is proposed to distribute the time-indexed points in the output space. An alternative to the distance-based formulations is the problem statement based on the Weyl's criterion to achieve uniform distribution in the feasible space under constraints. The ensuing chapter presents formulations and numerical solutions for the Weyl design and distribution in regressor and output space methods.

Chapter 5

# CONSTRAINED INPUT SIGNAL DESIGN FOR DATA-CENTRIC SYSTEM IDENTIFICATION: FORMULATIONS AND NUMERICAL SOLUTIONS

## 5.1 Overview

The general problem statements developed in Chapter 4 are formally posed as mathematical optimization problems in this chapter. The problem formulations are developed and numerically solved for linear time-invariant (LTI) and Hammerstein systems under time domain constraints on the input. In general, the resulting problems are challenging nonconvex optimization problems [94, 206]. The solution of these problems is proposed through nonlinear programming and semidefinite programming based relaxation for polynomial optimization problems. In certain cases, it is shown that useful bounds can be obtained on the objective under consideration. Numerical examples are used to illustrate the proposed input design formulations and assess their benefits.

The first approach for input signal design addresses the distribution of regressors and output in the finite dimensional space. For LTI systems, these correspond to nonconvex quadratic programs and for Hammerstein systems, these correspond to a general polynomial optimization problem, and are solved by building a hierarchy of convex relaxation and nonlinear programming. For the other approach using Weyl's criterion, the resulting optimization problem is nonconvex nonlinear program not amenable to traditional relaxation procedures though good solutions can be obtained through interior-point based nonlinear programming techniques [153]. For the Weyl's criterion formulation, numerical examples are presented using a hypothetical single-subject clinical trial for gabapentin in a pain treatment setting under categorical dosages.

The chapter is organized as follows: first, the problem formulations using the Weyl's criterion are discussed in Section 5.2 and the data-centric input design formulations using

distribution of regressors are presented in Section 5.3. Section 5.4 presents the formulation to achieve uniform coverage in the output space for highly interactive systems. The chapter ends with a summary and conclusions in Section 5.5.

## 5.2 Data-Centric Input Signal Design using Weyl's Criterion

This section mathematically formulates the problem statements using Weyl's criterion, introduced in Problem Statement 4 in Section 4.4.4, for data-centric input signal design to estimate an unknown dynamical system. This section proposes two problem formulations: one where the Weyl's criterion is directly minimized and the other where the objective is to achieve a desired input signal spectrum while Weyl's criterion is applied as a constraint. Both of these formulations are illustrated using a case study based on the drug gabapentin to show usefulness of the proposed input design.

- *Weyl's Criterion as the Objective Function*

  This formulation achieves a uniform distribution by minimizing Weyl's criterion under time domain constraints:

$$\min_{u \in \mathbb{U} \cap \mathbb{I}} \frac{1}{N} \sum_{k=1}^{N} e^{(2\pi \ell y(k))i}. \tag{5.1}$$

  This can be expanded as

$$\begin{aligned}
\min_{u,\delta} \quad & \delta \\
\text{s.t.} \quad & u_{\min} \leq u \leq u_{\max} \\
& |u(k+1) - u(k)| \leq b(k) \\
& u(k) \in \mathbb{I} \\
& \sum_{j=1}^{T_{\text{sw}}-1} (u(k) - u(k+j)) = 0 \quad \forall k = 1 + n_{\text{sw}} \times T_{\text{sw}},\ n_{\text{sw}} = 0, 1, 2, \ldots. \\
\text{LTI system output} \quad & \begin{cases} y_{\min} \leq y \leq y_{\max} \\ |y(k+1) - y(k)| \leq b_y(k) \end{cases}
\end{aligned} \tag{5.2}$$

$$\text{Weyl's criterion} \begin{cases} \text{Re}\left\{\frac{1}{N}\sum_{k=1}^{N} e^{(2\pi\ell y(k))i}\right\} \leq \delta \quad \forall \ell \in \mathbb{L} \subset \mathbb{Z} - \{0\} \\ \text{Im}\left\{\frac{1}{N}\sum_{k=1}^{N} e^{(2\pi\ell y(k))i}\right\} \leq \delta \quad \forall \ell \in \mathbb{L} \subset \mathbb{Z} - \{0\}. \end{cases}$$

The numerical solution for this formulation is shown in Section 5.2.3 when the switching time is fixed to be weekly ($T_{\text{sw}} = 7$).

- *Weyl's Criterion as a Constraint*

  This formulation achieves desired input signal spectrum $\gamma(\omega)$ under minimum possible bounds on Weyl's criterion:

$$\begin{aligned} \min_{u,t} \quad & t \\ \text{s.t.} \quad & -t + |\gamma(\omega_j)| \leq \Phi_u(\omega_j) \leq t + |\gamma(\omega_j)| \\ & 0 \leq \omega_j \leq \pi, j = 1, .., M \\ & u_{\min} \leq u \leq u_{\max} \\ & |u(k+1) - u(k)| \leq b(k) \\ & u(k) \in \mathbb{I} \\ & y_{\min} \leq y \leq y_{\max} \\ & |y(k+1) - y(k)| \leq b_y(k) \\ & \text{Re}\left\{\frac{1}{N}\sum_{k=1}^{N} e^{(2\pi\ell y(k))i}\right\} \leq \delta \quad \forall \ell \in \mathbb{L} \subset \mathbb{Z} - \{0\} \\ & \text{Im}\left\{\frac{1}{N}\sum_{k=1}^{N} e^{(2\pi\ell y(k))i}\right\} \leq \delta \quad \forall \ell \in \mathbb{L} \subset \mathbb{Z} - \{0\} \end{aligned} \tag{5.3}$$

  where $\delta$ is chosen such that a feasible solution can be obtained. The switching time constraint has been removed to help achieve the desired spectrum. Section 6.3 has more details on achieving specified input spectrum under constraints. As observed earlier, Weyl's criterion and the spectrum constraint are nonconvex and nonsparse in

$u$ as well as optimization problem is integer constrained: $u(k) \in \mathbb{I}\ \forall k$. The numerical solution for this formulation is showed in Section 5.2.4.

### *5.2.1 Numerical Examples and Computational Challenges*

The mixed integer nonlinear and nonconvex programs are, in general, NP-hard and hence computationally intractable (for global solution) unless $N$ is relatively small [206]. Based on the specific intervention studied in Chapter 2 and nature of data for most (finite $N$) clinical trials, the following specific observations can be made:

- The length of the clinical trial $N$ is not very large for pain interventions (less than 200). Also in a general case for system identification, 200 data points are large enough to assume the asymptotic results to hold true [45].
- The number of integer levels is a small finite number. Generally, it would be less than 10 levels. If the number of integer levels are very large, it may be best to simply approximate the continuous signal to the nearest integer. This is shown in Section 5.2.2 for the case of multisine signal.
- For minimizing the Weyl's criterion case, the criterion can be made close to zero. In any case, given limited data points, the formula is only approximately true. This, however, does not significantly affect the quality of the solution.
- For desired spectrum case, an 'exact' solution may not be necessary. In other words, no significant benefit may be obtained form solving the problem to global optimality (which is very difficult for nonconvex problems). If the procedure excites certain frequencies more than others, the objective for a flat spectrum can be achieved.
- As shown in (4.10), the problems (5.2) and (5.3) can be posed as nonlinear optimization by reformulating the integer constraints as polynomial equations.

A case study for input signal design is illustrated using a hypothetical clinical trial to treat neuropathic pain. The drug used in this study is gabapentin which has a broad

therapeutic window [77]. This implies that it is possible to vary the drug dosages over time and to observe corresponding changes in reported pain condition. Some of the features of the proposed trial are:

- Typical dosage: $1200 - 3600$ mg,
- Length of protocol : $3 - 8$ months or $90 - 240$ days,
- Dosage change size : $100, 300, 600, 900$ mg,
- Switching time: 1 day to 7 days.

It is important that the drug dosage should be gradually increased to and from 1200 mg level (baseline period) and similarly gradually decrease for washout period. This is achieved by padding the input signal with 'baseline' and 'washout' dosages. In addition, it is desired that the drug dosages do not change too abruptly between two samples and hence a maximum input move size of 900 mg is applied. The input signal is first generated on a magnitude of $-4$ to 4 and then scaled up to the desired drug concentrations of $1200 - 3600$ mg. Corresponding output is constrained and then scaled using a first order system with gain $K_p = -0.01235$ per mg of drug. Time constant is assumed to be $\tau = 5$ days. The simulation results are shown for two periods and nine levels of the input signal, with added baseline and washout periods. The corresponding parameters used for simulation are as follows:

- $N = 100$, $M = 50$,
- $n = 4$, $\mathbb{I} = \{-n, 1-n, \ldots, 0, \ldots, n-1, n\}$ (9 levels),
- $\omega^* = 0.4$: (based on dominant time constant $\tau = 5$),
- $u_{\max} = n$, $u_{\min} = -n$,
- $b(k) = 3$, $b_y(k) \to \infty$,
- (Section 5.2.3) $y_{\max,\min} = \pm 20$, $\mathbb{L} = \{-10, \ldots, 10\}$, $\epsilon = 20$

Table 5.1: Performance indices for different input signals generated in Section 5.2.2, Section 5.2.3 and Section 5.2.4.

| Signal | $x$ | CF($x$) | PIPS($x$) | max($\Delta x$) |
|---|---|---|---|---|
| Section 5.2.2 (multisine, $T_{\text{sw}} = 1$) | $u$ | 1.74 | 57.21 | 600 mg |
| | $y$ | 1.91 | 54.82 | 2.64% |
| Section 5.2.2 (multisine, $T_{\text{sw}} = 4$) | $u$ | 1.96 | 57.91 | 900 mg |
| | $y$ | 2.08 | 51.7 | 2.78% |
| Section 5.2.2 (multisine, $T_{\text{sw}} = 7$) | $u$ | 1.61 | 61.59 | 1500 mg |
| | $y$ | 2.03 | 51.5 | 3.39% |
| Section 5.2.3 (Weyl, $T_{\text{sw}} = 7$) | $u$ | 1.82 | 54.66 | 900 mg |
| | $y$ | 1.82 | 57.46 | 2.16% |
| Section 5.2.4 (Weyl, $T_{\text{sw}} = 1$) | $u$ | 1.84 | 53.77 | 900 mg |
| | $y$ | 1.88 | 54.45 | 2.55% |

- (Section 5.2.4) $\gamma_a = 3500$, $\gamma_b = 35$, $y_{\text{max,min}} = \pm 15$, $\mathbb{L} = \{-15, \ldots, 15\}$, $\delta = 0.5, \epsilon = 1$.

The formulations are written in the AMPL modeling language [172], with KNITRO as the nonlinear solver [179]. To overcome potentially poor local minima solutions, the solver is initiated with the 'multistart' option to enable a more global search. It is found that the relaxation approach for integer constraints results in good results for problems posed in this dissertation.

### *5.2.2 Approach using Approximated Multisine*

Before discussing the optimization based results, (integer) approximated multisine signals are briefly considered. The desired properties of input design can also be satisfied by multisine signals which are deterministic, periodic signals designed to contain specific frequency information

$$u(k) = \sum_{i=1}^{n_s} a_i \cos(\omega_i k T + \phi_i), \tag{5.4}$$

where $n_s$ is the number of harmonics, $T$ is the sampling time, $\omega_i$ are specified by the user and $a_i, \phi_i$ are selected by an algorithm. These multisines can be designed to reach a desired plant friendly metric such as the crest factor under time domain constraints [81]. But since the amplitude at a give time $k$ is expressed only as a sum of finite sinusoids, it may be

infeasible for the signal to take only categorical values. A practical way to archive this goal is to approximate average of the multisine signal over a predetermined switching time ($T_{\text{sw}}$) to the nearest integer. This can be written as

$$\bar{u}(k : k + T_{\text{sw}}) = u_I^*, \quad \forall k \in \{1, \ldots, N - T_{\text{sw}}\} \tag{5.5}$$

$$\text{s.t.} \quad \arg\min_{u_I} \{ \left| \frac{\sum_{i=k}^{k+T_{\text{sw}}} u(i)}{T_{\text{sw}}} - u_I \right| \}, \quad u_I \in \mathbb{I} \tag{5.6}$$

where $N$ is the signal length, $u_I^*$ is the nearest integer value, $u$ is the original multisine and $\bar{u}$ is the approximated signal. Clearly, this approximation is most accurate when the number of categorical levels is large and the switching time is short. This can be now shown for the gabapentin trial. The number of signal levels are assumed to be nine (i.e. minimum dosage size of 300 mg). A comparison of original multisine with the approximated signal is shown in Fig. 5.1. Dynamic simulation of pain response to an integer approximated Schroeder-phased multisine signal is shown in Fig. 5.2 with two periods of 96 data points. Fig. 5.6 shows comparison of the discrete power spectrum with increase in $T_{\text{sw}}$ from daily to weekly. It can be observed that increasing $T_{\text{sw}}$ results in an unavoidable loss of power at frequencies close to the desired bandwidth.

### *5.2.3 Weyl's Criterion as the Objective Function under Weekly Switching Time Constraint*

Dosage changes that happen daily may be excessive or impractical in some health intervention settings. In the joint input-output design, the aim is to obtain a signal that produces uniform changes in the output, while respecting input constraints including a weekly dosage change, i.e. $T_{\text{sw}} = 7$. The problem formulation shown in (5.2) is solved and the resulting time-domain signals are shown with two periods in Fig. 5.3. The condition expressed in (4.10) is used for (relaxed) integer constraints. Since the optimization-based design results in an input signal which fully covers the useful span, the patient experiences longer stretches of lower pain as a result of better utilization of the input. The optimization approach avoids the drawback of the approximated multisine where the user has no direct control over the

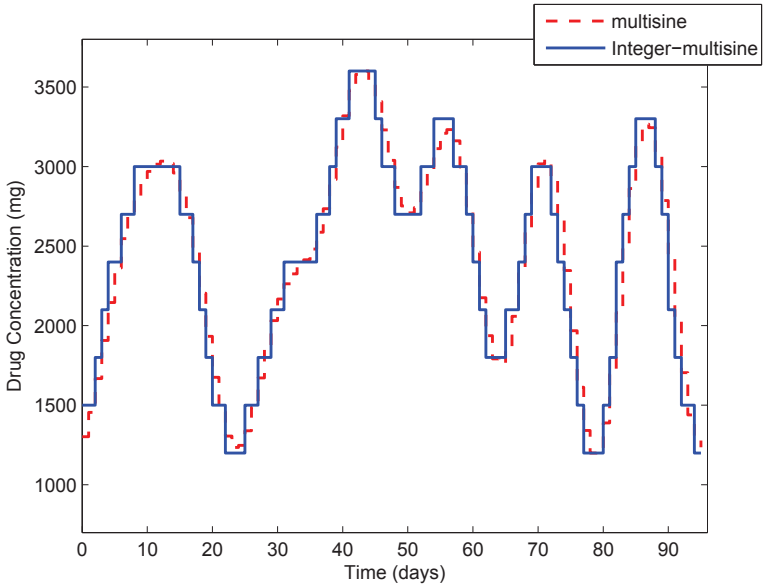


Figure 5.1: Comparison of Schroeder-phased multisine with a nine-level integer approximated multisine signal with daily switching ($T_{sw} = 1$). These signals are shown for one cycle.

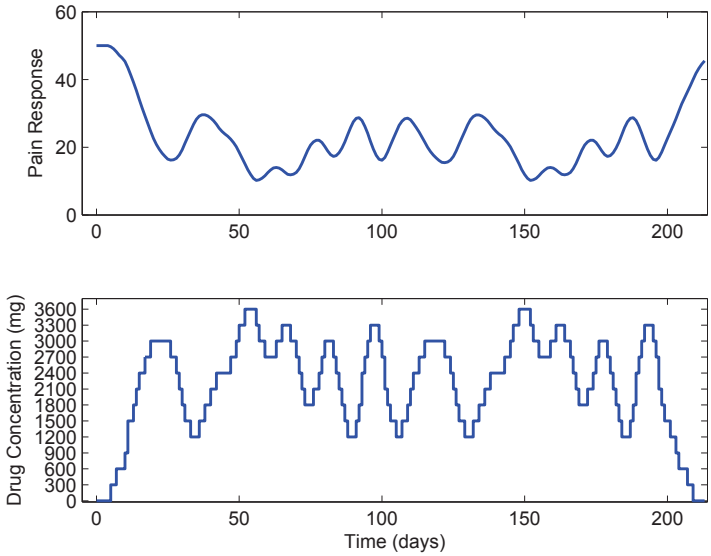


Figure 5.2: Dynamic simulation of pain response (from baseline 50) to a nine-level integer approximated Schroeder-phased multisine with daily switching ($T_{\mathrm{sw}} = 1$).

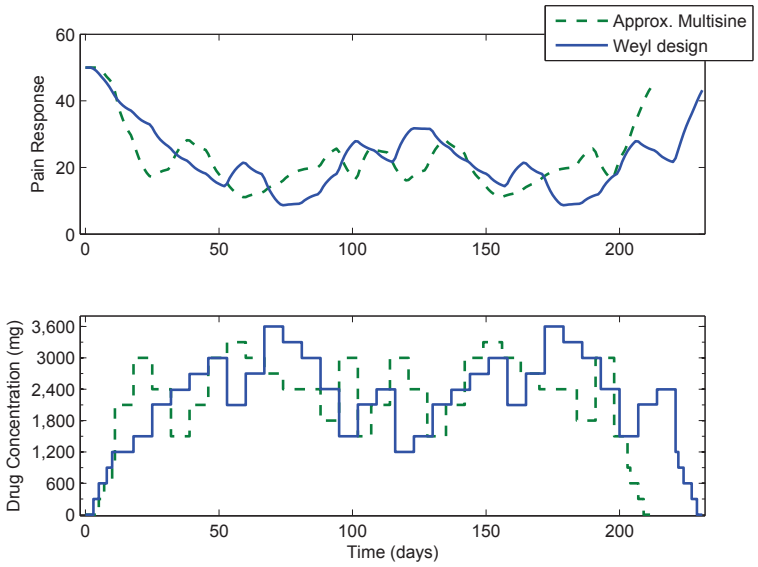


Figure 5.3: Dynamic simulation of pain response (from baseline 50) to a nine-level input signal under Weyl's criterion objective and constrained to a minimum weekly switching interval ($T_{\text{sw}} = 7$).

final realization (e.g. large move sizes as noted in Table 5.1). To ascertain the distribution of the output, the spread of $y$ to the corresponding changes in $y$ or $\Delta y = y(k+1) - y(k)$ can be observed. In Figure 5.4, the distribution ($y$ vs. $\Delta y$) for these two signals is compared where it can be observed that the Weyl design has a larger and more even distribution. It should also be noted that the two signals are of slightly different lengths.

### *5.2.4 Weyl's Criterion as a Constraint under a Desired Input Spectrum Objective*

In this section, the problem formulation shown in (5.3) is now considered which satisfies requirement on the input spectrum (flat over the desired bandwidth) and other time domain constraints on the input and output. When the problem is solved, the minimum value of $t$ obtained is 0.00559212 which implies that the approximation is quite good and inaccuracies only occur at higher frequencies in lower decibels, and the obtained input signal spectrum is shown in Fig. 5.6. Fig. 5.5 shows the dynamic simulation of pain response to the corresponding input signal. The dosage is varied between $1200 - 3600$ mg with maximum

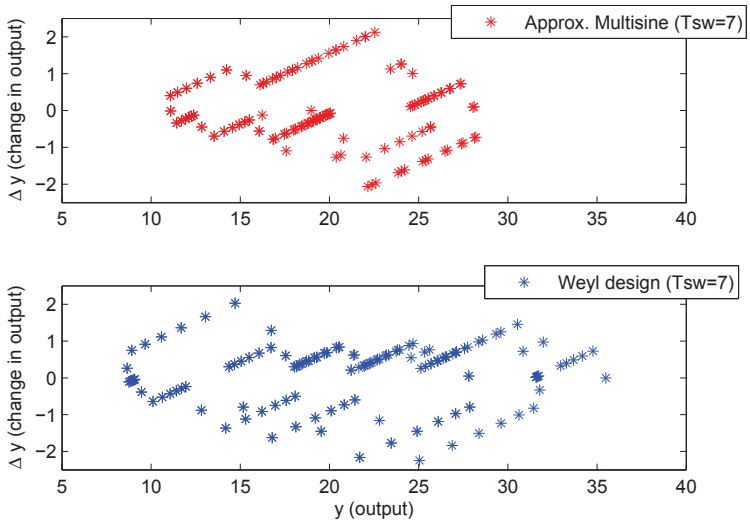


Figure 5.4: Comparison of distribution of output and rate of change of output for the approximated multisine (top) and optimization-based signal (bottom) for weekly switching ($T_{\text{sw}} = 7$) as discussed in Section 5.2.3.

move size of 900 mg as noted in Table 5.1. In Fig. 5.7, the integer constrained optimization based method can be contrasted with the approximated multisine result (with daily switching and on neglecting transients), where a more uniform spread of $y$ was observed with corresponding uniform changes in $\Delta y$, under integer constraints, for the Weyl design.

To conclude, this section described design of input signals using Weyl's criterion. This has been illustrated using a hypothetical clinical trial using the drug gabapentin. The drug dosage is manipulated over time to achieve variability in the pain response. It is shown in the numerical illustrations that the output signal covers more span that an ad-hoc design using multisine signals and thus provides better support for the estimator. As alluded to earlier, an alternative problem formulation could be derived using the regressor space for Weyl's criterion in lieu of in the output space. However, doing so will increase the difficulty of solving the resulting optimization problems given the higher dimension of the regressor space. The ensuing section discusses the data-centric input signal design using distribution of regressors which, unlike the Weyl's criterion, is more amenable for methods from convex

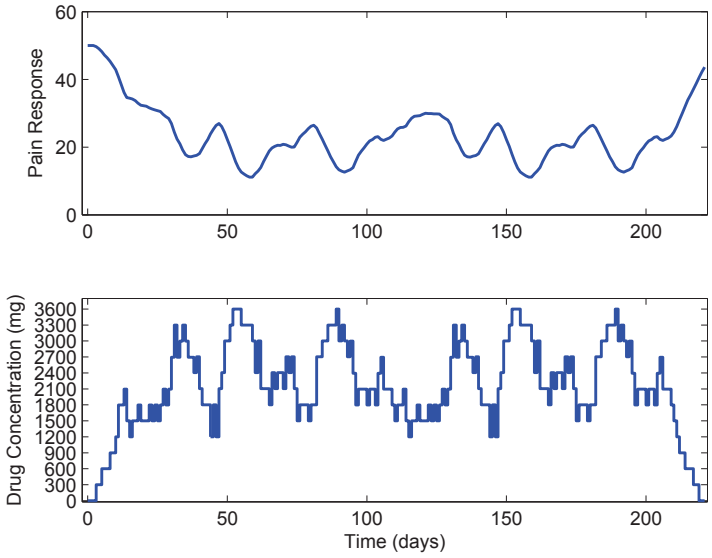


Figure 5.5: Dynamic simulation of pain response (from baseline 50) to a nine-level input signal under output Weyl's criterion constraints with daily switching ($T_{\text{sw}} = 1$) .

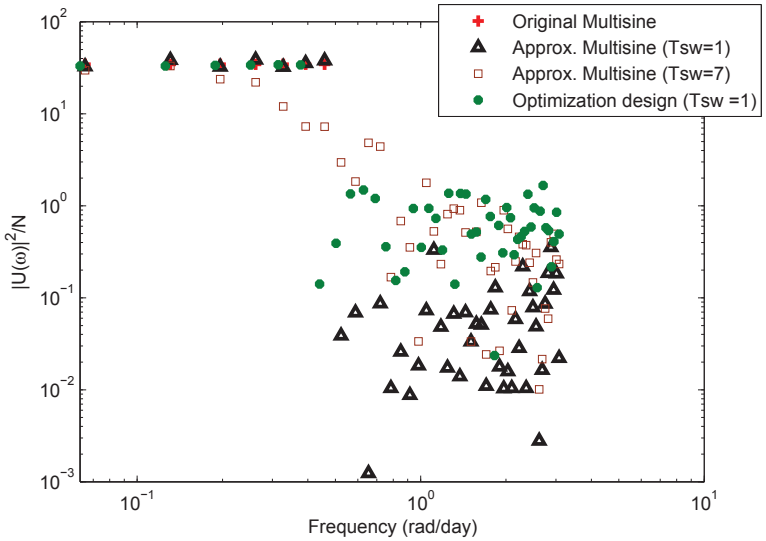


Figure 5.6: Comparison of periodogram of the original multisine with approximated multisine signals and Weyl optimization design.

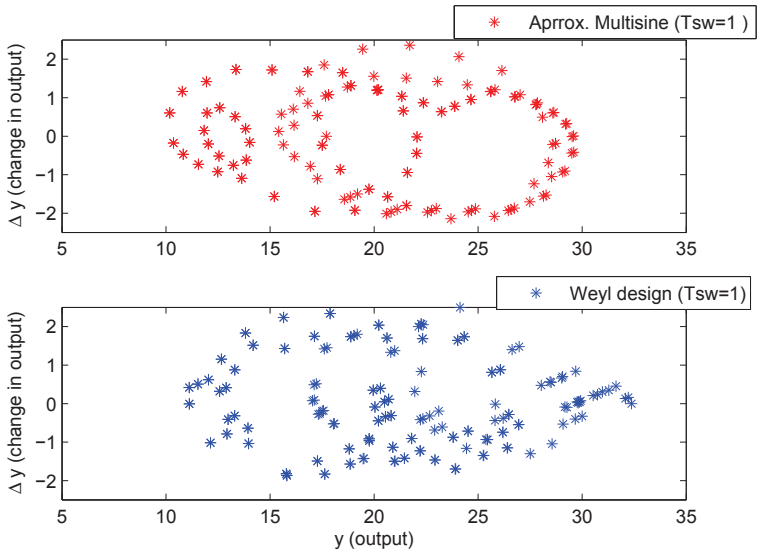


Figure 5.7: Comparison of distribution of output and rate of change of output for the approximated multisine (top) and optimization-based signal (bottom) for daily switching ($T_{\text{sw}} = 1$) as discussed in Section 5.2.4.

relaxation and polynomial optimization.

## 5.3 Data-Centric Input Signal Design using Distribution of Regressors

This section mathematically formulates the problem statements using distance measures, introduced in Section 4.4.1, for data-centric input signal design to estimate an unknown dynamical system. The regressor is expressed as a function of the input; the algorithm then distributes the regressors to cover the regressor space under time domain constraints on the input. First, this is developed for linear time-invariant systems where the subsequent optimization problems correspond to nonconvex quadratic programs. Later in the section, the problem formulations are extended by considering a more general formulation by incorporating multivariable and nonlinear nature of the system in the definition of the regressor. The resulting problems are nonconvex polynomial optimization problems. An initial formulation using semidefinite relaxation of one of these nonconvex quadratic problems was proposed in [84], and was improved by including both problem statements, as

developed in Section 4.4.1, under additional time domain constraints and signal realization techniques through randomization and nonlinear programming in [85]. An extension to Hammerstein systems using nonlinear programming was proposed in [100].

The rest of the section is arranged as follows: mathematical formulations are developed in Section 5.3.1 for LTI and Hammerstein systems. Section 5.3.2 provides a brief background on techniques in optimization over polynomials which are used in Section 5.3.3 and Section 5.3.4 to build a hierarchy of convex semidefinite optimization problems of increasing dimension to solve the input design problem. The remainder of the section presents numerical illustrations: Section 5.3.5 shows input design for LTI systems using SDP relaxation of nonconvex quadratic program, Section 5.3.6 shown input design for Hammerstein systems using nonlinear programming and Section 5.3.7 shows data-centric input signal design using sparse polynomial optimization.

### *5.3.1 Input Signal Design Formulations using Distribution of Regressors*

Two problem statements were introduced in Section 4.4.1 which describe two distinct ways of addressing distribution of regressors. These are first shown for LTI systems. The first formulation, based on Problem Statement 1, distributes the points as far apart as possible by maximizing the sum of regressor distances:

$$\begin{aligned} \max_{u} \quad & u^T \mathbf{Q} u \\ \text{s.t.} \quad & u \in \mathbb{U}, \end{aligned} \tag{5.7}$$

where $\mathbf{Q} = \sum_{i=1}^{N-1} \sum_{j=i+1}^{N} \mathbf{Q}_{ij}$. As $u^T \mathbf{Q}_{ij} u$ represents the square of the distance between $i$th and $j$th regressor, $\mathbf{Q}_{ij}$ is positive semidefinite ($\mathbf{Q}_{ij} \succeq 0$). This implies that $\mathbf{Q}$, the sum of positive semidefinite matrices, is also positive semidefinite ($\mathbf{Q} \succeq 0$). Hence the resulting quadratic maximization problem (or minimization of negative semidefinite problem) is NP-hard [94].

The second formulation, based on Problem Statement 2, distributes the points such that the magnitude of the minimum distance pair is maximized:

$$\begin{aligned} \max_{u,t} \quad & t \\ \text{s.t.} \quad & u^T \mathbf{Q}_{ij} u \geq t, \\ & u \in \mathbb{U}, \end{aligned} \tag{5.8}$$

where $i$ and $j$ are selected to define unique distance pairs as per the set $\mathcal{K}$. Given each $\mathbf{Q}_{ij}$ is positive semidefinite ($\mathbf{Q}_{ij} \succeq 0$), the feasible set lies outside the ellipsoid defined by $\mathbf{Q}_{ij}$ rendering the resulting problem nonconvex. Solution of these nonconvex quadratic programs is discussed in Section 5.3.5 and Section 5.3.7.

In comparison to LTI systems, input signal design for nonlinear systems is more challenging due to complexity associated with the structure which often results in very difficult problems [89, 207]. A general block-structured nonlinear system called Hammerstein-Wiener system, as represented in Fig. 5.8, is used to showcase the distribution of regressors for nonlinear systems. These are characterized by a static input nonlinearity $\mathcal{I}$ which accepts the system input followed by a linear time-invariant dynamical system $\mathcal{L}$ and finally a static output nonlinearity $\mathcal{O}$ whose output is measured. The internal signals $w_H, z_W$ are assumed to be unobservable. Note that this can be further generalized by incorporating noise in the measured $u, y$ and unmeasured $w_H, z_W$ signals. It is also possible to replace the static blocks with LTI blocks and vice-versa; this swapped system is called a Wiener-Hammerstein system [208]. Although chosen to have a particular structure, these parametrizations have been remarkably useful in practice [209]. Before discussing the input design formulations, it should be mentioned that the static nonlinearities have to be differentiable (smooth) to be used by most of the data-centric methods. Extensions to include the case of discontinuous nonlinearities have been proposed in the literature, but are not considered in this dissertation [210].

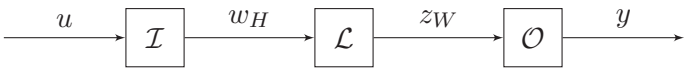


Figure 5.8: Noise-free input-output representation of a Hammerstein-Wiener system.

The Hammerstein-only system, which is defined by static input nonlinearity $\mathcal{I}$ followed by the LTI system $\mathcal{L}$, is considered for developing input design formulations. For this structure, Problem Statement 1 translates into the following nonconvex polynomial problem:

$$\begin{aligned} \max_{u} \quad & \mathcal{I}(u)^T \mathbf{Q} \mathcal{I}(u) \\ \text{s.t.} \quad & u \in \mathbb{U} \end{aligned} \tag{5.9}$$

and for Problem Statement 2, it results in the following problem

$$\begin{aligned} \max_{u,t} \quad & t \\ \text{s.t.} \quad & \mathcal{I}(u)^T \mathbf{Q}_{ij} \mathcal{I}(u) \geq t, \\ & u \in \mathbb{U}. \end{aligned} \tag{5.10}$$

Both of these optimization problem follow a similar structure to the LTI case except that the degree of the objective and that of the constraints is a function of the degree of the input nonlinearity. Solution of these nonconvex polynomial programs is discussed in Section 5.3.6 and Section 5.3.7.

Similar optimization problems can be derived for other block-structured nonlinear systems. For the simple purpose of illustration, consider the case of Wiener-only system where the input nonlinearity is one ($\mathcal{I} = 1$) and the output nonlinearity $\mathcal{O}$ is the power function

$$y(k) = (z_W(k))^{n_z} = ({h_k}^T u)^{n_z} \tag{5.11}$$

where $h_k$ is the row corresponding to the time instant $k$ in the matrix $G$ defined in (4.14). The ARX-type regressor can be written as

$$\varphi(k) = [({h_k}^T u)^{n_z} \ ... \ ({h_{k-n_a}}^T u)^{n_z} \ \ u(k-n_k) \ ... \ u(k-n_b-n_k+1)]^T. \tag{5.12}$$

The square of the distance between two regressors can be calculated using

$$d_{ij}^2 = (\varphi(i) - \varphi(j))^T(\varphi(i) - \varphi(j)) \tag{5.13}$$

which is a polynomial in $u$, and proceeding as earlier, can be used to formulate the polynomial optimization problems to distribute the regressors.

### *5.3.2 Background on Convex Relaxation and Optimization over Polynomials*

Nonconvex optimization problems are generally hard to solve; methods based on Karush-Kuhn-Tucker (KKT) conditions may give poor local solutions. A powerful approach to approximately solve some of these problems is through convex relaxation where the main source of nonconvexity is replaced with a 'relaxed' version that is convex and hence more tractable [168, 169, 170, 189]. The convex relaxation procedure provides a bound on the original objective function but generally no feasible solution unless the relaxation is tight. In some cases, feasible inputs can be generated using rank one approximation, randomization and nonlinear programming [168, 170]. Semidefinite programming (SDP) relaxation for the case of nonconvex quadratic problems has been particularly successful with proven bounds on the suboptimality, in polynomial time, for many scenarios [170, 211]. For general polynomial problems, effective solutions are possible under structured sparsity [212]. For overview of these methods with introduction to the notation and terminology, the reader is referred to the excellent review provided by Laurent [171].

Consider a general polynomial optimization problem $\mathbf{P}$ as follows:

$$\mathbf{P} : \min \{g_0(u) \ : \ u \in \mathbf{K}\} \tag{5.14}$$

where $g_0$ is a real valued polynomial, $u \in \mathbb{R}^N$ is the decision vector and $\mathbf{K} \subset \mathbb{R}^N$ is a basic closed semialgebraic set defined as:

$$\mathbf{K} = \{u \in \mathbb{R}^N \ : \ g_i(u) \geq 0, \quad i = 1, \ldots, m\}. \tag{5.15}$$

This structure accounts for large class of problems including linear, quadratic and integer programming. The problem $\mathbf{P}$ is, in general, difficult to solve to global optimality [213].

Given the smoothness of the underlying functions, local solutions can be generally found using powerful nonlinear programming solvers like KNITRO [214, 179]; however there are no guarantees on the quality of the solution. Recent work in real algebraic geometry and theory of moments applied to optimization has proposed to approximate the problem **P** by generating a hierarchy of convex relaxation by using representation of nonnegative polynomials as sum of squares polynomials and moments sequences [171]. For the purpose of explanation, in this section this relaxation approach is presented using the sum of squares representation. A similar, and in fact dual, representation can be obtained by using the theory of moments [215].

One of the central tools used in the construction of the relaxation procedure is that of sum-of-squares. It is known that checking whether a polynomial is nonnegative i.e. $g(u) \geq 0 \ \forall u$ is an intractable problem [171]. This requirement can be replaced with a simpler condition to test if there exists a sum-of-squares (SOS) decomposition[1]

$$g(u) = \sum_{i=1}^{p} p_i(u)^2 = v(u)^T \mathbf{V} v(u) \tag{5.16}$$

where $v$ is the vector of chosen monomials and $\mathbf{V} \succeq 0$. This can be checked by solving a SDP and is tractable in theory, and in practice, for many cases of interest [216]. This simple but powerful idea can be applied for solution of unconstrained optimization. Consider the following problem **P** shown earlier where the semialgebraic set **K** is the complete real space:

$$\mathbf{P} : \min \{g_0(u) \ : \ u \in \mathbb{R}^N\} \tag{5.17}$$

which can be equivalently written as:

$$\mathbf{P} : \max \lambda \text{ s.t. } g_0(u) - \lambda \geq 0. \tag{5.18}$$

The relaxation of this problem involves replacing the intractable condition of nonnegativity on the constraint polynomial by the condition that the polynomial is SOS [189]:

$$\mathbf{P_{SOS}} : \max \lambda \text{ s.t. } g_0(u) - \lambda \in \Sigma, \tag{5.19}$$

[1] In other words, if a polynomial can be decomposed as SOS, it also nonnegative but vice-versa is not true. Hence, the set of SOS polynomials $\Sigma$ lies in the set of nonnegative polynomials.

and this relaxation procedure produces an lower bound on the objective

$$g_{\text{SOS}} \leq g^*. \tag{5.20}$$

In other words, the global minima $g^*$ cannot exceed the bound provided through the relaxation. It should be noted that this bound may be trivial (i.e. $-\infty$) but in many cases meaningful bounds are obtained. Similarly, upper bound on the problem can be obtained by any of the nonlinear optimization routines. These gradient-based methods will be dependent on the initial point of search and thus using a randomly selected grid, a reasonable upper bound can be obtained. As previously noted, since the relaxation procedure provides a (lower) bound on the objective, it makes sense that no feasible minimizer can be directly obtained and if such a minimizer can be extracted, then the minima is the global solution. However, a feasible solution can always be obtained through the local nonlinear solver.

Using these insights from unconstrained optimization, a method can be proposed to solve the general case when $\mathbf{K}$ is semialgebraic as shown in (5.14). Towards this, a representation has to be found for the polynomial to be positive (or nonnegative) over the set $\mathbf{K}$. This is a significantly challenging task and several results in Positivstellensatze[2] (Psatz) have allowed for representation of this condition [217, 189]. One of the main result is called Krivine-Stengle's Psatz [189] for giving a certificate of positivity on any $\mathbf{K}$

$$g > 0 \text{ on } \mathbf{K} \Leftrightarrow g = \frac{1+q}{p} \tag{5.21}$$

where $p, q$ are polynomials from a preordered set [171, 189]. From an optimization perspective however, it does not allow for efficient representation due to the nonlinear product in its equation [171]. If the set $\mathbf{K}$ is assumed to be compact, a more simpler representation for strict positivity is known as Schmüdgen's Psatz [189], and which can be used in an optimization framework although it involves $2^m$ number of SOS condition where polynomials are selected from a preordered set.

[2]German for 'theorem of positives', similar to Hilbert's Nullstellensatz.

To develop efficient relaxation procedures in polynomial optimization, a refinement of previously stated Psatz conditions is required which is proposed in Putinar's Psatz. Towards this, first consider the following specific conditions based on the set $\mathbf{K}$:

**Definition 7.** *A set* $\mathbf{M}$

$$\mathbf{M}(g_1, \ldots, g_m) = \{s_0 + \sum_{j=1}^{m} s_j g_j,\ s_0, s_j \in \Sigma\} \tag{5.22}$$

*is called the quadratic module of the polynomials* $g_1, \ldots, g_m$*. The quadratic module is said to be Archimedean if* $\exists R_p \in \mathbb{N}$ *for which*

$$R_p - \sum_{k=1}^{N} u(k)^2 \in \mathbf{M}(g_1, \ldots, g_m). \tag{5.23}$$

Putinar's Psatz states that if the quadratic module is Archimedean, the condition that $g > 0$ on $\mathbf{K}$, is true iff $g \in \mathbf{M}$ [218]. This representation is more efficient as it allows for $m$ SOS constraint for representing positivity over set $\mathbf{K}$ and can be checked by solving a SDP. It is worth noting that the condition where the module $\mathbf{M}$ is Archimedean can be also be checked by solving a SDP. Using these results, a hierarchy of semidefinite programing relaxation can be proposed by relaxing the positivity condition on the polynomial by its SOS representation

$$\begin{aligned} \mathbf{P}^{\xi}_{\mathbf{SOS}}: \quad & \max_{\lambda, s_0, s_j} \ \lambda \\ & \text{s.t. } g_0(u) - \lambda = s_0 + \sum_{j=1}^{m} s_j g_j,\ s_0, s_j \in \Sigma \\ & \deg(s_0), \deg(s_j g_j) \leq 2\xi. \end{aligned} \tag{5.24}$$

The parameter $\xi$ is called the relaxation order where its lowest value is defined by the degree of the objective and constraints [171]. The degree of conservativeness of the relaxed problem depends inversely on the relaxation order $\xi$ and the accuracy of the approximation can be increased by increasing $\xi$ and hence the order of SOS multipliers $s_0, s_j$. More specifically, the optimum of the relaxed problem is guaranteed to converge monotonically to the global

optimum $g^*$ of the nonconvex problem as $\xi \to \infty$ [215, 171]. Recent results have also shown finite convergence [219], and also for the case of non-compact sets [220]. As an alternative interpretation, (5.24) can be understood as a generalized Lagrangian function formulation where the multipliers are nonnegative polynomials in contrast to nonnegative scalars [215].

The relationship shown in (5.16) can be restated as

$$g(u) = \sum_{i=1}^{p} p_i(u)^2 = v(u)^T \mathbf{V} v(u) = \mathrm{Tr}(vv^T \mathbf{V}) \tag{5.25}$$

where $\mathrm{Tr}(\cdot)$ is the trace operator. The matrix $vv^T$ is rank-one by construction and the problem can be reparametrized in new variables for each entry of the matrix $vv^T$. More formally, it can be interpreted in terms of truncated moment sequences [217, 171]. Using this understanding, a hierarchy of relaxation $\mathbf{P}^{\xi}_{\mathbf{MOM}}$ can be proposed using moment sequences which are shown to converge, as the SOS approach, to the global minimum [215]. Indeed, the method of SOS is dual to theory of moments where both conditions can be expressed as SDP. However, the moment approach has an unique advantage that it can allow for extraction of global minimizers where as the SOS approach natively can only provide with bounds on the minimum.

The size of the relaxed problem depends on the number of polynomial constraints of the original nonconvex problem, their degrees and on the dimension of the decision variable. The proposed relaxation approach $\mathbf{P}^{\xi}_{\mathbf{SOS}}, \mathbf{P}^{\xi}_{\mathbf{MOM}}$ is often called 'dense' convex relaxation [171] as it assumes that the polynomials $g_0, g_i$ are composed of all the possible monomials from all the elements $u(1), \ldots, u(N)$. To illustrate this point further, consider a polynomial of degree 2 and composed of variable $u(1), u(2)$. The possible monomial basis set for this polynomial can be written as:

$$v = \{1, u(1), u(2), u(1)^2, u(1)u(2), u(2)^2\}. \tag{5.26}$$

In general, for any given degree $d$, the number of elements in the basis set is given as $\binom{N+d}{d}$. Clearly, the number of monomials can increase exponentially as the degree of the polynomial

is increased even for fixed $N$. Furthermore, the number of variables for the relaxation in (5.24) is bounded by $\mathcal{O}(N^{2\xi})$. Indeed, this is why the traditional dense approach is limited to small sized problems. This is not surprising given that many of these problems are intractable and unless P=NP, it cannot be expected to solve all of these problems efficiently. However, in practice, many polynomials are composed of only select monomials and hence a representation which inherently assumes dense structure is restrictive. In [212] and [221], a 'sparse' convex relaxation procedure has been developed which utilizes the limited basis these polynomials may have. Thus, the resulting SDP is significantly smaller which allows solution of a larger sized problem. It is worth noting that just because a polynomial is composed of few monomials, it may not necessarily lead to efficient computation. In other words, a very specific condition is put on what is defined as sparse in [212, 221]. Consider that the elements of the decision variable $u = [u(1), \ldots, u(N)]^T \in \mathbb{R}^N$ can be split in to $p$ sets $I_1, \ldots, I_p$, each containing only few of the elements of $u$. The polynomial optimization problem is sparse under the following condition:

**Definition 8.** *Running intersection property (RIP) [221] is satisfied iff*

$$I_{\bar{k}+1} \cap \bigcup_{j=1}^{\bar{k}} I_j \subseteq I_s, \quad s \leq \bar{k}. \tag{5.27}$$

This implies if there exits a special ordering of the sets $I_1, \ldots, I_p$, the optimization problem is sparse. Earlier, a more specific requirement was developed in [212] based on the condition that a correlative sparsity pattern (csp) matrix $R$ has non-zero elements iff *any two elements from the decision variable appear in the monomial of the objective function $g_0$ or appear anywhere in the constraint $g_j$*. Subsequently, if $R$ is sparse then the problem is correlative sparse. However, the convergence of the resulting relaxation was not shown in [212] and was later proved in [221] using the presence of RIP condition. Similarly, a csp graph can be defined from which the sets $I_1, \ldots, I_p$ can be found as maximal cliques of a chordal extension of that graph, and thus the correlative sparsity condition is a subset of the RIP condition. More importantly, the detection of sparsity via sets $I_1, \ldots, I_p$ can

be efficiently automated for the correlative sparsity method [186] while it is nontrivial to arbitrarily find these sets in general.

Due to the specific construction by incorporating the algebraic structure, the complexity of solving the optimization is reduced. The sparse hierarchy of convex relaxation can be written as

$$\begin{aligned} \tilde{\mathbf{P}}^{\xi}_{\mathbf{SOS}}: \quad & \max_{\lambda, s_0, s_j} \ \lambda \\ & \text{s.t. } g_0(u) - \lambda = s_0 + \sum_{j=1}^{m} s_j g_j, \ s_0, s_j \in \Sigma(I_j) \\ & \deg(s_0), \deg(s_j g_j) \leq 2\xi \end{aligned} \tag{5.28}$$

where the polynomial multipliers $s_j$ are only function of variables as the constraint $g_j$. The number of variables for the relaxation in (5.28) is bounded by $\mathcal{O}(\kappa^{2\xi})$ where $\kappa \ll N$ is the maximum number of variables in the each monomial of the objective or the constraint polynomial [221]. It is worth noting the sparse relaxation is generally weaker than the classical dense relaxation, although good numerical results have been reported in literature [186, 222]. In the same way, testing Psatz condition using Putinar's result is weaker than the Krivine-Stengle's result [217]. Other ways to reduce the computational complexity is to exploit symmetry in the structure [171] and to use a user-defined basis for the polynomials based on an *a priori* knowledge. As a general comment, it is worth mentioning that solving the SOS problem is numerically challenging and use of reduced basis may induce further degeneration of the resulting SDP [216].

In conclusion to this section, an interesting special case is mentioned. When the polynomials are (nonconvex) quadratic functions, the $\xi = 1$ relaxation case corresponds to the standard semidefinite relaxation of nonconvex quadratic programs [215]. As is generally observed in the history of mathematics and science, this fact was discovered, formulated and then rediscovered through the general theory involving hierarchy of convex relaxation.

The construction of semidefinite relaxation for nonconvex quadratic programs involves linearization of quadratic terms as:

$$u^T \mathbf{Q} u = \mathrm{Tr}(\mathbf{Q}(uu^T)) = \mathrm{Tr}(\mathbf{Q}U), \tag{5.29}$$

$$uu^T = U = U^T \in \mathbb{R}^{N \times N}, \tag{5.30}$$

where $\mathrm{Tr}(\cdot)$ is the trace operator. In this way, the problem is posed as minimizing a linear functional subject to linear matrix inequalities which is essentially a semidefinite program. This variable transformation is similar to as shown in (5.25) and this convex relaxation procedure is a particular case of the general theory described earlier. The ensuing two sections are organized as follows: first, convex relaxation is applied to the case of LTI problems and it shown that useful bounds on the suboptimality of the relaxation can be derived. The following section presents general application of convex relaxation for data-centric input signal design with discussion focusing on addressing block-structured nonlinear systems.

### *5.3.3 Semidefinite Relaxation of Data-Centric Formulations for LTI Systems*

Semidefinite relaxation is used to approximately solve the nonconvex quadratic programs shown in Section 5.3.1. Consider the first problem formulation which considers maximization of sum of regressor distances as shown in (5.7). Using the variable transformation shown in (5.29), the original problem is 'lifted' in the space $(u, U)$ as:

$$\begin{aligned} \max_{u,U} \quad & \mathrm{Tr}(\mathbf{Q}U) \\ \text{s.t.} \quad & u \in \mathbb{U}, \\ & U = uu^T, \end{aligned} \tag{5.31}$$

and this can be written as a SDP problem by relaxing the constraint (5.30) as $U - uu^T \succeq 0$ and writing it in Schur complement form as:

$$\begin{bmatrix} U & u \\ u^T & 1 \end{bmatrix} \succeq 0. \tag{5.32}$$

For the case of amplitude-only constraints on the input, this problem can also be expressed as SDP by directly neglecting the rank constraint on $U$, as shown in [84]. Consider $\nu_{\text{QP}}$ as the objective value of the original nonconvex problem shown in (5.7). Let the objective of this SDP be $\nu_{\text{SDP}}$ with optimal variables $U^*$ and $u^*$, then the SDP relaxation gives an upper bound on the nonconvex maximization problem i.e. $\nu_{\text{QP}} \leq \nu_{\text{SDP}}$ [170, 211]. In case the rank $r$ of $U^*$ is not unity, the relaxation is not tight. Subsequently, the generation of input depends on the nature of the feasible set:

**Theorem 1** ([213])**.** *A convex (concave) function attains its global maximum (minimum) over a compact set $\mathcal{S}$ at an extreme point of $\mathcal{S}$.*

Hence, the maximum values will be obtained at the extreme of respective constraints e.g., when the input is either $u_{\min}$ or $u_{\max}$ and when the input changes the maximum allowed move $b$. If rank $r$ is low, an input $\bar{u}$ can be generated using best rank one approximation:

$$U^* = \sum_{j=1}^{r} \lambda_j q_j q_j^T, \quad \bar{u} = \sqrt{\lambda_1} q_1, \quad \lambda_1 \geq \lambda_2 \geq \cdots \geq \lambda_r > 0, \tag{5.33}$$

where $\lambda_j$ is the $j$th eigenvalue and $q_j$ is the corresponding eigenvector. Alternatively, an input can be generated using the process of randomization where an input $\bar{u} \sim \mathcal{N}(u^*, U^* - u^* u^{*T})$ can be repeatedly sampled such that the best objective is obtained [168, 170, 166]. It should be noted that both of these approaches do not guarantee a feasible input and a 'projection' in to the feasible set $\mathbb{U}$ is required. For the case of amplitude-only constraints, this is can be directly achieved by the signum function following Theorem 1. Moreover for amplitude constraints only, there also exists hard bounds on the suboptimality as follows:

**Theorem 2** (Nesterov [169], Ye [223], Manchester [161])**.** *Given the quadratic optimization problem (5.7) where $\mathbf{Q} \succeq 0$ under amplitude constraints only, the approximation bounds can be given by*

$$0.63\nu_{\text{SDP}} \leq \nu_{\text{QP}} \leq \nu_{\text{SDP}}. \tag{5.34}$$

This result holds for both FIR and ARX type regressors. For the FIR case, $\mathbf{Q}$ has additional properties and a tighter bound holds true:

**Theorem 3** (Goemans and Williamson [168])**.** *Given the quadratic optimization problem (5.7) where* $\mathbf{Q} \succeq 0$ *and all off-diagonal elements are nonpositive* ($\mathbf{Q}(c,d) \leq 0,\ c \neq d$) *under amplitude constraints only, the approximation bounds can be given by*

$$0.87\nu_{\text{SDP}} \leq \nu_{\text{QP}} \leq \nu_{\text{SDP}}. \tag{5.35}$$

The structure of $\mathbf{Q}$ can be confirmed based on (4.43) and (4.47). Theorems 2 and 3 imply that the exact global maximum is not known through relaxation but only that it lies inside the upper and lower bounds through SDP. Global solutions for NP-hard problems are difficult and may be found using branch-and-bound methods where the number of branching nodes can grow exponentially. Recently, methods have been proposed based on first-order KKT conditions and SDP relaxation using completely positive programs which yield finite branching for global optimality [224]. The performance of the proposed relaxation method is compared with the global method in Section 5.3.5. Under general linear equality and inequality constraints ($u \in \mathbb{U}$), such bounds on suboptimality generally do not exist [225]. Nevertheless, good objective values can be found using an input $\bar{u}$ generated through randomization and further refined to generate a feasible suboptimal solution using nonlinear programming methods such as sequential quadratic programming (SQP).

Similarly, for the second problem formulation which maximizes the minimum of regressor distances, semidefinite relaxation can be similarly constructed for problem formulated in (5.8). Given large number of nonconvex quadratic constraints, additional constraints using the reformulation-linearization technique (RLT) [226, 211] can be added to enforce stricter bounds on the matrix variable $U$. The resulting SDP can be written as:

$$\begin{aligned} \max_{u,U,t} \quad & t \\ \text{s.t.} \quad & \text{Tr}(\mathbf{Q}_{ij}U) \geq t, \end{aligned} \tag{5.36}$$

$$
\begin{aligned}
& u \in \mathbb{U}, \\
& U - u_{\min} u^T - u u_{\min}^T + u_{\min} u_{\min}^T \geq 0, \\
& U - u_{\max} u^T - u u_{\max}^T + u_{\max} u_{\max}^T \geq 0, \\
& U - u_{\min} u^T - u u_{\max}^T + u_{\min} u_{\max}^T \leq 0, \\
& \begin{bmatrix} U & u \\ u^T & 1 \end{bmatrix} \succeq 0,
\end{aligned}
$$

where $i$ and $j$ are selected to define unique distance pairs as per the set $\mathcal{K}$. The optimal solution includes the additional parameter $t^*$ which gives the upper bound on the maximum distance between two nearest regressors. A feasible input can be generated through randomization with further local refinement through nonlinear programming. To conclude, it can be noted that the numerical complexity of the both formulations for LTI systems using SDP relaxation is primarily a function of length of the input signal $N$ and less dependent on the dimension $m$ of the regressor space.

### *5.3.4 Sparse Polynomial Optimization of Data-Centric Formulations*

The relaxation procedure discussed in Section 5.3.2 is appealing from a theoretical point of view since it provides a systematic way for constructing a hierarchy of convex semidefinite relaxations guaranteed to converge to the global optimum of problem. However, due to the possible large size of the obtained SDP problem, a blind application of the 'dense' method to the input design problem is quite demanding in terms of computational resources due to an exponential increase in the size of the resulting SDP. Present SDP solver technology is in its infancy compared with solvers available for linear and quadratic programming which can handle millions of variables. The SDP relaxation introduced in the previous section is a special case applicable for approximate solution of LTI systems only. In other words, this implies that the traditional SDP relaxation has limited practical application unless a more efficient representation is found by exploiting the algebraic structure of the problem.

In Section 5.3.2, this was proposed as sparse polynomial optimization, and the concept of correlative sparsity and the running intersection property were introduced to detect underlying sparse structure of a given problem. Loosely speaking, the monomials of the objective and the polynomials in the constraint should be a function of only a few elements of the input $u$. This section explores the application of those methods to data-centric input signal design. The tractability of the numerical problem formulations developed in Section 5.3.1, for both LTI and Hammerstein systems, primarily depends on the following factors:

1. The nature of the input constraints expressed in the set $\mathbb{U}$ including the number of possible dosage levels (i.e., number of elements in the set $\mathbb{I}$), and the order of the polynomials $(u(k) - u_{-n})(u(k) - u_{1-n})...(u(k) - u_{n-1})(u(k) - u_n) = 0$.

2. The number of decision variable involved in the optimization problem or the length $N$ of the input signal $u$.

3. The parametrization of the regressor vector $\varphi(k)$

    - *ARX* which involves all the past variables through the output for a dynamic system,
    - *FIR* which involves limited past variables (although the dimension $m$ will be high).

4. The number of regressor distance pairs ($d_{ij}$) as shown in (4.45) and the metric, e.g. Euclidean distance vs Chebyshev distance, which is used to calculate the regressor distances $d_{ij}$.

5. The nature of system nonlinearities. For block-structured nonlinear system, the degree of the static nonlinearity $\mathcal{I}$ and $\mathcal{O}$.

Another way to look at the problem formulations is to examine what factors constitute the objective and what factors form part of the constraints. Based on the problem statements

developed in Section 4.4, for Problem Statement 1, $g_0$ is a function of regressor distance pairs ($d_{ij}$) and $\mathbf{K} \equiv \mathbb{U}$, and for Problem Statement 2, $g_0$ is linear and $\mathbf{K} \equiv \mathbb{U}$ and constraints involving the regressor distance pairs ($d_{ij}$). A natural first step is to detect the presence of native sparsity in input design problems. It is quite clear that the constraints on the shape of the input signal: amplitude, move size, switching constraint and integer constraint are function of only few elements of u. For the purpose of illustration, consider the following example:

**Example 1.** *Assume that* $N = 5$ *and* $u = [u(1), u(2), u(3), u(4), u(5)]^T$. *The optimization problem* $\mathbf{P}$ *where the set* $\mathbf{K}$ *is defined by amplitude, move size, switching constraints and three-level integer constraints can be written as*

$$
\begin{aligned}
\max_{u} \quad & g_0(u) \\
\text{s.t.} \quad & u_{\min} \le u(1) \le u_{\max} && \Rightarrow \{1\} \\
& \vdots \\
& u_{\min} \le u(5) \le u_{\max} && \Rightarrow \{5\} \\
& u(1) - u(2) \le \Delta u_{\max} && \Rightarrow \{1,2\} \\
& \vdots \\
& u(4) - u(5) \le \Delta u_{\max} && \Rightarrow \{4,5\} \\
& u(1) - u(2) = 0 && \Rightarrow \{1,2\} \\
& u(1) - u(3) = 0 && \Rightarrow \{1,3\} \\
& u(4) - u(5) = 0 && \Rightarrow \{4,5\} \\
& (u(1) - u_{-1})(u(1) - u_0)(u(1) - u_1) = 0 && \Rightarrow \{1\} \\
& (u(2) - u_{-1})(u(2) - u_0)(u(2) - u_1) = 0 && \Rightarrow \{2\} \\
& \vdots \\
& (u(5) - u_{-1})(u(5) - u_0)(u(5) - u_1) = 0 && \Rightarrow \{5\}
\end{aligned}
$$

*where* $\{\cdot\}$ *shows the involved variables in each constraint. Based on this information, the csp matrix* $R$ *can be written as*

$$R = \begin{pmatrix} 1 & 1 & 1 & 0 & 0 \\ 0 & 1 & 1 & 0 & 0 \\ 0 & 0 & 1 & 1 & 0 \\ 0 & 0 & 0 & 1 & 1 \\ 0 & 0 & 0 & 0 & 1 \end{pmatrix} \tag{5.37}$$

*which has a characteristic 'band' pattern [123, 212] implying that the input constraints are inherently sparse.*

It is interesting to note the input constraints are sparse irrespective of the objective $g_0$ which will depend on the estimator. For example, for classical linear statistical models [49], $g_0$ is some measure of the information matrix. Hence, the following proposition, for any input design problem under constraints, can be made:

**Proposition 2.** *The input constraints defined in* $\mathbb{U}$ *are correlative sparse where the csp matrix* $R \in \mathbb{R}^{N \times N}$ *has a band structure.*

Among other factors affecting the problem tractability, the number of input samples in the input sequence $N$ and the degree of the polynomials is dictated by the system dynamics, and thus does not provide scope for reformulation. The remaining factors in the optimization problem are how to parametrize the regressor vector and regressor distance pairs $d_{ij}$, and thus this is the central issue to be analyzed for data-centric input signal design. Towards this, in this dissertation two methods are developed:

1. First, a smaller set $\mathcal{J} \subset \mathcal{K}$ of distance pairs $d_{ij}$ is selected to make the problem amenable for sparse polynomial optimization as defined in [212, 221],

2. Second, using the fact that the distance $d_{ij}$ is already expressed as sum-of-squares to formulate a reduced-basis convex relaxation problem.

#### 5.3.4.1 Selected Regressor Distance Pairs

Since the regressor vector is parametrized, in general, by past inputs and past outputs, considering all the distance pairs from the set $\mathcal{K}$ will include polynomial equations which are dense and hence undesirable for sparsity-based methods. In other words, the distance pairs, unlike the input constraints, do not have inherent sparsity. This statement can be further clarified by the following example:

**Example 2.** *Consider the problem analyzed in Example 1. Assume that the regressor vector $\varphi(k)$ is composed to only past input i.e. FIR-type regressor with order $m = 2$*

$$\varphi(k) = [u(k-1)\ u(k-2)]^T. \tag{5.38}$$

*The regressor vectors can be enumerated as*[3]

$$\begin{aligned}
\varphi(1) &= [0\ 0]^T \\
\varphi(2) &= [u(1)\ 0]^T \\
\varphi(3) &= [u(2)\ u(1)]^T \\
\varphi(4) &= [u(3)\ u(2)]^T \\
\varphi(5) &= [u(4)\ u(3)]^T
\end{aligned}$$

*and the total number of distance pairs is given by $\frac{N(N-1)}{2} = \frac{5\times4}{2} = 10$, and can be written as*

$$\begin{aligned}
d_{12} &= f_d(u(1)) \\
d_{13} &= f_d(u(1), u(2)) \\
d_{14} &= f_d(u(2), u(3)) \\
d_{15} &= f_d(u(3), u(4))
\end{aligned}$$

[3]For simplicity, entries for 'negative time' are assumed to be zero and regressor vector upto $k = N$ are considered.

$$
\begin{aligned}
d_{23} &= f_d(u(1), u(2)) \\
d_{24} &= f_d(u(1), u(2), u(3)) \\
d_{25} &= f_d(u(1), u(3), u(4)) \\
d_{34} &= f_d(u(1), u(2), u(3)) \\
d_{35} &= f_d(u(1), u(2), u(3), u(4)) \\
d_{45} &= f_d(u(2), u(3), u(4))
\end{aligned}
$$

*where $f_d(\cdot)$ is a function to quantify the distance. The csp matrix $R$ for the all the distance pairs is dense:*

$$
R = \begin{pmatrix}
1 & 1 & 1 & 1 & 1 \\
1 & 1 & 1 & 1 & 1 \\
1 & 1 & 1 & 1 & 1 \\
1 & 1 & 1 & 1 & 1 \\
1 & 1 & 1 & 1 & 1
\end{pmatrix}. \tag{5.39}
$$

It is proposed in this work to chose select distance pairs such that they form a set $\mathcal{J} \subset \mathcal{K}$, and leads to the following problem statement:

**Problem Statement 5.** *Chose the distances $d_{ij}$ to form the set $\mathcal{J}$ such that running intersection property for sparse polynomial optimization is satisfied as well as the distance pairs provide enough coverage in the regressor space as argued in Section 4.4.*

More precisely, Problem Statement 5 argues that there are two aspects in choosing the distance pairs, first that the RIP condition is satisfied, and secondly that selected regressors pairs should make geometric sense in addition to satisfying the sparse property. As alluded to earlier, it is difficult to come up with sets $I_j$ for sparse polynomial optimization. Fortunately, for dynamical systems the regressor is not arbitrary and has a structure. For example, in the FIR-type regressor, each $\varphi(k)$ is distinct from $\varphi(k-1)$ and $\varphi(k+1)$ by one element of the vector as shown in Example 2. Thus, regressors closer in time $k$ are

also located closer geometrically in the vector space, and spreading these closer points will also force spreading of all other points in the regressor space. One of the possibilities is to consider the consecutive distances i.e. $d_{12}, d_{23}, d_{34}, d_{45}, \ldots$ and so on. In addition, from an algebraic point-of-view, it is easy to see that the consecutive distances are sparse as they satisfy RIP. Furthermore, the consecutive distances are more appealing for Problem Statement 2 as it maximizes the minimum distance and for regressors closely indexed by time, this may achieve a similar effect as choosing all the distance pairs. Thus, (5.8) and (5.10) are modified to include only selected distance pairs and upon analysis, the csp matrix for this selection has a band structure:

$$R = \begin{pmatrix} 1 & 1 & 1 & 0 & 0 \\ 1 & 1 & 1 & 1 & 0 \\ 1 & 1 & 1 & 1 & 1 \\ 0 & 0 & 1 & 1 & 1 \\ 0 & 0 & 0 & 1 & 1 \end{pmatrix} \tag{5.40}$$

and hence is sparse. Since the nonlinearity in block-structured systems is assumed to be memoryless or static, the sparse property is conserved for those systems. This idea can be extended by considering a cluster of near-by distances, for example, for $\varphi(k)$, distance two time indexes earlier and two time indexes later can be considered. Finally, this leads to the following proposition:

**Proposition 3.** *The qualified set of distance pairs can be obtained by selecting regressors which are close to each other as indexed by time $k$. In particular, the problem is sparsest if consecutive distance pairs are considered.*

Numerically it was observed that the minimum size of the maximum clique of the chordal extension of the csp graph is a bounded by the dimension of the FIR regressor $m$. This result is not difficult to understand based on the nature of resulting matrix $R$ due to consecutive distances and square of the distances calculated using the 2-norm. The exact

value of the clique sizes will depend on the actual number of distance pairs included in the design. Thus from a computational aspect, the number of variables appearing together $\kappa$ is only a function of $m$ where $N \gg m$ [221], and hence significant computational savings can be obtained for smaller $m$. Although very appealing in theory, it can be observed that the practical application of this method is quite limited if the dimension $m$ of the impulse response vector of the system is large. In that case, an approach is to make the impulse response vector $h$ as sparse as possible, for example by minimizing the 'zero-norm' of the impulse response vector $h$ of a given linear dynamical system:

$$\min_{h} \|h\|_0 \tag{5.41}$$

s.t. dynamical constraints are satisfied.

It is well known that this is a nonconvex optimization problem and can be relaxed by considering instead the 1-norm. Such specialized algorithms have been proposed in literature for FIR filter design [227]. In addition, a simple practical method is to approximate the small elements of $h$ to zero based on a user defined tolerance level. This approximation can result in considerable reduction in computational burden and has been using in example shown in Section 5.3.7. As an alternative, the system can be resampled at lower rate to reduce the dimension of the FIR regressor.

Finally, in conclusion to this section, it is important to note that there are many other possibilities to choose the distance pairs other than those pointed out earlier as long as the running intersection property is satisfied. For dynamical system, choosing nearby regressor vectors and coupled with Problem Statement 2, was found to provide useful results as shown in Section 5.3.7.

#### 5.3.4.2 Regressor Distance Pairs as Sum-of-Squares

In developing convex relaxation procedures, so far the fact that distance is always nonnegative $d_{ij} \geq 0$ as well as is already in sum-of-squares (SOS) form (e.g., for LTI systems: $d_{ij}^2 = u^T \mathbf{Q}_{ij} u$) has been neglected. The complexity of the solving the SDP for checking

SOS condition is dependent upon length of the monomial vector $v$ as defined in (5.16). The SOS module in MATLAB-based toolbox YALMIP offers many in-built functions aimed at reducing the size of the SDP problem by finding a better representation for the basis vector [216]. The following example compares the size reduction using YALMIP and size reduction by using the fact that the distances are already SOS.

**Example 3.** *Consider a Hammerstein system with input nonlinearity* $\mathcal{I} = 2.2u(k)^2 + 1.5u(k)^3$ *and with* $\mathcal{L} = \frac{1}{s+1}$. *The system is discretized at unit sampling and length of input signal is fixed at* $N = 10$. *The objective for problem formulation (5.10) is defined as sum of all the regressor distance pairs* $d_{ij}^2$ *which can be written as*

$$g(u) = \mathcal{I}(u)^T \mathbf{Q} \mathcal{I}(u) \tag{5.42}$$

*using notation from (5.16). The polynomial* $g(u)$ *is tested for SOS property by solving a SDP using YALMIP with features for dimensionality reduction turned on such as newton reduction, symmetry reduction and special post-processing developed in [216]. The size of the resulting* $\mathbb{V}$ *matrix is found to be* $126 \times 126$. *The problem is now solved with all dimensionality options tuned off while supplying the vector of monomials based on (5.42). The size of the resulting* $\mathbb{V}$ *is found to be* $20 \times 20$, *where the monomial vector can be written as*

$$v = [u(1)^2, \ldots, u(10)^2, u(1)^3, \ldots, u(10)^3]^T. \tag{5.43}$$

*Thus, the reduction in size is significant when the polynomial is known to be structured compared to using standard methods based on newton polytope and symmetry.*

The traditional sparse procedure developed in [212, 221] are developed for general polynomials and hence cannot make use of this specialized structure. The approach of using *a priori* structure has been previously used for unconstrained minimization in [222], and

hence can be conceptually extended to the case of constrained minimization. Towards this, the sparse SOS relaxation (5.28) can be modified as:

$$\tilde{\mathbf{P}}^{\xi}_{\mathbf{SOS}}: \quad \max_{\lambda, s_0, s_j} \ \lambda \tag{5.44}$$
$$\text{s.t. } g_0(u) - \lambda = s_0 + \sum_{j=1}^{m} s_j g_j, \ s_0 \in \Sigma_*, s_j \in \Sigma(I_j)$$
$$\deg(s_0), \deg(s_j g_j) \leq 2\xi$$

where the multiplier $s_0 \in \Sigma_*$, as shown in (5.44), is supplied by the user based on *a priori* knowledge of the distance pairs and the multipliers $s_j$ are function of only those variables which appear in respective constraints. However, unlike the sparse polynomial optimization introduced in previous sections where the convergence is guaranteed [221, 228], increasing the order of relaxation does not guarantee convergence and hence global solution cannot be certified for custom hierarchy developed in (5.44). If the constraints defined satisfy the Archimedean property, it could be shown that the solution can converge to the global minimum as argued in [228]. The formal analysis of convergence using these reduced basis formulation is not presented in this chapter and is an open research topic.

Instead, in this chapter, it is proposed that the SDP relaxation developed in (5.44) can be used to certify the quality of solution for any of the developed problem formulations from nonlinear programming. The proposed hierarchy has a distinct advantage over approaches using correlative sparsity and RIP condition that all of the regressor distance pairs from the set $\mathcal{K}$ can be considered irrespective of their parametrization (i.e. both FIR and ARX). This can be of help to calculate useful bounds on the local solution from nonlinear programming as discussed in Section 5.3.2. Similar bounding technique has been developed in Section 5.4 for highly interactive systems. The ensuing sections present numerical solution of the developed formulation using semidefinite relaxation of polynomial programs and using nonlinear programming.

### 5.3.5 Numerical Illustration: SDP Relaxation for LTI System Formulations

Consider a continuous-time second order system with a zero

$$G(s) = \frac{K_p(\tau_a s + 1)}{\tau^2 s^2 + 2\zeta\tau s + 1}, \tag{5.45}$$

where $K_p = 1$, $\tau_a = 2$, $\tau = 3$ and $\zeta = 0.6$. This model is discretized at unit sampling ($T = 1$) using a zero-order hold which can be fully parameterized by an ARX regressor of order [2 2 1]

$$\varphi(k) = [y(k-1)\ y(k-2)\ u(k-1)\ u(k-2)]^T, \tag{5.46}$$

$$\hat{y}(k) = \varphi(k)^T\theta, \tag{5.47}$$

where $\theta = [1.58, -0.6703, 0.2282, -0.1375]^T$.

Input signal design for data-centric methods is illustrated by comparing the two optimal inputs with the traditional pseudo random binary sequence (PRBS) [229] and Schroeder-phased multisine input [146]. Design of standard inputs in system identification is discussed in Section 3.4.1. The PRBS input is designed with switching time $T_{sw} = 2$ for $n_r = 5$ shift registers (see also [230] for the PRBS guidelines used) such that the length $N$ is 62. Similarly, a multisine signal $u(k) = \sum_{i=1}^{n_s} a_i \cos(\omega_i kT + \phi_i)$ was designed of same the length ($N = 62$) with $n_s = 10$, $a_i \in \mathbb{R}$ are constant for all $n_s$, frequencies $\omega_i$ uniformly spread over the desired bandwidth and phases $\phi_i$ determined by the Schroeder method [230, 146]. The input constraint set is defined by: $\tilde{\mathbb{U}} = \{u \in \mathbb{R}^N : u_{\min} \leq u \leq u_{\max}\} \subset \mathbb{U}$ where $u_{\min} = -\mathbf{1}$ and $u_{\max} = \mathbf{1}$ for the first optimal input and PRBS; for the second optimal input and the multisine signal, the amplitude was increased to $u_{\min} = -\mathbf{1.5}$ and $u_{\max} = \mathbf{1.5}$ to achieve a similar span in the regressor space for all cases. The SDP is coded in MATLAB with YALMIP [174] interface using SeDuMi [156] as the SDP solver, `quadprogbb` is used as the global solver for nonconvex quadratic program [224] and MATLAB function `fmincon` is used as the SQP nonlinear solver.

Table 5.2: Tabulation of sum of unique distances between all regressors for problem (5.7).

| Objective | Value |
|---|---|
| Upper bound ($\nu_{\text{SDP}}$) | 16038 |
| Lower bound ($0.63\nu_{\text{SDP}}$) | 10104 |
| Best objective from low rank approximation | $14921 \simeq (0.93\nu_{\text{SDP}})$ |
| PRBS objective | 10065 |
| Multisine objective | 4829 |
| Nonlinear programming objective | 12212 |
| Global objective from `quadprogbb` | 14927 |

First, the optimization formulation for maximizing the sum of regressor distances, as shown in (5.7) and (5.31), is solved. Extending the result from [84], the semidefinite relaxation is compared with the global solver and the standalone nonlinear solver. Upon solving the SDP (5.31)-(5.32), $\nu_{\text{SDP}} = 16038$ is the maximum value that can be attained by the maximization problem (5.7). Based on Theorem 2, a lower bound on the objective is 10104. The rank $r$ of $U$ was found to be equal to 3. Hence, a feasible solution can be generated through low rank approximation (or through randomization) with projection using the signum function. An objective function value $J_1$ of 14921 was obtained using the best rank one approximation and the corresponding optimal input signal is shown in Figure 5.9a. In comparison, the objective function values for PRBS and multisine signals are 10065 and 4829 respectively, which are lower than the guaranteed objective from the optimal input. In fact, randomization gave an objective function value improvement of 48.2% over the PRBS objective and 208.9% over the multisine objective. The global solution from [224] was found to be 14927, which is very close to the solution obtained from SDP relaxation (within 0.04%). Finally, using standalone nonlinear programming with 100 random initializations, the best objective function value achieved was only 12212. All these different objective values are noted in Table 5.2.

Similarly, the second optimization formulation for maximizing the minimum regressor distance pair, as shown in (5.8) and (5.36), is solved. The optimal input corresponding to

maximum $t$ from randomization and subsequent local refinement is selected and is shown in Figure 5.9a. A dynamical simulation for both optimal inputs is also shown in Figure 5.9a, with the distribution of regressors using the first two elements of the regressor in (5.46): $y(k-1)$ and $y(k-2)$ depicted in Figure 5.9b. The first optimal input switches less frequently to cover a larger output span, and thereby places elements towards the boundary of the set as shown in Fig. 5.10; in contrast, the second input switches more often, thus accomplishing a better fill-in of the regressor space. The solution presented in this section were computed on quadcore XEON machines using 16 GB RAM. Both the input design were run for $N = 62$. On the first problem, the solution times were quick, for example, it took around 15 sec to run the SDP problem. The second formulation is much harder to solve than the first formulation and thus takes longer time. For the second formulation, the SDP problem took around 58 sec to solve. To generate a feasible solution, one iteration of randomization plus local NLP refinement took 9 sec. This process of generating feasible input was repeated for 50 times and the best input was chosen. Thus, the total time for this execution was around 10 min.

It is interesting to evaluate the performance of data-centric estimators (such as MoD and DWO) for the two optimal inputs in comparison with traditional signals under noisy conditions. The two optimal inputs, PRBS and multisine signal, with their corresponding outputs are used to form a database of regressors which defines the estimation set. Two cycles of a test signal consisting of a combination of slow and fast dynamics with its corresponding output (as shown in Figure 5.9a) is used to form the validation set. The validation output is further corrupted by a zero mean Gaussian noise with standard deviation $\sigma_{\text{val}}$ ranging from no noise ($\sigma_{\text{val}} = 0$) to very noisy ($\sigma_{\text{val}} = 2$). The distribution of regressor components $(y(k-1), y(k-2))$ for used inputs and validation (noisy and noise-free) is shown in Fig. 5.11-Fig. 5.13. The function values are estimated from the MoD and DWO estimators and compared with the true predictions as per (5.47) using the validation dataset. The average root mean square (rms) errors calculated over 100 simulations for

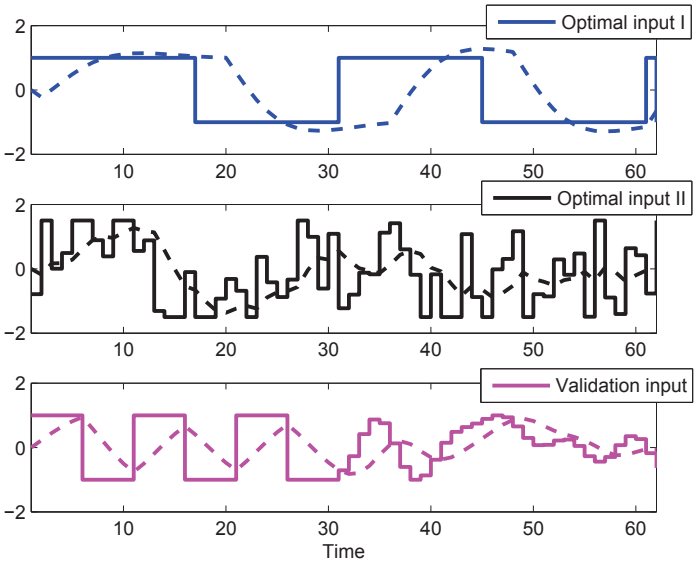


(a)

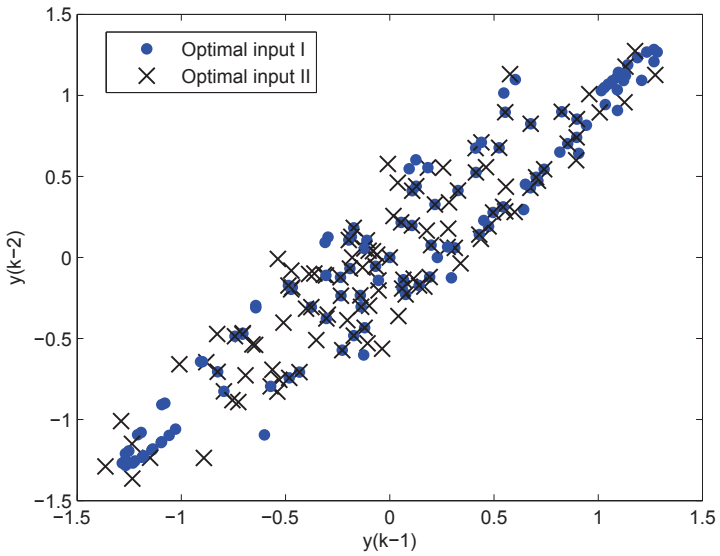


(b)

Figure 5.9: (a) Input-output dynamic simulation for both amplitude constrained optimal inputs (solid line) and the validation input. The corresponding outputs are shown by dashed lines. (b) Distribution of regressor components $(y(k-1), y(k-2))$ for both optimal inputs.

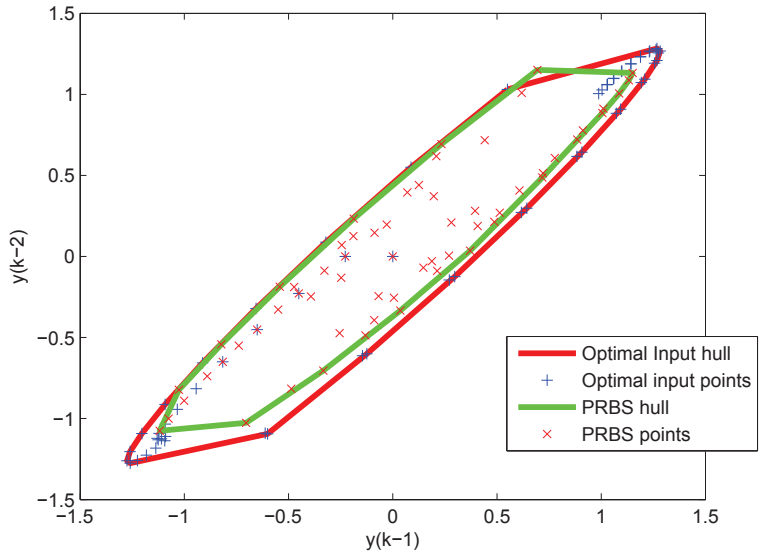


Figure 5.10: Comparison of convex hull for optimal input I and PRBS as shown for regressor components $y(k-1), y(k-2)$. The PRBS hull is almost entirely contained in the hull formed by the optimal input.

both estimators are tabulated in Table 5.3. Under low noise in the validation data, for instance $\sigma_{\text{val}} = 0.05$, the average rms error from the second optimal input was superior to the first optimal input, PRBS and multisine signal. This is a result of the greater uniformity in the regressor space for this design, leading to better estimates from both MoD and DWO estimators. As the noise in the validation set is increased (e.g, $\sigma_{\text{val}} = 1$ and $\sigma_{\text{val}} = 2$), the validation data regressors start to lie outside the range of estimation database, resulting in poorer estimates. Here, the first optimal input offers the lowest rms error as a result of maximally distributed regressors which minimize the effect of extrapolation for both estimators. Finally, one observes that for the first optimal input, the estimates from DWO are better than those from MoD, while for the second optimal input, the MoD estimates are generally better than those from DWO.

Table 5.3: Tabulation of average rms errors (over 100 simulations) from MoD and DWO estimators for amplitude-only constraints on the optimal inputs, PRBS and multisine signal.

| # | MoD [55] | | | | DWO [56] | | | |
|---|---|---|---|---|---|---|---|---|
| $\sigma_{\text{val}}$ | Opt. input # 1 | Opt. input # 2 | PRBS | Multisine | Opt. Input # 1 | Opt. Input # 2 | PRBS | Multisine |
| 0 | 0.12572 | 0.024389 | 0.047463 | 0.26038 | 0.10182 | 0.02515 | 0.053273 | 0.15167 |
| 0.05 | 0.12603 | 0.030049 | 0.050217 | 0.2618 | 0.10228 | 0.031072 | 0.055135 | 0.15215 |
| 0.1 | 0.12699 | 0.042586 | 0.057993 | 0.26687 | 0.10381 | 0.043876 | 0.060328 | 0.15339 |
| 0.5 | 0.15457 | 0.15766 | 0.14639 | 0.36948 | 0.1361 | 0.16092 | 0.13157 | 0.1824 |
| 1 | 0.21491 | 0.31028 | 0.2601 | 0.54546 | 0.19735 | 0.31411 | 0.23509 | 0.24174 |
| 2 | 0.39958 | 0.66205 | 0.53647 | 0.93183 | 0.36383 | 0.65529 | 0.48876 | 0.41795 |

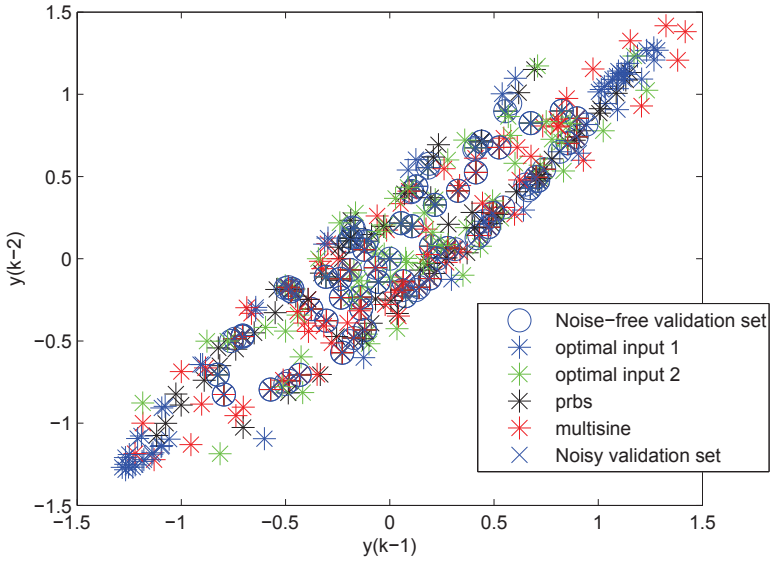


Figure 5.11: Distribution of regressor components $(y(k-1), y(k-2))$ for noise-free validation dataset, both optimal inputs, prbs input, multisine input, and the noisy validation dataset with $\sigma_{\text{val}} = 0$.

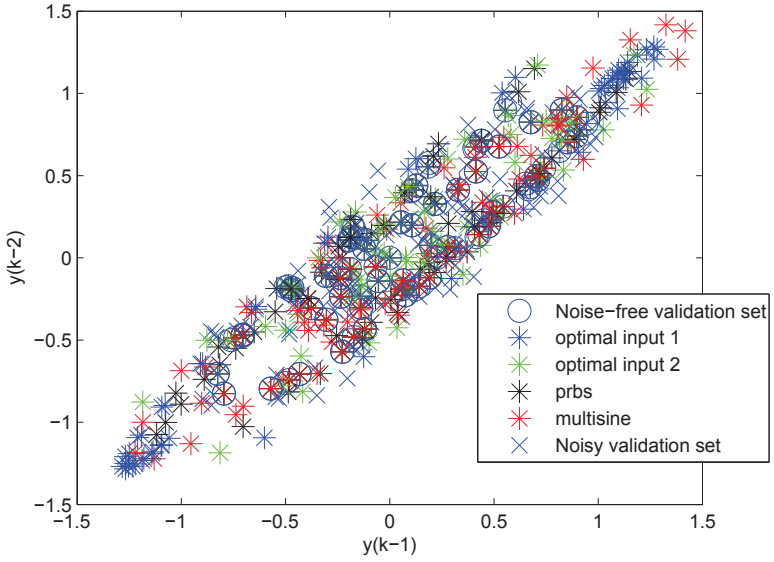


Figure 5.12: Distribution of regressor components $(y(k-1), y(k-2))$ for noise-free validation dataset, both optimal inputs, prbs input, multisine input, and the noisy validation dataset with $\sigma_{\text{val}} = 0.1$.

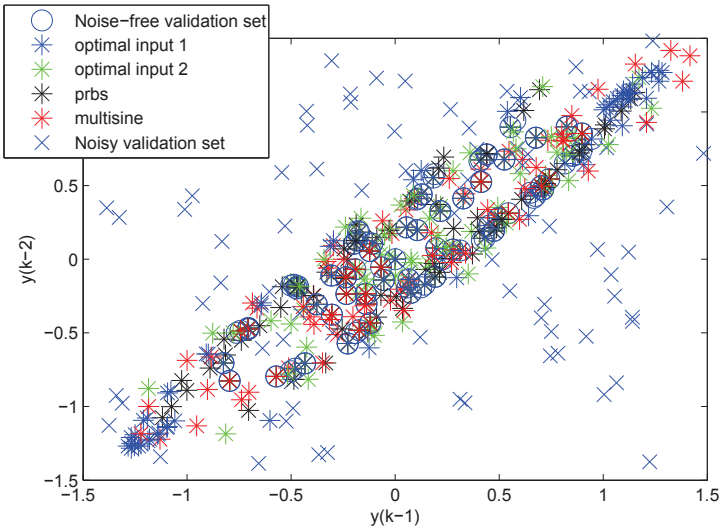


Figure 5.13: Distribution of regressor components $(y(k-1), y(k-2))$ for noise-free validation dataset, both optimal inputs, prbs input, multisine input, and the noisy validation dataset with $\sigma_{\text{val}} = 1$.

### *5.3.6 Numerical Illustration: Nonlinear Programming for Hammerstein System Formulations*

Consider the discrete-time LTI system $\mathcal{L}$ considered in Section 5.3.5. Assume that the input nonlinearity $\mathcal{I}$ is the power function

$$w_H(k) = (u(k))^{n_I} \quad \forall k. \tag{5.48}$$

Based on this relation, the regressor can be written as

$$\varphi(k) = \begin{bmatrix} P_k G \\ Q_k \end{bmatrix} \mathcal{I}(u) = \begin{bmatrix} P_k G \\ Q_k \end{bmatrix} [u(1)^{n_I}, \ldots, u(N)^{n_I}]^T. \tag{5.49}$$

In the subsequent numerical example, power nonlinearity is set to degree two, i.e. $n_I = 2$. The input signal is amplitude constrained as $u_{\min} \leq u \leq u_{\max}$ where $u_{\min} = -\mathbf{2}$ and $u_{\max} = \mathbf{2}$ so as to amplify (since $n_I > 1$) the input signal which should help increase the power, specially in the case of classical inputs.

Design of standard inputs in system identification is discussed in Section 3.4.1. For PRBS, based on $\tau_{\text{dom}}^{H} = \tau_{\text{dom}}^{L} = \tau_{\text{dom}} = 2.14$ (or $n_r = 5$, $T_{sw} = 2$), the length is found to be $N = N_{\text{cyc}} * T_{sw} = 62$ as shown in Fig. 5.14. For MLPRS, the design variables are chosen as $m_l = 3$, $q = 3$, $T_{sw} = 2$ to satisfy the high frequency limit and $n_r = 4$ to satisfy the low frequency limit. The length of the signal is $N = 160$ as shown in Fig. 5.15. The length of the uniform random signal was chosen to be as long the MLPRS to give enough power to this input as shown in Fig. 5.16.

The optimal input is generated by solving the problem (5.9) under amplitude constraints only and using a random initialization over 50 iterations. The length of the signal can be fixed rather arbitrarily ($N = 60$) and this feature has distinct advantages over the classical designs. The dynamic simulation of optimal input is shown in Fig. 5.17. To test the MoD estimator performance under various inputs, an independent noise-free validation dataset is created containing slow and fast dynamics of length $N = 124$ as shown in Fig. 5.18 using the true system shown in (5.47) and the regressor shown in (5.49). In comparison to the other inputs, the optimal signal naturally has more than two levels and it switches less often thus allowing the system to reach its maximum value, thus covering the regressor space. Table 5.4 shows the root mean square error (RMS) and maximum error (MAX) from the MoD estimator for simulation using a fixed validation dataset and fixed set of MoD settings. The lowest RMS is obtained for the optimal input which is a 16.6% improvement over the next best signal MLPRS, although MLPRS is almost three times as long as the optimal input. Further, it should be mentioned that the optimal input allows for inclusion of other input constraints such as move size constraints (4.3) which is not possible in the MLPRS design. The uniform random signal also does not cover the available span and gives higher RMS values although it is as long as the MLPRS signal. Finally, the PRBS gave the worst result because it is restricted to be binary.

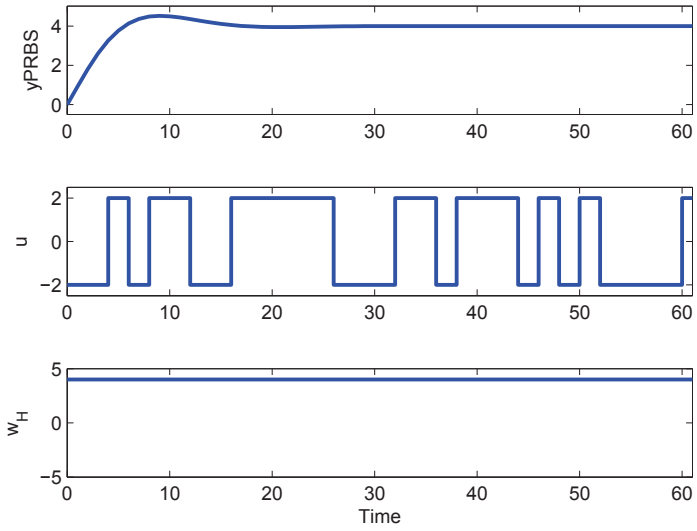


Figure 5.14: Dynamic simulation of PRBS signal ($u$) under amplitude constraints, intermediate signal ($w_H$) and the corresponding output $y$.

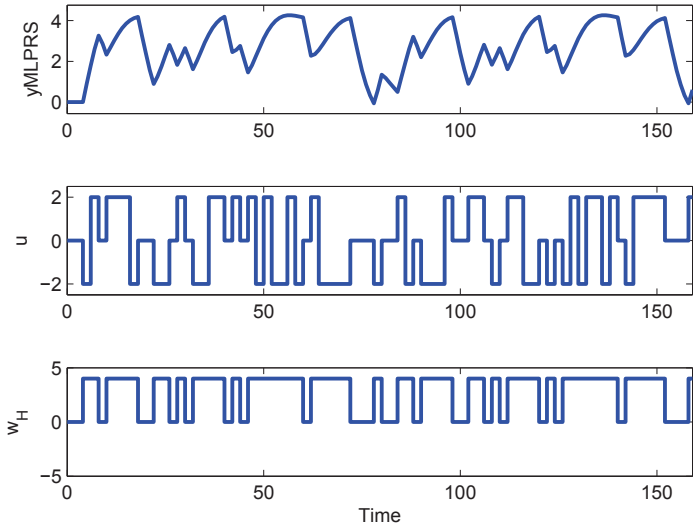


Figure 5.15: Dynamic simulation of MLPRS signal ($u$) under amplitude constraints, intermediate signal ($w_H$) and the corresponding output $y$.

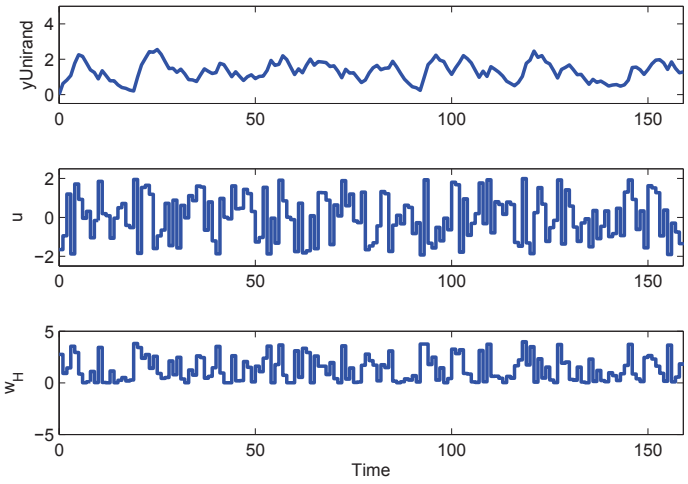


Figure 5.16: Dynamic simulation of uniform random signal ($u$) under amplitude constraints, intermediate signal ($w_H$) and the corresponding output $y$.

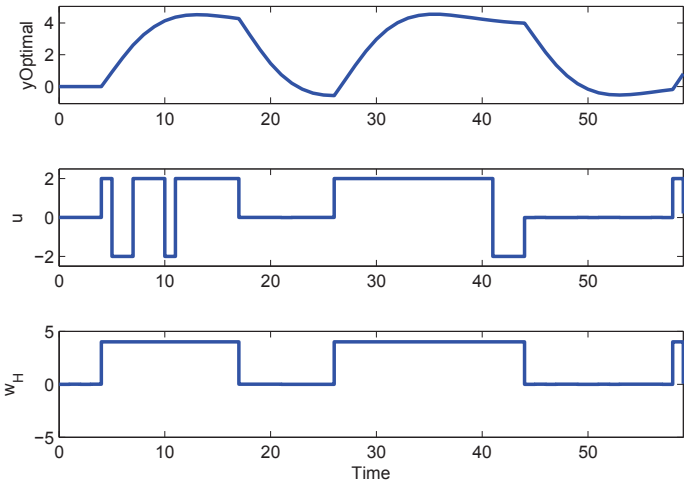


Figure 5.17: Dynamic simulation of optimal signal ($u$) under amplitude constraints, intermediate signal ($w_H$) and the corresponding output $y$.

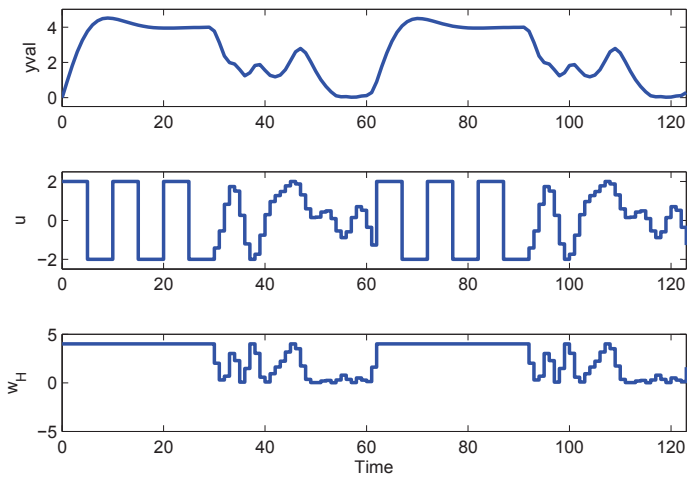


Figure 5.18: Dynamic simulation of validation signal ($u$), intermediate signal ($w_H$) and the corresponding output $y$.

Table 5.4: Tabulation of root mean square error (RMS) and maximum error (MAX) from the MoD estimator for simulation using a fixed validation dataset for problem (5.9).

| Input signal | RMS | MAX |
|---|---|---|
| PRBS ($N = 62$) | 2.0814 | 3.971 |
| MLPRS ($N = 160$) | 0.4764 | 0.9738 |
| Uniform random ($N = 160$) | 1.2407 | 2.879 |
| Optimal input ($N = 60$) | 0.39702 | 1.08 |

### *5.3.7 Numerical Illustration: Sparse Polynomial Optimization for Data-Centric Formulations*

In this section, application of sparse polynomial optimization using selective distance pairs is shown. Consider a linear first order system $\mathcal{L}$:

$$G(s) = \frac{K_p}{\tau s + 1} \tag{5.50}$$

where $K_p = 1$ and $\tau = 0.5$. The system is discretized at unit sampling and the resulting system can be represented using FIR-type regressor of dimension $m = 3$, which can be

written as: $\varphi(k) = [u(k-1)\ u(k-2)\ u(k-3)]^T$. The numerical example is shown for amplitude-only constraint: $u_{\min} \leq u \leq u_{\max}$ where $u_{\min} = -\mathbf{2}$ and $u_{\max} = \mathbf{2}$. Consequently, the regressor space is defined by a cube (polytope) and can be visually analyzed. For Hammerstein system, similar dynamics and constraints are considered where the input nonlinearity is assumed to a square nonlinearity $\mathcal{I} = u(k)^2$. The optimization problems are coded in MATLAB with the YALMIP toolbox [174] interfaced with the SparsePOP solver [186]. It is observed that the problems converge to optimal solution for finite value of the relaxation order $\xi \leq 3$.

First, problem formulations for LTI systems are solved. The problem formulation shown in (5.7) is solved by considering only consecutive distance pairs. Figure 5.19 shows the resulting input signal and the spread of the regressor in the regressor space ($m = 3$). Due to the objective to maximize the sum of all distance which are consecutive to each other, the resulting input switches very fast. In addition, the spread in the regressor space is also not very impressive as many regressor points overlap although the sum of distances are maximized. Next, Fig. 5.20 shows the input signal ($N = 30$) and the distribution of regressors for the problem formulation shown in (5.8). Since the optimization maximizes the minimum distance (which in this case is consecutive distances including the regressor at the origin), the regressor points lie on the boundary (and vertices) of the polytope defining the region and hence cover the regressor space. Fig. 5.21 shows the same problem but with increased signal length ($N = 60$) and additional limit on the move size of the input $|\Delta u| \leq 3.5$. The input signal now cannot switch the whole span due to move size limitation and the corresponding regressor spread reflects this behavior. Finally, for the Hammerstein system, Fig. 5.22 shows the resulting input signal under amplitude constraints and the spread in the regressor space for problem formulation (5.10). Since the input nonlinearity is square, the input automatically selects three levels to distribute the regressors. In both dynamical systems, it is observed that the regressors are well spread in the feasible space even though the formulation considered selected distance pairs with significantly longer

Table 5.5: Tabulation of objective values as lower bound from nonlinear programming and an upper bound from SDP relaxation of polynomial optimization for Hammerstein systems.

| NLP objective | SDP objective |
|---|---|
| 53269.17 | 63424 ($\xi = 3$) |

signal length ($N = 30, 60$) which are traditionally unsolvable through dense SDP relaxation.

Finally, the custom SOS hierarchy of SDP relaxation is used to generate useful bounds on the objective function. Consider the problem formulation solved for Hammerstein system in Section 5.3.6. For the length of the input signal $N = 60$, the best objective from NLP solver was found to be 53269.17. As argued earlier, by itself the NLP objective does not convey the quality of the solution. The problem methodology shown in (5.44) by supplying the following custom basis to the YALMIP SOS module:

$$v = [1, u(1), \ldots, u(60), u(1)^2, \ldots, u(60)^2, u(1)^3, \ldots, u(60)^3]^T, \tag{5.51}$$

and the relaxation order $\xi = 3$. The resulting objective value from solving the SDP is found to be 63424. Thus, it can be noted that the NLP solution is not arbitrarily bad and the global maximum lies between the two objective values found from NLP and SDP approach as shown in Table 5.5.

## 5.4 Input Signal Design for Highly Interactive Systems

This section proposes numerical solution for an representative highly interactive dynamical system shown in (4.67). As alluded to earlier, it is difficult to obtain information in the low gain direction using convention open-loop input signals and hence an input is required which can achieve a more uniform coverage by exciting both low and high gain directions [95]. In previous work, this was achieved using results from discrepancy theory [193] and the input design formulation minimizes the Weyl's criterion

$$\min_{u \in \mathbb{U}} \frac{1}{N} \sum_{k=1}^{N} e^{(2\pi i(\ell_1 y_1(k) + \ell_2 y_2(k)))} \tag{5.52}$$

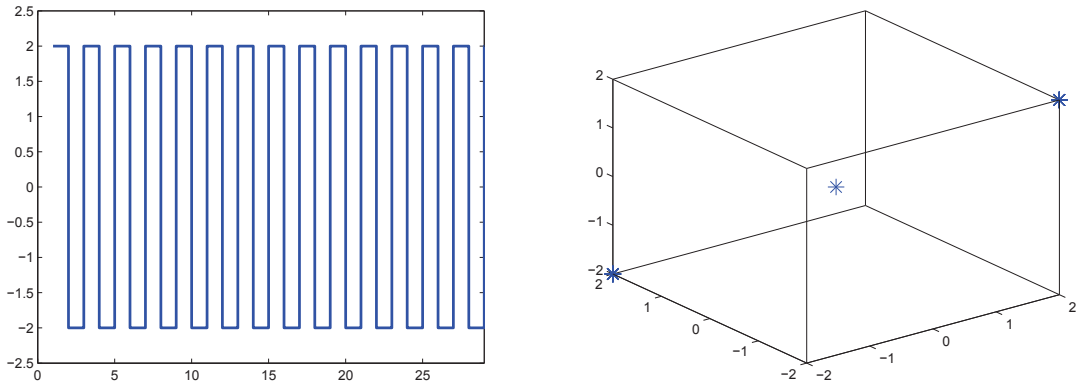


(a) Optimal input

(b) Distribution of regressors

Figure 5.19: Optimal input for LTI system ($N = 30$) using problem formulation (5.7) and the resulting distribution of regressors.

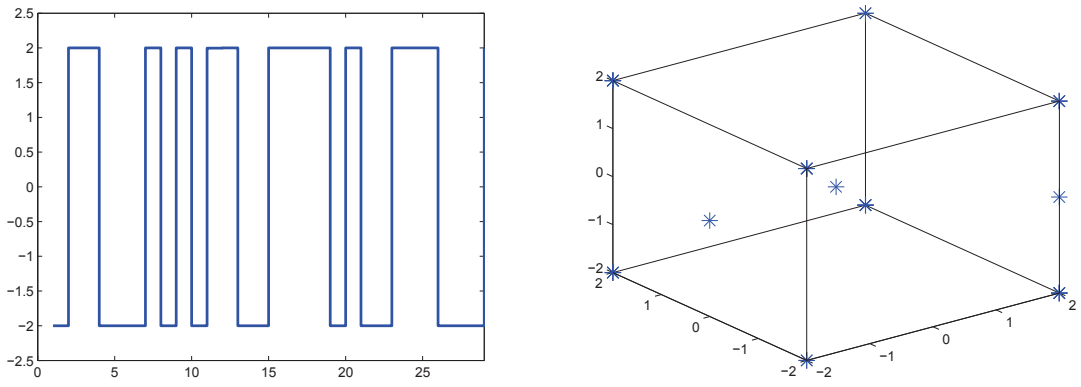


(a) Optimal input

(b) Distribution of regressors

Figure 5.20: Optimal input for LTI system ($N = 30$) using problem formulation (5.8) and the resulting distribution of regressors.

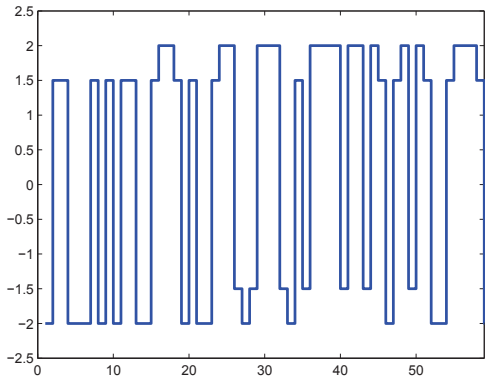


(a) Optimal input

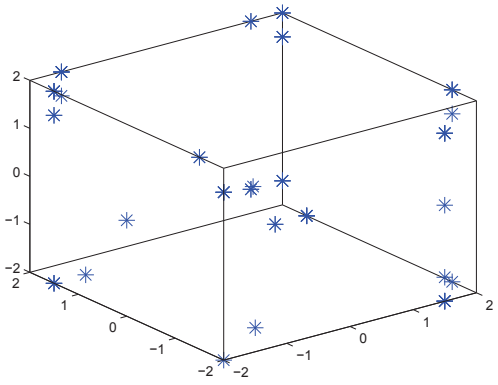


(b) Distribution of regressors

Figure 5.21: Optimal input for LTI system ($N = 60$) using problem formulation (5.8) and the resulting distribution of regressors under additional move size restriction $|\Delta u| \leq 3.5$.

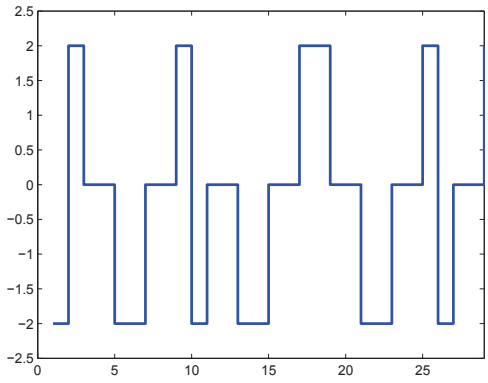


(a) Optimal input

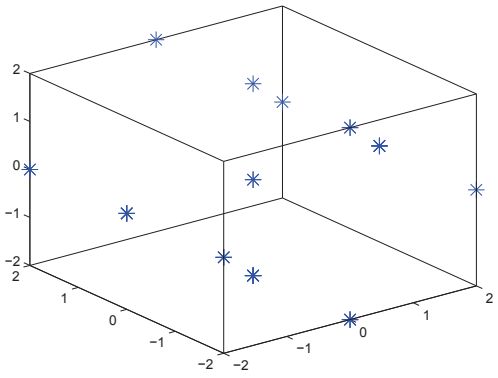


(b) Distribution of regressors

Figure 5.22: Optimal input for Hammerstein system ($N = 30$) using problem formulation (5.10) and the resulting distribution of regressors.

under constraints on the input to achieve uniform coverage in the output space [80, 153].

In this section, the problem formulation is developed on Problem Statement 3 which tries to maximize the minimum distance between output points in order to cover the space under constraints:

$$\begin{aligned} \max_{u,t} \quad & t \\ \text{s.t.} \quad & u^T \mathbf{Y}_{ij} u \geq t, \\ & u \in \mathbb{U}, \end{aligned} \tag{5.53}$$

where $\mathbf{Y}_{ij}$ is selected as per the set $\mathcal{K}_y$. It should be pointed out that additional constraints can be imposed on (5.53) to comply with certain directions in the output space. For LTI systems, such constraints can be written as a quadratic function of the variable $u$. For example, the optimization problem can be forced to excite the low-gain direction only by the following condition

$$y_1 y_2 \leq 0 \tag{5.54}$$

based on the partition of the output space into grids for high gain and low gain [95].

Similar to problems formulated for LTI systems in Section 5.3.1, the optimization problem (5.53) is a nonconvex quadratic program since $\mathbf{Y}_{ij} \succeq 0$ as the distance $dy_{ij} \geq 0$ is always nonnegative. As noted earlier, the nonconvex quadratic programs are, in general, NP-hard [94] and hence difficult to solve to global optimality. Since (5.53) is composed of smooth functions, it can be solved locally using standard nonlinear programming methods [124]. For example, the MATLAB function `fmincon` can used with the interior-point or sequential quadratic programming (SQP) algorithm where the best solution is chosen based on a random initialization over a finite number of runs.

Other than the clear drawback of local solution not necessarily being global, there is no certificate on the quality of the solution. An approach to construct bounds on nonconvex quadratic optimization is through relaxing the problem as a semidefinite program. As discussed in previous sections, the relaxation procedure involves replacing the nonconvexity

of the problem with a convex condition which is, in theory, more tractable [170]. For completeness, the procedure of developing SDP relaxation is restated for this problem. For the case of quadratic objective and constraints, the procedure involves linearization as follows:

$$u^T \mathbf{Y}_{ij} u = \mathrm{Tr}(\mathbf{Y}_{ij}(uu^T)) = \mathrm{Tr}(\mathbf{Y}_{ij}U), \tag{5.55}$$

$$U = uu^T = U^T \in \mathbb{R}^{2N\times 2N} \iff U \succeq 0,\ \mathrm{rank}(U) = 1 \tag{5.56}$$

where $\mathrm{Tr}(\cdot)$ is the matrix trace operator. Using the variable transformation shown in (5.55), the problem (5.53) can be written as

$$\begin{aligned} \max_{u,U,t} \quad & t \\ \text{s.t.} \quad & \mathrm{Tr}(\mathbf{Y}_{ij}U) \geq t, \\ & u \in \mathbb{U}, \\ & \begin{bmatrix} U & u \\ u^T & 1 \end{bmatrix} \succeq 0 \end{aligned} \tag{5.57}$$

where (5.56) has been relaxed and written in the Schur complement form [85]. As before, more stricter bounds can be added on the matrix variable $U$ by adding redundant constraints through the reformulation-linearization technique [226]:

$$U - u_{\min}u^T - uu_{\min}^T + u_{\min}u_{\min}^T \geq 0, \tag{5.58}$$

$$U - u_{\max}u^T - uu_{\max}^T + u_{\max}u_{\max}^T \geq 0, \tag{5.59}$$

$$U - u_{\min}u^T - uu_{\max}^T + u_{\min}u_{\max}^T \leq 0. \tag{5.60}$$

where $u_{\min} = [u_{\min 1}^T u_{\min 2}^T]^T$ and $u_{\max} = [u_{\max 1}^T u_{\max 2}^T]^T$.

Unlike nonlinear programming, the semidefinite relaxation procedure does not yield a feasible input unless the relaxation is tight. The optimal variable $t^*$ provides an upper bound on the minimum distance between two points in the output space while the best nonlinear solution will provide the lower bound on the maximization problem. Thus the

SDP relaxation at least provides a certificate for the quality of solution from nonlinear techniques.

Numerical examples are now shown to highlight the proposed method by comparing the results from optimization-based formulation with the input design based on Weyl's criterion. Consider the $2 \times 2$ system shown in (4.67). The system is discretized using zero-order hold with unit sampling resulting in discrete-time relationship, as shown in (4.64)-(4.65), where the length of the input signal is chosen to be $N = 50$. In this section, the optimization (5.53) is solved using nonlinear programming and the solution is certified by solving a relaxed version using semidefinite programming as shown in (5.57). The program is coded in MATLAB with YALMIP interface [174], with MOSEK as the SDP solver [183] and `fmincon` as the nonlinear solver using the SQP algorithm. For both problems, the amplitude of the output variable is restricted while no restriction is imposed on the input signal

$$-\infty < u_i(k) < \infty \quad \forall k \tag{5.61}$$

$$-200 \leq y_i(k) \leq 200 \quad \forall k. \tag{5.62}$$

Fig. 5.23 shows the optimal input and resulting noise-free output signals. Based on the ill-conditioned system (4.67), in order to excite the low gain direction, it is expected that large changes are required as is observed in Fig. 5.23. The optimization formulation naturally generates high amplitude correlated inputs to excite both low and high gain regions. The best objective from nonlinear programming was found to be $J = 4275.8$ where as the upper bound from SDP relaxation was found to be $t^* = 12042$. As discussed in earlier sections, the global solution lies between these two values and the SDP relaxation provides a reference for the quality of the solution as shown in Table 5.6.

The optimization-based results are contrasted with the Weyl's criterion based design shown in (5.52). More details on the computational aspects of Weyl design can be found in [95, 153]. Since Weyl's criterion is true only asymptotically, for a fairer comparison the

Table 5.6: Tabulation of objective values as lower bound from nonlinear programming and an upper bound from SDP relaxation of nonconvex quadratic programs for highly interactive systems.

| NLP objective | SDP objective |
|---|---|
| 4275.8 | 12042 ($\xi = 2$) |

length of the input signal is increased to $N = 100$. Fig. 5.24 shows the input using Weyl's criterion and the resulting noise-free output. Similar conclusion can be drawn as for the optimization inputs that large changes have to be made to excite the low gain direction. The difference between two approaches can be seen in the output distribution as shown in Fig. 5.25. The Weyl design suffers primarily because of finite length of the input signal where as the geometric objective in the optimization-based design performs much better by offering a more uniform coverage at input length half of the Weyl design. In addition, the optimization-based approach is computationally less intensive than the Weyl design, as well as can be complemented by SDP relaxation approaches where as the Weyl design is not amenable to traditional relaxation methods.

## 5.5 Chapter Summary and Conclusions

This chapter presented the problem formulations and their numerical solutions for constrained input signals for data-centric estimation methods. Broadly, the data-centric input design is shown using two approaches: one based on Weyl's criterion, and the other based on distribution of regressors and outputs.

To accomplish the Weyl design, a time-domain approach for input signal synthesis is presented which is motivated by the requirements of clinical trials for pain treatment intervention. This design considers constraints on signal magnitude, move sizes, and the categorical nature of the input signal. A joint input-output design is presented to achieve a uniform distribution in the output. The resulting optimization problems are integer-

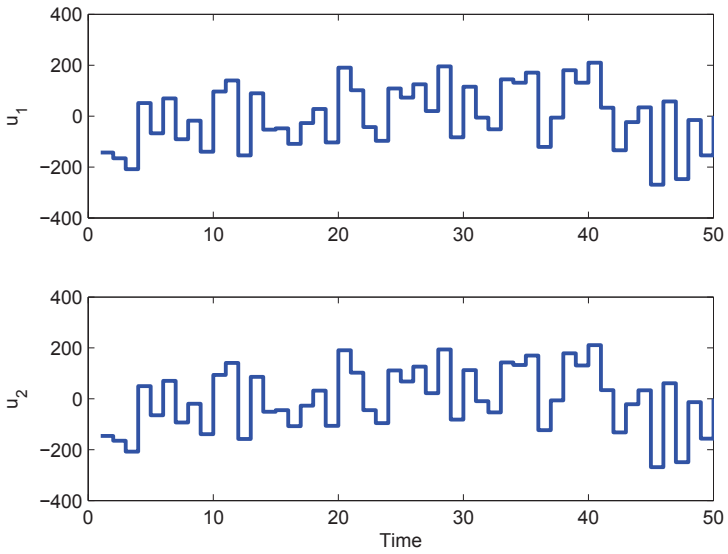


(a) Input signals.

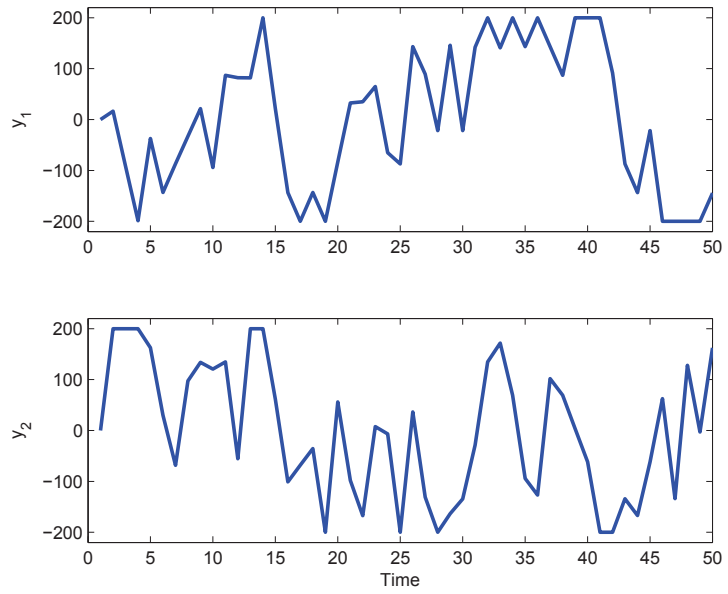


(b) Noise-free output signals.

Figure 5.23: Optimal input ($N = 50$) for problem formulation (5.53) under constraints on the output for system shown in (4.67).

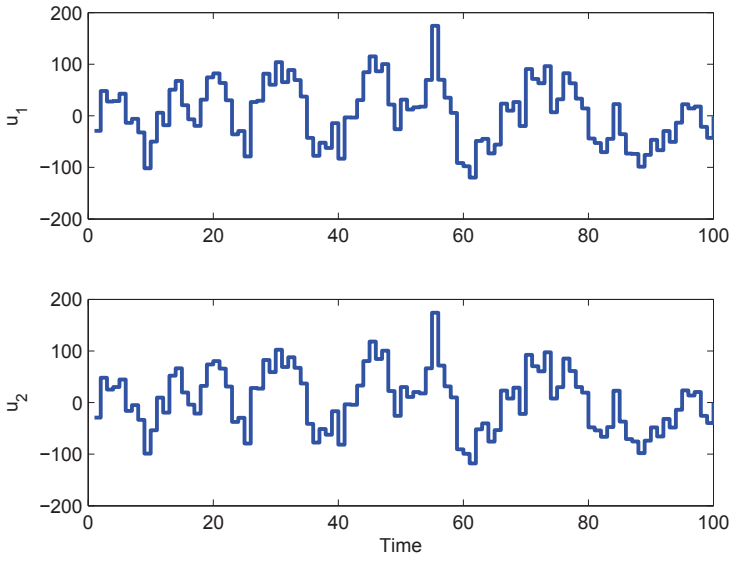


(a) Input signals.

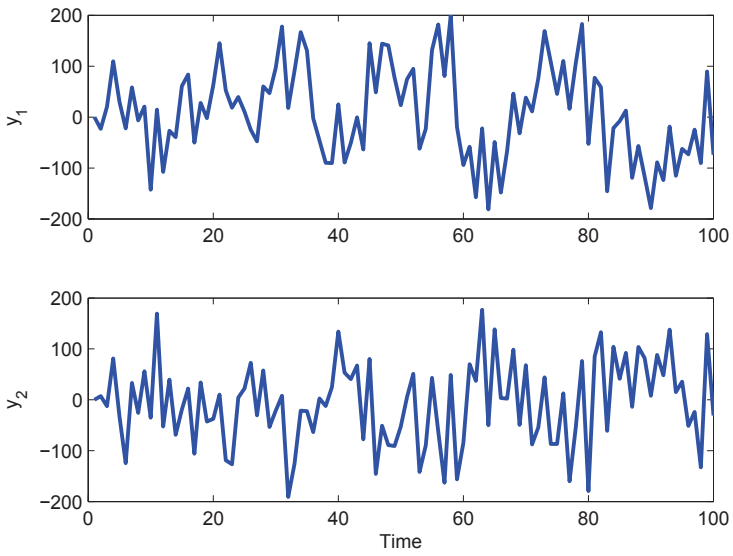


(b) Noise-free output signals.

Figure 5.24: Weyl input ($N = 100$) for problem formulation (5.52) under constraints on the output for system shown in (4.67).

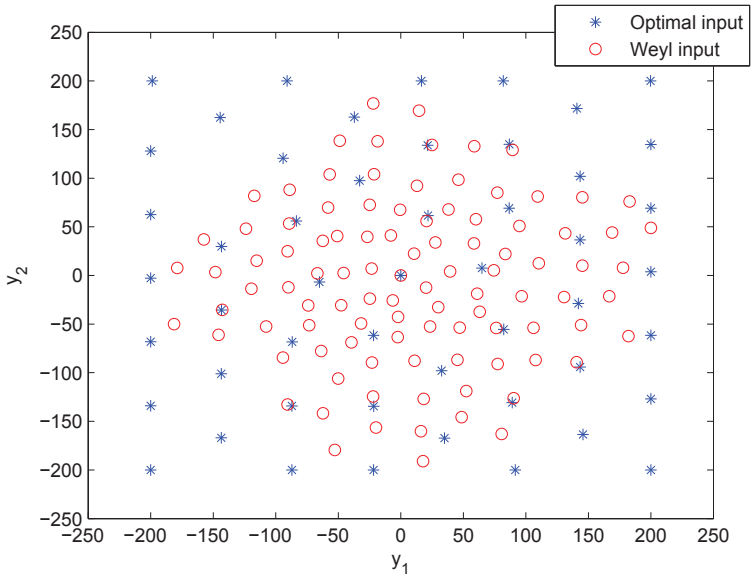


Figure 5.25: Comparison of distribution of output components $(y_1(k), y_2(k))$ for optimization-based design and Weyl design for system shown in (4.67).

constrained nonlinear programming problems. A polynomial-based static relaxation for the integer constraints is used so that the problem can be solved by nonlinear programming. A hypothetical gabapentin-based clinical trial is shown to illustrate the usefulness of the proposed design. Best optimization results in comparison to approximated multisines are obtained when a minimum weekly switching time is required between dosage changes.

For the distribution of regressors, two formulations are proposed towards achieving constrained input signal design for data-centric estimation methods. The objective is to distribute regressors, as measured by their Euclidean distances, in a given finite dimensional regressor space. The first formulation maximizes the total sum of all regressor pair distances under input constraints, while the second formulation maximizes the minimum distance pair under input constraints. These are developed for LTI systems subject to patient-friendly constraints on the input such as amplitude constraints, move size constraints and switching constraints. The resulting nonconvex quadratic optimization problems are approximately solved through the method of semidefinite relaxation. For the case of amplitude-only con-

straints in the first formulation, hard bounds exist on the suboptimality. A numerical example contrasts the proposed input signal designs, including their relative performance for MoD and DWO estimation. For Hammerstein systems, the problem formulation are solved using nonlinear programming and sparse polynomial optimization. It is shown that the optimal input performs better than ad-hoc inputs with added flexibility of addressing different input constraints.

This chapter also proposes a method to generate data-centric input signals for highly interactive dynamical systems. The objective of the formulation is to distribute the time-indexed output points in the output space under constraints on the input to achieve uniform coverage. The resulting optimization problem is derived as nonconvex quadratic optimization which is solved using nonlinear programming and semidefinite relaxation methods. A numerical example is shown using $2\times2$ LTI approximation of high-purity distillation column under amplitude constraints on the output signal, where an improved spread is obtained using distance-based formulation over the design based on Weyl's criterion in presence of finite data.

Finally, in this chapter the possibility of using methods from semidefinite programming approaches for polynomial optimization has been explored. It is shown that the input constraints defined in the set $\mathbb{U}$ and the integer constraints are naturally correlative sparse. The regressor distance pairs, on the other hand, are not sparse. To solve the input design problems using sparse polynomial optimization, two approaches have been proposed: first, by choosing selected distance pairs such that the distance pairs are sparse and secondly, by developing a custom SOS hierarchy of SDP relaxation based on the monomial basis supplied based on the fact that distance pairs are already sum-of-squares. Numerical examples are shown for applicability of convex relaxation in data-centric input signal design.

# Chapter 6

# CONSTRAINED INPUT SIGNAL DESIGN FOR DESIRED OBJECTIVES

## 6.1 Overview

The previous two chapters presented input signal design for data-centric system identification methods under time-domain constraints. On the other hand, the input signal design formulations discussed in this chapter are generated to achieve a *desired* objective function, and do not require setting of data-centric estimation. In some cases, the desired objective function is known *a priori*, for example, in the context of human behavior change [78] and in other cases, as a way to guarantee persistence of excitation in LTI system identification [45, 46]. As illustrated in the previous chapters, the input design formulations are posed as optimization problem in the decision variable $u$ to address time domain constraints. The formulations are grouped based on their primary focus on:

1. *Achieving a desired output trajectory under constraints.* Based on domain knowledge, it is desired that the output signal profile follow a set trajectory over time. In this formulation, the input signal is design to achieve this goal and the problem is solved using convex optimization. Numerical examples are presented to showcase the utility of the proposed formulation including an example from single-subject clinical design for improving physical activity.

2. *Achieving a desired input spectrum under constraints.* The persistence of excitation condition quantifies a necessary requirement on the input signal for linear parametric system identification. The problem formulation generates a deterministic input signal to achieve input spectrum under time-domain constraints on the input. The minimum parameter variance optimal input design under constraints is also discussed.

The chapter is organized in the following sections: Section 6.2 proposes generating input signal for desired output under constraints. Section 6.3 deals with generation of input signal under requirements on the input signal spectrum. The chapter ends with a summary in Section 6.4.

## 6.2 Achieving a Desired Output under Constraints

The traditional focus of input design formulations has been on reducing the estimation error by choosing, for example, the input signal spectrum or distribution of regressors [52, 53, 85]. This section develops an input signal design formulation without considering the specifics of the estimator, but rather by forcing the output $y$ of the system to reach a certain goal $y_{\text{des}}$. In addition, the goals must be reached under patient-friendly constraints for applications in behavioral health and medicine. The requirement of *a priori* knowledge of desired output ($y_{\text{des}}$) might seem as very narrow and hence restrictive, but in many practical scenarios the user has access to a desired output for data generation. Indeed, the desired output itself becomes a design variable and influences the quality of resulting data.

To motivate this further, consider an experiment to test the effect of rewards over time to reinforce the behavior of taking part in physical activity [231]. With increasing use of smart and connected devices, there is an opportunity to implement real-time algorithms to make decisions using behavioral theories such as social cognitive theory [38]. A single-subject clinical design for improving physical activity can be proposed by designing the input (reward) over time to test the dynamics of rewards to physical activity (such as number of steps taken per day). Standard input signals used in system identification such as PRBS or optimal inputs designed in previous chapter may not be typically used in such behavioral setting as it would cause large unwanted changes in behavior. In fact, what is required is that the input signal should cause systematic progression or drift in the observed behavior as a consequence of applied rewards. Hence, the input-output data observed in experiments designed to reach a desired goal can better capture the dynamical relationship

in certain behavioral settings [78]. Another situation which may warrant such a requirement is generation of a 'grid' or spread of operating points under amplitude constraints [232, 233].

The desired output input signal design can be posed as an open-loop finite-time optimal control problem:

$$\begin{aligned} \min_{u} \quad & \|y - y_{\text{des}}\| \\ \text{s.t.} \quad & u \in \mathbb{U} \end{aligned} \tag{6.1}$$

where $\mathbb{U}$ is defined by constraints on the input signal as defined in Section 4.2. Assuming the linear system description developed in (4.13) and (4.58), the problem formulation (6.1) can be expanded as:

$$\begin{aligned} \min_{u} \quad & \|Gu - y_{\text{des}}\| \\ \text{s.t.} \quad & u_{\min} \leq u \leq u_{\max} \\ & Au \leq b \\ & u(k) \in \mathbb{I} \\ & y_{\min} \leq y \leq y_{\max} \\ & A(Gu) \leq b_y \end{aligned} \tag{6.2}$$

by incorporating additional categorical constraints on the input signal and constraints on the output signal. The resulting optimization problem (6.2) is a convex mixed-integer second order cone program (or equivalently a quadratically constrained quadratic program). This can be globally solved, without integer constraints, in polynomial time using several optimization solvers. For the case of integer constraints, modern solver technology allows efficient solution of hundreds of variables in reasonable time [177, 178]. It should be mentioned that the requirement on persistent of excitation in the input is not enforced in the design but can always be evaluated *a posteriori*. Simulation examples are shown in the ensuing section to illustrate how this requirement can be satisfied under constraints.

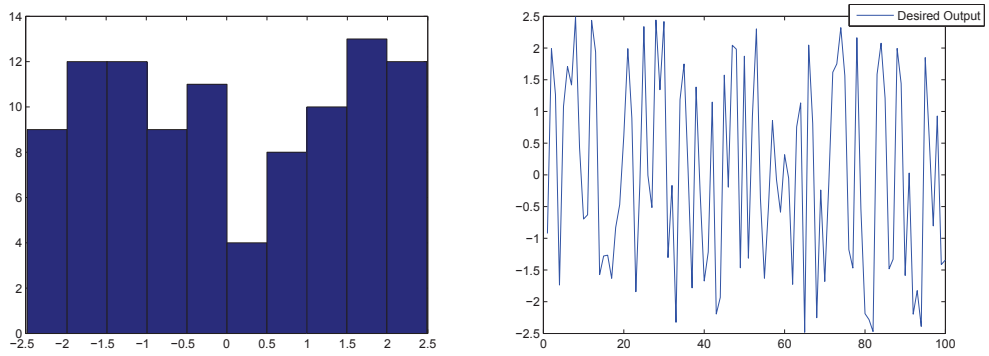


(a) (b)

Figure 6.1: (a) Histogram and (b) time plot of desired output sampled from a uniform probability distribution $\mathcal{U}$ with bounds equal to $y_{\min} = -2.5, y_{\max} = 2.5$ with $N = 100$.

### *6.2.1 Numerical Examples*

Consider a first order continuous-time system

$$G(s) = \frac{K_p}{\tau_p s + 1} \tag{6.3}$$

where $K_p = 5$ and $\tau_p = 5$. The desired output is assumed to be sampled from a uniform distribution

$$y(k) \sim \mathcal{U}(y_{\min}, y_{\max}) \tag{6.4}$$

defined using scalar amplitude bounds on the output signal. Fig. 6.1 shows the histogram of desired output vector sampled from a uniform probability distribution with amplitude bounds corresponding to $\pm 2.5$ with length of input signal $N = 100$. The aim of the input design is to follow the desired output profile as closely as possible. The problem is coded in MATLAB using the YALMIP interface [174] and Gurobi [177] as the MIQCP solver.

The first simulation is shown in Fig. 6.2 under only the amplitude constraints on the input as $-\mathbf{4} \leq u \leq \mathbf{4}$. The simulated output is compared with the desired output in Fig. 6.2a with the corresponding optimal input shown in Fig. 6.2b. The objective value is found to be 0.7903. The second simulation, shown in Fig. 6.3, considers previous amplitude constraints

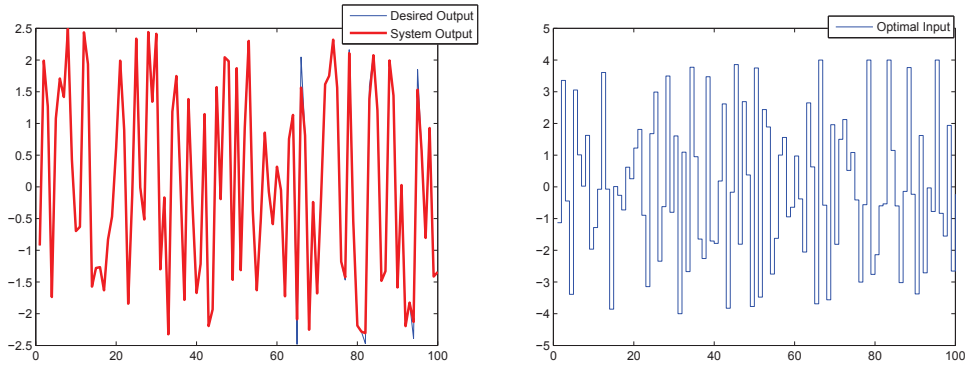


(a) (b)

Figure 6.2: (a) Simulation output compared with desired output, as shown in Fig. 6.1, under amplitude constraints on the input. The input-output model used is as shown in (6.3). The corresponding optimal input is shown in (b). The objective value is 0.7903.

and move size constraints $|u(k+1) - u(k)| \leq 4$ on the input. The simulated output is compared with the desired output in Fig. 6.3a with the corresponding optimal input shown in Fig. 6.3b. The objective value is found to be 3.4587, higher than the first simulation due to restrictions on the input. The third simulation, shown in Fig. 6.4, considers three constraints: amplitude constraints, move size constraints as previous simulation and adds switching constraints $T_{\text{sw}} = 2$ on the input. The simulated output is compared with the desired output in Fig. 6.4a with the corresponding optimal input shown in Fig. 6.4b. The objective value is found to be 10.3134, higher than the first and second simulations due to more restrictions on the input.

The fourth and final simulation for this numerical example, shown in Fig. 6.5, shows the case when amplitude constraints, move size constraints and *integer* constraints $u(k) \in \mathbb{I}$ are imposed on the input. It is well known that the problem is now NP-hard, and in this case is solved within 12% of global optimality (given enough time, the solution will converge to the global solution). The simulated output is compared with the desired output in Fig. 6.5a with the corresponding optimal input shown in Fig. 6.5b. The objective value (for up to 12% of global optimality) is found to be 4.3134. In conclusion, the simulations show that

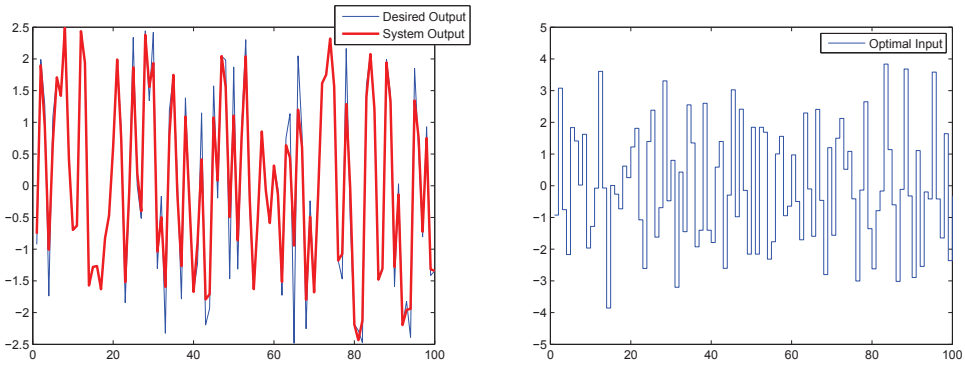


(a) (b)

Figure 6.3: (a) Simulation output compared with desired output, as shown in Fig. 6.1, under amplitude constraints and move size constraints on the input. The input-output model used is as shown in (6.3). The corresponding optimal input is shown in (b). The objective value is 3.4587.

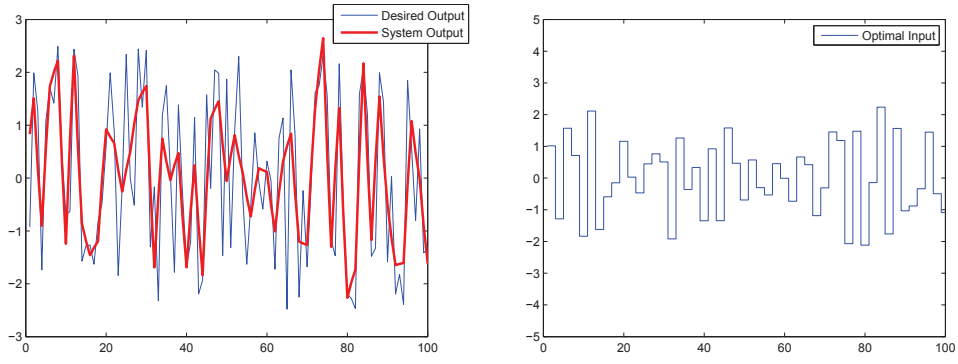


(a) (b)

Figure 6.4: (a) Simulation output compared with desired output, as shown in Fig. 6.1, under amplitude constraints, move size constraints and switching constraints on the input. The input-output model used is as shown in (6.3). The corresponding optimal input is shown in (b). The objective value is 10.3134.

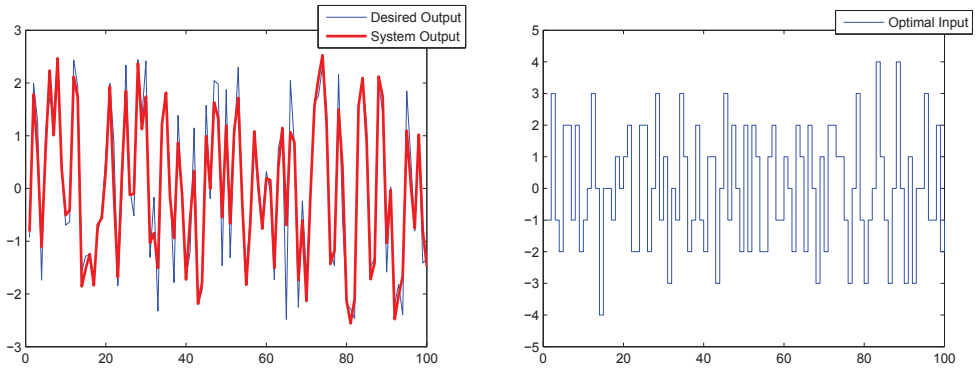


(a) (b)

Figure 6.5: (a) Simulation output compared with desired output, as shown in Fig. 6.1, under amplitude constraints, move size constraints and integer constraints on the input. The input-output model used is as shown in (6.3). The corresponding optimal input is shown in (b). The objective value (for up to 12% of global optimality) is 4.3134.

the output from the dynamical system tracks the desired output under constraints where with additional restrictions on the input, the tracking performance deteriorated.

To briefly illustrate the desired output design applied to a behavioral problem, consider the previously described example of an intervention aimed for improving physical activity. The goal of the input design is provide generate a binary input (i.e. reward or no reward) such that the number of steps taken by the participant per day match daily goals as close as possible under other factors. This will help understand the complex relationship, through experimental data, between rewards and their effect on improving the physical activity of that individual [78]. The optimized experiment takes advantage of the dynamical model developed from behavioral theory, specifically social cognitive theory [38], to determine theorized "optimal" delivery of the intervention component over time. This optimization is performed under constraints that reflect clinical and practical guidelines. Fig. 6.6 shows the optimal input for a simulation. Using a dynamical system informed from experimental data [38], which is found to be closed to an integrating system, it is interesting to observe that the optimal input naturally 'dies off' towards the end of the time period as the ob-

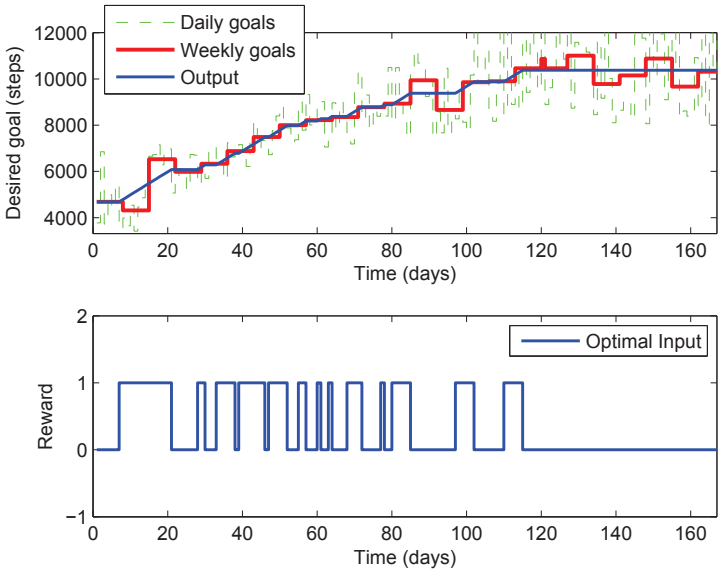


Figure 6.6: Dynamic simulation of steps per day (from baseline of 5000 steps) to a binary reward input for an intervention aimed at improving physical activity among adults. The weekly goals are derived from averaging the daily goal setpoint.

served behavior is closer to the goal. Typical input signals in system identification such as PRBS will continue to switch on and off, and hence are not beneficial in such applications. The optimized experiment is expected to result in superior information within allowable constraints in a single-subject fashion. The proposed input design can be extended to incorporate other manipulated variables as well as logical conditions on the delivery of these components such as rewards will be not be assigned unless the previous day goals have been reached [78].

Finally, it is worth mentioning that simple extensions can be proposed to the input design formulation shown in this section. For example, it can be used injunction with minimum parameter variance optimal input design, as described in Section 3.4.3, to satisfy the patient friendly requirements. The optimal design procedure yields an optimal spectrum and an input can be found using the method of spectral factorization [142, 154]. In general, the spectral factorization procedure does not guarantee that any patient friendly

requirements are satisfied. In such a scenario, the desired output is known from the optimal design, and hence an input can be designed to reach this output while satisfying time domain constraints as shown in (6.2). Some of the properties of the optimal spectrum may be lost but as a trade-off to satisfy time-domain constraints. The problem formulation can also be extended to include an *a priori* model uncertainty which can be formulated in terms of impulse response coefficients

$$G = G_0 + \Delta \tag{6.5}$$

where $G_0$ is the true model as described in (4.14) and $\Delta \in \mathbb{R}^{N\times N}$ is a matrix capturing the model uncertainty on the impulse response parameters. The input design problem (6.1) can be modified and posed as a robust optimization problem.

## 6.3 Input Signal Design for a Desired Spectrum under Constraints

Frequency domain requirements, discussed in Section 4.2, are enforced as a way to satisfy persistence of excitation of the input signal. Section 3.4.3 presented design of optimal input using the parametrization in terms of the autocorrelation coefficients. The aim of the input signal design formulation in this section is to find a realization of the signal, under time domain constraints, such that the signal spectrum ($\Phi_u(\omega)$) approximates a desired spectrum ($\gamma(\omega)$). In many circumstances, very little *a priori* knowledge of the system is available, so a "flat" spectrum over a bandwidth is a reasonable approximation

$$\Phi_u(\omega) \approx \gamma(\omega) = \begin{cases} \gamma_a & \omega_* \leq \omega \leq \omega^* \\ \gamma_b & \omega > \omega^*, \end{cases} \tag{6.6}$$

where $\gamma_a$ and $\gamma_b$ are real numbers defining the magnitude and $\omega^*$ denotes the desired bandwidth. Based on the discussion in previous chapters, the following properties are desired from an input signal:

- *Frequency range of interest.* The input signal should be persistently exciting with significant power over the required bandwidth. Since the model may be intended for

control design, the signal bandwidth should cover the frequency range of interest for control. Such bounds can be approximately calculated using dominant time constant estimates ($\tau^H_{\text{dom}}, \tau^L_{\text{dom}}$) of the system based on the high ($\alpha_s$) and low ($\beta_s$) frequency information as:

$$\omega_* = \frac{1}{\beta_s \tau^H_{\text{dom}}} \leq \omega \leq \frac{\alpha_s}{\tau^L_{\text{dom}}} = \omega^*, \tag{6.7}$$

where typically $\alpha_s = 2$ and $\beta_s = 3$ [80].

- *Periodicity.* Applying multiple cycles of a periodic input makes it possible to obtain estimation and validation data sets, thus facilitating crossvalidation. Also, a periodic input creates a natural time window for the identification experiment, allowing the user to examine the data while the clinical trial is underway. Hence the input design can be modified after the end of a period to better conform to the observed dynamics.

- *Change in levels.* Having multiple levels in the input signal can be beneficial, particularly if the plant under study is nonlinear in nature [45].

Using the parametrization developed in Section 4.2, the condition expressed in (6.6) is considered, i.e. when a particular spectrum must be matched exactly. This Chebychev type of problem [158] can be stated as

$$\min_u \quad |\Phi_u(\omega) - |\gamma(\omega)||, \tag{6.8}$$

and can be reformulated by using an auxiliary variable $t$, as:

$$|\Phi_u(\omega) - |\gamma(\omega)|| \leq t \tag{6.9}$$

$$\text{or}, -t \leq \Phi_u(\omega) - |\gamma(\omega)| \leq t \tag{6.10}$$

$$\text{or}, -t + |\gamma(\omega)| \leq \Phi_u(\omega) \leq t + |\gamma(\omega)|, \tag{6.11}$$

and hence the original problem (6.8) can be written as

$$\min_{u\in\mathbb{U}\cap\mathbb{I}} \quad |\Phi_u(\omega) - |\gamma(\omega)|| \equiv \begin{cases} \min\limits_{u,t} & t \\ \text{s.t.} & -t + |\gamma(\omega)| \leq \Phi_u(\omega) \leq t + |\gamma(\omega)| \\ & \omega \in [0, \pi] \\ & u_{\min} \leq u \leq u_{\max} \\ & |u(k+1) - u(k)| \leq b(k) \\ & u(k) \in \mathbb{I}. \end{cases}$$

The following can be said regarding the optimization problem (6.8):

- The spectrum is parametrized using the relation shown in (4.20).
- In addition to this optimization being mixed-integer nonlinear constrained problem, (6.11) makes the problem semi-infinite due to the continuous variable $\omega \in [0, \pi]$. A numerical approach to address this is to use a discretized spectral space [234] on finite ($M$) numbers. This is shown in (6.12).
- The constraint $-t + |\gamma(\omega)| \leq \Phi_u(\omega)$ is nonconvex as discussed in Section 4.2. It is also non-sparse given it involves all the decision variables (samples $u(k)$) in a fully coupled way. In other words, the problem does not enjoy any particular sparsity structure.
- The optimization problem is integer constrained: $u(k) \in \mathbb{I}\ \forall k$. This makes the problem NP-hard. One way to handle this is to replace it with polynomial inequalities as shown in (4.10).

Consequently, the optimization problem can now be restated as:

$$\begin{aligned} \min_{u,t} \quad & t \\ \text{s.t.} \quad & -t + |\gamma(\omega_j)| \leq \Phi_u(\omega_j) \leq t + |\gamma(\omega_j)| \\ & 0 \leq \omega_j \leq \pi, j = 1, \ldots, M \end{aligned} \tag{6.12}$$

$$u_{\min} \leq u \leq u_{\max}$$

$$|u(k+1) - u(k)| \leq b(k)$$

$$|\prod_{i \in \mathbb{I}} (u(k) - i)| \leq \epsilon$$

The problem (6.12) can be solved using standard nonlinear programming tools to obtain a local solution. Numerical solution have been discussed in the context of Weyl design in Section 5.2.4 to show the quality of the numerical solution, where Fig. 5.6 shows the comparison of various input spectrum with desired spectrum. The optimization (6.12) can also be used to implement input spectrum obtained from minimum parameter variance optimal designs [80]. The ensuing section discusses input signal design to minimize parameter variances under time-domain constraints.

### *6.3.1 Classical Minimum Parameter Variance Input Design under Constraints*

This section briefly discusses generalization of persistence of excitation on the input signal in terms of size of the parameter covariance matrix or in the maximum likelihood framework, size of the Fisher information matrix. Primarily for computational reasons, the classical optimal input design problems are parametrized in terms of input spectrum (or the auto-correlation coefficients) which can be posed as convex optimization problems [162], where it is difficult to directly address critical time domain constraints. In fact, the only definite way to address the time domain constraints is to formulate the information matrix directly as function of the input.

For FIR and ARX model structure, the estimation problem is linear least squares and hence the estimated parameter $\hat{\theta} \in \mathbb{R}^{n_\theta}$ can be written as

$$\hat{\theta} = (X^T X)^{-1} X^T Y \tag{6.13}$$

where $X$ is a matrix formed using the regressors $\varphi(k)$ and $Y$ is a vector of observed outputs. The term $X^T X \in \mathbb{R}^{n_\theta \times n_\theta}$ captures the associated estimation error [46], and hence

minimization (in some sense using function $\mu$ typically matrix trace or determinant [49]) of that term would yield smaller error for the given signal-to-noise ratio

$$\begin{aligned} \max_{u} \quad & \mu(X^T X) \\ \text{s.t.} \quad & u \in \mathbb{U}. \end{aligned} \tag{6.14}$$

In general, the information matrix can be written in terms of quadratic functions

$$I(u) = \begin{bmatrix} u^T F_1^T F_1 u & \cdots & u^T F_1^T F_{n_\theta} u \\ \vdots & \cdots & \vdots \\ u^T F_{n_\theta}^T F_1 u & \cdots & u^T F_{n_\theta}^T F_{n_\theta} u \end{bmatrix} \in \mathbb{R}^{n_\theta \times n_\theta} \tag{6.15}$$

where $n_\theta$ is the order of the model and the derivation of specific quadratic forms $(F_1, \ldots, F_{n_\theta})$ can be found in [161, 51]. In [161], this has been posed as a maximization of a convex function under affine constraints and was solved using the method of SDP relaxation of nonconvex quadratic programs.

In particular, for the FIR case, the average information matrix is known to be

$$I(u) = \frac{1}{N} \sum_{k=1}^{N} \varphi(k)\varphi(k)^T = \frac{1}{N} \sum_{k=1}^{N} \begin{bmatrix} u^2(k-1) & \cdots & u(k-1)u(k-n_\theta) \\ \vdots & \cdots & \vdots \\ u(k-n_\theta)u(k-1) & \cdots & u^2(k-n_\theta) \end{bmatrix}. \tag{6.16}$$

based on relationship shown in (3.11). It can be noted that the off diagonal terms are related to the autocorrelation of the input signal. Thus, an input signal which is a white will make the off-diagonal terms zero and hence is optimal for D-optimal designs [46, 235]. In addition, due to the FIR structure, the problem (6.14) is sparse and hence can be solved using sparse polynomial optimization with details as discussed in Section 5.3.2. For the purpose of simple illustration, consider the example system in Section 5.3.5 parametrized using FIR regressor of order $n_\theta = 25$. The resulting input signal and its autocorrelation for $N = 50$ is shown in Fig. 6.7. It can be observed that the relaxation based procedure naturally procedures an input signal which is finite length, deterministic and white. Thus,

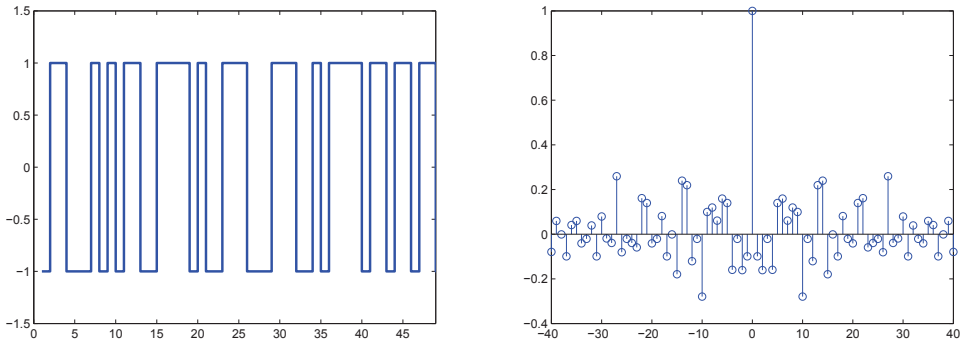


(a) (b)

Figure 6.7: (a) Optimal input to minimize the trace of the information matrix under amplitude constraints shown in (6.14). The input signal autocorrelation is shown in (b).

this provides an approach to generate persistently exciting input signal of arbitrary length, under constraints, as defined in Section 3.4.1. Further model quality constraints, which are expressed as a function of the information matrix, could be represented in terms of the input. In future work, other cases where the optimization problem (6.14) is sparse can be analyzed.

## 6.4 Chapter Summary

This chapter proposed input signal design under user-specified objective function. Broadly, two formulation are presented: where a desired output trajectory is defined and the other formulation where the desired input signal spectrum is defined under time domain constraints. The desired output formulation is posed as convex optimization problem with illustration using an input signal design for a physical activity intervention. The desired input spectrum problem formulation is posed as a nonlinear program. Additional discussion is also presented in posing the minimum parameter variance input design problem using sparse optimization, and a numerical example is used to show that a finite length persistently exciting input signal can be generated using the optimization procedure.

# Chapter 7

# EXTENSIONS TO HYBRID MODEL PREDICTIVE CONTROL

## 7.1 Overview

This chapter extends the hybrid model predictive control (HMPC) formulation introduced in Chapter 2. The improvement is proposed in two ways: first, by incorporating requirements on switching time of the manipulated inputs and secondly, by enabling manipulation of one input at a time among multiple inputs. This is achieved by extending the traditional mixed logical dynamical (MLD) framework, first introduced in [92], by representing the desired requirements as linear equality constraints and mixed-integer linear inequality constraints respectively. It is worth mentioning that the necessity for considerations of hybrid dynamics arises from the fact that the dosages of intervention components may be required to take only categorical values. In this dissertation, the two proposed updates are expressed using the inputs applied externally to the system, where the states and the outputs of the dynamical system are assumed to vary continuously. Numerical examples are shown using the previous problem of treatment plan for fibromyalgia as discussed in Chapter 2.

The rest of the chapter is organized in the following sections: Section 7.2 re-states the hybrid model predictive control formulation for completeness. Section 7.3 describes the switching time strategy for HMPC with numerical illustration and Section 7.4 describes the procedure for manipulating one input at a time among multiple inputs. The chapter summary is presented in Section 7.5.

## 7.2 HMPC as a Decision Framework

Model predictive control (MPC) is an online optimization based control technique where a finite-horizon, open-loop, discrete-time optimal control problem is solved at any given time

$k$ over the horizon $m$. The resulting optimization problems for LTI systems can be shown to be a convex quadratic programs (QP) [236] and for LTI hybrid system as convex mixed-integer quadratic programs (MIQP) [92]. Next, only the first value of the calculated optimal input is applied to system, and the process is repeated for the next sampling instance. This 'receding-horizon' framework ensures that the final control law is closed-loop and resolving the problem at each instance makes the control system more robust to uncertainty and disturbances. The MPC technology is particularly suited to be used in clinical applications due to the flexibility it offers to address design objectives and constraints. Examples of application of HMPC in behavioral interventions can be found in [21, 16, 103, 237].

In this chapter, a formulation for hybrid model predictive control with three degree-of-freedom (3 DoF) tuning developed in [96, 97] is used as the basis for making updates. The optimal control is obtained by solving the following mixed-integer quadratic optimization problem based on a quadratic cost function

$$\begin{aligned}\min_{\rho=\{[u(k+i)]_{i=0}^{m-1},\,[\delta(k+i)]_{i=0}^{p-1},\,[z(k+i)]_{i=0}^{p-1}\}} & \sum_{i=1}^{p}\|(y(k+i)-y_r)\|_{Q_y}^2+\sum_{i=0}^{m-1}\|(\Delta u(k+i))\|_{Q_{\Delta u}}^2\\ &+\sum_{i=0}^{m-1}\|(u(k+i)-u_r)\|_{Q_u}^2+\sum_{i=0}^{p-1}\|(\delta(k+i)-\delta_r)\|_{Q_d}^2\\ &+\sum_{i=0}^{p-1}\|(z(k+i)-z_r)\|_{Q_z}^2 \qquad (7.1)\end{aligned}$$

$$\text{s.t.}\quad y_{\min}\le y(k+i)\le y_{\max},\ i\in\mathcal{T}_p \qquad (7.2)$$

$$u_{\min}\le u(k+i)\le u_{\max},\ i\in\mathcal{T}_m \qquad (7.3)$$

$$\Delta u_{\min}\le \Delta u(k+i)\le \Delta u_{\max},\ i\in\mathcal{T}_m \qquad (7.4)$$

$$\text{Dynamics}\begin{cases}x(k+1)=Ax(k)+B_1u(k)+B_2\delta(k)+B_3z(k)+B_dd(k)\\ y(k)=Cx(k)+d'(k)+\nu(k)\end{cases} \qquad (7.5)$$

$$\text{MLD}\left\{E_2\delta(k)+E_3z(k)\le E_5+E_4y(k)+E_1u(k)-E_dd(k)\right. \qquad (7.6)$$

where $\mathcal{T}_p=\{1,\dots,p\}$, p is the prediction horizon, $\mathcal{T}_m=\{0,\dots,m-1\}$, m is the control horizon, $y_r$ is the reference, $Q_*$ are the penalty weights. Specific details of the formulation

can be found in Chapter 2 where it was used to assign dosages of naltrexone for treatment of fibromyalgia.

The enhancements suggested in this chapter assume linear dynamics and incorporate the desired requirements on the manipulated inputs, thus creating the functionality needed by the control algorithm to make decisions within a receding horizon framework. The flexibility associated with HMPC is used to incorporate two requirements frequently desired in clinical applications:

1. Switching time constraints,

2. Manipulating one input at a time among multiple inputs.

The ensuing sections discusses these two formulations to meet requirements of decision policies in adaptive interventions.

## 7.3 Switching Time Strategy

Due to clinical and resource considerations, it is often desirable to make decisions at frequencies other than the regular sampling interval. For example, the participant may visit the clinic, say, every other Monday (the assessment cycle) while data is collected daily through self-monitoring. In this situation, it is desirable to make decisions on intervention components on a weekly or multi-weekly basis, despite daily sampling of intervention outcomes. In other words, the control decisions are required to be made at an *a priori* known integer multiple $T_{\text{sw}}$ of the system sample time $T$ in addition to the previously discussed constraints. This section describes the algorithm for making the control decisions at such known samples of time. It should be noted that this requirement is different from specifications of multirate control as all the variables considered are sampled at the same rate. It is also distinct from move blocking strategies [238] which are aimed at computational burden reduction.

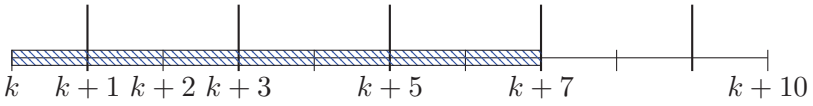


Figure 7.1: Control horizon $m = 7$ for HMPC at any time $k$ for switching time $T_{\text{sw}} = 2$.

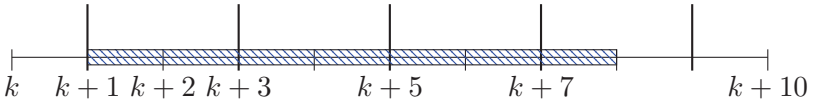


Figure 7.2: Control horizon $m = 7$ for HMPC at any time $k+1$ for switching time $T_{\text{sw}} = 2$.

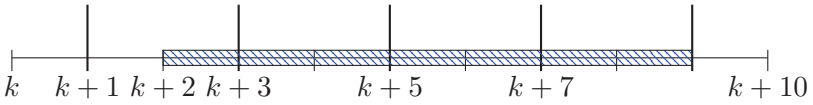


Figure 7.3: Control horizon $m = 7$ for HMPC at any time $k+2$ for switching time $T_{\text{sw}} = 2$.

This algorithm is referred to in this chapter as a switching time strategy and this is achieved by enforcing control move size $\Delta u(k)$ to be zero over the control horizon except when decisions have to be made. Fig. 7.1 shows the control horizon $m = 7$ for any given time $k$ when the switching time $T_{\text{sw}} = 2$. The sample points in time where the control decision has to be made is shown by longer vertical lines in Fig. 7.1-Fig. 7.3. As the horizon moves forward for the next iteration at sample $k + 1$ as shown in Fig. 7.2, the points where the control decisions are made have moved relative to the horizon. Similarly, for the next iteration at sample $k + 2$, the horizon is shown in Fig. 7.3. Thus, the constraints describing the switching behavior have to be updated by taking the receding horizon nature of HMPC into account, and this can be written as time-dependent linear equality constraint:

$A_{T_{\text{sw}}}(k)u = 0$. The matrix $A_{T_{\text{sw}}}(k)$ has a block-diagonal structure, for example,

$$\begin{bmatrix} \star & & & & & & & & & & \\ & \star & \star & & & & & & & & \\ & \star & & \star & & & & & & & \\ & & & \mathbf{0} & & & & & & & \\ & & & & \star & \star & & & & & \\ & & & & \star & & \star & & & & \\ & & & & \star & & & \star & & & \\ & & & & & & & \ddots & & & \\ & & & & & & & & \mathbf{0} & & \\ & & & & & & & & & \star & \star \\ & & & & & & & & & \star & \end{bmatrix} \begin{bmatrix} u(k) \\ u(k+1) \\ \vdots \\ u(k+m-1) \end{bmatrix} = \begin{bmatrix} \star \\ 0 \\ \vdots \\ 0 \end{bmatrix} \tag{7.7}$$

where rows with $\star$ entries and $\mathbf{0}$ (row of zeros) are assigned by the algorithm. The rest of the entries in the matrix are zero. One of the ways to generate this matrix at each sampling instant $k$ is as following:

1. Given the control horizon $m$ and switching time $T_{\text{sw}}(\leq m)$, calculate the number of blocks $\texttt{numblocks} = \lfloor \frac{m-1}{T_{\text{sw}}} \rfloor + 1$. If the $\texttt{numblocks} \geq 3$, define number of block excluding the first and last block: $\texttt{midblocks} = \texttt{numblocks} - 2$. The term 'switching sample' will be used to denote sample when the control is allowed to change its value i.e. $\texttt{iff rem}(\frac{k}{T_{\text{sw}}}) = 0$, where $\texttt{rem}$ is the remainder.

2. The matrix $A_{T_{\text{sw}}}(k)$ is populated by $0, 1$ or $-1$ to implement the move size restriction, and its size is determined by length of control horizon and size of $\texttt{numblocks}$: $A_{T_{\text{sw}}}(k) \in \mathbb{R}^{(T_{\text{sw}}+\texttt{midblocks}\times(T_{\text{sw}}-1)+\texttt{rem}(\frac{m-1}{T_{\text{sw}}})+1)\times m}$.

3. The rows in $A_{T_{\text{sw}}}(k)$ corresponding to switching samples will be set to zero; otherwise the rows will be populated to implement $\Delta u(k+i) = 0$.

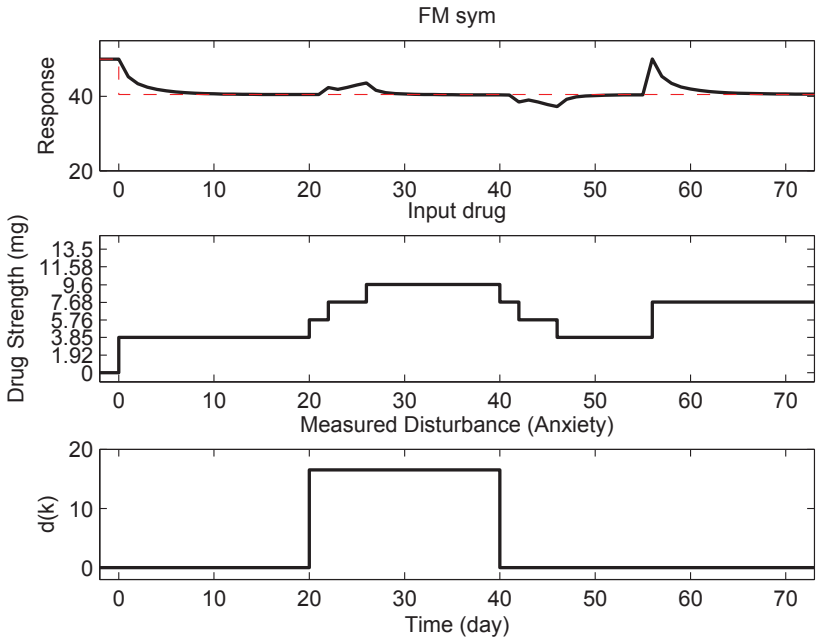


Figure 7.4: Performance of hybrid MPC (eight levels) with tuning parameter $(\alpha_r, \alpha_d, f_a) = (0.5, 0.5, 0.5)$ under $T_{\text{sw}} = 2$ for fibromyalgia problem considered in Chapter 2.

4. Finally, the first sample $u(k)$ is assigned the previously calculated optimal value i.e. $u(k) = u^*$ when $k$ does not correspond to the switching sample (as per the receding horizon framework).

This algorithm can be demonstrated using the example problem considered in Section 2.5.1 for nominal performance. The simulations are repeated under same parameter values with additional enforcement of the switching constraint. Fig. 7.4 shows the case when the switching time is 2 days or, the control input can change every other day. Similarly, Fig. 7.5 shows the case for switching time of 5 days and Fig. 7.6 shows the case when the switching time is 7 days or weekly. With this additional constraint, there is a natural degradation in performance as changes in the input are not allowed at every sample.

Finally, while mathematically the switching time strategy is similar to move blocking strategies used in MPC [238], the difference, besides the process of generating the matrix

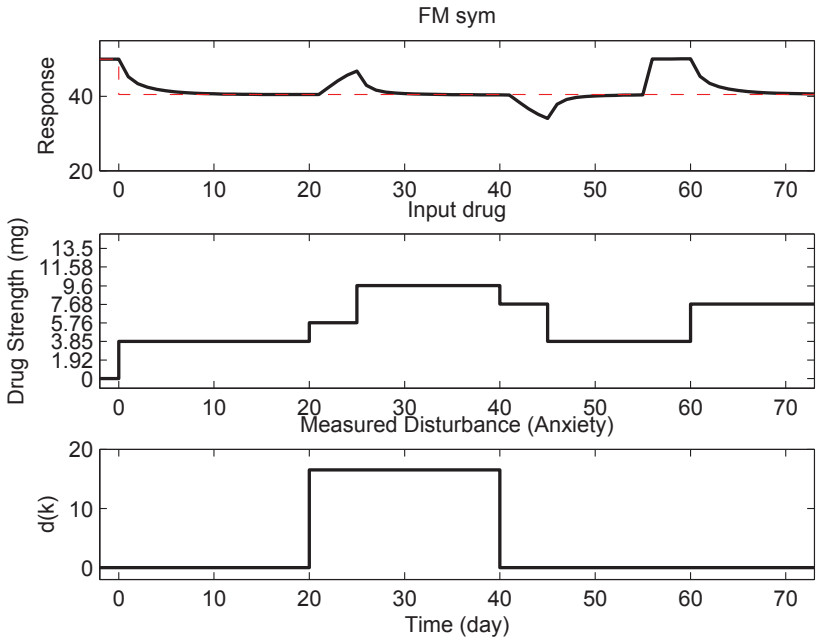


Figure 7.5: Performance of hybrid MPC (eight levels) with tuning parameter $(\alpha_r, \alpha_d, f_a) = (0.5, 0.5, 0.5)$ under $T_{\text{sw}} = 5$ for fibromyalgia problem considered in Chapter 2.

$A_{T_{\text{sw}}}(k)$, lies in the fact that in move blocking strategies, the idea is to decrease the dimension of the decision variable to reduce the computational burden, whereas here the requirement is to apply controls only at specified samples while the size of the decision variable remains the same, and is enforced as a constraint in the HMPC optimization problem.

## 7.4 Selection of Single Input in a Multi-Input Scenario

Many adaptive interventions usually require that only one component or input may change dosage at any given time. This may be necessary to prevent the participant from being uncomfortable due to any dramatic unknown interactions between different components of the treatment. This basically implies that the controller can only choose one input to incur change at each sampling time, and the other input changes have to be zero at that time instant. Of course, there is no restriction on *which* input among given inputs should

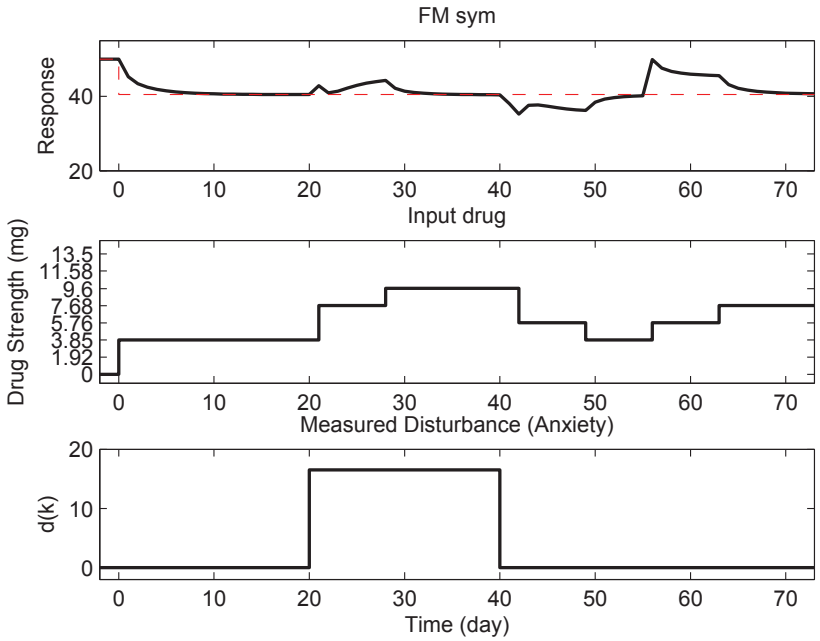


Figure 7.6: Performance of hybrid MPC (eight levels) with tuning parameter $(\alpha_r, \alpha_d, f_a) = (0.5, 0.5, 0.5)$ under $T_{\text{sw}} = 7$ for fibromyalgia problem considered in Chapter 2.

change at given time. Thus, the HMPC problem should be formulated in such a way that the controller chooses an input to change based on goals, dynamics and a logical statement describing the selection of single input in a multi-input scenario.

The HMPC problem formulated in (7.1)-(7.6) contains the following vector of decision variables

$$\rho = \left[ [u(k+i)]_{i=0}^{m-1},\ [\delta(k+i)]_{i=0}^{p-1},\ [z(k+i)]_{i=0}^{p-1} \right]^T. \tag{7.8}$$

In this section, selection of one input at a time is enforced by forcing the move size of other inputs as zero. Towards this, additional binary variables $\phi$ are augmented to the decision vector to achieve this functionality. In the following, the associated logical specifications are derived and converted into linear inequalities, and are implemented by appending them to the MLD equation.

For the purpose of illustration, consider a multi-input system with $n_x$ manipulated

inputs. The number of the additional binary variables corresponds to the number of the manipulated inputs or, in other words, $n_x$ binary variables ($\phi_1$, $\phi_2$, ..., $\phi_{n_x}$) are augmented into the vector of binary variables $\delta$ in (7.8). The selection of one input change can be logically expressed as follows,

$$\phi_1(k) = 1 \Leftrightarrow \begin{cases} |\Delta u_1(k)| > 0, \\ \Delta u_2(k) \ = \cdots = \Delta u_{n_x}(k) = 0 \end{cases} \tag{7.9}$$

$$\phi_2(k) = 1 \Leftrightarrow \begin{cases} |\Delta u_2(k)| > 0, \\ \Delta u_1(k) \ = \cdots = \Delta u_{n_x}(k) = 0 \end{cases} \tag{7.10}$$

$$\vdots \tag{7.11}$$

$$\phi_{n_x}(k) = 1 \Leftrightarrow \begin{cases} |\Delta u_{n_x}(k)| > 0, \\ \Delta u_1(k) \ = \cdots = \Delta u_{n_x-1}(k) = 0 \end{cases} \tag{7.12}$$

$$\phi(k) \odot \Delta u(k)_{\min} \leq \Delta u(k) \leq \phi(k) \odot \Delta u(k)_{\max} \tag{7.13}$$

$$\sum_{i=1}^{n_x} \phi_i(k) \leq 1 \tag{7.14}$$

$$\text{where} \quad \phi(k) = [\phi_1(k) \quad \phi_2(k) \ \ldots \ \phi_{n_x}(k)]^T \tag{7.15}$$

$$\Delta u(k) = [\Delta u_1(k) \quad \Delta u_2(k) \ \ldots \ \Delta u_{n_x}(k)]^T \tag{7.16}$$

$$\Delta u(k)_{\max} = [\Delta u_1(k)_{\max} \quad \Delta u_2(k)_{\max} \ \ldots \ \Delta u_{n_x}(k)_{\max}]^T \tag{7.17}$$

$$\Delta u(k)_{\min} = [\Delta u_1(k)_{\min} \quad \Delta u_2(k)_{\min} \ \ldots \ \Delta u_{n_x}(k)_{\min}]^T \tag{7.18}$$

and $\odot$ is the Hadamard product. The logical specifications in (7.9) - (7.13) can be expressed as linear inequalities related with $u(k)$ over the $m$ control horizon, and $\phi(k)$ over the $p$ prediction horizon, (7.14) is augmented after the linear inequalities of binary variables $\delta(k)$ in (7.8) over the $p$ prediction horizon. The resulting optimization remain a mixed-integer quadratic program (MIQP) with additional binary variables to determine which input should change at a given time instant. For brevity, a numerical illustration is

not shown in this section. This algorithm has been applied to the problem of managing gestational weight gain (GWG) among pregnant women where different intervention components such as healthy eating and physical activity cannot change simultaneously and is shown with a numerical illustration in [103].

## 7.5 Chapter Summary

In summary, this chapter has introduced two specific concepts relating to improvements in hybrid model predictive control: a switching time strategy and selection of a single input in a multi-input scenario. Both conditions are proposed as an extension of the mixed logical dynamical (MLD) framework and are implemented as a time-dependent linear equality and mixed-integer linear inequality constraints. For the switching time scenario, numerical examples are presented to show the effect of switching constraint on the performance of HMPC for the simulated fibromyalgia intervention. This work demonstrates the potential for real-world applications of an adaptive intervention by employing control-oriented approach and the flexibility associated with the model predictive control framework. The HMPC formulation proposed in this dissertation can also be extended to incorporate fully time dependent constraints developed using linear temporal logic. It should be noted that these clinically-motivated enhancement do not guarantee recursive feasibility and ultimately closed-loop stability of this improved HMPC formulation, and other methods have to be developed to address this issue. Future work will analyze the issues of stability and recursive feasibility in a 3 DoF tuning framework.

In conclusion, the MPC framework can also be modified to include more complicated nonlinear models as long as they can be written in predictive forms. On the other hand, the controller can be also built to utilize local models for such nonlinear cases. Once such example is called Model-On-Demand Model Predictive Control (MoDMPC) [54, 89, 91]. In this approach, a local linear model (as shown in (3.23)) is obtained from the MoD estimator at each sampling time. This model can be converted to the standard state-space

MLD structure by rearranging (3.23) in output predictor format as shown in [91]. Since the model is changed at each sampling instant, it can capture autonomous events in hybrid systems [239, 240] where as the non-autonomous events are captured by the original MLD equation [91, 92]. With optimal input signal design for data-centric methods introduced in earlier chapters, a more informative dataset can be obtained. This in turn will lead to better local models which can be directly used by the controller for improved closed-loop performance. Analysis of the effect of input signal design on MoDMPC represents an interesting topic for future research.

# Chapter 8

# SUMMARY AND FUTURE WORK

## 8.1 Summary of the Dissertation

The design of input signals for system identification under constraints on the input and output signals is examined in this dissertation. A major emphasis of this work has been to integrate the requirements originating from clinical practice with the requirements for data-centric system identification methods such as Model-On-Demand (MoD). The concept of "patient-friendly" design has been introduced by making a case for how the current approaches to population-level clinical trials may fall short of producing informative data for identifying dynamics through system identification. Hence an improved design can be systematically obtained through the use of input signals as a means to operationalize single-subject clinical trials. For data-centric methods, a novel framework using geometrical distribution of regressors in the finite dimensional regressor space has been proposed. It has been extended for highly interactive systems by addressing distribution of time-indexed output points in the finite dimensional output space. Extension to the case of multi-input single-output multivariable systems has also been proposed.

The formulated problems are difficult nonconvex optimization problems and hence tractable relaxations have been proposed for an efficient solution. The set of input constraints from the set $\mathbb{U}$ and set $\mathbb{I}$ which are shown to be naturally sparse. In addition, it is shown that the data-centric formulations are amenable to sparse polynomial optimization under selected regressor distances pairs using FIR parametrization and user-defined custom monomial basis. Numerical examples are presented to illustrate the benefit of proposed input design formulations for both LTI systems and Hammerstein systems, and are contrasted with design based on the Weyl's criterion. Through numerical examples, a case has also been made for the utility of the convex relaxation procedures by generating useful

bounds on the objective function value.

Additional input design formulations have also been proposed to achieve a desired output under constraints, specific input spectrum under input constraints and minimization of the parameter uncertainty in a least-squares type estimator in system identification. The process of input design is complemented by showcasing a secondary data analysis of naltrexone intervention for fibromyalgia, and its limitations, with subsequent closed-loop control using simulation.

As the end-use of informative data is better models and improved closed-loop performance, the mixed logical dynamical framework for hybrid model predictive control is extended to incorporate a switching time strategy, where the decisions are made at some integer multiple of the sample time, and for enabling manipulation of only one input at a given sample time among multiple inputs. Numerical examples are shown for the case of switching time by using the problem for the naltrexone intervention for fibromyalgia under two days, five days and weekly switching time.

The major contributions of this dissertation can be listed as:

- Proof-of-concept secondary analysis of fibromyalgia clinical data for identification and control. Chapter 2 shows a secondary data analysis conducted on a clinical trial data where a linear parametric model is derived and is used by a hybrid model predictive controller to assign dosages over time. Various cases of relevance to clinical practice have been considered.

- Elucidation of various constraints for identification and control originating from the demands of practice. In particular, the focus has been on requirements from the fields of behavioral health and medicine resulting in patient-friendly designs. The constraints considered include limits on signal amplitude, rate of change, switching time and categorical levels as discussed in Section 4.2.

- The input design problems are formulated to directly address time domain constraints. Hence, the decision variable is the finite dimensional deterministic input signal $u$. Specifically, to address the requirements of data-centric estimation methods, broadly two designs approaches are proposed:
  - Design based on Weyl's criterion,
  - Design based on optimal distribution of regressors and time-indexed output points using two methods:
    * Maximize the sum of all distance pairs,
    * Maximize the minimum of all distance pairs.
- A design approach based on Weyl's criterion results in uniform distribution in the output space. Numerical examples are based on a hypothetical clinical trial and various simulations based on practical scenarios are conducted.
- A design approach based on distribution of regressors is aimed to cover the regressor space so as to generate sufficient support for the estimator. The subsequent optimization problem for LTI systems and Hammerstein systems is solved using nonlinear programming, SDP relaxation of nonconvex quadratic program and sparse polynomial optimization.
- A design approach using distribution of time-indexed output points is aimed to generate uniform coverage in the ill-conditioned output space. The subsequent optimization problem for LTI systems is solved using nonlinear programming and SDP relaxation of nonconvex quadratic program.
- Input signal design problems are also developed for desired objectives. For a desired output trajectory over time, the optimization problem is shown to be convex mixed-integer quadratic programming problem. The formulation is illustrated on a

hypothetical intervention for improving physical activity using the dynamical model derived from social cognitive theory (SCT).

- Extensions to the hybrid model predictive control formulation through incorporation of two logical conditions on the input change which are frequently encountered in practice: switching time constraint and manipulation of only one input in a multi-input scenario.

The ensuing section discusses directions for future work.

## 8.2 Directions for Future Work

There are many interesting open research problems in the context of data-centric input signal design, and automated dosage assignment in behavioral health and medicine settings using control systems. Among the future topics of interest for constrained input signal design problem are:

1. For data-centric input signal design, a useful extension would be to analyze the direct effect of distribution of regressors on the estimation error *globally*. In other words, it would be interesting to derive stronger statistical arguments for the objective of distribution of regressors.

2. The problem formulations can be extended to include distribution of regressors and output points under uncertainty. In Chapter 4, it is shown that for a linear system under noise with zero mean and known covariance, the average distribution of regressor is same as the deterministic objective. A comprehensive exploration can be conducted for the cases where such results holds true.

3. Extension of the method of distribution of regressors to other block-structured system such as Hammerstein-Wiener (H-W) systems and other nonlinear system written in the regressor form.

4. Additional interesting cases can be examined for highly interactive systems such as distribution of output points when the input is amplitude or power constrained and excitation of only certain region in the output space. The presented input design approach can also be compared with other input design methods in literature for ill-conditioned systems.

5. More efficient parametrization of the regressor distance pairs can be explored from a computational point-of-view so that the formulation is more suited for sparse polynomial optimization methods without sacrificing any of the distance pairs. This can include using the $\ell_\infty$ distance and an affine transformation of the decision variable $u$ to some other variable $x$ such that $x = Zu$ where $Z$ is chosen to induce sparsity.

For automated dosage assignment using hybrid model predictive control, additional improvements can be made in the following areas:

- Incorporation of local linear dynamical models from data-centric estimators such as MoD as a means for implementing nonlinear control. The effect of focused data-centric input design on the closed-loop performance can also be quantified.

- The logical constraints such as switching constraints and choosing one input only can be further generalized by incorporating more complicated conditions, such as, for example, the first input may change only when the second input has reach a particular value, using linear temporal constraints.

- It is arbitrarily difficult to assign 'exact' setpoints in many clinical problems. Moreover, the measurements are often faulty and corrupted by noise and hence, it is more practical to require the controller to keep the controlled variables in a desired setpoint band rather than a fixed setpoint. The HMPC formulation can be the modified such that the setpoint tracking is not part of the objective ($Q_y = 0$) and specific setpoint

band is enforced through a constraint added to the original formulation including output prediction considering uncertainty.

In conclusion, this dissertation has tried to address problems arising from requirements of clinical practice together with local modeling in system identification. It is hoped that this will motivate future work in this area towards addressing open problems of theoretical and practical nature.

BIBLIOGRAPHY

[1] P. O'Shea. Future medicine shaped by an interdisciplinary new biology. *The Lancet*, 379(9825):1544–1550, 2012.

[2] M. A. Hamburg and F. S. Collins. The path to personalized medicine. *New England Journal of Medicine*, 363(4):301–304, 2010.

[3] A. Committee on a Framework for Development a New Taxonomy of Disease; National Research Council. *Toward Precision Medicine: Building a Knowledge Network for Biomedical Research and a New Taxonomy of Disease*. The National Academies Press, 2011.

[4] A. C. Ahn, M. Tewari, C.-S. Poon, and R. S. Phillips. The clinical applications of a systems approach. *PLoS Med*, 3(7):e209, 05 2006.

[5] D. E. Rivera, M. D. Pew, and L. M. Collins. Using engineering control principles to inform the design of adaptive interventions: A conceptual introduction. *Drug and Alcohol Dependence*, 88(2):S31–S40, 2007.

[6] D. E. Rivera. Optimized behavioral interventions: what does system identification and control engineering have to offer? In *Proceedings of 16th IFAC Symposium on System Identification*, pages 882–893, July 2012.

[7] A. X. Garg, N. J. Adhikari, H. McDonald, and et al. Effects of computerized clinical decision support systems on practitioner performance and patient outcomes: A systematic review. *Journal of the American Medical Association*, 293(10):1223–1238, 2005.

[8] W. T. Riley, D. E. Rivera, A. A. Atienza, W. Nilsen, S. M. Allison, and R. Mermelstein. Health behavior models in the age of mobile interventions: are our theories up to the task? *Translational Behavioral Medicine*, 1:53–71, 2011.

[9] I. Sim, P. Gorman, R. A. Greenes, R. B. Haynes, B. Kaplan, H. Lehmann, and P. C. Tang. Clinical decision support systems for the practice of evidence-based medicine. *Journal of the American Medical Informatics Association*, 8(6):527–534, 2001.

[10] L. M. Collins, S. A. Murphy, and K. L. Bierman. A conceptual framework for adaptive preventive interventions. *Prevention Science*, 5:185–196, 2004.

[11] B. Chakraborty and S. A. Murphy. Dynamic treatment regimes. *Annual Review of Statistics and Its Application*, 1(1):447–464, 2014.

[12] S. Kumar, W. Nilsen, M. Pavel, and M. Srivastava. Mobile health: Revolutionizing healthcare through transdisciplinary research. *Computer*, 46(1):28–35, 2013.

[13] P. Molenaar. Dynamic assessment and adaptive optimization of the psychotherapeutic process. *Behavioral Assessment*, 9:389–416, 1987.

[14] D. E. Davison, R. Vanderwater, and K. Zhou. A control-theory reward-based approach to behavior modification in the presence of social-norm pressure and conformity pressure. In *Proceedings of the 2012 American Control Conference*, pages 4076–4052, 2012.

[15] K. P. Timms, D. E. Rivera, L. M. Collins, and M. E. Piper. A dynamical systems approach to understanding self-regulation in smoking cessation behavior change. *Nicotine & Tobacco Research*, 16(Suppl 2):S159–S168, 2014.

[16] Y. Dong, D. E. Rivera, D. S. Downs, J. S. Savage, D. M. Thomas, and L. M. Collins. Hybrid model predictive control for optimizing gestaional weight gain behavioral interventions. In *Proceedings of the 2013 American Control Conference*, pages 1973–1978, 2013.

[17] R. Spanagel. Alcoholism: A systems approach from molecular physiology to addictive behavior. *Physiological Reviews*, 89(2):649–705, 2009.

[18] S. Ching, S. Sarma, and M. B. Westover. Emerging applications in systems and control theory for neuroscience and neural medicine, June 2013. Pre-conference workshop during the *2013 American Control Conference*.

[19] J. Shi, O. Alagoz, F. Erenay, and Q. Su. A survey of optimization models on cancer chemotherapy treatment planning. *Annals of Operations Research*, pages 1–26, 2011.

[20] A. Nacev, A. Komaee, A. Sarwar, R. Probst, S. Kim, M. Emmert-Buck, and B. Shapiro. Towards control of magnetic fluids in patients: Directing therapeutic nanoparticles to disease locations. *IEEE Control Systems*, 32(3):32–74, June 2012.

[21] S. Deshpande, N. N. Nandola, D. E. Rivera, and J. Younger. A control engineering approach for designing an optimized treatment plan for fibromyalgia. In *Proceedings of the 2011 American Control Conference*, pages 4798–4803, June 2011.

[22] S. Deshpande. A control engineering approach for designing an optimized treatment plan for fibromyalgia. Master's thesis, Electrical Engineering, Arizona State University, USA, 2011.

[23] M. A. Thompson, J. A. Aberg, J. F. Hoy, and et al. Antiretroviral treatment of adult HIV infection: 2012 recommendations of the international antiviral society USA panel. *Journal of the American Medical Association*, 308(4):387–402, 2012.

[24] B. Buckingham, H. P. Chase, E. Dassau, E. Cobry, P. Clinton, V. Gage, K. Caswell, J. Wilkinson, F. Cameron, H. Lee, B. W. Bequette, and F. J. Doyle. Prevention of Nocturnal Hypoglycemia Using Predictive Alarm Algorithms and Insulin Pump Suspension. *Diabetes Care*, 33(5):1013–1017, 2010.

[25] H. Lee, B. Buckingham, D. Wilson, and B. Bequette. A closed-loop artificial pancreas using model predictive control and a sliding meal size estimator. *Journal of Diabetes Science and Technology*, 3(5):1082–1090, 2009.

[26] L. Zadeh. From circuit theory to system theory. *Proceedings of the IRE*, 50(5):856–865, 1962.

[27] N. Wiener. *Cybernetics or the Control and Communication in the Animal and the Machine*. MIT Press, 1965.

[28] K. Åström and R. Murray. *Feeback Systems: An Introduction for Scientists and Engineers*. Princeton University Press, 2009.

[29] B. A. Ogunnaike and W. H. Ray. *Process Dynamics, Modeling, and Control*. Oxford University Press, 1994.

[30] F. Holzapfel and S. Theil. *Advances in Aerospace Guidance, Navigation and Control: Selected Papers of the 1st CEAS Specialist Conference on Guidance, Navigation and Control*. Springer, 2011.

[31] S. M. Amin. Smart grid: Overview, issues and opportunities: Advances and challenges in sensing, modeling, simulation, optimization and control. *European Journal of Control*, 17(5-6):547–567, 2011.

[32] J. L. Hellerstein, Y. Diao, S. Parekh, and D. M. Tilbury. *Feedback Control of Computing Systems*. John Wiley and Sons, 2004.

[33] G. B. West. The importance of quantitative systemic thinking in medicine. *The Lancet*, 379(9825):1551–1559, 2012.

[34] O. Wolkenhauer, H. Kitano, and K.-H. Cho. Systems biology. *IEEE Control Systems Magazine*, 23(4):38–48, Aug. 2003.

[35] B. Ghosh and C. Martin. Guest editorial - special issue on systems and control problems in medicine. *IEEE Transactions on Automatic Control*, 43(6):763–764, june 1998.

[36] M. Khammash, C. J. Tomlin, and M. Vidyasagar. Guest editorial - special issue on systems biology. *IEEE Transactions on Automatic Control*, 53(Special Issue):4–7, 2008.

[37] C. S. Carver and M. F. Scheier. *On the self-regulation of behavior*. Cambridge University Press, 1998.

[38] C. A. Martin, D. E. Rivera, W. Riley, E. Hekler, M. Buman, M. Adams, and A. King. A dynamical systems model of social cognitive theory. In Proceedings of the 2014 *American Control Conference* (to appear), 2014.

[39] E. B. Hekler, P. Klasnja, J. E. Froehlich, and M. P. Buman. Mind the theoretical gap: Interpreting, using, and developing behavioral theory in HCI research. In *Proceedings of the SIGCHI Conference on Human Factors in Computing Systems*, CHI '13, pages 3307–3316, 2013.

[40] E. Sontag. *Mathematical Control Theory: Deterministic Finite Dimensional Systems*. Springer, 1998.

[41] S. Skogestad and I. Postlethwaite. *Multivariable Feedback Control: Analysis and Design*. John Wiley & Sons, 1996.

[42] V. Dhar. Data science and prediction. *Communications of the ACM*, 56(12):64–73, December 2013.

[43] S. Staff. Challenges and opportunities. *Science*, 331(6018):692–693, 2011.

[44] R. G. Baraniuk. More is less: Signal processing and the data deluge. *Science*, 331(6018):717–719, 2011.

[45] L. Ljung. *System identification: theory for the user*. Prentice Hall PTR, Upper Saddle River, NJ, 2nd edition, 1999.

[46] G. C. Goodwin and R. L. Payne. *Dynamic system identification: experiment design and data analysis*. Academic Press, 1977.

[47] M. G. Safonov. Origins of robust control: Early history and future speculations. *Annual Reviews in Control*, 36(2):173–181, 2012.

[48] L. Ljung. Perspectives on system identification. *Annual Reviews in Control*, 34(1):1–12, 2010.

[49] F. Pukelsheim. *Optimal Design of Experiments*. SIAM, 2006.

[50] D. E. Rivera, H. Lee, M. W. Braun, and H. D. Mittelmann. Plant-friendly system identification: a challenge for the process industries. In *Proceedings of the 13th IFAC Symposium on System Identification*, pages 917–922, 2003.

[51] R. Mehra. Optimal input signals for parameter estimation in dynamic systems–survey and new results. *IEEE Transactions on Automatic Control*, 19(6):753–768, 1974.

[52] M. Gevers, X. Bombois, R. Hildebrand, and G. Solari. Optimal experiment design for open and closed-loop system identification. *Communications in Information and Systems*, 11(3):197–224, 2011.

[53] L. Pronzato. Optimal experimental design and some related control problems. *Automatica*, 44(2):303–325, 2008.

[54] A. Stenman. *Model on demand: Algorithms, analysis and applications*. PhD thesis, Linköping University, Sweden, 1999.

[55] M. Braun, D. E. Rivera, and A. Stenman. A 'Model-on-Demand' identification methodology for non-linear process systems. *International Journal of Control*, 74(18):1708–1717, 2001.

[56] J. Roll, A. Nazin, and L. Ljung. Nonlinear system identification via direct weight optimization. *Automatica*, 41(3):475–490, 2005.

[57] S. Deshpande, D. E. Rivera, and J. Younger. Towards patient-friendly input signal design for optimized pain treatment interventions. In *Proceedings of the 16th IFAC Symposium on System Identification*, pages 1311–1316, July 2012.

[58] C. Kreutz and J. Timmer. Systems biology: experimental design. *FEBS Journal*, 276(4):923–942, 2009.

[59] J. F. Apgar, J. E. Toettcher, D. Endy, F. M. White, and B. Tidor. Stimulus design for model selection and validation in cell signaling. *PLoS Computational Biology*, 4(2):e30, 02 2008.

[60] S. Mukherjee. *The Emperor of All Maladies: A Biography of Cancer*. Scribner, 2010.

[61] S.-C. Chow and J.-P. Liu. *Design and Analysis of Clinical Trials: Concepts and Methodologies*. John Wiley and Sons, 2004.

[62] P. L. Bonate. *Pharmacokinetic-pharmacodynamic modeling and simulation*. Springer, 2005.

[63] T. D. Cook and D. L. DeMets. *Introduction to Statistical Methods for Clinical Trials*. Chapman and Hall/CRC, 2007.

[64] J. Pearl. *Causality: Models, Reasoning, and Inference*. Cambridge University Press, 2000.

[65] M. D. Boissevain and G. A. McCain. Toward an integrated understanding of fibromyalgia syndrome. i. medical and pathophysiological aspects. *Pain*, 45(3):227–238, 1991.

[66] M. D. Boissevain and G. A. McCain. Toward an integrated understanding of fibromyalgia syndrome. ii. psychological and phenomenological aspects. *Pain*, 45(3):239–248, 1991.

[67] J. Younger and S. Mackey. Fibromyalgia symptoms are reduced by low-dose naltrexone: A pilot study. *Pain Medicine*, 10(4):663–672, 2009.

[68] J. Younger, N. Noor, R. McCue, and S. Mackey. Low-dose naltrexone for the treatment of fibromyalgia: Findings of a small, randomized, double-blind, placebo-controlled, counterbalanced, crossover trial assessing daily pain levels. *Arthritis & Rheumatism*, 65(2):529–538, 2013.

[69] S. Deshpande, N. N. Nandola, D. E. Rivera, and J. Younger. A system identification and control engineering approach for designing an optimized treatment plan for fibromyalgia, Oct. 2011. 2011 AIChE Annual Meeting. Paper 764c.

[70] D. E. Rivera, N. N. Nandola, and S. Deshpande. Robust optimal decision policies for adaptive, time-varying interventions using model predictive control, April 2011. Invited Symposium: Drawing on Ideas from Engineering and Computer Science to Build Better Behavioral Interventions. *2011 Annual Meeting of the Society of Behavioral Medicine*, Washington, D.C.

[71] T. A. Walls and J. L. Schafer, editors. *Models for Intensive Longitudinal Data*. Oxford University Press, 2006.

[72] L. M. Arnold, E. V. Hess, J. I. Hudson, J. A. Welge, S. E. Berno, and P. E. Keck. A randomized, placebo-controlled, double-blind, flexible-dose study of fluoxetine in the treatment of women with fibromyalgia. *The American Journal of Medicine*, 112(3):191–197, 2002.

[73] M. Hersen and D. H. Barlow. *Single-case experimental designs: strategies for studying behavior change*. Pergamon Press, 1976.

[74] E. O. Lillie, B. Patay, J. Diamant, B. Issell, E. J. Topol, and N. J. Schork. The n-of-1 clinical trial: the ultimate strategy for individualizing medicine? *Personalized Medicine*, 8(2):161–173, 2011.

[75] J. Dallery, R. N. Cassidy, and B. R. Raiff. Single-case experimental designs to evaluate novel technology-based health interventions. *Journal of Medical Internet Research*, 15(2):1–17, 2013.

[76] E. B. Hekler, M. P. Buman, N. Poothakandiyil, D. E. Rivera, J. M. Dzierzewski, A. Aiken Morgan, C. S. McCrae, B. L. Roberts, M. Marsiske, and P. R. Giacobbi. Exploring behavioral markers of long-term physical activity maintenance: A case study of system identification modeling within a behavioral intervention. *Health Education & Behavior*, 40(1 suppl):51S–62S, 2013.

[77] A. Siler, H. Gardner, K. Yanit, T. Cushman, and M. McDonagh. Systematic review of the comparative effectiveness of antiepileptic drugs for fibromyalgia. *Journal of Pain*, 12(4):407–415, Oct. 2011.

[78] C. A. Martin, S. Deshpande, E. B. Hekler, and D. E. Rivera. A system identification procedure for behavioral interventions based on social cognitive theory. Submitted to the *53rd IEEE Conference on Decision and Control*, 2014.

[79] H. Lee and B. Bequette. A closed-loop artificial pancreas based on model predictive control: Human-friendly identification and automatic meal disturbance rejection. *Biomedical Signal Processing and Control*, 4(4):347–354, 2009.

[80] D. E. Rivera, H. Lee, H. Mittelmann, and M. Braun. High-purity distillation: using plant-friendly multisine signals to identify a strongly interactive process. *IEEE Control Systems Magazine*, 27(5):72–89, Oct. 2007.

[81] D. E. Rivera, H. Lee, H. Mittelmann, and M. Braun. Constrained multisine input signals for plant-friendly identification of chemical process systems. *Journal of Process Control*, 19(4):623–635, 2009.

[82] K. Godfrey, editor. *Perturbation signals for system identification*. Prentice Hall, 1993.

[83] D. G. Luenberger. *Optimization by vector space methods*. John Wiley and Sons, 1969.

[84] S. Deshpande and D. E. Rivera. Optimal input signal design for data-centric estimation methods. In *Proceedings of the 2013 American Control Conference*, pages 3930–3935, June 2013.

[85] S. Deshpande and D. E. Rivera. Constrained optimal input signal design for data-centric estimation methods. *IEEE Transactions on Automatic Control* (to appear), 2014.

[86] C. Rojas, J.-C. Agüero, J. Welsh, G. Goodwin, and A. Feuer. Robustness in experiment design. *IEEE Transactions on Automatic Control*, 57(4):860–874, April 2012.

[87] H. Jansson and H. Hjalmarsson. Input design via LMIs admitting frequency-wise model specifications in confidence regions. *IEEE Transactions on Automatic Control*, 50(10):1534–1549, Oct. 2005.

[88] J. Sjöberg, Q. Zhang, L. Ljung, A. Benveniste, B. Delyon, P.-Y. Glorennec, H. Hjalmarsson, and A. Juditsky. Nonlinear black-box modeling in system identification: a unified overview. *Automatica*, 31(12):1691–1724, 1995.

[89] M. Braun. *Model-on-demand nonlinear estimation and model predictive control: Novel methodologies for process control and supply chain management*. PhD thesis, Chemical Engineering, Arizona State University, USA, 2001.

[90] E.-W. Bai and Y. Liu. Recursive direct weight optimization in nonlinear system identification: A minimal probability approach. *IEEE Transactions on Automatic Control*, 52(7):1218–1231, 2007.

[91] N. N. Nandola and D. E. Rivera. Model-on-Demand predictive control for nonlinear hybrid systems with application to adaptive behavioral interventions. In *Proceedings of the 49th IEEE Conference on Decision and Control*, pages 6113–6118, Dec. 2010.

[92] A. Bemporad and M. Morari. Control of systems integrating logic, dynamics, and constraints. *Automatica*, 35:407–427, 1999.

[93] S. Karaman, R. Sanfelice, and E. Frazzoli. Optimal control of mixed logical dynamical systems with linear temporal logic specifications. In *Proceedings of the 47th IEEE Conference onDecision and Control*, pages 2117–2122, Dec 2008.

[94] P. Pardalos and S. Vavasis. Quadratic programming with one negative eigenvalue is NP-hard. *Journal of Global Optimization*, 1:15–22, 1991.

[95] H. Lee. *A plant-friendly multivariable system identification framework based on identification test monitiring*. PhD thesis, Chemical Engineering, Arizona State University, USA, 2006.

[96] N. N. Nandola and D. E. Rivera. A novel model predictive control formulation for hybrid systems with application to adaptive behavioral interventions. In *Proceedings of the 2010 American Control Conference*, pages 6286–6292, June 2010.

[97] N. N. Nandola and D. E. Rivera. An improved formulation of hybrid model predictive control with application to production-inventory systems. *IEEE Transactions on Control Systems Technology*, 21(1):121–135, Jan. 2013.

[98] S. Deshpande, N. N. Nandola, D. E. Rivera, and J. W. Younger. Optimized treatment of fibromyalgia using system identification and hybrid model predictive control. Conditionally accepted to *IFAC Control Engineering Practice*, 2014.

[99] S. Deshpande, D. E. Rivera, J. Younger, and N. N. Nandola. A control systems engineering approach for designing optimized adaptive interventions: An illustration

from the treatment of fibromyalgia. Submitted to *Translational Behavioral Medicine*, 2014.

[100] S. Deshpande and D. E. Rivera. A data-centric system identification approach to input signal design for Hammerstein systems. In *Proceedings of the 52nd IEEE Conference on Decision and Control (CDC)*, pages 5192–5197, Dec. 2013.

[101] S. Deshpande and D. E. Rivera. Data-centric input signal design for highly interactive dynamical systems. Submitted to the *53rd IEEE Conference on Decision and Control*, 2014.

[102] S. Deshpande and D. E. Rivera. Towards data-centric input signal design using sparse polynomial optimization. Submitted to the *53rd IEEE Conference on Decision and Control*, 2014.

[103] Y. Dong, S. Deshpande, D. E. Rivera, D. S. Downs, and J. S. Savage. Hybrid model predictive control for sequential decision policies in adaptive behavioral interventions. In *Proceedings of the 2014 American Control Conference* (to appear), 2014.

[104] P. L. dos Santos, S. Deshpande, D. E. Rivera, T.-P. A. Perdicoulis, J. A. Ramos, and J. Younger. Identification of affine linear parameter varying models for adaptive interventions in fibromyalgia treatment. In *Proceedings of the 2013 American Control Conference*, pages 1976–1981, June 2013.

[105] P. L. dos Santos, T.-P. A. Perdicoulis, J. A. Ramos, S. Deshpande, D. E. Rivera, and J. L. M. de Carvalho. LPV system identification using a separable least squares support vector machines approach. Submitted to the *53rd IEEE Conference on Decision and Control*, 2014.

[106] P. Wellstead, E. Bullinger, D. Kalamatianos, O. Mason, and M. Verwoerd. The role of control and system theory in systems biology. *Annual Reviews in Control*, 32(1):33–47, 2008.

[107] F. S. Collins. The future of personalized medicine. *NIH Medline Plus*, 5:2–3, 2010.

[108] A. Zafra-Cabeza, D. E. Rivera, L. Collins, M. Ridao, and E. Camacho. A risk-based model predictive control approach to adaptive interventions in behavioral health. *IEEE Transactions on Control Systems Technology*, 19(4):891–901, July 2011.

[109] F. Wolfe, H. A. Smythe, M. B. Yunus, R. M. Bennett, C. Bombardier, D. L. Goldenberg, P. Tugwell, S. M. Campbell, M. Abeles, P. Clark, A. G. Fam, S. J. Farber,

J. J. Fiechtner, C. Michael Franklin, R. A. Gatter, D. Hamaty, J. Lessard, A. S. Lichtbroun, A. T. Masi, G. A. Mccain, W. John Reynolds, T. J. Romano, I. Jon Russell, and R. P. Sheon. The American College of Rheumatology 1990 criteria for the classification of fibromyalgia. *Arthritis & Rheumatism*, 33(2):160–172, 1990.

[110] F. Wolfe, D. J. Clauw, M.-A. Fitzcharles, D. L. Goldenberg, R. S. Katz, P. Mease, A. S. Russell, I. J. Russell, J. B. Winfield, and M. B. Yunus. The American College of Rheumatology preliminary diagnostic criteria for fibromyalgia and measurement of symptom severity. *Arthritis Care & Research*, 62(5):600–610, 2010.

[111] S. Perrot. Fibromyalgia syndrome: a relevant recent construction of an ancient condition? *Current Opinion in Supportive and Palliative Care*, 2(2):122–127, 2008.

[112] Y. Lee, N. Nassikas, and D. Clauw. The role of the central nervous system in the generation and maintenance of chronic pain in rheumatoid arthritis, osteoarthritis and fibromyalgia. *Arthritis Research and Therapy*, 13(2):211, 2011.

[113] T. M. Mattiloi, B. Milne, and C. Cahill. Ultra-low dose naltrexone attenuates chronic morphine-induced gliosis in rats. *Molecular Pain*, 6(22):1–11, 2010.

[114] P. Molenaar and C. Campbell. The new person-specific paradigm in psychology. *Current Directions in Psychological Science*, 18:112–117, 2009.

[115] M. Gevers, L. Miskovic, D. Bonvin, and A. Karimi. Identification of multi-input systems: variance analysis and input design issues. *Automatica*, 42(4):559–572, 2006.

[116] G. Box, G. M. Jenkins, and G. Reinsel. *Time Series Analysis: Forecasting and Control*. Prentice Hall, 1994.

[117] S. J. Qin and T. A. Badgwell. A survey of industrial model predictive control technology. *Control Engineering Practice*, 11(7):733–764, 2003.

[118] R. Zurakowski and A. R. Teel. A model predictive control based scheduling method for HIV therapy. *Journal of Theoretical Biology*, 238(2):368–382, 2006.

[119] Y. Wang, E. Dassau, and F. Doyle. Closed-loop control of artificial pancreatic $\beta$-cell in type 1 diabetes mellitus using model predictive iterative learning control. *IEEE Transactions on Biomedical Engineering*, 57(2):211–219, Feb. 2010.

[120] J. Lee and Z. Yu. Tuning of model predictive controllers for robust performance. *Comp. and Chem. Engg.*, 18(1):15–37, 1994.

[121] W. Wang and D. E. Rivera. Model predictive control for tactical decision-making in semiconductor manufacturing supply chain management. *IEEE Transactions on Control Systems Technology*, 16(5):841–855, Sep. 2008.

[122] M. Morari and E. Zafiriou. *Robust Process Control*. Prentice Hall, Englewood Cliffs, NJ, 1989.

[123] S. Boyd and L. Vandenberghe. *Convex Optimization*. Cambridge University Press, 2004.

[124] J. Nocedal and S. Wright. *Numerical Optimization*. Springer, 2006.

[125] S. S. Carey. *A Beginner's Guide to Scientific Method*. Wadsworth Publishing, 2011.

[126] P. Godfrey-Smith. The strategy of model-based science. *Biology and Philosophy*, 21:725–740, 2006.

[127] P. A. Tipler. *Physics*. Worth Publishers, 1976.

[128] K. F. Gauss. *Theory of Motion of the Heavenly Bodies Moving About the Sun in Conic Sections: A Translation of Theoria Motus*. Dover Publications, 2004. An english translation of theoria motus corporum coelestium in sectionibus conicis solem ambientium.

[129] G. Aad and et al. Observation of a new particle in the search for the standard model higgs boson with the ATLAS detector at the LHC. *Physics Letters B*, 716(1):1–29, 2012. ATLAS collaboration. Full author list at `http://www.sciencedirect.com/science/article/pii/S037026931200857X`.

[130] S. Chatrchyan and et al. Observation of a new boson at a mass of 125 GeV with the CMS experiment at the LHC. *Physics Letters B*, 716(1):30–61, 2012. CMS collaboration. Full author list at `http://www.sciencedirect.com/science/article/pii/S0370269312008581`.

[131] P. A. R. Ade and et al. BICEP2 I: Detection of B-mode polarization at degree angular scales. *arXiv:1403.3985*, 2014.

[132] D. E. Rivera. ChE 494/598: Introduction to system identification, 2009. Class notes.

[133] G.-P. Bonneau, T. Ertl, and G. Nielson, editors. *Scientific Visualization: The Visual Extraction of Knowledge from Data*. Springer, 2006.

[134] D. Luenberger. *Introduction to dynamic systems: theory, models, and applications*. Wiley, 1979.

[135] C. E. Rasmussen and C. K. I. Williams. *Gaussian Processes for Machine Learning*. MIT Press, 2006.

[136] S. O. Haykin. *Neural Networks and Learning Machines*. Prentice Hall, 2008.

[137] W. H. Greene. *Econometric Analysis*. Prentice Hall, 2011.

[138] G. L. Lilien, P. Kotler, and K. S. Moorthy. *Marketing Models*. Prentice Hall, 1991.

[139] L. Zadeh. On the identification problem. *IRE Transactions on Circuit Theory*, 3(4):277–281, 1956.

[140] L. Ljung, H. Hjalmarsson, and H. Ohlsson. Four encounters with system identification. *European Journal of Control*, 17(5-6):449–471, 2011.

[141] B. Ninness, H. Hjalmarsson, and F. Gustafsson. The fundamental role of general orthonormal bases in system identification. *IEEE Transactions on Automatic Control*, 44(7):1384–1406, July 1999.

[142] H. Jansson. *Experiment design with applications in identification for control*. PhD thesis, Royal Institute of Technology (KTH), Sweden, 2004.

[143] J. Fan and I. Gijbels. *Local polynomial modeling and its applications*. Chapman & Hall, 1996.

[144] E.-W. Bai. Non-parametric nonlinear system identification: An asymptotic minimum mean squared error estimator. *IEEE Transactions on Automatic Control*, 55(7):1615–1626, July 2010.

[145] J. Roll. *Local and piecewise affine approaches to system identification*. PhD thesis, Linköping University, Sweden, 2003.

[146] M. Schroeder. Synthesis of low-peak-factor signals and binary sequences with low autocorrelation. *IEEE Transactions on Information Theory*, 16(1):85–89, 1970.

[147] P. A. Ioannou. *Robust Adaptive Control*. Prentice Hall PTR, 1995.

[148] D. E. Rivera, X. Chen, and D. S. Bayard. Experimental design for robust process control using schroeder-phased input signals. In *Proceedings of the 1993 American Control Conference*, pages 895–899, June 1993.

[149] M. Braun, R. Ortiz-Mojica, and D. E. Rivera. Application of minimum crest factor multisinusoidal signals for plant-friendly identification of nonlinear process systems. *Control Engineering Practice*, 10(3):301–313, 2002.

[150] R. Steenis. *Plant-friendly input signal design for system identification and robust control performance*. PhD thesis, Electrical Engineering, Arizona State University, USA, 2009.

[151] R. Steenis and D. E. Rivera. Plant-friendly signal generation for system identification using a modified simultaneous perturbation stochastic approximation (SPSA) methodology. *IEEE Transactions on Control Systems Technology*, 19(6):1604–1612, Nov. 2011.

[152] G. V. Pendse. Optimization based formulations using the Weyl criterion for input signal design in system identification. Master's thesis, Mathematics and Statistics, Arizona State University, USA, 2004.

[153] H. D. Mittelmann, G. Pendse, D. E. Rivera, and H. Lee. Optimization-based design of plant-friendly multisine signals using geometric discrepancy criteria. *Computational Optimization and Applications*, 38(1):173, 2007.

[154] M. Annergren and C. Larsson. MOOSE: Model based optimal input design toolbox for Matlab. Technical report, Royal Institute of Technology (KTH), Sweden, 2011.

[155] CVX: Matlab software for disciplined convex programming, version 2.0 beta. CVX Research Inc. `http://cvxr.com/cvx`, September 2012.

[156] J. Sturm. Using SeDuMi 1.02, a MATLAB toolbox for optimization over symmetric cones. *Optimization Methods and Software*, 11–12:625–653, 1999.

[157] S. Boyd, L. E. Ghaoui, E. Feron, and V. Balakrishnan. *Linear Matrix Inequalities in System and Control Theory*. Society for Industrial and Applied Mathematics (SIAM), 1994.

[158] S.-P. Wu, S. Boyd, and L. Vandenberghe. FIR filter design via semidefinite programming and spectral factorization. In *Proceedings of the 35th IEEE Conference on Decision and Control (CDC)*, volume 1, pages 271–276, Dec. 1996.

[159] L. Gerencsér, H. Hjalmarsson, and J. Mårtensson. Identification of ARX systems with non-stationary inputs - asymptotic analysis with application to adaptive input design. *Automatica*, 45(3):623–633, 2009.

[160] E. A. Morelli. *Practical Input Optimization for Aircraft Parameter Estimation Experiments*. PhD thesis, The George Washington University, USA, 1993.

[161] I. Manchester. Input design for system identification via convex relaxation. In *Proceedings of the 49th IEEE Conference on Decision and Control (CDC)*, pages 2041 –2046, Dec. 2010.

[162] S. Narasimhan and R. Rengaswamy. Plant friendly input design: Convex relaxation and quality. *IEEE Transactions on Automatic Control*, 56(6):1467–1472, 2011.

[163] D. E. Kirk. *Optimal control theory: an introduction*. Dover Publications, 2004.

[164] G. G. Magaril-Il'yaev and V. M. Tikhomirov. *Convex Analysis: Theory and Applications*. American Mathematical Society, 2003.

[165] R. Rockafellar. Lagrange multipliers and optimality. *SIAM Review*, 35(2):183–238, 1993.

[166] A. Ben-Tal and A. Nemirovski. *Lectures on Modern Convex Optimization*. SIAM, 2001.

[167] M. Grötschel, editor. *Optimization Stories*, volume Extra Volume ISMP (2012). DOCUMENTA MATHEMATICA, Journal der Deutschen Mathematiker-Vereinigung, 2012.

[168] M. Goemans and D. Williamson. Improved approximation algorithms for maximum cut and satisfiability problems using semidefinite programming. *Journal of the ACM*, 42(6):1115–1145, 1995.

[169] Y. Nesterov. Semidefinite relaxation and nonconvex quadratic optimization. *Optimization Methods and Software*, 9(1-3):141–160, 1998.

[170] Z.-Q. Luo, W.-K. Ma, A. So, Y. Ye, and S. Zhang. Semidefinite relaxation of quadratic optimization problems. *IEEE Signal Processing Magazine*, 27(3):20–34, May 2010.

[171] M. Laurent. Sums of squares, moment matrices and optimization over polynomials. In M. Putinar and S. Sullivant, editors, *Emerging Applications of Algebraic Geometry*, volume 149 of *The IMA Volumes in Mathematics and its Applications*, pages 157–270. Springer New York, 2009.

[172] R. Fourer, D. M. Gay, and B. W. Kernighan. *AMPL: A Modeling Language for Mathematical Programming*. Duxbury Press, 2003.

[173] R. E. Rosenthal. *GAMS - A User's Guide*. GAMS Development Corporation, 2012.

[174] J. Löfberg. YALMIP : a toolbox for modeling and optimization in matlab. In *2004 IEEE International Symposium on Computer Aided Control Systems Design*, pages 284–289, 2004.

[175] TOMLAB optimizer reference manual, February 2013. TOMLAB Optimization. `http://tomopt.com/tomlab/`.

[176] J. Czyzyk, M. P. Mesnier, and J. J. Moré. The NEOS server. *IEEE Computational Science & Engineering*, 5(3):68–75, July 1998.

[177] Gurobi optimizer reference manual, 2012. Gurobi Optimization Inc. `http://www.gurobi.com`.

[178] IBM ILOG CPLEX optimizer reference manual, February 2013. International Business Machines (IBM) Corp. `http://www-01.ibm.com/software/integration/optimization/cplex-optimizer/`.

[179] KNITRO, a solver for nonlinear optimization, September 2011. Ziena Optimization LLC. `http://www.ziena.com/knitro.htm`.

[180] P. Belotti. Couenne, an exact solver for nonconvex minlps, September 2011. `https://projects.coin-or.org/Couenne`.

[181] P. Bonami. Bonmin (basic open-source nonlinear mixed integer programming), September 2011. `https://projects.coin-or.org/Bonmin`.

[182] K. C. Toh, M. J. Todd, and R. H. Tutuncu. SDPT3 - a matlab software package for semidefinite programming, version 1.3. *Optimization Methods and Software*, 11(1-4):545–581, 1999.

[183] J. Dahl. Semidefinite optimization with MOSEK, Oct. 2013. INFORMS Annual Meeting.

[184] The Mathworks. *Optimization Toolbox, MATLAB User Manual for version R2012b*, 2012.

[185] D. Henrion, J. B. Lasserre, and J. Löfberg. GloptiPoly 3: moments, optimization and semidefinite programming. *Optimization Methods and Software*, 24(4-5):761–779, 2009.

[186] H. Waki, S. Kim, M. Kojima, M. Muramatsu, and H. Sugimoto. Algorithm 883: SparsePOP—a sparse semidefinite programming relaxation of polynomial optimization problems. *ACM Transactions on Mathematical Software*, 35:15:1–15:13, July 2008.

[187] Y. Nesterov. Smooth minimization of non-smooth functions. *Mathematical Programming*, 103:127–152, 2005.

[188] M. Backonja and R. L. Glanzman. Gabapentin dosing for neuropathic pain: Evidence from randomized, placebo-controlled clinical trials. *Clinical Therapeutics*, 25(1):81–104, 2003.

[189] G. Blekherman, P. A. Parrilo, and R. R. Thomas, editors. *Semidefinite Optimization and Convex Algebraic Geometry*. SIAM, 2013.

[190] X. Bombois, G. Scorletti, M. Gevers, P. V. den Hof, and R. Hildebrand. Least costly identification experiment for control. *Automatica*, 42(10):1651–1662, 2006.

[191] P. Guillaume, J. Schoukens, R. Pintelon, and I. Kollar. Crest-factor minimization using nonlinear Chebyshev approximation methods. *IEEE Transactions on Instrumentation and Measurement*, 40(6):982–989, Dec. 1991.

[192] K. Godfrey, H. Barker, and A. Tucker. Comparison of perturbation signals for linear system identification in the frequency domain. *IEE Proceedings Control Theory and Applications*, 146(6):535–548, Nov. 1999.

[193] J. Matoušek. *Geometric Discrepancy: An Illustrated Guide*. Springer, 1999.

[194] H. Weyl. Über die gleichverteilung von zahlen mod. eins. *Mathematische Annalen*, 77:313–352, 1916.

[195] A. Nazin, J. Roll, and L. Ljung. Direct weight optimization for approximately linear functions: optimality and design. In *Proceedings of 14th IFAC Symposium on System Identification*, pages 796–801, 2006.

[196] A. Nazin, J. Roll, L. Ljung, and I. Grama. Direct weight optimization in statistical estimation and system identification. In *The Seventh International Conference on System Identification and Control Problems*, 2008.

[197] V. V. Fedorov, G. Montepiedra, and C. J. Nachtsheim. Design of experiments for locally weighted regression. *Journal of Statistical Planning and Inference*, 81(2):363–382, 1999.

[198] M. Johnson, L. Moore, and D. Ylvisaker. Minimax and maximin distance designs. *Journal of Statistical Planning and Inference*, 26(2):131–148, 1990.

[199] A. Brøndsted. *An Introduction to Convex Polytopes*. Springer, 1983.

[200] J. A. Rice. *Mathematical Statistics and Data Analysis*. Wadsworth & Brooks/Cole Advanced Books & Software, 1988.

[201] L. Pronzato and E. Walter. Experiment design in a bounded-error context: Comparison with D-optimality. *Automatica*, 25(3):383–391, 1989.

[202] Y. Zhu. *Multivariable System Identification For Process Control*. Pergamon Elsevier Science, 2001.

[203] Y. Zhu and P. Stec. Simple control-relevant identification test methods for a class of ill-conditioned processes. *Journal of Process Control*, 16(10):1113–1120, 2006.

[204] O. R. Vaillant, A. S. R. Kuramoto, and C. Garcia. Effectiveness of signal excitation design methods for identification of ill-conditioned and highly interactive processes. *Industrial & Engineering Chemistry Research*, 52(14):5120–5135, 2013.

[205] E. W. Jacobsen and S. Skogestad. Inconsistencies in dynamic models for ill-conditioned plants: Application to low-order models of distillation columns. *Industrial & Engineering Chemistry Research*, 33(3):631–640, 1994.

[206] S. Burer and A. N. Letchford. Non-convex mixed-integer nonlinear programming: A survey. *Surveys in Operations Research and Management Science*, 17(2):97–106, 2012.

[207] M. Gevers, M. Caenepeel, and J. Schoukens. Experiment design for the identification of a simple Wiener system. In *Proceedings of the 51st IEEE Conference on Decision and Control (CDC)*, pages 7333–7338, 2012.

[208] F. Giri and E.-W. Bai, editors. *Block-oriented Nonlinear System Identification*. Springer, 2010.

[209] H. Hjalmarsson, C. R. Rojas, and D. E. Rivera. System identification: A Wiener-Hammerstein benchmark. *Control Engineering Practice*, 20(11):1095–1096, 2012.

[210] H. Ohlsson, J. Roll, A. Brun, H. Knutsson, M. Andersson, and L. Ljung. Direct weight optimization applied to discontinuous functions. In *Proceedings of the 47th IEEE Conference on Decision and Control*, pages 117–122, Dec. 2008.

[211] X. Bao, N. Sahinidis, and M. Tawarmalani. Semidefinite relaxations for quadratically constrained quadratic programming: A review and comparisons. *Mathematical Programming*, 129:129–157, 2011.

[212] H. Waki, S. Kim, M. Kojima, and M. Muramatsu. Sums of squares and semidefinite program relaxations for polynomial optimization problems with structured sparsity. *SIAM Journal on Optimization*, 17(1):218–242, 2006.

[213] R. Horst, P. Pardalos, and N. Thoai. *Introduction to global optimization*. Kluwer academic publishers, 1995.

[214] R. H. Byrd, M. E. Hribar, and J. Nocedal. An interior point algorithm for large-scale nonlinear programming. *SIAM Journal on Optimization*, 9:877–900, April 1999.

[215] J. B. Lasserre. Global optimization with polynomials and the problem of moments. *SIAM Journal on Optimization*, 11(3):796–817, 2001.

[216] J. Löfberg. Pre- and post-processing sum-of-squares programs in practice. *IEEE Transactions on Automatic Control*, 54(5):1007–1011, May 2009.

[217] P. A. Parrilo. Semidefinite programming relaxations for semialgebraic problems. *Mathematical Programming*, 96(2):293–320, 2003.

[218] M. Putinar. Positive polynomials on compact semi-algebraic sets. *Indiana University Mathematics Journal*, 42(3):969–984, 1993.

[219] J. Nie. Optimality conditions and finite convergence of Lasserre's hierarchy. *Mathematical Programming*, pages 1–25, 2013.

[220] V. Jeyakumar, J. B. Lasserre, and G. Li. On Polynomial Optimization over Non-compact Semi-algebraic Sets. *ArXiv e-prints*, April 2013.

[221] J. B. Lasserre. Convergent SDP-relaxations in polynomial optimization with sparsity. *SIAM Journal on Optimization*, 17(3):822–843, 2006.

[222] J. Nie. Sum of squares method for sensor network localization. *Computational Optimization and Applications*, 43:151–179, 2009.

[223] Y. Ye. Approximating quadratic programming with bound and quadratic constraints. *Mathematical Programming*, 84:219–226, 1999.

[224] J. Chen and S. Burer. Globally solving nonconvex quadratic programming problems via completely positive programming. *Mathematical Programming Computation*, 4:33–52, 2012.

[225] Y. Nesterov. Global quadratic optimization via conic relaxation. In R. Saigal, L. Vandenberghe, and H. Wolkowicz, editors, *Handbook of Semidefinite Programming*. Kluwer Academic Publishers, 2000.

[226] K. Anstreicher. Semidefinite programming versus the reformulation-linearization technique for nonconvex quadratically constrained quadratic programming. *Journal of Global Optimization*, 43:471–484, 2009.

[227] T. Baran, D. Wei, and A. Oppenheim. Linear programming algorithms for sparse filter design. *IEEE Transactions on Signal Processing*, 58(3):1605–1617, 2010.

[228] D. Grimm, T. Netzer, and M. Schweighofer. A note on the representation of positive polynomials with structured sparsity. *Archiv der Mathematik*, 89(5):399–403, 2007.

[229] W. D. T. Davies. *System identification for self-adaptive control*. John Wiley and Sons, 1970.

[230] J. Álvarez, J. Guzmán, D. E. Rivera, M. Berenguel, and S. Dormido. Perspectives on control-relevant identification through the use of interactive tools. *Control Engineering Practice*, 21(2):171–183, 2013.

[231] A. C. King, E. B. Hekler, L. A. Grieco, S. J. Winter, J. L. Sheats, M. P. Buman, B. Banerjee, T. N. Robinson, and J. Cirimele. Harnessing different motivational frames via mobile phones to promote daily physical activity and reduce sedentary behavior in aging adults. *PLoS ONE*, 8(4):e62613, 04 2013.

[232] A. Khalate, X. Bombois, R. Toth, and R. Babuska. Optimal experimental design for LPV identification using a local approach. In *Proceedings of the 15th IFAC Symposium on System Identification*, 2009.

[233] K. Fang and D. Lin. Uniform experimental designs and their applications in industry. *Handbook of statistics*, 22:131–170, 2003.

[234] R. Reemtsen and J.-J. Rückmann. *Semi-infinite programming*. Kulwer academic publishers, 1998.

[235] I. J. Leontaritis and S. A. Billings. Experimental design and identifiability for non-linear systems. *International Journal of Systems Science*, 18(1):189–202, 1987.

[236] E. F. Camacho and C. Bordons. *Model predictive control*. Springer, 1999.

[237] K. P. Timms, D. E. Rivera, M. E. Piper, and L. M. Collins. A hybrid model predictive control strategy for optimizing a smoking cessation intervention. In Proceedings of the 2014 *American Control Conference* (to appear), 2014.

[238] R. Cagienard, P. Grieder, E. Kerrigan, and M. Morari. Move blocking strategies in receding horizon control. In *Proceedings of the 43rd IEEE Conference on Decision and Control (CDC)*, volume 2, pages 2023–2028, Dec. 2004.

[239] H. Williams. *Model Building in Mathematical Programming*. John Wiley and Sons, 4 edition, 1999.

[240] W. P. M. H. Heemels, B. D. Schutter, and A. Bemporad. Equivalence of hybrid dynamical models. *Automatica*, 37:1085–1091, 2001.